# HIGH-FREQUENCY OSCILLATIONS IN THE HIPPOCAMPUS AS BIOMARKERS OF PATHOLOGY AND HEALTHY BRAIN FUNCTION

EDITED BY: Johannes Sarnthein, Julia Jacobs and Maeike Zijlmans
PUBLISHED IN: Frontiers in Neurology and Frontiers in Human Neuroscience

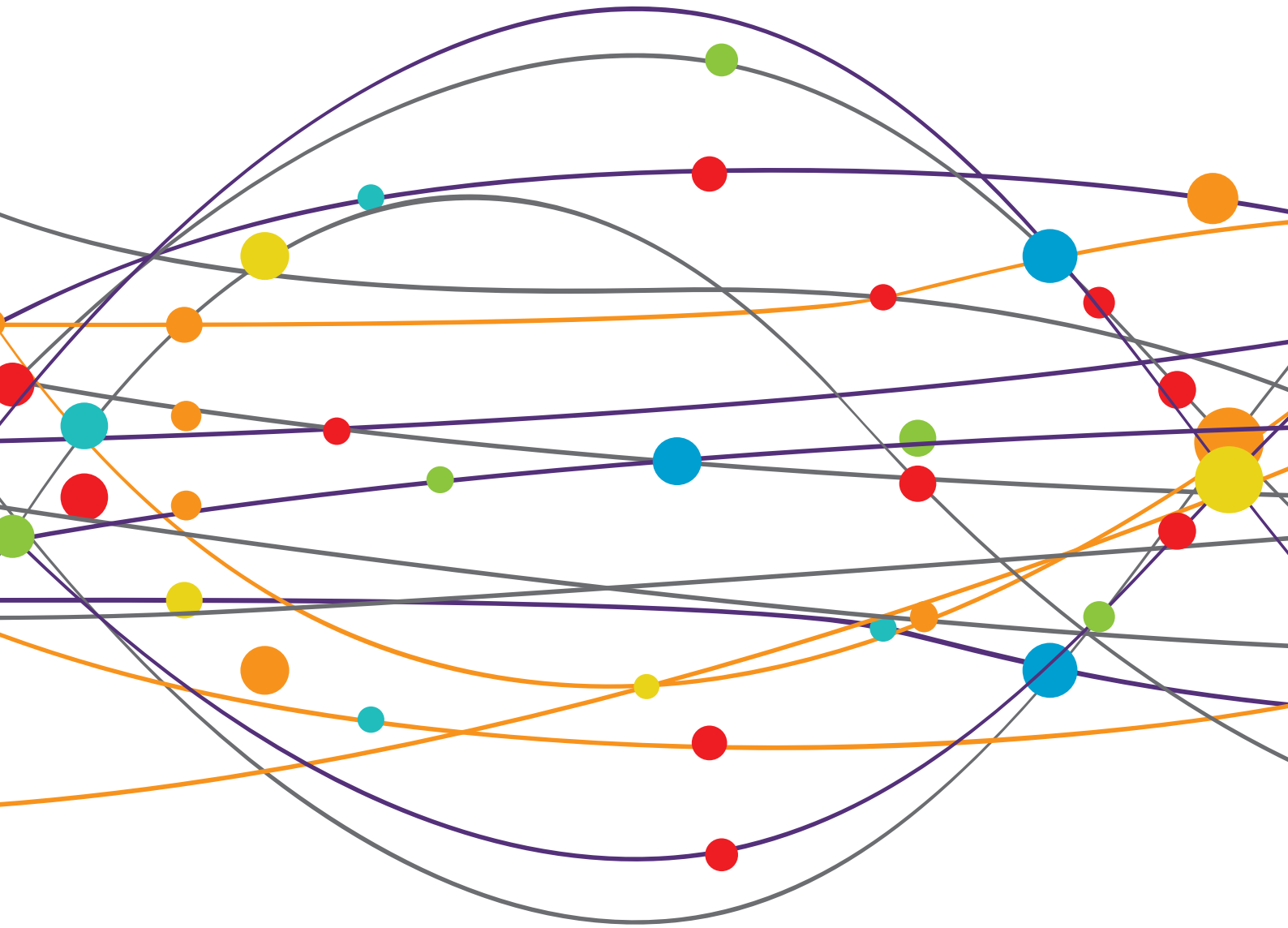

frontiers Research Topics

**Frontiers eBook Copyright Statement**

The copyright in the text of individual articles in this eBook is the property of their respective authors or their respective institutions or funders. The copyright in graphics and images within each article may be subject to copyright of other parties. In both cases this is subject to a license granted to Frontiers.

The compilation of articles constituting this eBook is the property of Frontiers.

Each article within this eBook, and the eBook itself, are published under the most recent version of the Creative Commons CC-BY licence. The version current at the date of publication of this eBook is CC-BY 4.0. If the CC-BY licence is updated, the licence granted by Frontiers is automatically updated to the new version.

When exercising any right under the CC-BY licence, Frontiers must be attributed as the original publisher of the article or eBook, as applicable.

Authors have the responsibility of ensuring that any graphics or other materials which are the property of others may be included in the CC-BY licence, but this should be checked before relying on the CC-BY licence to reproduce those materials. Any copyright notices relating to those materials must be complied with.

Copyright and source acknowledgement notices may not be removed and must be displayed in any copy, derivative work or partial copy which includes the elements in question.

All copyright, and all rights therein, are protected by national and international copyright laws. The above represents a summary only. For further information please read Frontiers' Conditions for Website Use and Copyright Statement, and the applicable CC-BY licence.

ISSN 1664-8714
ISBN 978-2-88971-689-0
DOI 10.3389/978-2-88971-689-0

## About Frontiers

Frontiers is more than just an open-access publisher of scholarly articles: it is a pioneering approach to the world of academia, radically improving the way scholarly research is managed. The grand vision of Frontiers is a world where all people have an equal opportunity to seek, share and generate knowledge. Frontiers provides immediate and permanent online open access to all its publications, but this alone is not enough to realize our grand goals.

## Frontiers Journal Series

The Frontiers Journal Series is a multi-tier and interdisciplinary set of open-access, online journals, promising a paradigm shift from the current review, selection and dissemination processes in academic publishing. All Frontiers journals are driven by researchers for researchers; therefore, they constitute a service to the scholarly community. At the same time, the Frontiers Journal Series operates on a revolutionary invention, the tiered publishing system, initially addressing specific communities of scholars, and gradually climbing up to broader public understanding, thus serving the interests of the lay society, too.

## Dedication to Quality

Each Frontiers article is a landmark of the highest quality, thanks to genuinely collaborative interactions between authors and review editors, who include some of the world's best academicians. Research must be certified by peers before entering a stream of knowledge that may eventually reach the public - and shape society; therefore, Frontiers only applies the most rigorous and unbiased reviews.
Frontiers revolutionizes research publishing by freely delivering the most outstanding research, evaluated with no bias from both the academic and social point of view. By applying the most advanced information technologies, Frontiers is catapulting scholarly publishing into a new generation.

## What are Frontiers Research Topics?

Frontiers Research Topics are very popular trademarks of the Frontiers Journals Series: they are collections of at least ten articles, all centered on a particular subject. With their unique mix of varied contributions from Original Research to Review Articles, Frontiers Research Topics unify the most influential researchers, the latest key findings and historical advances in a hot research area! Find out more on how to host your own Frontiers Research Topic or contribute to one as an author by contacting the Frontiers Editorial Office: frontiersin.org/about/contact

# HIGH-FREQUENCY OSCILLATIONS IN THE HIPPOCAMPUS AS BIOMARKERS OF PATHOLOGY AND HEALTHY BRAIN FUNCTION

Topic Editors:
**Johannes Sarnthein,** University of Zurich, Switzerland
**Julia Jacobs,** University of Freiburg Medical Center, Germany
**Maeike Zijlmans,** University Medical Center Utrecht, Netherlands

**Citation:** Sarnthein, J., Jacobs, J., Zijlmans, M., eds. (2021). High-Frequency Oscillations in the Hippocampus as Biomarkers of Pathology and Healthy Brain Function. Lausanne: Frontiers Media SA. doi: 10.3389/978-2-88971-689-0

# Table of Contents

frontiers in Human Neuroscience

EDITORIAL
published: 29 September 2021
doi: 10.3389/fnhum.2021.763881

# Editorial: High-Frequency Oscillations in the Hippocampus as Biomarkers of Pathology and Healthy Brain Function

*Johannes Sarnthein*[1]*, *Julia Jacobs*[2] and *Maeike Zijlmans*[3,4]

[1] University Hospital and University of Zurich, Zurich, Switzerland, [2] Alberta Children's Research Institute, University of Calgary, Calgary, AB, Canada, [3] University Medical Center Utrecht, Utrecht, Netherlands, [4] Stichting Epilepsie Instellingen Nederland (SEIN), Heemstede, Netherlands

**Keywords: high frequency oscillation, epilepsy, memory, hippocampus, cognition, ripple, fast ripple**

**Editorial on the Research Topic**

**High-Frequency Oscillations in the Hippocampus as Biomarkers of Pathology and Healthy Brain Function**

Functional and anatomical aspects of the hippocampus are unique compared to other brain regions. Brain signals recorded from this structure are indicators for function especially memory, but also diseases like epilepsy or dementia. The hippocampus was the first structure in which High frequency oscillations (HFO > 80 Hz) were discovered. From recent research it is also the place where HFO are most abundant. This discovery raises an important question: are these oscillations reflecting function or pathology?

A clear link between HFO and pathology has been found for patients with epilepsy. Animal models suggest that epileptic HFO only occur in rodents that develop spontaneous seizures after induced status epilepticus. If HFOs are detected in the tissue during the invasive pre-surgical examination in patients with refractory epilepsy, the resection of this tissue is a specific predictor for postoperative seizure freedom. While first identified over the hippocampus, the validity of HFO as biomarker for epilepsy extends to all other brain lobes.

Similarly, there is no question that HFO contribute to important physiological functions in the hippocampus. Physiological HFO were first identified in rat hippocampus, where ripples (80–250 Hz) contribute to spatial processing. The visual cortex and the somatosensory cortex abound with HFO that seem unrelated to the epileptogenicity of the tissue—they mask possible pathological HFO and render HFO analysis not applicable in these brain areas. HFO are certainly a part of the repertoire of oscillations in the healthy cortex.

Therefore, in the MTL, both pathological and healthy HFO are of high scientific interest and we have to pose the following question: Is the co-existence of physiological and epileptic HFO a confounding factor for using HFO in diagnostics? Can the overlap in frequencies also be an opportunity to learn about both function and pathology in the hippocampus? We therefore designed a Research Topic with a specific focus on these questions. In the following papers you will find a wide range of methods and questions all aimed to discuss "High-Frequency Oscillations in the hippocampus as biomarkers of pathology and in healthy brain function."

Contributions in this special issue span from improvements in the methodology of analyzing HFO to investigating the link between HFO and function/pathology. At this point, there is no agreement on the actual definition and mechanisms of HFO. These questions are first addressed from a signal processing perspective (Thomschewski et al.) and from a physiological perspective to advance our understanding on a microscopic level (Naggar et al.; Weiss et al.). Naggar et al.

OPEN ACCESS

***Edited and reviewed by:***
*Björn H. Schott,*
*Leibniz Institute for Neurobiology (LG), Germany*

***Correspondence:**
*Johannes Sarnthein*
*johannes.sarnthein@usz.ch*

***Specialty section:***
*This article was submitted to Brain Health and Clinical Neuroscience, a section of the journal Frontiers in Human Neuroscience*

***Received:*** *24 August 2021*
***Accepted:*** *30 August 2021*
***Published:*** *29 September 2021*

***Citation:***
*Sarnthein J, Jacobs J and Zijlmans M (2021) Editorial: High-Frequency Oscillations in the Hippocampus as Biomarkers of Pathology and Healthy Brain Function. Front. Hum. Neurosci. 15:763881. doi: 10.3389/fnhum.2021.763881*

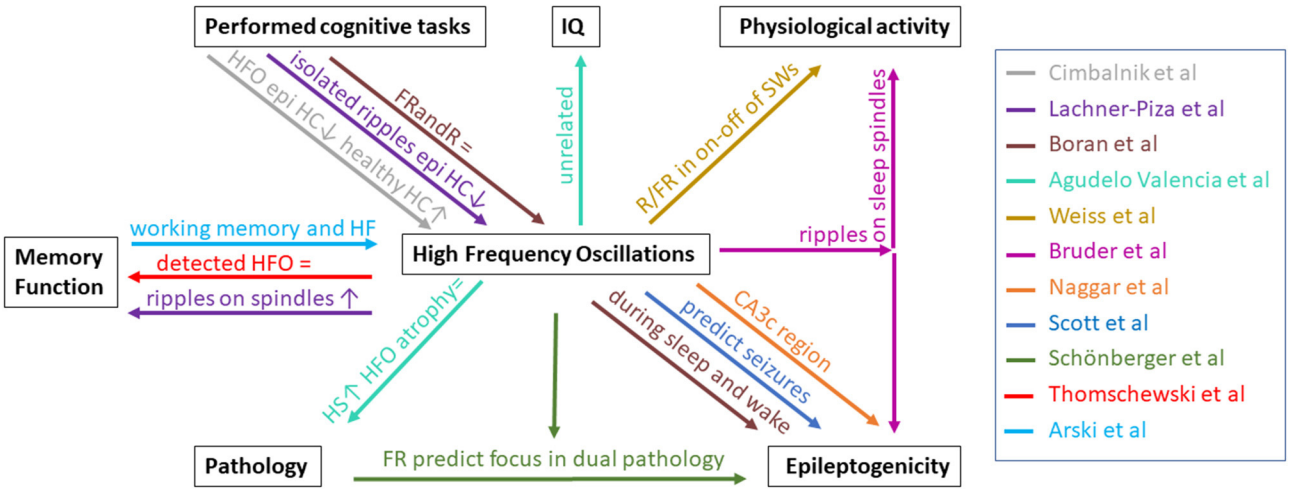


**FIGURE 1 |** Overview of relationships between HFO and pathology, memory function, performed cognitive tasks, IQ, physiological activity, and epileptogenicity described by the papers in this Research Topic. Each paper is represented by a color. HS, hippocampal sclerosis; HC, hippocampus; epi, epileptic; FRandR, fast ripples combined with ripples; R, ripple; FR, fast ripple; SW, slow waves; ↑, increase/positive relation; =, no effect; ↓, decrease/negative relation.

showed that in rat brains hippocampal slices HFOs had the highest amplitude over the CA3c region. Weiss et al. showed that epileptiform ripples occurred mostly during the on-off state transition of hippocampal slow waves. Additionally, one of the contributions reviews how different EEG frequencies have been linked to memory and come to the conclusion that t higher frequencies appear most interesting to study memory functioning (Arski et al.).

Several contributions in this collection aim to shed light on the differences between physiological and epileptic HFO. In this effort two principal approached were used. First, studies analyzed changed in HFO occurrence and rate during cognitive tasks. Second, HFO were not analyzed as stand-alone events but in their occurrence with other markers like epileptic spikes or sleep spindles.

Cimbalnik et al. show in 24 patients with bilateral stereo-EEG implantations that cognitive tasks reduced epileptiform activity in the diseased hippocampus. At the same time, brain activity in the healthy hippocampus shifted toward higher frequencies. With machine learning they created a predictive model for the diseased hippocampus based on HFOs, connectivity and spikes.

A set of studies focused on comparing distribution and changes in subsets of ripples, namely in isolated ripples (maybe physiological), spindle-ripples (likely physiological) and epileptic spikes coupled ripples. Bruder et al. focused on describing the occurrence of sleep-spindle coupled ripples. The latter are believed to be a subset of ripples, linked to physiological task. In the present study they were identified most frequently but not limited to the hippocampal structure. As second study investigated how cognitive tasks modulate the above described ripples subtypes (Lachner-Piza et al.). While cognitive tasks reduced the number of isolated ripples in the diseased hippocampus, no effect was observed for ripples co-occurring with spikes. Most importantly, authors found a positive correlation between performance improvement and spindle-ripple rates in a spatial navigation task. This finding suggests that spindle ripples actually select a physiological subpopulation of all HFO. Moreover, that rates of physiological HFO might allow us to measure function.

Interestingly, a similar correlation could not be found in other studies, which may relate to the specific definition of what is an epileptic HFO or a physiological HFO. Thomschewski et al. found no relation between performance of memory tasks and number of automatically detected HFOs. Agudelo Valencia et al. also showed no relation between ripples (either normal or prolonged) and IQ scores. As a further null-finding, Boran et al. did not find an effect of cognitive tasks on HFO rates. More specifically fast-ripples co-occurring with ripples were not altered during the task. This finding is reassuring, as ripples with fast ripples can be used for pre-surgical evaluations and seem to occur independent of behavioral changes.

In keeping with the tradition of HFO as biomarker for epilepsy, several contributions in the collection focus on the relation of HFO with the underlying pathology and epileptic activity. In the past several studies focused on the question whether HFO are linked to abnormal "lesional" brain tissue in general more specifically reflect the epileptic potential of this tissue. Agudelo Valenca et al. confirmed that high HFO rates occur in brain regions with hippocampal sclerosis. Interestingly the same was not true for areas which only showed atrophy. In the study of Schönberger et al. fast ripples, but not ripples or spikes, could predict the epileptogenic focus in case of dual pathology (lesions and hippocampal sclerosis). Boran et al. reported a higher HFO rate in the seizure onset zone not only during deep sleep but even during wakefulness while performing cognitive tasks. These studies can be viewed as additional evidence that HFO are not just reflecting general anatomical changes but

are more specific for epilepsy. One contribution reports that HFO might even serve as predictors of imminent seizures in 10 out of 27 patients, mostly with temporal lobe epilepsy (Scott et al.).

Neuroscientists and epileptologists have long known that physiological function and epileptic activity co-exist in the human brain even within small substructures like the hippocampus. The present collection of articles focusses on investigating the value of HFO in this triangle between different cognitive functions and brain pathology. **Figure 1** summarizes the different interactions investigated. As expected, this summary cannot give a final answer to all open questions and some findings are slightly contradictory. If anything, these papers confirm the complex relations between HFOs and physiological functioning as well as with pathology and epileptogenicity.

Overall we have to keep in mind that the term HFO simply describes a frequency band and not all oscillations in this frequency serve the same purpose. Thereby, this Research Topic exemplifies the current research directions in the fields of HFO in healthy brain function and in epilepsy. It can be seen as guide suggesting new methods and pathways to separating physiology and pathology within the epileptic hippocampus.

## AUTHOR CONTRIBUTIONS

All authors listed have made a substantial, direct and intellectual contribution to the work, and approved it for publication.

## FUNDING

We acknowledge the ERC starting grant 803880 to MZ and the SNSF grant 176222 to JS.

**Conflict of Interest:** The authors declare that the research was conducted in the absence of any commercial or financial relationships that could be construed as a potential conflict of interest.

**Publisher's Note:** All claims expressed in this article are solely those of the authors and do not necessarily represent those of their affiliated organizations, or those of the publisher, the editors and the reviewers. Any product that may be evaluated in this article, or claim that may be made by its manufacturer, is not guaranteed or endorsed by the publisher.

*Copyright © 2021 Sarnthein, Jacobs and Zijlmans. This is an open-access article distributed under the terms of the Creative Commons Attribution License (CC BY). The use, distribution or reproduction in other forums is permitted, provided the original author(s) and the copyright owner(s) are credited and that the original publication in this journal is cited, in accordance with accepted academic practice. No use, distribution or reproduction is permitted which does not comply with these terms.*

frontiers in Neurology

BRIEF RESEARCH REPORT
published: 24 March 2020
doi: 10.3389/fneur.2020.00174

# Ripples Have Distinct Spectral Properties and Phase-Amplitude Coupling With Slow Waves, but Indistinct Unit Firing, in Human Epileptogenic Hippocampus

*Shennan A. Weiss[1], Inkyung Song[1], Mei Leng[2], Tomás Pastore[3], Diego Slezak[3], Zachary Waldman[1], Iren Orosz[4], Richard Gorniak[5], Mustafa Donmez[1], Ashwini Sharan[6], Chengyuan Wu[6], Itzhak Fried[7], Michael R. Sperling[1], Anatol Bragin[4], Jerome Engel Jr.[4,8,9,10], Yuval Nir[11] and Richard Staba[4]**

[1] Department of Neurology and Neuroscience, Thomas Jefferson University, Philadelphia, PA, United States, [2] Department of Medicine, Statistics Core, David Geffen School of Medicine at UCLA, Los Angeles, CA, United States, [3] Department of Computer Science, University of Buenos Aires, Buenos Aires, Argentina, [4] Department of Neurology, David Geffen School of Medicine at UCLA, Los Angeles, CA, United States, [5] Department of Neuroradiology, Thomas Jefferson University, Philadelphia, PA, United States, [6] Department of Neurosurgery, Thomas Jefferson University, Philadelphia, PA, United States, [7] Department of Neurosurgery, David Geffen School of Medicine at UCLA, Los Angeles, CA, United States, [8] Department of Neurobiology, David Geffen School of Medicine at UCLA, Los Angeles, CA, United States, [9] Department of Psychiatry and Biobehavioral Sciences, David Geffen School of Medicine at UCLA, Los Angeles, CA, United States, [10] Brain Research Institute, David Geffen School of Medicine at UCLA, Los Angeles, CA, United States, [11] Department of Physiology and Pharmacology, Sackler School of Medicine and Sagol School of Neuroscience, Tel Aviv University, Tel Aviv-Yafo, Israel

OPEN ACCESS

**Edited by:**
*Maeike Zijlmans, University Medical Center Utrecht, Netherlands*

**Reviewed by:**
*Stiliyan Nikolov Kalitzin, Epilepsy Institutions Netherlands Foundation, Netherlands*
*Pierre-Pascal Lenck-Santini, Institut National de la Santé et de la Recherche Médicale (INSERM), France*

***Correspondence:**
*Richard Staba*
*rstaba@mednet.ucla.edu*

**Specialty section:**
*This article was submitted to Epilepsy, a section of the journal Frontiers in Neurology*

**Received:** *24 November 2019*
**Accepted:** *24 February 2020*
**Published:** *24 March 2020*

**Citation:**
*Weiss SA, Song I, Leng M, Pastore T, Slezak D, Waldman Z, Orosz I, Gorniak R, Donmez M, Sharan A, Wu C, Fried I, Sperling MR, Bragin A, Engel J Jr, Nir Y and Staba R (2020) Ripples Have Distinct Spectral Properties and Phase-Amplitude Coupling With Slow Waves, but Indistinct Unit Firing, in Human Epileptogenic Hippocampus. Front. Neurol. 11:174. doi: 10.3389/fneur.2020.00174*

Ripple oscillations (80–200 Hz) in the normal hippocampus are involved in memory consolidation during rest and sleep. In the epileptic brain, increased ripple and fast ripple (200–600 Hz) rates serve as a biomarker of epileptogenic brain. We report that both ripples and fast ripples exhibit a preferred phase angle of coupling with the trough-peak (or On-Off) state transition of the sleep slow wave in the hippocampal seizure onset zone (SOZ). Ripples on slow waves in the hippocampal SOZ also had a lower power, greater spectral frequency, and shorter duration than those in the non-SOZ. Slow waves in the mesial temporal lobe modulated the baseline firing rate of excitatory neurons, but did not significantly influence the increased firing rate associated with ripples. In summary, pathological ripples and fast ripples occur preferentially during the On-Off state transition of the slow wave in the epileptogenic hippocampus, and ripples do not require the increased recruitment of excitatory neurons.

**Keywords: sleep, high-frequency oscillation, slow wave, epilepsy, hippocampus, ripple, fast ripple**

## INTRODUCTION

In the epileptic brain, ripple oscillations (80–200 Hz) exhibit increased rates in epileptogenic mesial-temporal regions (1, 2). In the normal brain, ripples are important in memory consolidation during rest and sleep (3). Neocortical ripples during the trough-peak (or On-Off) state transition of the non-rapid eye movement (NREM) sleep slow wave are found at a higher density in epileptogenic tissue and are considered pathological (4–6) (**Figures 1A,B**). In the epileptogenic

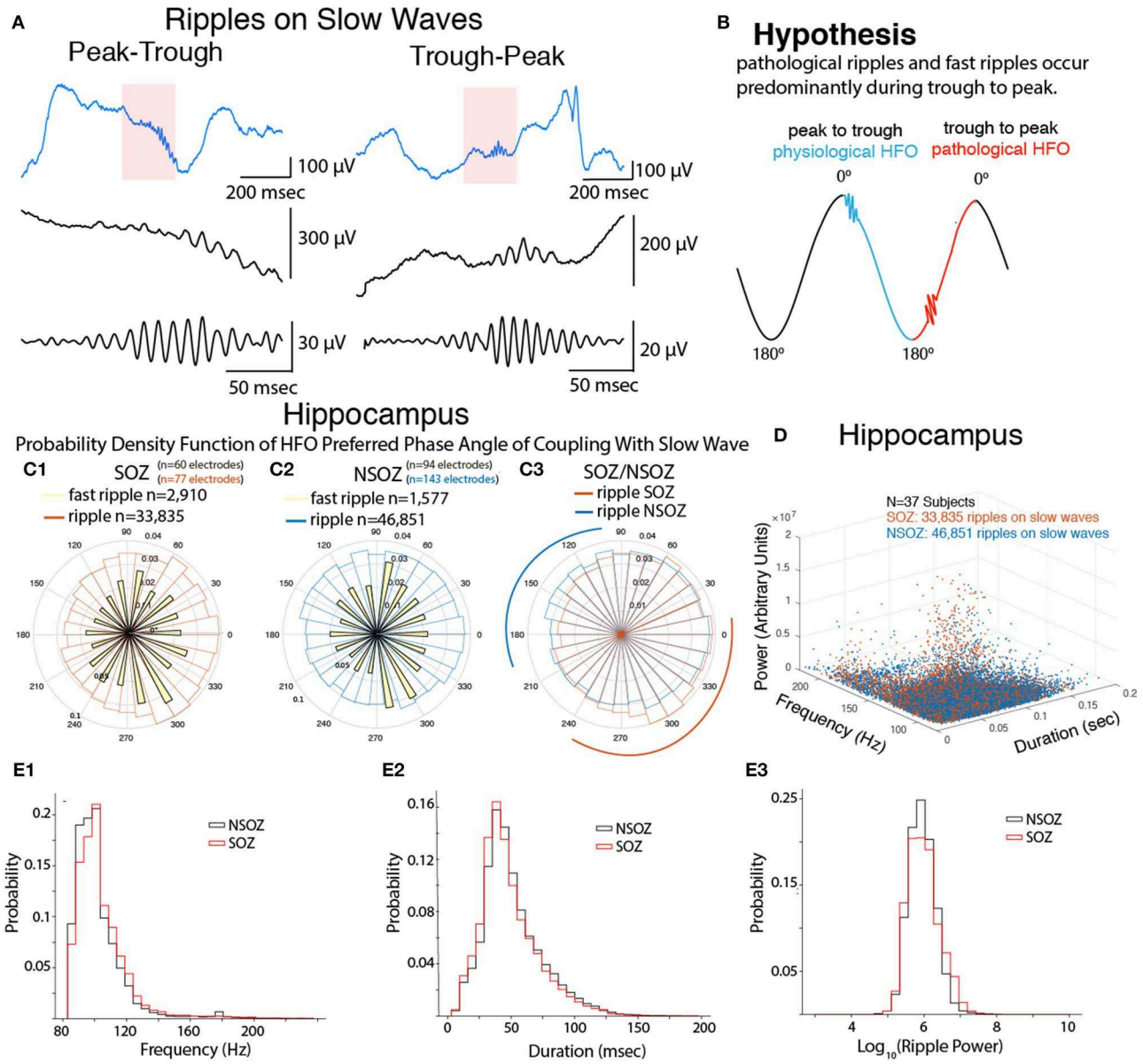


**FIGURE 1 |** Fast ripples and ripples in the hippocampal seizure-onset zone (SOZ) are coupled with the trough-peak of the slow wave and exhibit distinct properties. **(A)** Example of ripples on slow waves during the peak-trough (or Off-On; left) and trough-peak (or On-Off; right) transition, (middle) ripples at an expanded time scale, (bottom) band-pass filtered ripples. **(B)** Illustration of main hypothesis pathological ripples and fast ripples preferentially occur during the trough-peak transition of the slow wave. **(C)** Normalized circular histogram [i.e., probability density function(PDF)] of fast ripple (yellow) and ripple [SOZ: red, non-SOZ(NSOZ): blue] preferred phase angle of coupling with respect to the slow wave measured in the SOZ **(C1)** and NSOZ **(C2)**. A direct comparison of ripple preferred phase angle of coupling in the SOZ and NSOZ is shown in **(C3)** where arcs represent regions where the SOZ PDF exceed the NSOZ PDF (red) and vice versa (blue). **(D)** Three dimensional scatter plot of ripple on slow wave properties in the SOZ (red) and NSOZ (blue). **(E)** Normalized histogram of the ripple on slow wave properties in the SOZ (red) and NSOZ (black).

mesial temporal lobe, however, it is not clear if specific phases of the slow wave are associated with the generation of pathological ripples or fast ripples (200–600 Hz) (7, 8).

In the normal rat hippocampus CA1, ripples superimpose on sharp waves (<3 mV, 30–150 ms duration), which have the largest negative polarity in stratum radiatum and positive polarity in stratum pyramidale and oriens (9). Ripples are associated with a 5- to 6-fold increase in stratum pyramidale principal cell firing and 2- to 3-fold increase in stratum pyramidale and oriens non-principal firing. Both cell types discharge during the ripple trough, but non-principal cell firing is shifted a half-cycle with respect to principal cell discharges (10–12). Normal ripples are involved with memory consolidation and generated preferentially during the Off-On transition of the neocortical slow wave (13).

In the rat epileptogenic hippocampus, ripples can superimpose on interictal spikes (>4 mV, <30 ms) or on interictal spikes that have a positive polarity in stratum radiatum and negative polarity in stratum pyramidale and oriens (9, 14). Pathological ripples represent summated principal cell discharges with reduced non-principal firing (15–17) and could occur during On-Off transition of the slow wave.

Separating normal and pathological ripples in clinical studies, as in rat studies, would require electrodes with high spatial resolution, unit recordings, and precise anatomical localization of recording sites (18). This is not possible with clinical intracranial EEG (iEEG) electrodes, but these electrodes can record ripples during sleep slow waves and, combined with microelectrode recordings, could identify differences in EEG and unit firing that help to separate normal and pathological ripples. In the current study, we hypothesized that in the human epileptogenic hippocampus (i.e., seizure onset zone or SOZ), pathological ripples are generated during a preferred phase of the NREM sleep slow wave and involve a different level of principal cell firing than hippocampal ripples outside the SOZ. To evaluate this hypothesis, we analyzed iEEG and single unit recordings from the mesial temporal lobe of patients with drug-resistant focal epilepsy during NREM sleep.

# METHODS

iEEG recordings that contained large amplitude slow wave activity associated with NREM sleep were retrospectively collected from 37 patients with mesial temporal or neocortical focal epilepsy. All patients underwent intracranial monitoring with depth electrodes between 2014 and 2018 at the University of California Los Angeles (UCLA) and Thomas Jefferson University (TJU) for the purpose of localization of the SOZ (**Supplementary Table 1**). The inclusion criteria for this patient cohort were a minimum of 4 h of interictal EEG recorded overnight that contained NREM sleep lasting between 10 and 60 min, sampled at 1 or 2 kHz, and was relatively free of muscle artifact. The 4-h recording criterion was used to exclude pre-ictal, ictal, and post-ictal episodes and to ensure sufficient epochs of slow wave sleep.

A second patient cohort included iEEG and single unit recordings from Behnke-Fried hybrid macro-micro electrodes obtained from five patients with focal epilepsy at UCLA who were monitored between 2007 and 2010 (19). In this second cohort, each of the macroelectrodes contained eight 40 μm platinum-iridium microwires that were designed to extend 3–5 mm beyond the distal tip and record extracellular wide bandwidth (1–6,000 Hz), local field potentials (LFP), and neuronal spikes (**Supplementary Table 2**). Both cohorts consisted of patients with mesial-temporal lobe and neocortical epilepsy who had similar medical histories and clinical features. This retrospective study was approved by the UCLA and TJU institutional review boards. All patients gave informed consent prior to participating in this research.

## Data Acquisition

The UCLA recordings were referenced to scalp electrode Cz, and the TJU recordings were referenced to an iEEG electrode positioned in the white matter per clinical protocol. Local field potential recordings were referenced locally to a ninth non-insulated microwire and synchronized with the iEEG recordings using a TTL pulse (19). For these sleep study recordings the iEEG recordings were synchronized with EOG and EMG recordings and the iEEG signals were referenced to earlobe electrodes for accurate comparison with scalp recordings (19). These recordings were part of a prior, larger study that included analysis of neocortical slow waves (19). NREM sleep was characterized by the predominance of irregular, large amplitude EEG activity comprised of slow waves, K-complexes, and spindles. Clinical iEEG sleep recordings at both UCLA and TJU (0.016–600 Hz) were acquired from 7 to 16 contact depth electrodes using a Nihon-Kohden 256-channel JE-120 long-term monitoring system (Nihon-Kohden America, Foothill Ranch, CA, USA) for patient cohort one, and a stellate EEG amplifier (XLTEK, San Diego, CA, USA) for patient cohort two. LFP recordings were acquired using a Neuralynx Cheetah (Neualynx, Bozeman, MT, USA) at a sampling rate of 28/30 kHz and bandpass-filtered between 1 and 6,000 Hz (19).

## Neuroimaging

The positions of surface and depth electrode contacts were obtained for all subjects from post-implantation computed tomography (CT) scans. Pre-implantation volumetric T1-weighted magnetic resonance imaging (MRI) scans were co-registered to the CT scans as well as to the Montreal Neurological Institute 152 (MNI152) standard brain to enable comparison of recording sites in a common space across subjects. Anatomic locations of the recording sites were derived by converting MNI coordinates to Talairach coordinates and querying the Talairach daemon. The SOZ was defined by visual inspection of ictal iEEG by clinicians at each of the data collection sites.

## Slow Wave-HFO Detection and Quantification

All iEEG recordings were imported from EDF format into Matlab v2017b (Natick, MA, USA). Subsequent processing steps for those recordings from macroelectrodes deemed suitable on the basis of visual inspection using Micromed™ Brainquick™ (Veneto TV, Italy) were performed using custom software developed in Matlab. The custom software generated HFO and EEG spike annotations in Brainquick™ that could be used to visually validate the accuracy of the detector (20).

In brief, the HFO detector reduced muscle and electrode artifacts in the iEEG recordings using a custom independent component analysis (ICA)-based algorithm (21). After applying this ICA-based method, ripples were detected in the referential and bipolar montage iEEG recordings per contact by utilizing a Hilbert detector, in which (i) a 1,000th order symmetric finite impulse response (FIR) band-pass filter (80–600 Hz) was applied, and (ii) a Hilbert transform was applied to calculate the instantaneous amplitude of this time series according to the analytic signal z(t), described in Weiss et al. (20) and Shimamoto et al. (21).

$$z(t) = a(t)\, e^{\wedge} i\phi(t) \quad (1)$$

where a(t) is the instantaneous amplitude and ø(t) is the instantaneous phase of z(t). Following the Hilbert transform, (iii) the instantaneous HFO amplitude function [a(t)] was smoothed using moving window averaging, (iv) the smoothed instantaneous HFO amplitude function was normalized using the mean and standard deviation of the time series, and (v) a custom statistical threshold defined by the skewness of the normalized time series was used to detect the onset and offset of discrete/potential events.

HFO-like events can arise due to Gibb's phenomenon, i.e., high-pass filtering sharp transients, including epileptiform spikes. To distinguish authentic HFO during slow waves from authentic HFO on EEG spikes or spurious HFO due to filter ringing, we used a custom algorithm that performed topographic analysis of time-frequency plots for each HFO (22). The algorithm also measured the power, spectral content, and duration of each HFO. Both true HFO on EEG spikes and spurious HFOs were discarded from further analysis.

We identified ripple on slow wave (RoSW) events using the following approach. We first applied an optimized Hamming-windowed FIR band-pass filter between 0.1 and 2 Hz (eegfiltnew.m; EEGLAB, https://sccn.ucsd.edu/eeglab) to all the iEEG recordings optimally reducing phase distortion (6, 23). We then calculated the normalized instantaneous amplitude of the Hilbert transformed band-pass filtered signal (Equation 1). We used independent onset and offset normalized minimum amplitude (z-score) and duration criteria defined on the basis of visual inspection of the algorithm results to identify epochs in which slow oscillatory epochs appeared (6). After identifying the slow epochs, the corresponding epoch time stamps were used to classify the RoSW.

## Calculation of Ripple Phasors During Sleep Slow Wave

To assess phase-amplitude coupling we transformed each HFO into a HFO phasor (6), as described in Equation (2).

$$ve^{i\theta} = \sum_{t}^{T} a\,(t)\; e^{i\phi(t)} \tag{2}$$

where $v$ is the vector strength of the phasor, theta its preferred slow-wave phase angle, and $a(t)$ and $\phi(t)$ the respective instantaneous HFO amplitude iEEG slow wave phase during the ripple across its duration $[t{:}T]$, where $t$ is the onset of the HFO and $T$ is the offset. Thus, the preferred phase angle represents the mean phase angle of coupling between the ripple and slow wave.

## Single Unit Analysis

Extracellular action potentials were detected by high-pass filtering the microelectrode recordings above 300 Hz and applying a threshold at 5 SD above the median noise level (19). Detected events were categorized as noise, single-, or multi-unit activity using superparamagnetic clustering for unsupervised classification of each spike waveform (19). The stability of unit firing throughout the recording was assessed by inspecting the spike waveforms and inter-spike interval histograms. An inter-spike interval histogram with a clear refractory period of 2 ms or greater was considered a putative single unit; otherwise it was considered multiunit activity.

For each single unit mean action potential waveform we measured the peak amplitude asymmetry, a measurement of the relative differences in the peaks prior to and following the depolarizing spikes, the duration between the trough and the following peak, and half-width duration at half amplitude of the action potential waveform (19). We quantified single unit firing before, during, and after RoSW to generate binary vectors of the action potentials in 1-ms bins. For a 10 min episode of NREM sleep we computed the instantaneous phase value of the slow wave activity with respect to each action potential, and then repeated this analysis after removing action potentials associated with a ripple, i.e., action potentials within 250 ms a ripple. This interval surrounding the ripple was based on an analysis that found 47 ± 28% of all ripples occurred with an inter-ripple interval of <500 ms. Spike trains were smoothed with a 100 ms Gaussian kernel and then down-sampled to 100 Hz for comparison with ripples. A long-duration kernel was used because of the relatively sparse unit firing.

## Statistical Analysis

We used a non-linear, logistic mixed effects model to derive the probability for predicting the SOZ using the sin and cos of the slow-ripple phase angle and controlling for the following: duration, spectral frequency, and power of the ripple; and patient's gender, race, seizure type, seizure location, montage, reference electrode, risk factor, and MRI and PET findings. We used a log transformation on variables with non-normal distributions. Measures were clustered by patient by the random effect model. The analysis was stratified by anatomical location. $P$-values $<0.05$ were considered statistically significant. All analyses will be performed using SAS v. 9.4 (SAS Institute Inc., Cary, NC, USA).

A linear, mixed effects model in SAS v. 9.4 was used to analyze changes in firing rate during the slow-ripple events (ripple peak amplitude ±25 ms) with respect to baseline firing. Two sets of analyses were performed. The first considered trials clustered by unit then by patient using unit-within-patient nested random effects. In the second, units were clustered by electrode using electrode-within-patient nested random effects. The models controlled for location, spectral frequency and power of the ripples, slow wave-ripple coupling as defined by slow wave peak-trough or trough-peak distribution, and location within the SOZ (i.e., etiology). Similar models were used to test the baseline firing rate and the overall firing rate.

# RESULTS

We analyzed iEEG recordings during NREM sleep episodes from 37 patients with medically refractory epilepsy and electrodes implanted in the hippocampal gray matter (**Supplementary Table 1**). To examine if the phase of the slow wave correlates with the generation of fast ripples and ripples (**Figures 1A,B**) first we compared the probability density function (PDF) of the phase angles of coupling between fast ripples and slow waves (**Figure 1C1**), and the PDF of ripples

and slow waves in the seizure onset zone (SOZ, **Figure 1C1**). Fast ripples were phase locked with the slow wave (Rayleigh's test, $Z = 33.4$, $p <$ 1e-9) at a mean phase angle of 334 ± 121° and a maxima of 310° [trough-peak]. Ripples also exhibited strong phase locking with the slow wave ($Z = 418$, $p <$ 1e-9) at a mean phase angle of 356 ± 121° and a maxima at 310° (**Figure 1C1**). By comparison, fast ripples in the NSOZ were not nearly as strongly phase locked as those in the SOZ (**Figure 1C2**, Rayleigh's test, $Z = 9.16$, $p =$ 1e-4). The mean phase angle for fast ripples in the NSOZ was 19 ± 130° and the maxima was 290° (**Figure 1C2**). Ripples in the NSOZ were strongly phase locked to the slow wave but not as strong as in the SOZ ($Z = 176$, $p <$ 1e-9), and at a different mean phase angle of 42 ± 140° and maxima of 10° (**Figure 1C2**).

Next, we compared ripples in the SOZ to those in the NSOZ (**Figure 1C3**). The PDF for ripples in the SOZ indicated ripples were more likely to occur between 240 and 10° [trough-peak] of the slow wave, whereas in the NSOZ ripples were more likely to occur between 90 and 200° [peak-trough] of the slow wave (**Figure 1C3**). A comparison of the ripple phase angles in the SOZ and NSOZ using both circular statistical methods (Kuiper's $p < 0.001$) and a logistic regression model (LRM, $p < 0.0001$) confirmed that the phase angles for ripple-slow wave coupling in the SOZ and NSOZ were distinct. The remaining analyses focused on ripples since, unlike fast ripples, they support physiological functions such as memory consolidation during sleep in the hippocampus, and our objective was to distinguish physiological from pathological ripples.

We hypothesized that ripples on slow waves (RoSW) in the SOZ would have different spectral frequency, power, and duration than those in the NSOZ because pathological ripples with distinct properties should be over expressed in the SOZ. Analysis of these properties revealed an overlap of values between RoSW in the SOZ and NSOZ (**Figures 1D,E**). In spite of the overlap, however, the LRM found RoSW in the hippocampus SOZ had a higher spectral frequency (**Figure 1E1**, $p < 0.001$), shorter duration (**Figure 1E2**, $p < 0.005$), and lower power (**Figure 1E3**, $p < 0.005$) than those recorded in the NSOZ. As predicted by the LRM, there were more RoSW between 90 and 200° (peak-trough) transition with lower spectral content (**Figure 2C**), a longer duration (**Figure 2A**), and greater power (**Figure 2B**) in the NSOZ than in the SOZ (**Figure 2**). Other factors in the LRM, such as recording montage (referential or bipolar), electrode reference, and clinical metadata, did not affect these results.

Evidence suggests slow waves modulate unit firing and, in the hippocampus, RoSW could have a stronger effect on unit firing both in the SOZ and, possibly, remote brain areas. To evaluate unit firing modulation, we analyzed slow waves and ripples recorded from the most distal contact on the macroelectrode and single unit firing from the adjacent microelectrode during NREM sleep from five patients with medically refractory epilepsy (**Supplementary Table 2**). We isolated 59 (39 in SOZ and 20 in NSOZ) putative excitatory and one inhibitory single unit on the basis of waveform morphology and firing rate characteristics from 430 min of

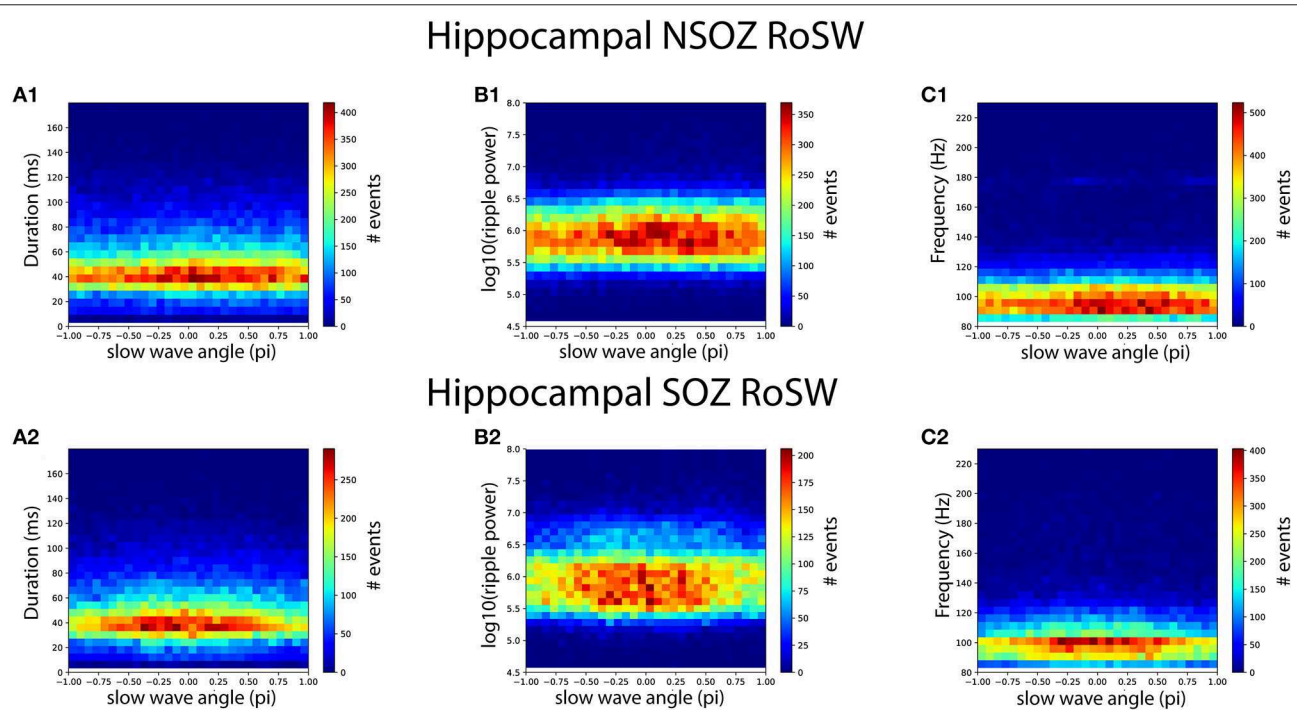


**FIGURE 2 |** Longer duration, higher power, lower spectral content ripples on slow waves (RoSW) during the peak-trough transition were more frequent in the hippocampal non-seizure onset zone (NSOZ) than the SOZ. Histograms quantifying the number of RoSW events binned by **(A1,A2)** duration, **(B1,B2)** spectral power, and **(C1,C2)** spectral frequency and by the phase angle of coupling recorded from the NSOZ (top row) and the SOZ (bottom row).

sleep recorded in these 5 patients from hippocampal and extra-hippocampal structures.

First we analyzed unit firing modulation during all slow wave activity and then repeated the analysis after removing action potentials associated with ripples (see section Methods). For the 39 neurons in the SOZ, unit firing was strongly modulated by the slow wave ($Z = 45.4$, $p <$ 1e-9) and the highest firing probability was at a mean phase angle of 332 ± 80° ($n =$ 109,559). After ripple-related (i.e., ± 250 ms) action potentials were removed the modulation of unit firing remained, but the magnitude was lower ($Z = 26.6$, $p <$ 1e-9) and the mean phase angle was similar (357 ± 80°; $n =$ 76,158). For the 20 neurons in the NSOZ, unit firing was also modulated by the slow wave, but the magnitude was much lower than in the SOZ ($Z = 12.6$, $p < 0.001$) and the highest firing probability shifted to 25 ± 80° ($n =$ 38,019). After removing ripple-related action potentials, unit firing modulation decreased ($Z = 9.74$, $p < 0.001$) but the mean phase angle was similar (50 ± 80°; $n =$ 28,080).

Next, we examined the firing rate from all of the excitatory single units during RoSW using a linear mixed-effects model. The lone inhibitory unit precluded any meaningful analysis of this cell type. We found that all 59 excitatory single units firing increased at the time of the RoSW ($n =$ 62,040 RoSW, $p < 0.001$, **Figure 3A**). Moreover, the increase in the excitatory neuron firing rate correlated with greater iEEG RoSW power ($F =$ 41.26, $p < 0.001$, **Figure 3A1**) and was dependent on unit identity (i.e., unit number, $p < 0.005$). Neither the location of the unit nor the SOZ had an effect on excitatory firing, demonstrating that individual single units had diverse firing properties during the local RoSW. Thirteen out of fifty-nine of the units (22%) consistently fired during each RoSW recorded by the macroelectrode.

Similar to hippocampal RoSW in the larger cohort of patients, ripples occurred during all phase angles of the slow wave irrespective of the neuroanatomic location of the macroelectrode. Thus, for the next analysis, we separated RoSW in to two distributions, labeled Dist1 and Dist2, based on the phase-amplitude coupling results illustrated in **Figure 1C3**. Dist1 consisted of RoSW during the trough-peak (250–70°) transition and Dist2 were RoSW during the peak-trough (70–250°) transition (**Figure 3B**). The axis was shifted slightly to reflect the deviation evident in the data. Analysis found an increase in spike firing during RoSW with respect to baseline that was similar for Dist1 and Dist2 ($p =$ 0.11, **Figure 3C**). Neither the neuroanatomical location of the single unit nor the location of the SOZ had an effect on excitatory unit firing during the RoSW ($p > 0.05$).

Lastly, the firing rate of the excitatory single units preceding and following RoSW (±500 ms) was significantly greater in Dist1 than in Dist2 ($p < 0.001$, **Figure 3C**), as expected based on the robust change in firing rates associated with different phases of slow wave activity (19). The increased baseline firing rate of excitatory single units for RoSW in Dist1 was not significantly correlated with the neuroanatomical location of the excitatory single unit ($p > 0.05$) or the location of the SOZ ($p > 0.05$).

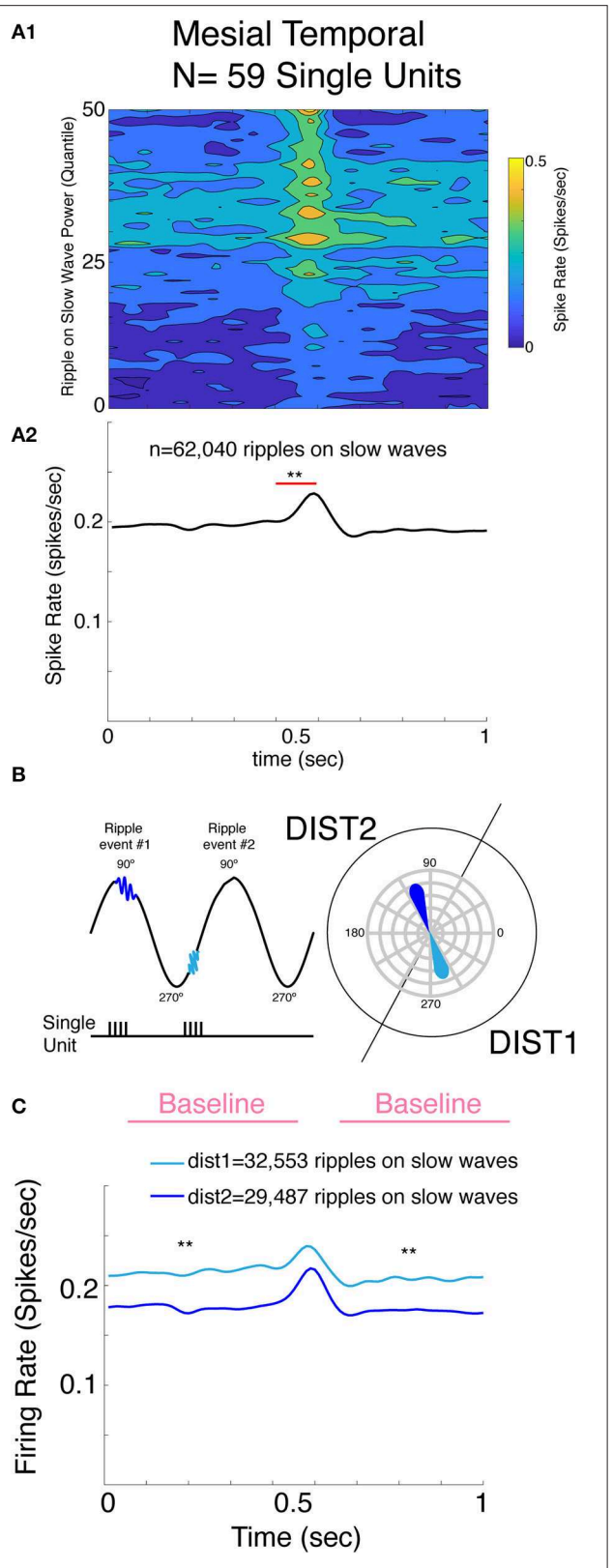


**FIGURE 3 |** Mesial temporal lobe single unit spiking increases proportional to the RoSW power recorded from the adjacent macroelectrode, and units are

*(Continued)*

**FIGURE 3 |** only weakly modulated by the On and Off state. **(A)** Mesial temporal single unit spike rates increased around RoSW onset ($p < 0.001$, **A1,A2**). The increase in firing was proportional to the power of the RoSW recorded by the macroelectrode ($p < 0.001$, **A1**). **(B)** Illustration of derivation of single unit firing on the unit circle and definition of distribution 1 (DIST1) and DIST2. Note the two RoSW events and corresponding phasors on the unit circle. **(C)** Baseline mesial temporal single unit spike rate was greater for RoSW in DIST1 (cyan) than RoSW in DIST2 (blue, $p < 0.001$). However, the increase in the firing rate during the ripple with respect to the baseline firing was not statistically different. $^{**}p < 0.001$.

## DISCUSSION

We show in the hippocampal SOZ and NSOZ, fast ripples occur preferentially during the trough-peak or On-Off state transition of the slow wave. In the SOZ, RoSW also have a higher probability of coupling during the On-Off state, but in the NSOZ, RoSW are more likely to couple during the Off-On state transition. The wide range of phase angles associated with RoSW could be due to a mixture of pathological and normal ripples in epileptogenic and irritative tissue (1–3). Hippocampal RoSW during the On-Off state transition found here is consistent with results of neocortical RoSW in prior studies that show that ripples in the SOZ or resected regions are more likely to be coupled to the On-Off state, whereas ripples in healthy brain regions are more likely to be coupled to the Off-On state (4–6). These results may signify that the On-Off transition provides a more powerful depolarizing volley that promotes their generation (19).

The mechanisms responsible for ripple and fast ripple coupling with the slow wave were not fully elucidated in this study. The increase in excitatory single unit firing was similar for RoSW during the Off-On and the On-Off transition, but ripples during the On-Off transition had higher background firing rates. It is unlikely ripples alone could explain differences in background firing since removal of ripple-related firing only reduced, but did not eliminate, firing modulation. Rather, unit firing is also modulated by the slow wave and the fact that modulation of excitatory unit firing was stronger in the SOZ could be one factor contributing to the generation of pathological ripples.

Overall, only a minority of recorded neurons participated in ripple generation as reflected by the weak, yet significant, modulation (24). Interestingly, recent work in epileptic rats found pathological ripples recruit fewer neurons than ripples in healthy rats (25). Thus, in patients with epilepsy, pathological ripples might also recruit fewer neurons than normal ripples. This concept is inconsistent with a prior report (26) and what would be expected during fast ripples (15). However, in support of this concept, we found hippocampal ripples in the SOZ had lower spectral power and higher spectral frequency than ripples in the NSOZ, and spectral power was proportional to the increase in excitatory neuron firing (27). Fast ripples and unit firing were not studied here due to the challenges of isolating single unit waveforms during the fast ripple field potential, which represents population spikes consisting of summated neuronal spikes (15). Our results of RoSW in the NSOZ recapitulate other studies of normal hippocampal ripples on sharp waves that occur preferentially during the Off-On state transition (13). We also found longer duration ripples in the NSOZ than in the SOZ, which is consistent with the results from others (28).

In clinical epilepsy, the hippocampus may not be the ideal location to utilize slow wave phase-amplitude coupling to distinguish normal from pathological ripples (5). One reason may be that local slow waves propagate throughout the mesial temporal lobe and only moderately influence baseline firing rate (19). Another could be the architecture of the hippocampus and non-orthogonal orientation of the electrodes in relation to the cell layers and dipole generators. This could increase variability between patients and the slow wave On-Off state transition. Despite these technical issues, quantifying phase-amplitude coupling between slow waves and fast ripples has been shown to correlate with severity of epileptogenicity in patients with epileptic spasms (29), and our study suggests that these measures could also assist in surgical planning for mesial-temporal lobe epilepsy. RoSW phase-amplitude coupling may also assist researchers in identifying physiological ripples associated with memory encoding, consolidation, and recall in the human hippocampus. Our results are similar to those from human memory studies and suggest phase-amplitude could provide additional information for identifying physiological ripples in the human hippocampus (30).

## DATA AVAILABILITY STATEMENT

The raw data supporting the conclusions of this article will be made available by the authors, without undue reservation, to any qualified researcher.

## ETHICS STATEMENT

The studies involving human participants were reviewed and approved by UCLA and TJU. The patients/participants provided their written informed consent to participate in this study.

## AUTHOR CONTRIBUTIONS

SW, IS, and RS conceived and designed the experiments. AS, CW, and IF performed the experiments, the remainder of the authors analyzed the data. SW and RS wrote the manuscript.

## FUNDING

SW was supported by the NIH/NINDS awards 1K23NS094633-01A1 and 1K23NS094633-02A1, and a Junior Investigator Award from the American Epilepsy Society. RS was supported by NINDS award 5R01NS106957-02.

## SUPPLEMENTARY MATERIAL

The Supplementary Material for this article can be found online at: https://www.frontiersin.org/articles/10.3389/fneur.2020.00174/full#supplementary-material

## REFERENCES


1. Jacobs J, LeVan P, Chander R, Hall J, Dubeau F, Gotman J. Interictal high-frequency oscillations (80-500 Hz) are an indicator of seizure onset areas independent of spikes in the human epileptic brain. *Epilepsia*. (2008) 49:1893–907. doi: 10.1111/j.1528-1167.2008.01656.x
2. Jacobs J, Banks S, Zelmann R, Zijlmans M, Jones-Gotman M, Gotman J. Spontaneous ripples in the hippocampus correlate with epileptogenicity and not memory function in patients with refractory epilepsy. *Epilepsy Behav*. (2016) 62:258–66. doi: 10.1016/j.yebeh.2016.05.025
3. Axmacher N, Elger CE, Fell J. Ripples in the medial temporal lobe are relevant for human memory consolidation. *Brain J Neurol.* (2008) 131:1806–17. doi: 10.1093/brain/awn103
4. Frauscher B, von Ellenrieder N, Ferrari-Marinho T, Avoli M, Dubeau F, Gotman J. Facilitation of epileptic activity during sleep is mediated by high amplitude slow waves. *Brain J Neurol.* (2015) 138:1629–41 doi: 10.1093/brain/awv073
5. von Ellenrieder N, Frauscher B, Dubeau F, Gotman J. Interaction with slow waves during sleep improves discrimination of physiologic and pathologic high-frequency oscillations (80-500 Hz). *Epilepsia*. (2016) 57:869–78. doi: 10.1111/epi.13380
6. Song I, Orosz I, Chervoneva I, Waldman ZJ, Fried I, Wu C, et al. Bimodal coupling of ripples and slower oscillations during sleep in patients with focal epilepsy. *Epilepsia.* (2017) 58:1972–84. doi: 10.1111/epi.13912
7. Clemens Z, Mölle M, Eross L, Barsi P, Halász P, Born J. Temporal coupling of parahippocampal ripples, sleep spindles and slow oscillations in humans. *Brain*. (2007) 130:2868–78. doi: 10.1093/brain/awm146
8. Staresina BP, Bergmann TO, Bonnefond M, van der Meij R, Jensen O, Deuker L, et al. Hierarchical nesting of slow oscillations, spindles and ripples in the human hippocampus during sleep. *Nat Neurosci.* (2015) 18:1679–86. doi: 10.1038/nn.4119
9. Buzsáki G. Hippocampal sharp waves: their origin and significance. *Brain Res.* (1986) 398:242–52. doi: 10.1016/0006-8993(86)91483-6
10. Csicsvari J, Hirase H, Czurkó A, Mamiya A, Buzsáki G. Fast network oscillations in the hippocampal CA1 region of the behaving rat. *J Neurosci.* (1999) 19:RC20. doi: 10.1523/JNEUROSCI.19-16-j0001.1999
11. Buzsáki G, Horváth Z, Urioste R, Hetke J, Wise K. High-frequency network oscillation in the hippocampus. *Science*. (1992) 256:1025–7. doi: 10.1126/science.1589772
12. Ylinen A, Bragin A, Nádasdy Z, Jandó G, Szabó I, Sik A, et al. Sharp wave-associated high-frequency oscillation (200 Hz) in the intact hippocampus: network and intracellular mechanisms. *J Neurosci.* (1995) 15:30–46. doi: 10.1523/JNEUROSCI.15-01-00030.1995
13. Isomura Y, Sirota A, Ozen S, Montgomery S, Mizuseki K, Henze DA, et al. Integration and segregation of activity in entorhinal-hippocampal subregions by neocortical slow oscillations. *Neuron.* (2006) 52:871–82. doi: 10.1016/j.neuron.2006.10.023
14. Buzsáki G, Hsu M, Slamka C, Gage FH, Horváth Z. Emergence and propagation of interictal spikes in the subcortically denervated hippocampus. *Hippocampus*. (1991) 1:163–80. doi: 10.1002/hipo.450010205
15. Bragin A, Benassi SK, Kheiri, F, Engel J Jr. Further evidence that pathologic high-frequency oscillations are bursts of population spikes derived from recordings of identified cells in dentate gyrus. *Epilepsia.* (2011) 52:45–52. doi: 10.1111/j.1528-1167.2010.02896.x
16. Bragin A, Wilson CL, Almajano J, Mody I, Engel J Jr. High-frequency oscillations after status epilepticus: epileptogenesis and seizure genesis. *Epilepsia*. (2004) 45:1017–23. doi: 10.1111/j.0013-9580.2004.17004.x
17. Engel J Jr, Bragin A, Staba R, Mody I. High-frequency oscillations: what is normal and what is not? *Epilepsia*. (2009) 50:598–604. doi: 10.1111/j.1528-1167.2008.01917.x
18. Buzsáki G. Hippocampal sharp wave-ripple: a cognitive biomarker for episodic memory and planning. *Hippocampus*. (2015) 25:1073–188. doi: 10.1002/hipo.22488
19. Nir Y, Staba RJ, Andrillon T, Vyazovskiy VV, Cirelli C, Fried I, et al. Regional slow waves and spindles in human sleep. *Neuron*. (2011) 70:153–69. doi: 10.1016/j.neuron.2011.02.043
20. Weiss SA, Berry B, Chervoneva I, Waldman Z, Guba J, Bower M, et al. Visually validated semi-automatic high-frequency oscillation detection aides the delineation of epileptogenic regions during intra-operative electrocorticography. *Clin Neurophysiol.* (2018) 129:2089–98. doi: 10.1016/j.clinph.2018.06.030
21. Shimamoto S, Waldman ZJ, Orosz I, Song I, Bragin A, Fried I, et al. Utilization of independent component analysis for accurate pathological ripple detection in intracranial EEG recordings recorded extra- and intra-operatively. *Clin Neurophysiol.* (2018) 129:296–307. doi: 10.1016/j.clinph.2017.08.036
22. Waldman ZJ, Shimamoto S, Song I, Orosz I, Bragin A, Fried I, et al. A method for the topographical identification and quantification of high frequency oscillations in intracranial electroencephalography recordings. *Clin Neurophysiol.* (2018) 129:308–18. doi: 10.1016/j.clinph.2017.10.004
23. Widmann A, Schröger E, Maess B. Digital filter design for electrophysiological data–a practical approach. *J Neurosci Methods*. (2015) 30:34–46. doi: 10.1016/j.jneumeth.2014.08.002
24. Stark E, Roux L, Eichler R, Senzai Y, Royer S, Buzsáki G. Pyramidal cell-interneuron interactions underlie hippocampal ripple oscillations. *Neuron*. (2014) 83:467–80. doi: 10.1016/j.neuron.2014.06.023
25. Ewell LA, Fischer KB, Leibold C, Leutgeb S, Leutgeb JK. The impact of pathological high-frequency oscillations on hippocampal network activity in rats with chronic epilepsy. *Elife*. (2019) 8:e42148. doi: 10.7554/eLife.42148.025
26. Guragain H, Cimbalnik J, Stead M, Groppe DM, Berry BM, Kremen V, et al. Spatial variation in high-frequency oscillation rates and amplitudes in intracranial EEG. *Neurology*. (2018) 90:e639–46. doi: 10.1212/WNL.0000000000004998
27. Khodagholy D, Gelinas JN, Buzsáki G. Learning-enhanced coupling between ripple oscillations in association cortices and hippocampus. *Science.* (2017) 358:369–37. doi: 10.1126/science.aan6203
28. Fernández-Ruiz, A, Oliva A, Fermino de Oliveira E, Rocha-Almeida F, Tingley D, Buzsáki G. Long-duration hippocampal sharp wave ripples improve memory. *Science*. (2019) 364:1082–6. doi: 10.1126/science.aax0758
29. Iimura Y, Jones K, Takada L, Shimizu I, Koyama M, Hattori K, et al. Strong coupling between slow oscillations and wide fast ripples in children with epileptic spasms: investigation of modulation index and occurrence rate. *Epilepsia*. (2018) 59:544–54. doi: 10.1111/epi.13995
30. Vaz AP, Inati SK, Brunel N, Zaghloul KA. Coupled ripple oscillations between the medial temporal lobe and neocortex retrieve human memory. *Science*. (2019) 363:975–8. doi: 10.1126/science.aau8956


**Conflict of Interest:** SW is founder of Fastwave LLC, a Neurology software company. ZW and DS are cofounders and hold more than 5% equity interest in Fastwave LLC.

The remaining authors declare that the research was conducted in the absence of any commercial or financial relationships that could be construed as a potential conflict of interest.

*Copyright © 2020 Weiss, Song, Leng, Pastore, Slezak, Waldman, Orosz, Gorniak, Donmez, Sharan, Wu, Fried, Sperling, Bragin, Engel, Nir and Staba. This is an open-access article distributed under the terms of the Creative Commons Attribution License (CC BY). The use, distribution or reproduction in other forums is permitted, provided the original author(s) and the copyright owner(s) are credited and that the original publication in this journal is cited, in accordance with accepted academic practice. No use, distribution or reproduction is permitted which does not comply with these terms.*

frontiers in Neurology

ORIGINAL RESEARCH
published: 22 April 2020
doi: 10.3389/fneur.2020.00326

# High Frequency Oscillations in Rat Hippocampal Slices: Origin, Frequency Characteristics, and Spread

*Isaac Naggar*[1], *Mark Stewart*[2,3] *and Rena Orman*[3]*

[1] EEG Section, NINDS, National Institutes of Health, Bethesda, MD, United States, [2] Department of Neurology, State University of New York Downstate Medical Center, Brooklyn, NY, United States, [3] Department of Physiology and Pharmacology, State University of New York Downstate Medical Center, Brooklyn, NY, United States

Field potential oscillations reflect repetitive firing and synaptic activity by ensembles of neurons in certain areas of the brain. They can be distinguished as slow (e.g., alpha, delta, and theta), fast (e.g., beta and gamma), and high frequency oscillations (HFOs). Neuronal oscillations are involved in a variety of physiological and pathophysiological states such as cognition, consciousness, and seizures. The laminar structure of rat hippocampus affords a way to study these oscillations in hippocampal slices. Rat ventral hippocampal brain slices were cut and maintained in a recording chamber that permitted 64 simultaneous extracellular recordings in the presence of artificial CSF. Brief single stimulus pulses were applied with bipolar electrodes to the CA3 or CA1 regions of hippocampus. Single pulses triggered epileptiform population events that included HFOs in the 150–250 Hz range in the presence of $GABA_A$ receptor blockade or kainic acid. HFOs also occurred spontaneously in the presence of kainic acid. The oscillations had the largest amplitude in the CA3c cell layer, regardless of the drug, and were synchronized throughout the cell layer. AMPA receptor blockade stopped these HFOs, whereas NMDA receptor blockade did not. Gap junction activation did not restore HFOs in the presence of AMPA receptor blockade. Our findings suggest that a population of excitatory neurons in CA3c may be a primary focus of seizure-like activity in Ammon's Horn. We suggest that the interconnection of CA3c is different from the rest of CA3.

**Keywords: CA3c, ripples, very fast oscillations, bicuculline, kainic acid, carbenoxolone, gap junctions, electrode array**

OPEN ACCESS

***Edited by:***
*Johannes Sarnthein, University of Zurich, Switzerland*

***Reviewed by:***
*Massimo Avoli, McGill University, Canada*
*Pierre-pascal Lenck-Santini, Institut National de la Santé et de la Recherche Médicale (INSERM), France*

***Correspondence:**
*Rena Orman*
*rena.orman@downstate.edu*

***Specialty section:***
*This article was submitted to Epilepsy, a section of the journal Frontiers in Neurology*

***Received:*** *21 January 2020*
***Accepted:*** *03 April 2020*
***Published:*** *22 April 2020*

***Citation:***
*Naggar I, Stewart M and Orman R (2020) High Frequency Oscillations in Rat Hippocampal Slices: Origin, Frequency Characteristics, and Spread. Front. Neurol. 11:326. doi: 10.3389/fneur.2020.00326*

## INTRODUCTION

Field potential oscillations reflect synchronized rhythmic synaptic potentials and/or firing by populations of neurons. High frequency oscillations (HFOs), in some studies referred to as "ripples," exist in the 80–600 Hz range. It has been proposed that this broad frequency range reflects different kinds of activity, and recent reviews have outlined the possibilities for HFO generation involving synaptic and non-synaptic mechanisms as well as the challenges associated with identification of mechanism in brain (1, 2). HFOs can be observed in limbic structures and all over neocortex (3–6) in both pathologic contexts like seizures (7, 8) and in normal contexts such as cognition and sleep (9, 10). The oscillatory periods tend to be of shorter duration and amplitude on account of the neuronal synchrony necessary to achieve them (11).

Pathologic HFOs tend to be of higher frequency than physiologic HFOs (7) and are thought to be a feature of the seizure onset zone in patients with epilepsy (12, 13). HFOs of around 200 Hz have been described under normal conditions in the CA1 pyramidal cell layer of awake immobile rats.

Population bursts of the CA3 network occurring during eating, drinking, slow-wave sleep, and awake immobility are thought to be field excitatory post-synaptic potentials (EPSPs) that depolarize CA1 pyramidal cells via the Schaffer collaterals (10) and the dentate gyrus (14). These in turn are thought to produce the HFOs in the 200 Hz range in normal rats (9). The bursts of sinusoidal activity last 5 to 15 cycles with peak-to-peak amplitudes less than 500 microvolts (10).

Laminar profiles of these oscillations have shown that the oscillations restrict themselves to the pyramidal cell layer with almost no phase lag over 2 mm distance (15), even up to 5 mm in the rat (10). The ability to extend over this amount of space essentially shows there is an underlying network that must generate the oscillations, as it cannot arise from single neurons with propagation from cell to cell (16).

Two main hypotheses have been offered as the mechanism for these oscillations (1, 2). One is that there is a synaptic basis for the oscillations with both excitatory and inhibitory control (9, 15). The other hypothesis states that gap junctions are responsible for the oscillations (17, 18). A third and contributing theory posits there may be some role for local field effects in the amplitude of the oscillation (19).

Evidence supporting a synaptic mechanism has shown that the oscillations are related to variations in pyramidal cell and interneuron activity (20). High frequency 200 Hz oscillations within CA1 reflect synchronized IPSPs in the perisomatic region of CA1 pyramidal cells (15). The probability of pyramidal cell firing is greatest during the negative peaks of the oscillations, indicating a degree of excitatory synchrony. Thus, long-range inhibitory control superimposed over a depolarizing input can produce synchronized oscillations (10). In addition to high-density connection basket cells that produce local inhibition, long-range inhibitory control via interneurons with axonal length of 20 to 100 mm has been described (21). Evidence against the synaptic hypothesis includes the presence of 150–200 Hz oscillations in the absence of extracellular calcium ions, which are required for chemical synapses (17).

Evidence for the gap junction hypothesis includes abolition of the HFOs in the presence of gap junction blockers, including halothane, carbenoxolone, and octanol (17). However, multiple blockers have been used since specific gap junction blockade has not been achieved (22). Spontaneous HFOs have been shown to be less frequent in connexin 36-deficient mice (22). There is also evidence of electrical coupling between hippocampal principal cells (23–25), which suggests the presence of gap junctions. The oscillations are thought to arise via gap junctions between axons of pyramidal cells (18). In one study, gap junctions were identified in mossy fibers in CA3b (total of 10 axoaxonic pairs) and CA3c (one axoaxonic pair) using electron microscopy and immunogold labeling (26).

In a study of mouse brain slices, D'Antuono et al. (27) showed that HFOs occurred in slices disinhibited with picrotoxin, depended on non-NMDA glutamatergic receptors, did not depend on gap junction availability, and could occur in isolated dentate gyrus sub-slices. These authors did note that initiation of HFO/ripple activity appeared to be in either CA3 or entorhinal cortex, depending upon the particular slice being studied. These results point away from inhibitory circuits or gap junctions for HFO generation.

We sought to explore the origins of HFO in rat brain slices where would could apply 64-electrode array recordings to define the spatio-temporal distribution of high frequency oscillations and relate them to their inhibitory and excitatory controls.

## MATERIALS AND METHODS

All procedures were approved by the University's Animal Care and Use Committee and conform to NIH guidelines.

### Slice Preparation and Maintenance

Male Sprague-Dawley albino rats (150–200 g; 3–5 weeks old) were anesthetized with halothane and decapitated. Each brain was removed from the skull, bisected, and placed briefly in ice cold artificial CSF. Thick slices of tissue (about 1–2 mm thick) were cut horizontally from the intact hemispheres with its dorsal face at about the level of the hippocampal genu. These thick sections were mounted in a Leica VT1000S sectioning system (Leica; Nussloch, Germany), which was used to cut brain slices for physiological study (350–400 μm). Final slices were simple horizontal sections trimmed with a cut perpendicular to the midline on the rostral side of area CA3 and the level of the slices corresponded to a range of about 2.6–4.6 mm above the interaural line (28). Slices were maintained in a holding chamber containing oxygenated artificial cerebrospinal fluid (see below).

From the holding chamber, single slices were placed in the MED64 chamber (Panasonic MED64; Osaka, Japan). The MED64 chamber is a 22 mm diameter well formed from a plastic ring cemented to a glass base that contains the electrodes. Conductive strips embedded in the glass base terminate in platinum-platinum black electrodes that are nearly flush with the well floor. Flow is regulated such that slices are just below an interface configuration. The perfusion solution (1 ml/min) was composed of (in mM): NaCl 125, KCl 2.5 to 5, $CaCl_2$ 1.7, $MgCl_2$ 1.2, $NaHCO_3$ 26, and glucose 10; pH 7.4 when exposed to 95% $O_2$ and 5% $CO_2$. The temperature of the MED64 chamber was maintained at 30°C by warming the perfusate with an inline heater. The ventral horizontal slice preparation contains area CA1 and many of the surrounding areas, including: CA3, subiculum, presubiculum, and entorhinal cortex (29–31).

### Recording and Stimulating Techniques

The MED64 chamber allows simultaneous extracellular recordings from 64 electrodes (50 μm squares). Each electrode is a platinum black-plated square embedded in the floor of the recording chamber. Inter-electrode distances (center to center) were 100, 150, or 300 μm. Recording electrode impedances are 22 kΩ (at 1 kHz) and each is referred to a set of four reference electrodes in the periphery of the chamber that are electrically connected. The recording electrodes are arranged

in an 8 x 8 array embedded on the bottom of the chamber. Brief stimulating pulses were delivered using platinum-iridium parallel bipolar stimulating electrodes (150 μm tip separation; FHC; Bowdoinham, ME) with <100 kΩ electrode impedances. Stimuli were biphasic pulses (50–100 μs in total duration) applied to the CA3 or CA1 regions of hippocampus through constant current stimulus isolation units. The bipolar stimulating electrode was placed from the top side of the slice. Data were digitized at 20 kHz per channel and stored on disk using MED64 Conductor software. Events could be viewed offline using the MED64 Conductor software.

## Pharmacology

All drugs were applied to the bath by adding them to the perfusate reservoir. The concentrations given are concentrations that exist in the reservoir and were achieved in the recording chamber over a period of minutes. Recordings in the presence of all drugs were taken after sufficient time for equilibration in the recording chamber. Equilibration was apparent in recordings as a change in evoked response. Bicuculline (bicuculline methiodide; 50 μM), AP-5 (DL-(2)-2- amino-5-phosphonopentanoic acid; 40 μM), CPP (3 ((RS)-2-carboxypiperazin-4-yl)-propyl-1-phosphonic acid; 20 μM), carbenoxolone (100 μM) and CNQX (6-cyano-7-nitroquinoxaline-2,3-dione or 6-cyano-7-nitroquinoxaline-2,3-dione disodium; 20 μM), and trimethylamine (TMA; 4 mM) were obtained from Sigma (Sigma-Aldrich; St. Louis, MO). Kainic acid (15 nM) was obtained from Abcam (Cambridge, MA). Some batches of CNQX were obtained from Tocris Bioscience (Ellisville, MO). Bicuculline was used to antagonize $GABA_A$ receptors, and kainic acid was used as a kainate receptor agonist. AP-5 and CPP were used as NMDA receptor antagonists, and CNQX was used as an AMPA receptor antagonist. Carbenoxolone was used to block gap junctions and TMA was used to activate gap junctions.

## Data Analysis

Analysis of the electrode recordings was done using Matlab with the Signal Processing Toolbox (Mathworks; Natick, MA) as well as with the Joint Time-Frequency Analyzer software (National Instruments; Austin, TX).

Color spectrograms of raw data from individual recordings were made using the Joint Time Frequency Analyzer software. The recordings chosen were the ones with greatest amplitude oscillation, as found by using the Fast Fourier Transform (FFT). High frequency oscillations were noted to all be within the 150–250 Hz range, and beginning and end times of the oscillations

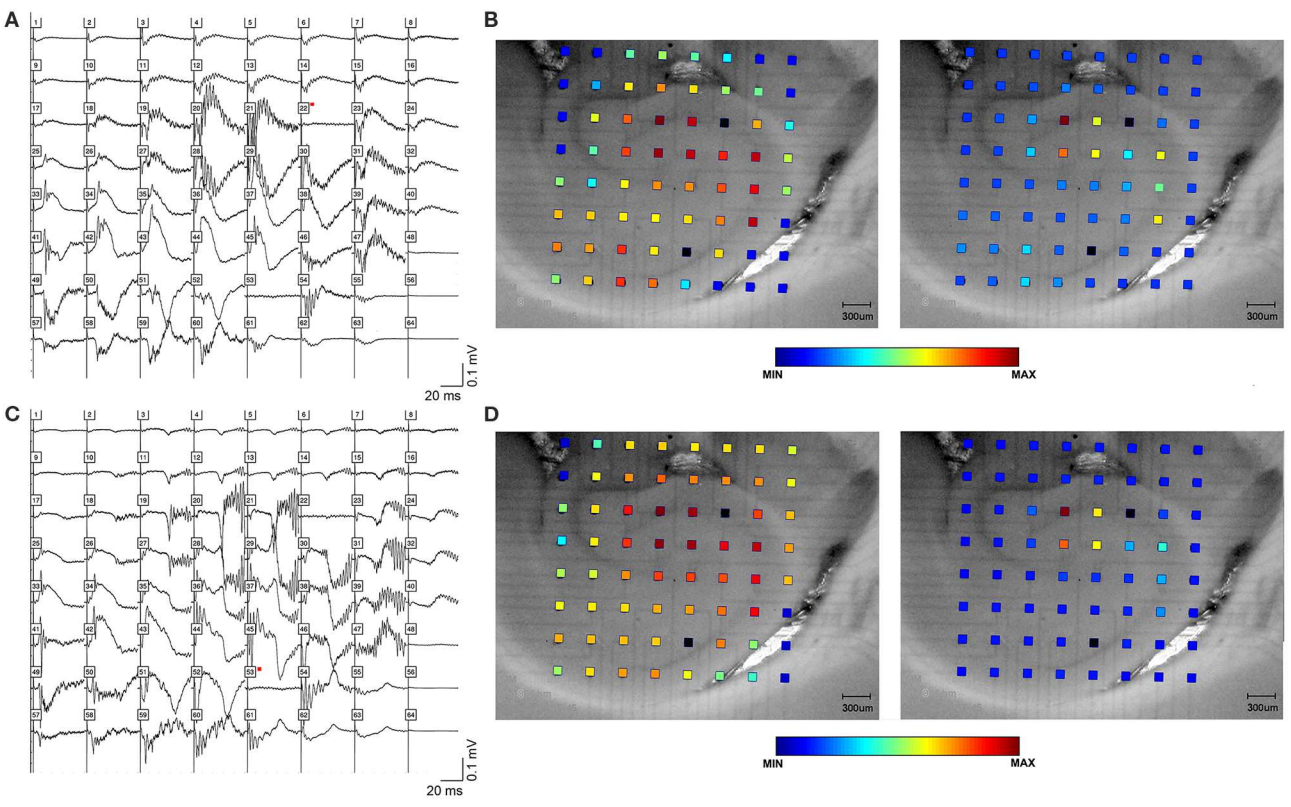


**FIGURE 1 |** High frequency oscillations in the presence of bicuculline. HFOs can be observed in rat hippocampal slices containing CA3, CA1, subiculum and dentate gyrus. **(A)** depicts field potentials evoked by a single stimulus pulse applied in area CA3 (black square in the cell layer). **(B)** Maximum amplitude and frequency were recorded in area CA3. The color grid indicates the exact location of recording electrodes. The dark red color of the calibration spectrum represents the maximum oscillation amplitude (right panel) and maximum log of the amplitude (left panel) for the CA3 stimulating site. **(C,D)** show the same oscillations, this time evoked by a single pulse applied at stimulating site in area CA1 (black square in the proximal stratum radiatum of mid-CA1, i.e., close to the cell layer).

were found using a set threshold amplitude within this range from instantaneous FFTs. The time of maximum oscillatory amplitude in the 150–250 Hz range was also located. In total, 20 slices (17 rats) with oscillations after application of bicuculline and 13 slices (10 rats) after application of kainic acid (all slices under electrical stimulation) were studied in this way. A total of 6 slices (4 rats) with kainic acid displayed spontaneous oscillations, and these were also analyzed in the same fashion.

The rest of the data analysis was conducted with Matlab. Descriptive statistics of each slice among all electrodes included (1) the time of greatest oscillatory activity, (2) the amplitude of the oscillation given by the power of the FFT, and (3) the frequency of the oscillatory activity. As a measure of sustainability of the oscillation, (4) the amount of time from greatest oscillatory activity to the end of the oscillation was calculated. For a given slice, the above parameters were calculated for each of the 64 channels over 8 representative sweeps, which could be found in a subset of the slices (An exception was made in 2 of the slices with spontaneous oscillations in kainic acid, for which only 5 or 6 events could be recorded). The results were subsequently averaged across the 8 sweeps for each channel. A series of short time Fourier transforms (STFTs) were calculated for each channel to identify the time of peak oscillatory activity in the high frequency oscillation frequency range. The presence of high frequency oscillations was determined with an amplitude threshold of the FFT in the HFO range that was initially verified manually as the absence of significant oscillation. The 13 ms of data before and after the calculated time were mean detrended, and the point at which the oscillations reached an absolute maximum in magnitude was taken to be the precise peak time of oscillations. The amplitude of the oscillations was determined as the amplitude of the FFT at that time. Alternatively, the voltage difference between the largest peak and valley of the oscillations was used as a measure of the amplitude of the oscillations; this was done to compare slices with bicuculline or kainic acid that had CPP or AP-5 added to them. To calculate the frequency, the three oscillations before and after the peak oscillatory time were located using a threshold-lockout algorithm and their frequency was averaged. The end oscillatory time was found by taking

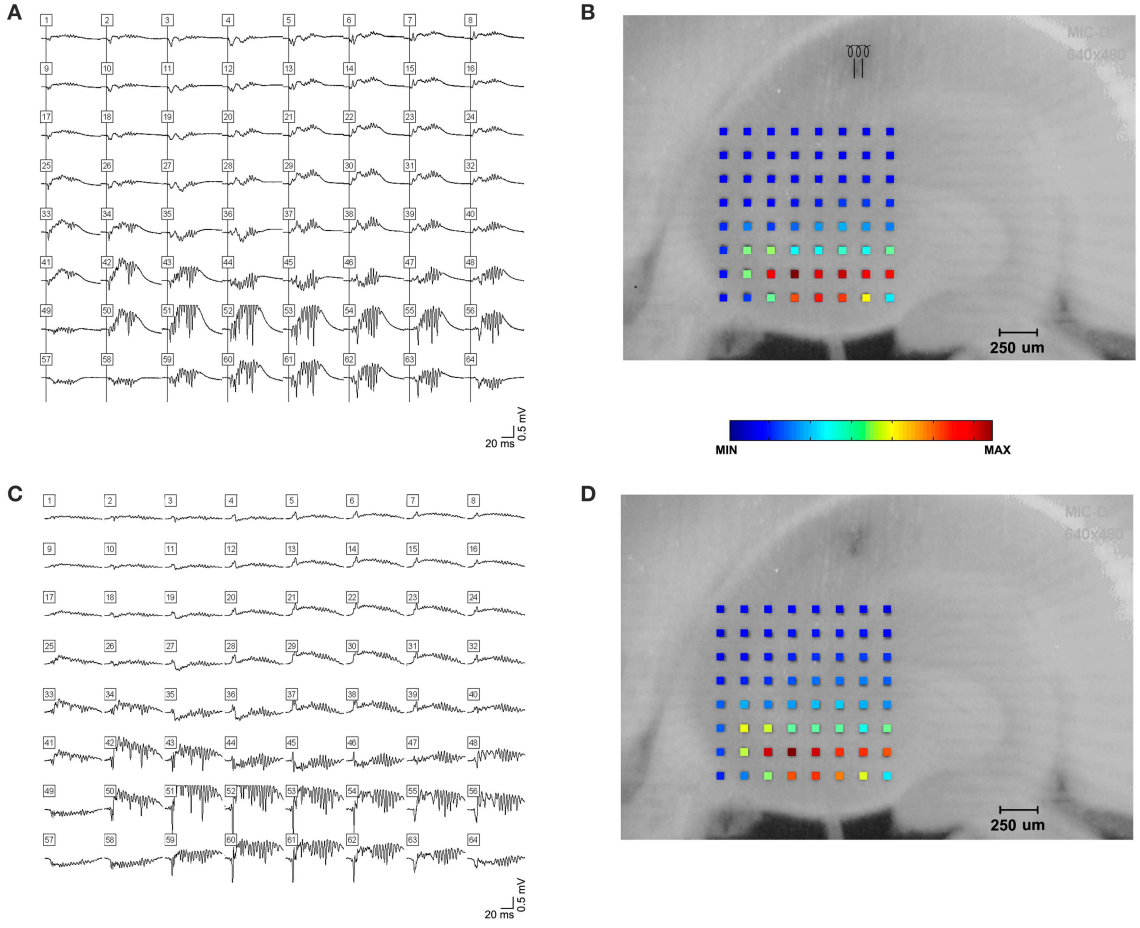


**FIGURE 2 |** High frequency oscillations in the presence of kainic acid. HFOs could be observed in rat hippocampal slices bathed in kainic acid. **(A)** shows field potentials evoked by a single stimulus pulse, which is shown in **(B)**. Stimulus electrode location is distal stratum radiatum in mid-CA1, i.e., away from the cell layer. Raw amplitude data is denoted by the color spectrum of the electrode grid. **(C,D)** demonstrate spontaneous high frequency oscillations in the presence of kainic acid.

consecutive FFTs after the peak oscillatory time and finding the first FFT over the 150–250 Hz range to return as below the set threshold.

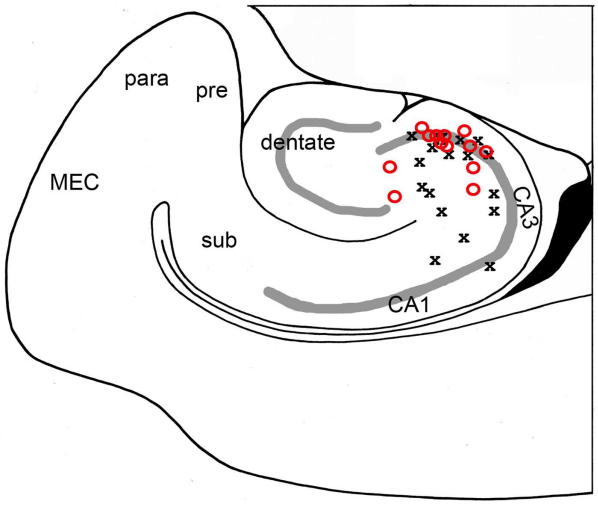


**FIGURE 3 |** High frequency oscillations are maximal in area CA3c. The channel with greatest oscillatory activity was found for each slice and correlated with its anatomical position. Both bicuculline- (red O; $N = 17$ slices) and kainic acid- (black X; $N = 13$ slices) treated slices showed maximal oscillatory in area CA3c, most notably in the cell layer.

The above methods could not be used for the slices to which kainic acid was applied, since some of them had their peak time too early in the sweep. Instead, the methods described below were used. Results from these calculations were validated by applying them to data from bicuculline-treated slices and comparing to existing calculations from the previous methods described. As with the slices in the bicuculline bath, calculations were averaged over 8 sweeps of the 64-channel data. Each sweep and channel had to have the beginning and end of oscillatory activity identified by hand after applying a band-stop filter of 0–70 Hz. The sum of the absolute value of the points between the selected points was taken as the full-wave rectified area under the curve. This value was divided by the length of time of oscillation to yield average amplitude, or intensity, of the oscillations. The peak time of oscillation was taken as the point at which the oscillation reached its maximum absolute value. The length of the oscillations from peak to end of the oscillations could then also be determined. The frequency of the oscillations was determined by taking the frequency with maximum amplitude in the FFT of the entire oscillatory period.

Color maps of oscillation intensity over all 64 electrodes were also made. These could be superimposed upon the slice images to appreciate the areas of greatest oscillatory activity. Depth profile plots of a single sweep were made by examining an electrode row or column of interest perpendicular to the cell layer. The signals from these channels were mean detrended, band-stop filtered (0–70 Hz), and subsequently plotted. The voltage at a specific

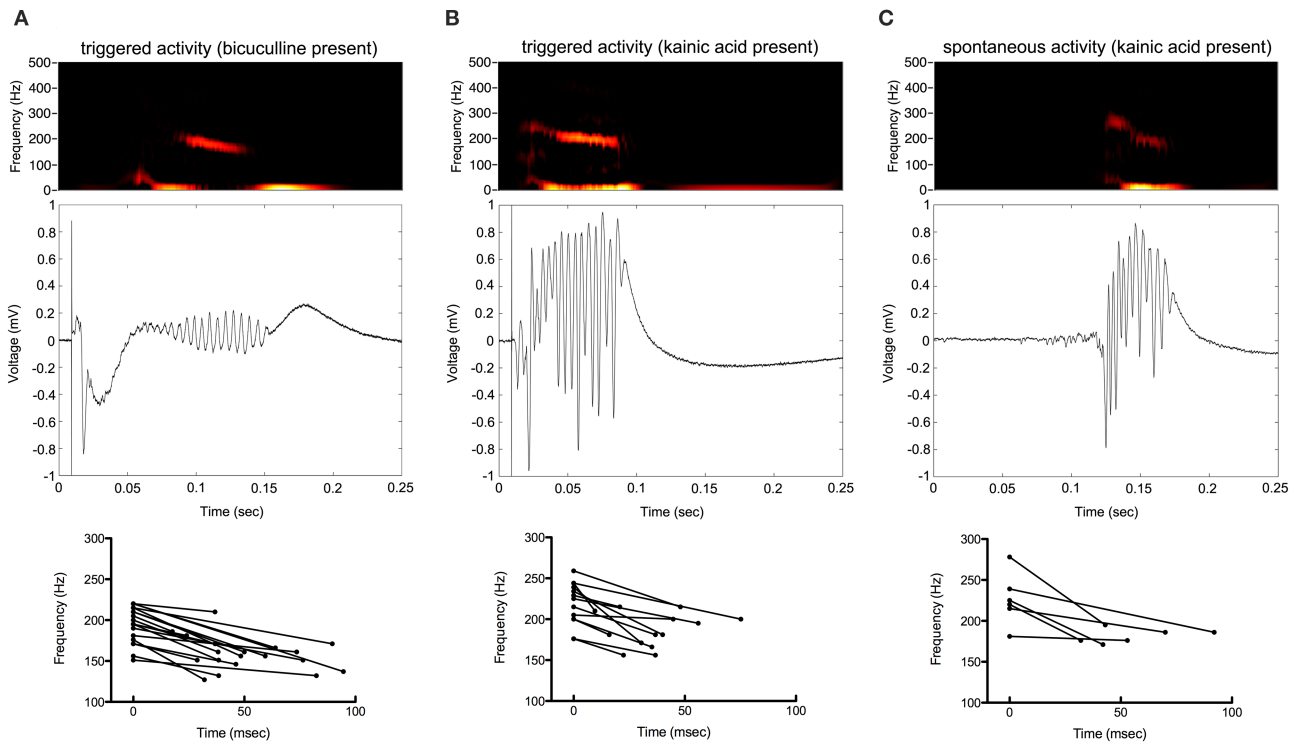


**FIGURE 4 |** Frequency of the oscillations decrease over time. Color spectrograms and raw data of representative recordings from the electrode with greatest oscillatory activity are shown in **(A–C)**. Start and end frequencies, as well as duration of oscillatory activity over time, are shown determined from the electrodes with greatest oscillatory activity from each of the slices.

point in time was taken as the value of the filtered data at that time point for each of the electrodes. In a manner similar to the depth profiles, profile plots along the cell layer were made. Electrodes along the cell layer were located, and their data was band-pass filtered (70–350 Hz) and subsequently plotted. Peaks and valleys were found within the oscillations of each electrode using a threshold-lockout algorithm.

Cross-correlation between electrodes along the cell layer and the electrode with maximal oscillatory activity was calculated. First, for each sweep analyzed, the collection of electrodes along the cell layer was identified. Four sweeps from each slice were taken and band-stop filtered (0–70 Hz). Using MATLAB's xcorr function, the $r^2$ and lag values were calculated for the electrodes compared to the electrode with most oscillatory activity. For bicuculline-treated slices, the data used was from the peak of the oscillation until its end of each individual channel. Data from the beginning to end of the oscillations in kainic acid-treated slices could be used. Maximum $r^2$ values with their associated lag times were taken. The resulting values were averaged across the sweeps. Distances between each of the electrodes in the slices were calculated, which allowed for creating a composite correlation using data from all slices.

Data are reported as means ± SD, unless the measurements are means themselves, in which case data are reported as means ± SEM. All statistics were computed with Minitab 18 (Minitab, Inc., State College, PA, USA). Unless otherwise noted, parameters calculated from slices with bicuculline or kainic acid (triggered or spontaneous) were compared using ANOVA with Tukey's *post-hoc* analysis. Paired *t*-tests were used to compare bicuculline- and kainic acid-treated slices before and after the addition of CPP or AP-5. In general, a $p$-value $< 0.05$ was considered to be statistically significant. Significant $p$-values are denoted in figures with asterisks (*).

# RESULTS

## Spatio-Temporal Description of Hippocampal HFOs

A total of 41 animals were used, with 41 bicuculline-treated slices (31 rats) and 13 kainic acid-treated slices (10 rats). Single pulses in the presence of bicuculline (**Figure 1**) or kainic acid (**Figure 2**) triggered epileptiform events that contained episodes of high frequency oscillations lasting 50–150 ms. Of the kainic acid-treated slices, 6 slices (4 rats) had spontaneous oscillations for at least 5 sweeps (**Figure 2**). Stimulation at CA3 and CA1 produced similar responses (**Figure 1**), with oscillations of maximal amplitude in area CA3c for both kainic acid—and bicuculline—treated slices (**Figure 3**).

Oscillations began 25–125 ms from the beginning of stimulation. They appeared to be maximal in frequency at their beginning and decrease in frequency over time. The amplitude of oscillations was maximal in the middle of the oscillatory period (**Figure 4**).

The frequency of HFOs and the duration of the oscillatory period were measured at the channel in which the oscillations had greatest amplitude (**Figure 5**). Peak frequency was 196 ± 22, 227 ± 21, and 233 ± 24 Hz for bicuculline triggered ($n$ = 20; 17 rats), kainic acid triggered ($n$ =13; 10 rats), and kainic acid spontaneous events ($n$ = 6; 4 rats), respectively. There was no difference in duration of the oscillations (bicuculline triggered 54 ± 24 ms vs. kainic acid triggered 36 ± 18 ms vs. kainic acid spontaneous 55 ± 22 ms), although there was a trend toward a difference in these groups $p = 0.07$. *Post-hoc* analysis revealed the trend to be a difference in the triggered bicuculline and kainic acid treated slices ($p = 0.08$).

Oscillations appeared to originate from the cell layer in both bicuculline- and kainic acid-treated slices (**Figure 6**). Depth profile analysis showed reversal of the voltage just apical to the cell layer of CA3c or other segments of CA3. The apical negativity in voltage profiles is consistent with excitatory synaptic activity and was consistent across spontaneous and evoked HFOs seen in disinhibited slices or slices activated by kainic acid. Moving along the cell layer, the temporal shifting of peaks suggests a spread velocity of ≤ 1 m/s (1 mm/ms) (**Figure 7**), also consistent with spread times for epileptiform activity in hippocampus [e.g., (32)].

The oscillatory coherence decreased with distance from the channel of maximal oscillatory amplitude along the cell layer (**Figure 8A**), yet with little to no lag in all slices except for kainic acid-treated slices with spontaneous oscillation (**Figure 8B**). There appeared to be greater correlation over larger distances among bicuculline-treated slices than kainic acid-treated slices.

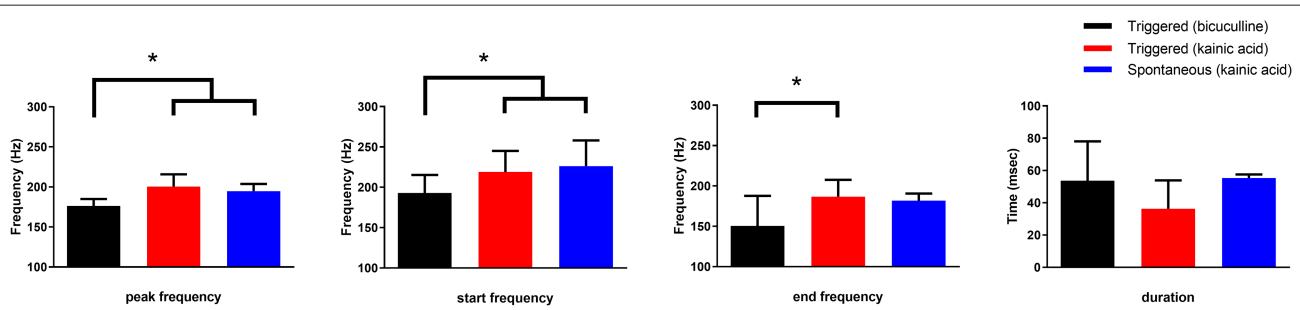


**FIGURE 5 |** Frequency and duration characteristics of oscillations in the presence of bicuculline or kainic acid. Slices with kainic acid (either triggered events or spontaneous) had a higher starting and peak frequency than those slices with triggered events in bicuculline after *post-hoc* analysis (*$p < 0.004$ and 0.001, respectively). The frequency at the end of the oscillations were different for only the triggered bicuculline and kainic acid slices after *post-hoc* analysis (*$p = 0.004$). There was no difference in duration of the oscillations, although there was a trend toward a difference between spontaneous and triggered oscillations in the presence of kainic acid (*post-hoc* analysis $p = 0.058$).

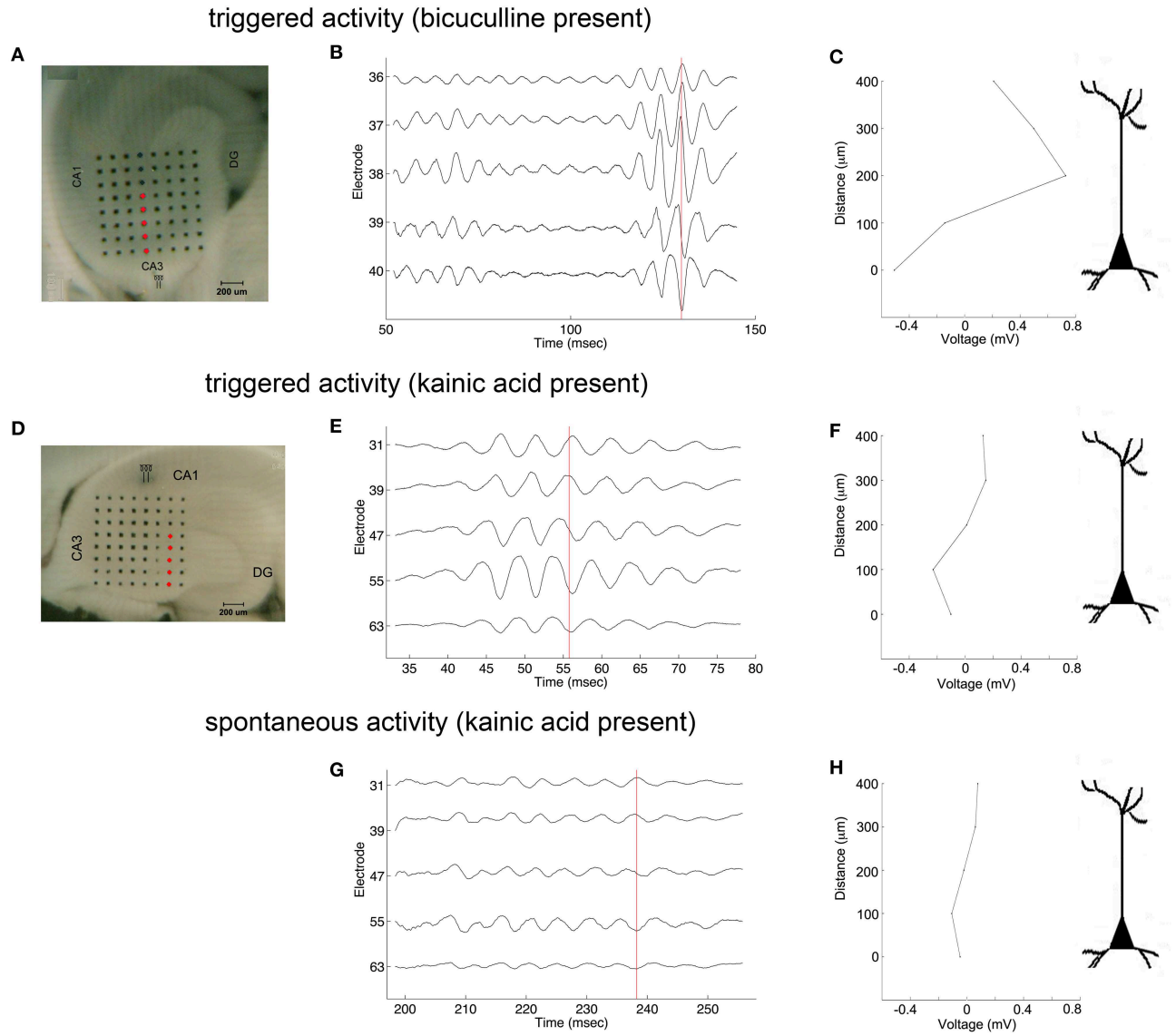


**FIGURE 6 |** Coarse voltage depth profile analysis in the presence of bicuculline or kainic acid. **(A,D)** show images of slices in bicuculline and kainic acid, respectively. Recordings of electrodes marked in red in those images are shown in **(B,E,G)** for triggered activity in bicuculline, triggered activity in kainic acid, and spontaneous activity in kainic acid, respectively. **(C,F,H)** plot the raw voltages marked by the red lines going through the records in **(B,E,G)**, respectively to show a phase reversal over the cell layer. Stimulus location in **(A)** is the white matter near the fimbria, below the cell layer. Stimulus location in **(D)** is stratum radiatum in mid-CA1.

We made recordings of evoked HFOs in CA1 of 13 slices (6 rats) after CA3 was cut off from the rest of the slice. Oscillations occurred as part of triggered events in CA1, but these were not as well synchronized as events recorded in CA3 or in CA1 of intact slices. This is illustrated in **Figure 9**.

## Pharmacology of Hippocampal HFOs

Comparison of all channels in slices in bicuculline and kainic acid was undertaken. The time to peak oscillatory activity after electrical stimulation was greater in the bicuculline-treated slices than in the kainic acid-slices (**Table 1**; 80 ± 9 vs. 33 ± 6 ms; Student's *t*-test, $p = 0.003$). HFOs in bicuculline were slower than those in kainic acid in general ($p < 0.002$). The time from the peak frequency to the end of the oscillation was not different between groups, but spontaneous oscillations appeared to last longer than triggered ones in kainic acid ($p = 0.058$).

Comparison of oscillations before and after application of CPP to 6 slices (6 rats) bathed in bicuculline was performed. Also, in slices bathed in bicuculline (6 slices; 5 rats) and kainic acid (5 slices; 5 rats), the effect of application of AP-5 was evaluated. As shown in **Table 2**, there was significant increase in frequency after application of CPP to slices bathed in bicuculline (174 ± 3 vs. 184 ± 3 Hz; $p = 0.0033$). Increase in frequency was also observed after application of AP-5 to slices bathed in bicuculline (169 ± 3 vs. 178

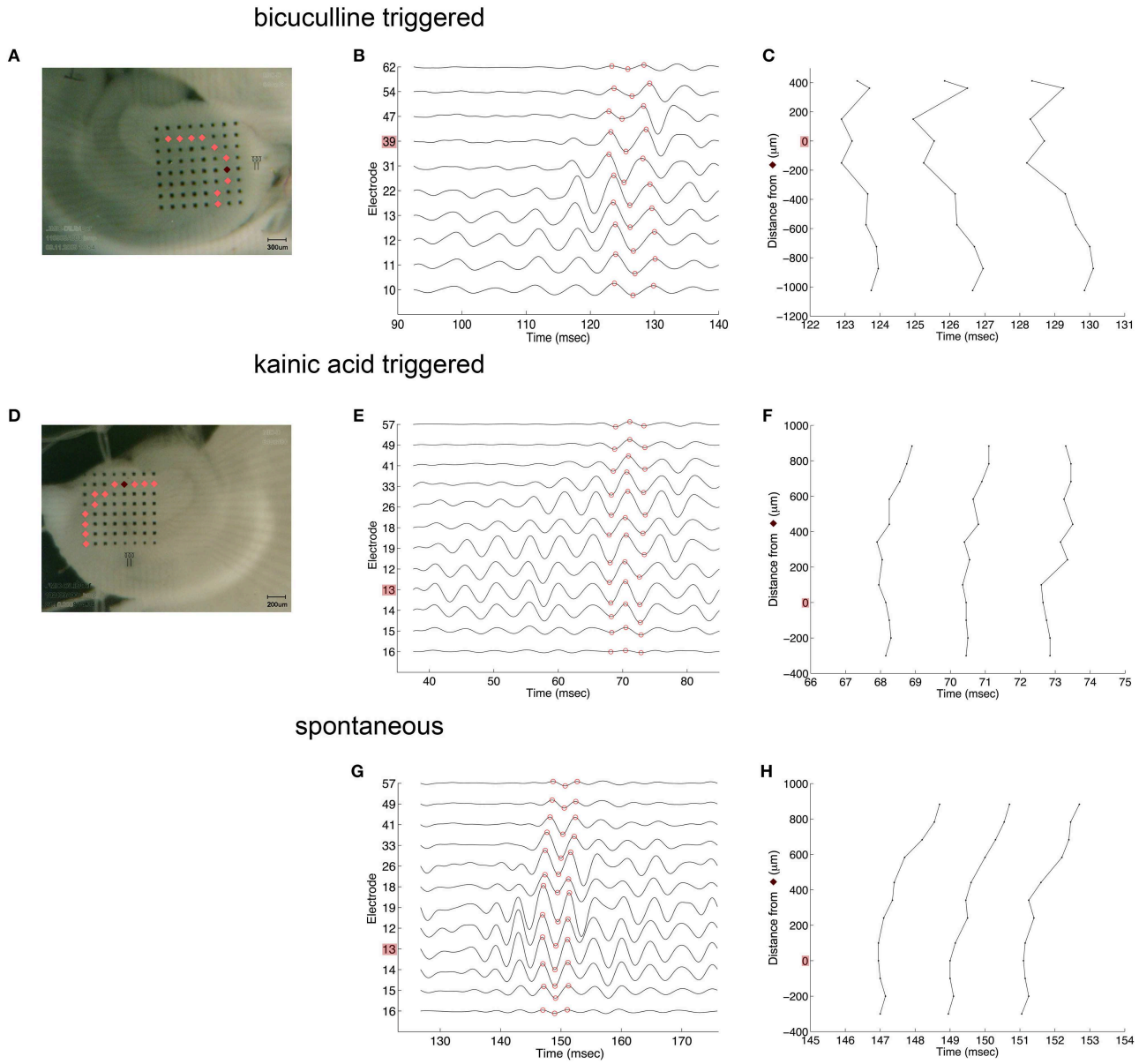


**FIGURE 7 |** Coarse voltage profile analysis over the cell layer in the presence of bicuculline or kainic acid. **(A,D)** show images of slices in bicuculline and kainic acid, respectively. Recordings of electrodes over the cell layer marked in pink in those images are shown in **(B,E,G)** for triggered activity in bicuculline, triggered activity in kainic acid, and spontaneous activity in kainic acid, respectively. The electrodes marked in dark red in **(A,D)** denote the sites of greatest overall oscillatory activity. **(C,F,H)** plot the time at which the recordings reach their peaks and troughs [marked in red circles in **(B,E,G)**, respectively]. These show little to no lag of the oscillation along the cell layer. Stimulus location in **(A)** is the white matter near the fimbria, below the cell layer. Stimulus location in **(D)** is stratum radiatum in mid-CA1.

$\pm$ 3 Hz; $p = 0.011$), and the time to the end of the oscillation was decreased (46 $\pm$ 3 vs. 36 $\pm$ 3 ms; $p = 0.043$). There was no change in any of measured parameters to slices bathed in kainic acid after application of AP-5.

Application of CNQX to bicuculline-treated slices caused cessation of the oscillations (**Figure 10A**). A desynchronization effect similar to that described by Foffani et al. (33) is evident as the CNQX effect develops. Addition of TMA to these slices increased spontaneous single and multi-unit spiking activity, but did not restore high frequency oscillations (**Figure 10B**). And, further addition of carbenoxolone abolished the single and multi-unit spiking activity (**Figure 10C**). The addition of carbenoxolone to slices with only bicuculline did not cause cessation of the oscillations, but it did decrease the frequency of spontaneous episodes of oscillatory activity during recordings. In 8 slices (8 rats), carbenoxelone tested in bicuculline-exposed slices did not disrupt HFOs. Interestingly, the only effect that we detected was that occasionally, the stimulus trigger pulse

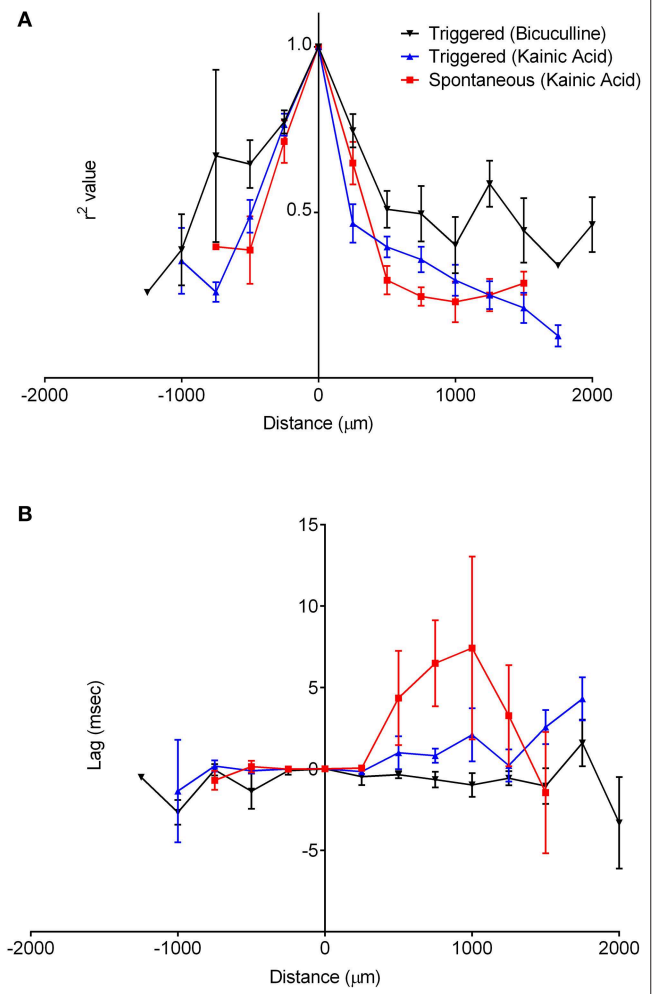


**FIGURE 8 |** Correlation of oscillations with the origin site in CA3. The recordings along the cell layer were compared with recordings from the maximal oscillatory activity for all slices. **(A)** shows that for recordings with both drugs, correlation of the oscillations decreases as a function of distance over the cell layer. It appears to decrease faster in slices bathed in kainic acid than those in bicuculline. The lag time compared to the maximal oscillatory electrode appeared to be constant over the cell layer, as in **(B)**.

did not trigger a population event. The maximal failure rate was 1 failure/3 stimulus trigger pulses. Population events that did occur were indistinguishable in duration, amplitude, or frequency characteristics from events triggered in the presence of bicuculline only.

## DISCUSSION

Using the laminar characteristic of the rat hippocampus, the rat hippocampal slice model is ideal for studying HFOs in hippocampus. We found HFOs to occur either after direct electrical stimulation in the presence of $GABA_A$ receptor blockade or kainic acid, or spontaneously in the presence of kainic acid. These oscillations had the largest amplitude and earliest onset in area CA3c cell layer, regardless of the drug, and their synchronization/spread extended over distances greater than 1 mm. The frequency of the oscillations was in the 150–250 Hz range, and the frequency decreased over time within a single oscillatory epoch. HFOs also tended to be higher frequency and the oscillatory period lasted longer in the presence of kainic acid than in the presence of a $GABA_A$ receptor blocker. NMDA antagonism did not significantly alter oscillations either in the presence of $GABA_A$ blockade or in kainic acid, except for a small increase in the frequency of the oscillations. Oscillations appeared to require AMPA receptor activity, as the HFOs stopped in bicuculline with the addition of an AMPA receptor antagonist, although there was still action potential activity in the slices. Addition of a gap junction opener increased the single and multi-unit action potential activity, but did not restore HFOs. Collectively, we conclude that $\approx$ 200 Hz HFOs depend upon glutamatergic synaptic transmission for synchronization of action potentials generated by various mechanisms, including disinhibition, convulsant action, and possibly the presence of gap junctions. Disruption of either the mechanism of synchronization or the action potential activity substrate to be synchronized can eliminate these HFOs.

### Importance of CA3c in High Frequency Oscillations

Others have recorded HFOs simultaneously in areas such as CA3 and CA1 (34) in normal behaving rats or in areas such as entorhinal cortex, dentate gyrus, and CA3 in disinhibied brain slices (27), this is the first study of HFOs in rat hippocampus with high spatial resolution of activity as a result of multiple simultaneous recordings from multiple hippocampal structures. The results of our spatio-temporal analysis suggest that there may be an important difference in the way pyramidal cells are interconnected in CA3c, and that this region may be involved in the generation of high frequency oscillations in hippocampus, which may contribute to the epileptogenic properties area CA3 in hippocampus. The difference in connectivity likely reflects quantitative difference in either strength or frequency of excitatory connections.

This quantitative difference in synaptic connectivity is further supported by our data that oscillations were less pronounced in CA1 after CA3 was physically removed from the slice by microknife cut. As illustrated, HFOs occurred as part of the CA1 events, but the amplitude was less and higher frequency features were evident as a result of activity losses in a manner consistent with the mechanism proposed by Foffani et al. (33).

With a relatively high density recording array, the laminar profiles of HFO are available in each structure together with accurate timing data for studies of activity spread. The variance in proposed mechanisms and locations of origin suggest that multiple forms of HFOs may exist in the hippocampus, but our finding of very similar properties for HFOs facilitated by disinhibition or by glutamate receptor activation suggests that there may be regional

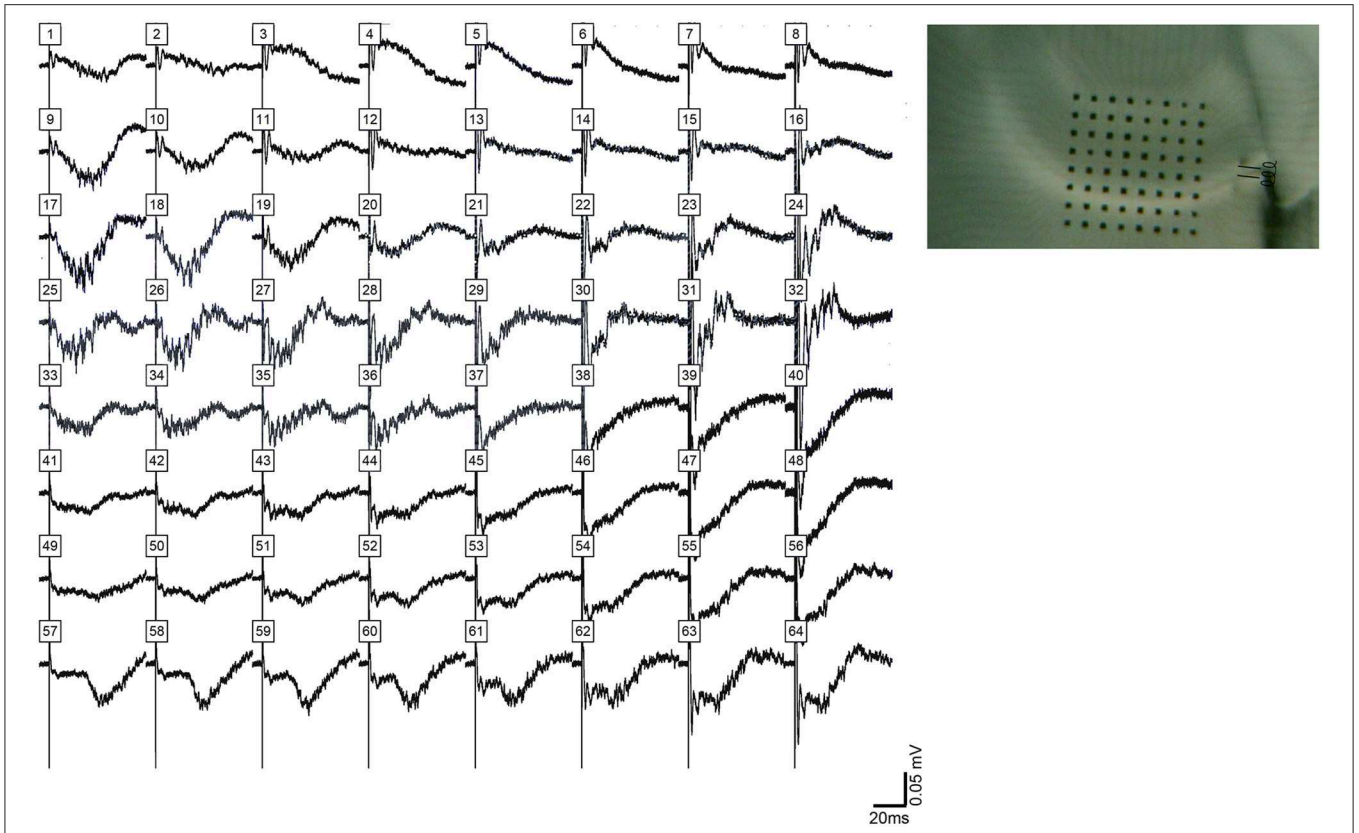


**FIGURE 9 |** HFOs evoked in CA1 after removal of CA3 from the slice. **(Left)** shows filed potentials evoked by a single stimulus pulse applied to the alveus on the CA3 (proximal) side of CA1 after area CA3 was separated from the slice by knife cut, which is shown in **(Right)**. The amplitude and synchrony of HFOs in CA1 under these conditions was less than HFOs observed in CA3 or in CA1 in intact slices.

**TABLE 1 |** Characteristics of hippocampal triggered and spontaneous VFOs in presence of bicuculline or kainic acid.

| | **Triggered Bic (*N* = 12)** | **Triggered KA (*N* = 11)** | **Spontaneous KA (*N* = 6)** | ***p*-value (B-KA)** | ***p*-value (B-KAs)** | ***p*-value (KA-KAs)** | ***p*-value (all)** |
|---|---|---|---|---|---|---|---|
| Peak time of oscillatory activity (ms) | 80 ± 9 | 33 ± 6 | N/A | N/A | N/A | N/A | 0.0003 |
| Frequency of peak oscillatory activity (Hz) | 172 ± 2 | 182 ± 2 | 184 ± 2 | 0.001 | 0.002 | 0.828 | 0.0003 |
| Time to end of oscillation (ms) | 42 ± 3 | 33 ± 4 | 50 ± 8 | 0.31 | 0.47 | 0.058 | 0.065 |

*Bic, bicuculline; KA, kainic acid (triggered); KAs, kainic acid (spontaneous).*

differences that emerge when the primary initiation point is removed.

Our data include area CA2 in nearly all recordings (see **Figures 1**, **2**, **7** as examples). Whereas, Oliva et al. (35) showed that CA2 appeared to be the origin for synchronous activity, in our recordings, CA2 did not lead CA3c in the oscillations no matter what the stimulus location was nor if the HFOs were part of spontaneous events.

One possible explanation for the localization of oscillations in area CA3 is the likelihood that mossy fiber axons have the highest density in this part of the slice. In addition, axonal gap junctions have been demonstrated in mossy fibers (26) and may contribute to pyramidal cell synchronization. Proximal CA3b and the CA3c subregions send their axons predominantly to the CA1 region. A fraction of collaterals also project to the dentate gyrus (36, 37). Our spatial account of the oscillations can be explained, therefore, on the basis of hippocampal connectivity.

Interestingly, the study by Foffani et al., which demonstrated the emergence of very high frequency oscillations from HFOs or ripple activity (33) also points to CA3c as a spatial focal point. As HFOs are the required substrate for very high frequency oscillations, it is to be expected that their spatial localization overlaps. Further, this points to a linkage between normal HFOs and what may be considered pathological very high frequency oscillations.

**TABLE 2 |** Effect of CPP or AP-5 to slices bathed in bicuculline or kainic acid.

| | Bicuculline | CPP | *p*-value |
|---|---|---|---|
| **Bicuculline + CPP (*N* = 6)** | | | |
| Peak time of oscillatory activity (ms) | 73 ± 13 | 61 ± 7 | 0.32 |
| Amplitude of oscillatory activity (au) | 13 ± 9 | 20 ± 14 | 0.30 |
| Peak-to-valley oscillation amplitude (mV) | 0.19 ± 0.04 | 0.22 ± 0.05 | 0.16 |
| Frequency of peak oscillatory activity (Hz) | 174 ± 3 | 184 ± 3 | 0.0033 |
| Time to end of oscillation (ms) | 37 ± 5 | 28 ± 2 | 0.17 |
| | **Bicuculline** | **AP-5** | ***p*-value** |
| **Bicuculline + AP-5 (*N* = 6)** | | | |
| Peak time of oscillatory activity (ms) | 86 ± 12 | 92 ± 8 | 0.50 |
| Amplitude of oscillatory activity (au) | 10 ± 3 | 15 ± 4 | 0.14 |
| Peak-to-valley oscillation amplitude (mV) | 0.18 ± 0.02 | 0.20 ± 0.02 | 0.24 |
| Frequency of peak oscillatory activity (Hz) | 169 ± 3 | 178 ± 3 | 0.011 |
| Time to end of oscillation (ms) | 46 ± 3 | 36 ± 3 | 0.043 |
| | **Kainic acid** | **AP-5** | ***p*-value** |
| **Kainic acid + AP-5 (*N* = 5)** | | | |
| Peak time of oscillatory activity (ms) | 26 ± 4 | 26 ± 4 | 0.87 |
| Amplitude of oscillatory activity (au) | 486 ± 111 | 597 ± 213 | 0.54 |
| Peak-to-valley oscillation amplitude (mV) | 0.37 ± 0.06 | 0.58 ± 0.13 | 0.11 |
| Frequency of peak oscillatory activity (Hz) | 192 ± 13 | 192 ± 12 | 0.93 |
| Time to end of oscillation (ms) | 44 ± 10 | 28 ± 3 | 0.22 |

## Synaptic Control of High Frequency Oscillations

Our study indicates that either $GABA_A$ inhibition or activation of kainate receptors is sufficient for the emergence of robust HFOs. Our data indicate that oscillations require AMPA receptors, but not NMDA receptors, the latter of which has previously been shown (17). Our findings are further supported by evidence that HFOs are dependent on both inhibitory and excitatory control (20), and they can thus be driven by loss of one or gain of the other.

In optogenetically induced HFOs, loss of excitation of increases in inhibition aborted the oscillations (38). The increased frequency of the oscillations while inhibition is still present in the slice illustrates a paradoxical effect of inhibition of increasing the circuit's frequency. The difference in duration of the events under disinhibition and excitation suggests an intrinsic oscillatory circuit that is modulated more by inhibition than by limitation of excitation. This may be related to the observation that HFOs occurred spontaneously in the presence of kainic acid but not bicuculline.

HFO activity was triggered from multiple sites within hippocampus (different subregions and different layers within subregions) and all stimulus sites led to the same finding that oscillations appeared to originate in area CA3c (see **Figure 3**). Direct and antidromic activation of neurons certainly occurred with our single pulse stimulation. The best evidence for this is the single population spike that remains after CNQX exposure (**Figure 10**). The long latency for population events containing high frequency oscillations (**Figure 1**) when stimuli were applied to CA1 is another indicator that cell-to-cell connectivity (synaptic or otherwise) is necessary for the generation of events containing HFOs.

## Gap Junctions Affect Neuronal Activity but Not Neuronal Synchrony

Our work shows that while gap junctions may impact the frequency of firing of neurons in a population, the synchronization of that activity does not appear to require gap junctions. Specific gap junction blockade cannot be done with precision with any available drug, and therefore, while a number of gap junction "blockers" can stop HFOs (17), this may be due to other effects of the various gap junction blockers. Gap junction activation in the presence of glutamate blockade did not aid in HFO formation, but did increase the overall amount of neuronal activity. Gap junction blockade clearly reduced the amount of neuronal activity (**Figure 10C**). These results are consistent with the view that both a means to generate activity and a means to synchronize such activity are necessary for population oscillations. Our findings clearly illustrate how gap junction activity can contribute to the presence of neuronal activity that might become synchronous, but gap junctions do not appear to be the synchronization mechanism. Glutamate receptors appear to be the critical synchronization mechanism. We speculate that if gap junctions do exist in mossy fibers at mixed chemical and electric synapses and the mossy fiber density is greatest in CA3 (26), gap junctions in area CA3c may thus account for our observation that HFOs originate and have such large amplitudes in area CA3c.

## Clinical Significance

HFOs are known to occur frequently in mesial temporal lobe epilepsy (39). These areas are additionally thought to be an indicator of the seizure onset zone independent of interictal spikes (40). Further, seizure outcomes have been found to be better with removal of a larger extent of tissue with HFOs (41). However, the scale at which HFOs are detected cannot easily resolve particular hippocampal substructures. Our work contributes to the idea that HFOs arising within the mesial temporal lobe reflect epileptogenicity in that we show a specific circuit that is pre-disposed to HFO generation in the setting of abnormal excitation or disinhibition. We propose that this intrinsic circuit may play a role in the generation of HFOs and epileptogenicity in mesial temporal lobe epilepsy.

## Limitations

One limitation of this work is that while HFOs exist in normal and pathologic contexts, this study uses a brain slice model to study them. Additionally, the effects of synaptic disinhibition or excitation on generation of HFOs may not necessarily reflect synchrony in the generation of seizures. However, this study does nonetheless describe an intrinsic circuit that may be important in seizure generation.

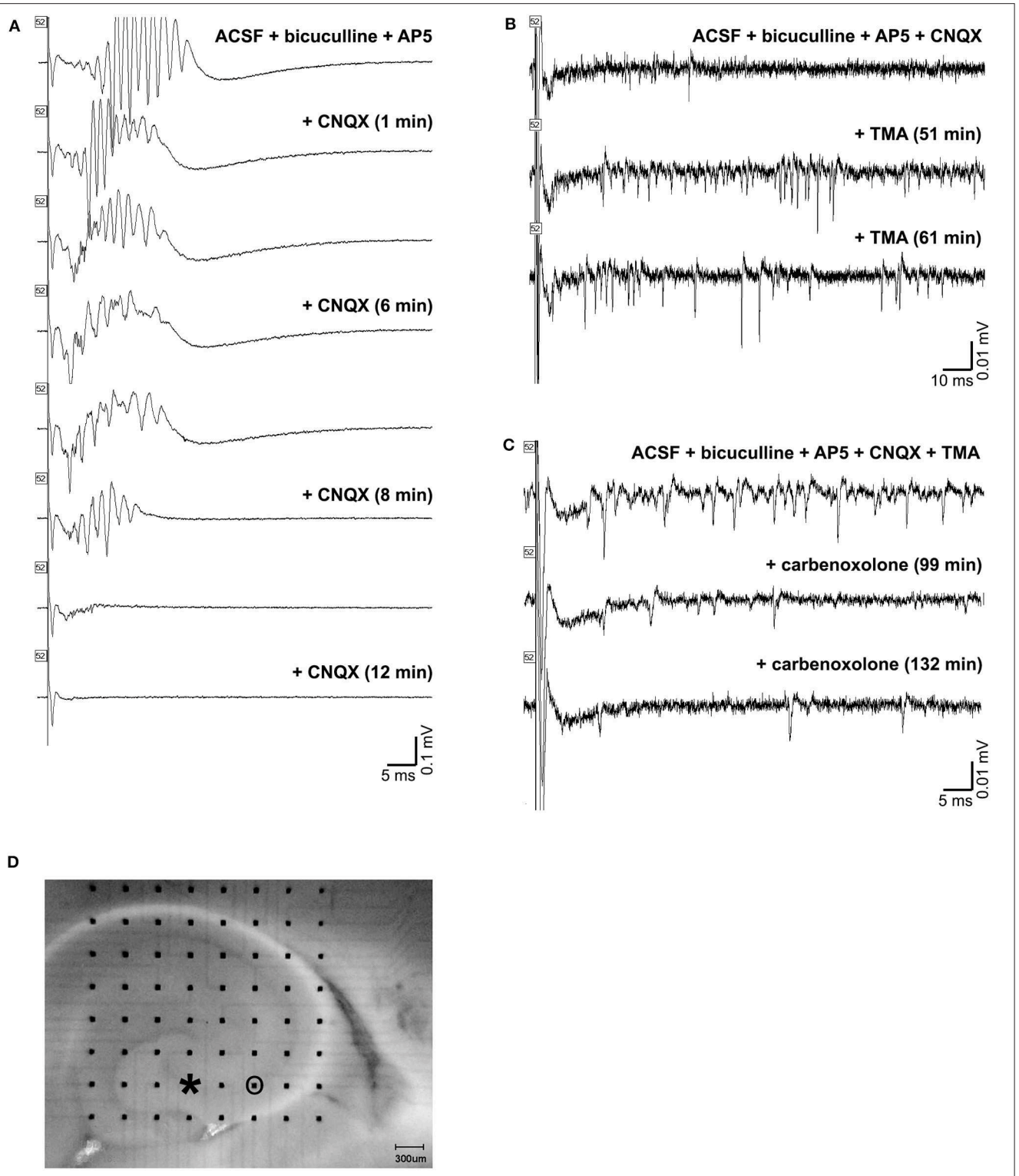


**FIGURE 10 |** Gap junction and synaptic control over high frequency oscillations. **(A)** shows a triggered HFO in the presence of bicuculline and AP-5 in the top tracing. Addition of CNQX caused cessation of the oscillations in the bottom tracings. The addition of TMA to these slices increased activity, but did not restore high frequency oscillations, as shown in the tracings in **(B)**. Further addition of carbenoxolone abolished the increased activity, as in the tracings in **(C)**. An image of the slice used is shown in **(D)**. The electrode used for stimulation is marked with an asterisk (at the end of CA3 inside the hilus), and the electrode used for recordings in **(A,B,C)** is circled.

## DATA AVAILABILITY STATEMENT

The datasets generated for this study are available on request to the corresponding author.

## ETHICS STATEMENT

The animal study was reviewed and approved by Animal Care and Use Committee, SUNY Downstate Medical Center.

## AUTHOR CONTRIBUTIONS

RO designed the study and performed the experiments. MS and IN performed the data analysis. RO and IN prepared the figures. IN wrote the manuscript, which was revised by RO, MS, and IN.

## FUNDING

This work was supported by the State University of New York and private philanthropic contributions.

## REFERENCES


1. Jefferys JG, Menendez De La Prida L, Wendling F, Bragin A, Avoli M, Timofeev I, et al. Mechanisms of physiological and epileptic HFO generation. *Prog Neurobiol.* (2012) 98:250–64. doi: 10.1016/j.pneurobio.2012.02.005
2. Jiruska P, Alvarado-Rojas C, Schevon CA, Staba R, Stacey W, Wendling F, et al. Update on the mechanisms and roles of high-frequency oscillations in seizures and epileptic disorders. *Epilepsia.* (2017) 58:1330–9. doi: 10.1111/epi.13830
3. Jones MS, Barth DS. Spatiotemporal organization of fast (>200 Hz) electrical oscillations in rat Vibrissa/Barrel cortex. *J Neurophysiol.* (1999) 82:1599–609. doi: 10.1152/jn.1999.82.3.1599
4. Amassian VE, Stewart M. Motor cortical and other cortical interneuronal networks that generate very high frequency waves. *Suppl Clin Neurophysiol.* (2003) 56:119–42. doi: 10.1016/S1567-424X(09)70214-4
5. Traub RD, Whittington MA. *Cortical Oscillations in Health and Disease*. New York, NY: Oxford University Press (2010).
6. Uhlhaas PJ, Singer W. Oscillations and neuronal dynamics in schizophrenia: the search for basic symptoms and translational opportunities. *Biol Psychiatry.* (2015) 77:1001–9. doi: 10.1016/j.biopsych.2014.11.019
7. Alkawadri R, Gaspard N, Goncharova Ii, Spencer DD, Gerrard JL, Zaveri H, et al. The spatial and signal characteristics of physiologic high frequency oscillations. *Epilepsia.* (2014) 55:1986–95. doi: 10.1111/epi.12851
8. Frauscher B, Bartolomei F, Kobayashi K, Cimbalnik J, Van 'T Klooste MA, Rampp S, et al. High-frequency oscillations: the state of clinical research. *Epilepsia.* (2017) 58:1316–29. doi: 10.1111/epi.13829
9. Buzsaki G, Horvath Z, Urioste R, Hetke J, Wise K. High-frequency network oscillation in the hippocampus. *Science.* (1992) 256:1025–7. doi: 10.1126/science.1589772
10. Chrobak JJ, Buzsaki G. High-frequency oscillations in the output networks of the hippocampal-entorhinal axis of the freely behaving rat. *J Neurosci.* (1996) 16:3056–66. doi: 10.1523/JNEUROSCI.16-09-03056.1996
11. Staba RJ. Normal and pathologic high-frequency oscillations. In: Noebels JL, Avoli M, Rogawski MA, Olsen RW, Delgado-Escueta AV, editors. *Jasper's Basic Mechanisms of the Epilepsies.* 4th ed. Bethesda, MD: National Center for Biotechnology Information. (2012) 285–301.
12. Bragin A, Engel J Jr, Wilson CL, Fried I, Buzsaki G. High-frequency oscillations in human brain. *Hippocampus.* (1999) 9:137–42. doi: 10.1002/(SICI)1098-1063(1999)9:2<137::AID-HIPO5>3.0.CO;2-0
13. Andrade-Valenca L, Mari F, Jacobs J, Zijlmans M, Olivier A, Gotman J, et al. Interictal high frequency oscillations (HFOs) in patients with focal epilepsy and normal MRI. *Clin Neurophysiol.* (2012) 123:100–5. doi: 10.1016/j.clinph.2011.06.004
14. Penttonen M, Kamondi A, Sik A, Acsady L, Buzsaki G. Feed-forward and feed-back activation of the dentate gyrus *in vivo* during dentate spikes and sharp wave bursts. *Hippocampus.* (1997) 7:437–50. doi: 10.1002/(SICI)1098-1063(1997)7:4<437::AID-HIPO9>3.0.CO;2-F
15. Ylinen A, Bragin A, Nadasdy Z, Jando G, Szabo I, Sik A, et al. Sharp wave-associated high-frequency oscillation (200 Hz) in the intact hippocampus: network and intracellular mechanisms. *J Neurosci.* (1995) 15:30–46. doi: 10.1523/JNEUROSCI.15-01-00030.1995
16. Draguhn A, Traub RD, Bibbig A, Schmitz D. Ripple (approximately 200-Hz) oscillations in temporal structures. *J Clin Neurophysiol.* (2000) 17:361–76. doi: 10.1097/00004691-200007000-00003
17. Draguhn A, Traub RD, Schmitz D, Jefferys JG. Electrical coupling underlies high-frequency oscillations in the hippocampus *in vitro*. *Nature.* (1998) 394:189–92. doi: 10.1038/28184
18. Traub RD, Schmitz D, Jefferys JG, Draguhn A. High-frequency population oscillations are predicted to occur in hippocampal pyramidal neuronal networks interconnected by axoaxonal gap junctions. *Neuroscience.* (1999) 92:407–26. doi: 10.1016/S0306-4522(98)00755-6
19. Weiss SA, Faber DS. Field effects in the CNS play functional roles. *Front Neural Circuits.* (2010) 4:15. doi: 10.3389/fncir.2010.00015
20. Csicsvari J, Hirase H, Czurko A, Mamiya A, Buzsaki G. Oscillatory coupling of hippocampal pyramidal cells and interneurons in the behaving Rat. *J Neurosci.* (1999) 19:274–87. doi: 10.1523/JNEUROSCI.19-01-00274.1999
21. Sik A, Penttonen M, Ylinen A, Buzsaki G. Hippocampal CA1 interneurons: an *in vivo* intracellular labeling study. *J Neurosci.* (1995) 15:6651–65. doi: 10.1523/JNEUROSCI.15-10-06651.1995
22. Maier N, Guldenagel M, Sohl G, Siegmund H, Willecke K, Draguhn A. Reduction of high-frequency network oscillations (ripples) and pathological network discharges in hippocampal slices from connexin 36-deficient mice. *J Physiol.* (2002) 541:521–8. doi: 10.1113/jphysiol.2002.017624
23. Macvicar BA, Dudek FE. Electrotonic coupling between granule cells of rat dentate gyrus: physiological and anatomical evidence. *J Neurophysiol.* (1982) 47:579–92. doi: 10.1152/jn.1982.47.4.579
24. Perez-Velazquez JL, Valiante TA, Carlen PL. Modulation of gap junctional mechanisms during calcium-free induced field burst activity: a possible role for electrotonic coupling in epileptogenesis. *J Neurosci.* (1994) 14:4308–17. doi: 10.1523/JNEUROSCI.14-07-04308.1994
25. Valiante TA, Perez Velazquez JL, Jahromi SS, Carlen PL. Coupling potentials in CA1 neurons during calcium-free-induced field burst activity. *J Neurosci.* (1995) 15:6946–56. doi: 10.1523/JNEUROSCI.15-10-06946.1995
26. Hamzei-Sichani F, Kamasawa N, Janssen WG, Yasumura T, Davidson KG, Hof PR, et al. Gap junctions on hippocampal mossy fiber axons demonstrated by thin-section electron microscopy and freeze fracture replica immunogold labeling. *Proc Natl Acad Sci USA.* (2007) 104:12548–53. doi: 10.1073/pnas.0705281104
27. D'antuono M, De Guzman P, Kano T, Avoli M. Ripple activity in the dentate gyrus of dishinibited hippocampus-entorhinal cortex slices. *J Neurosci Res.* (2005) 80, 92–103. doi: 10.1002/jnr.20440
28. Paxinos G, Watson C. *The Rat Brain in Stereotaxic Coordinates*. San Diego, CA: Academic Press (2005).
29. Stewart M. Columnar activity supports propagation of population bursts in slices of rat entorhinal cortex. *Brain Res.* (1999) 830:274–84. doi: 10.1016/S0006-8993(99)01404-3
30. Harris E, Witter MP, Weinstein G, Stewart M. Intrinsic connectivity of the rat subiculum: I. Dendritic morphology and patterns of axonal arborization by pyramidal neurons. *J Comp Neurol.* (2001) 435:490–505. doi: 10.1002/cne.1046
31. Kunitake A, Kunitake T, Stewart M. Differential modulation by carbachol of four separate excitatory afferent systems to the rat subiculum *in vitro*. *Hippocampus.* (2004) 14:986–99. doi: 10.1002/hipo.20016

32. Orman R, Von Gizycki H, Lytton WW, Stewart M. Local axon collaterals of area CA1 support spread of epileptiform discharges within CA1, but propagation is unidirectional. *Hippocampus.* (2008) 18:1021–33. doi: 10.1002/hipo.20460
33. Foffani G, Uzcategui YG, Gal B, Menendez De La Prida L. Reduced spike-timing reliability correlates with the emergence of fast ripples in the rat epileptic hippocampus. *Neuron.* (2007) 55:930–41. doi: 10.1016/j.neuron.2007.07.040
34. Csicsvari J, Hirase H, Czurko A, Mamiya A, Buzsaki G. Fast network oscillations in the hippocampal CA1 region of the behaving rat. *J Neurosci.* (1999) 19:RC20. doi: 10.1523/JNEUROSCI.19-16-j0001.1999
35. Oliva A, Fernandez-Ruiz A, Buzsaki G, Berenyi A. Role of hippocampal CA2 region in triggering sharp-wave ripples. *Neuron.* (2016) 91:1342–55. doi: 10.1016/j.neuron.2016.08.008
36. Ishizuka N, Weber J, Amaral DG. Organization of intrahippocampal projections originating from CA3 pyramidal cells in the rat. *J Comp Neurol.* (1990) 295:580–623. doi: 10.1002/cne.902950407
37. Li XG, Somogyi P, Ylinen A, Buzsaki G. The hippocampal CA3 network: an *in vivo* intracellular labeling study. *J Comp Neurol.* (1994) 339:181–208. doi: 10.1002/cne.903390204
38. Stark E, Roux L, Eichler R, Senzai Y, Royer S, Buzsaki G. Pyramidal cell-interneuron interactions underlie hippocampal ripple oscillations. *Neuron.* (2014) 83:467–80. doi: 10.1016/j.neuron.2014.06.023
39. Levesque M, Shiri Z, Chen LY, Avoli M. High-frequency oscillations and mesial temporal lobe epilepsy. *Neurosci Lett.* (2018) 667:66–74. doi: 10.1016/j.neulet.2017.01.047
40. Jacobs J, Levan P, Chander R, Hall J, Dubeau F, Gotman J. Interictal high-frequency oscillations (80-500 Hz) are an indicator of seizure onset areas independent of spikes in the human epileptic brain. *Epilepsia.* (2008) 49:1893–907. doi: 10.1111/j.1528-1167.2008.01656.x
41. Jacobs J, Zijlmans M, Zelmann R, Chatillon CE, Hall J, Olivier A, et al. High-frequency electroencephalographic oscillations correlate with outcome of epilepsy surgery. *Ann Neurol.* (2010) 67:209–20. doi: 10.1002/ana.21847


**Conflict of Interest:** The authors declare that the research was conducted in the absence of any commercial or financial relationships that could be construed as a potential conflict of interest.

*Copyright © 2020 Naggar, Stewart and Orman. This is an open-access article distributed under the terms of the Creative Commons Attribution License (CC BY). The use, distribution or reproduction in other forums is permitted, provided the original author(s) and the copyright owner(s) are credited and that the original publication in this journal is cited, in accordance with accepted academic practice. No use, distribution or reproduction is permitted which does not comply with these terms.*

frontiers in Neurology

ORIGINAL RESEARCH
published: 30 September 2020
doi: 10.3389/fneur.2020.573975

# Interictal Fast Ripples Are Associated With the Seizure-Generating Lesion in Patients With Dual Pathology

*Jan Schönberger*[1,2,3,4]*, *Charlotte Huber*[2,3], *Daniel Lachner-Piza*[1,3], *Kerstin Alexandra Klotz*[1,2,3,4], *Matthias Dümpelmann*[1,3], *Andreas Schulze-Bonhage*[1,3] and *Julia Jacobs*[2,3,5,6]

[1] Epilepsy Center, Medical Center, University of Freiburg, Freiburg, Germany, [2] Department of Neuropediatrics and Muscle Disorders, Medical Center, University of Freiburg, Freiburg, Germany, [3] Faculty of Medicine, University of Freiburg, Freiburg, Germany, [4] Berta-Ottenstein-Programme, Faculty of Medicine, University of Freiburg, Freiburg, Germany, [5] Department of Paediatrics and Department of Neuroscience, Cumming School of Medicine, University of Calgary, Calgary, AB, Canada, [6] Hotchkiss Brain Institute and Alberta Children's Hospital Research Institute, University of Calgary, Calgary, AB, Canada

**Rationale:** Patients with dual pathology have two potentially epileptogenic lesions: One in the hippocampus and one in the neocortex. If epilepsy surgery is considered, stereotactic electroencephalography (SEEG) may reveal which of the lesions is seizure-generating, but frequently, some uncertainty remains. We aimed to investigate whether interictal high-frequency oscillations (HFOs), which are a promising biomarker of epileptogenicity, are associated with the primary focus.

**Methods:** We retrospectively analyzed 16 patients with dual pathology. They were grouped according to their seizure-generating lesion, as suggested by ictal SEEG. An automated detector was applied to identify interictal epileptic spikes, ripples (80–250 Hz), ripples co-occurring with spikes (IES-ripples) and fast ripples (250–500 Hz). We computed a ratio R to obtain an indicator of whether rates were higher in the hippocampal lesion (R close to 1), higher in the neocortical lesion (R close to −1), or more or less similar (R close to 0).

**Results:** Spike and HFO rates were higher in the hippocampal than in the neocortical lesion ($p < 0.001$), particularly in seizure onset zone channels. Seizures originated exclusively in the hippocampus in 5 patients (group 1), in both lesions in 7 patients (group 2), and exclusively in the neocortex in 4 patients (group 3). We found a significant correlation between the patients' primary focus and the ratio $R_{\text{fast ripples}}$, i.e., the proportion of interictal fast ripples detected in this lesion ($p < 0.05$). No such correlation was observed for interictal epileptic spikes ($p = 0.69$), ripples ($p = 0.60$), and IES-ripples ($p = 0.54$). In retrospect, interictal fast ripples would have correctly "predicted" the primary focus in 69% of our patients ($p < 0.01$).

**Conclusions:** We report a correlation between interictal fast ripple rate and the primary focus, which was not found for epileptic spikes. Fast ripple analysis could provide helpful information for generating a hypothesis on seizure-generating networks, especially in cases with few or no recorded seizures.

**Keywords: epilepsy, dual pathology, stereotactic electroencephalography, interictal, high-frequency oscillations, fast ripples**

OPEN ACCESS

***Edited by:***
*Johannes Sarnthein, University of Zurich, Switzerland*

***Reviewed by:***
*Giovanni Pellegrino, McGill University, Canada*
*Manuel Toledo, Vall d'Hebron University Hospital, Spain*

***Correspondence:**
*Jan Schönberger*
*jan.schoenberger@yahoo.de*

***Specialty section:***
*This article was submitted to Epilepsy, a section of the journal Frontiers in Neurology*

***Received:*** *18 June 2020*
***Accepted:*** *31 August 2020*
***Published:*** *30 September 2020*

***Citation:***
*Schönberger J, Huber C, Lachner-Piza D, Klotz KA, Dümpelmann M, Schulze-Bonhage A and Jacobs J (2020) Interictal Fast Ripples Are Associated With the Seizure-Generating Lesion in Patients With Dual Pathology. Front. Neurol. 11:573975. doi: 10.3389/fneur.2020.573975*

# INTRODUCTION

Temporal lobe epilepsy is the most frequent cause for drug-resistant seizures (1). These patients have a higher chance of achieving seizure freedom if treated by epilepsy surgery rather than prolonged medical therapy (2, 3) and surgical outcomes are better if imaging revealed a potentially epileptogenic lesion (4, 5). Some individuals, however, have two lesions: One in the hippocampus and another one in the neocortex. In these "dual pathology" (6) patients, it is often unclear which lesion is seizure-generating, or if both lesions have such potential. Stereotactic electroencephalography (SEEG) may be helpful, but especially if only few seizures were captured, remaining uncertainty is considerable (7)—and patients rarely become seizure-free (1).

Even more in such scenarios, analysis of interictal activity may contribute substantially to presurgical evaluation. Most clinicians have focused on interictal epileptic spikes for decades and resection of spike-generating tissue correlates to some degree with post-surgical outcome in neocortical epilepsy (8). More recent studies suggest that high-frequency oscillations (HFOs), divided into ripples (80–250 Hz) and fast ripples (250–500 Hz), might have additional value when it comes to understanding epileptic networks and identifying epileptic foci. Resection of HFO-generating areas was associated with seizure-free outcome in several collectives (9–12), their rates increased after reduction of antiepileptic medication (13) and they may be involved in seizure generation (14–17). Many key studies on HFOs relied on visual identification, which is extremely time-consuming. During the past years, however, several automatic detectors have been developed (18–22). These tools now enable us to analyze HFOs in a clinical routine setting.

In this study, we hypothesized that interictal HFOs are associated with the seizure-generating lesion in patients with dual pathology. We applied an automated detector, compared spike, and HFO rates between the two lesions and examined whether this ratio correlates with the primary focus, as identified by ictal SEEG. Finally, we reviewed individual patients to estimate the value of our tool for clinical decision-making.

# METHODS

## Patient Selection

We considered all patients with drug-resistant temporal lobe epilepsy who, as part of their evaluation for epilepsy surgery, had undergone stereotactic electroencephalography (SEEG) recordings at the Freiburg Epilepsy Center between 2012 and 2019. From these, subjects with two potentially epileptogenic lesions on neuroimaging were selected. All our patients had one lesion in the hippocampus and the other one in the temporal neocortex on the same side. In a few patients, radiologic findings were equivocal or only suggestive of a lesion. From these, we only included subjects with a lesion confirmed by histology. This study was approved by the Ethics Commission at the University Medical Center Freiburg and written informed consent was obtained from all patients.

## Grouping of Patients

Depth electrodes (Ad-Tech Medical Instrument Corporation, Racine, WI) had been implanted based on their estimated value for clinical decision-making. Electrode contacts located inside the hippocampal or neocortical lesion were identified based on post-implantation MRI. We grouped our patients according to their seizure-generating lesion (**Figure 1**):

- Group 1: All recorded seizures generated in the hippocampal lesion
- Group 2: Some seizures generated in the hippocampal and some in the neocortical lesion, or onset more or less simultaneous in the two lesions
- Group 3: All recorded seizures generated in the neocortical lesion.

Grouping was performed based on our patients' medical reports only. Thus, regarding the decision of whether a seizure originated from the hippocampus or neocortex, we relied on the assessment of a board-certified neurologist who was blind to the purpose of this study.

## Interictal SEEG Data

SEEG was recorded with a Neuvo system (Compumedics, Abbotsford, Victoria, Australia). The sampling rate was 2 kHz and a low-pass filter with 800 Hz cut-off frequency was applied. For each patient, we selected a 1-h segment of slow-wave sleep, at least 2 h before and after a seizure. To determine if a contact was considered part of the seizure onset zone (SOZ), or not (non-SOZ), we used the judgement the independent clinical neurophysiologist made at the time of recording and clinical decision making.

## Detection of Interictal Epileptic Spikes and HFOs

We applied a recently developed automatic detector (23) to determine the rates of interictal epileptic spikes (IES), ripples (80–250 Hz), ripples co-occurring with spikes (IES-ripples), and fast ripples (250–500 Hz). This algorithm is based on a support vector machine, which is combined with a radial basis function kernel for non-linear classification. Simulated IES from a publicly available database (24) and visually identified HFOs were used for training. This detector has been tested against simulated and visually identified gold standards and, regarding HFOs, benchmarked against previously published algorithms. A detailed description of this method can be found in the original publication.

## Ratio R and $R_{\text{fast ripples}}$ in Individual Patients

We computed a ratio R of mean rates (hippocampus—neocortex)/(hippocampus + neocortex) for each of these events. Thus, we obtained an indicator of whether

- events were more frequent in the hippocampal lesion (R close to 1)
- more or less similar in the two lesions (R close to 0) or
- more frequent in the neocortical lesion (R close to −1).

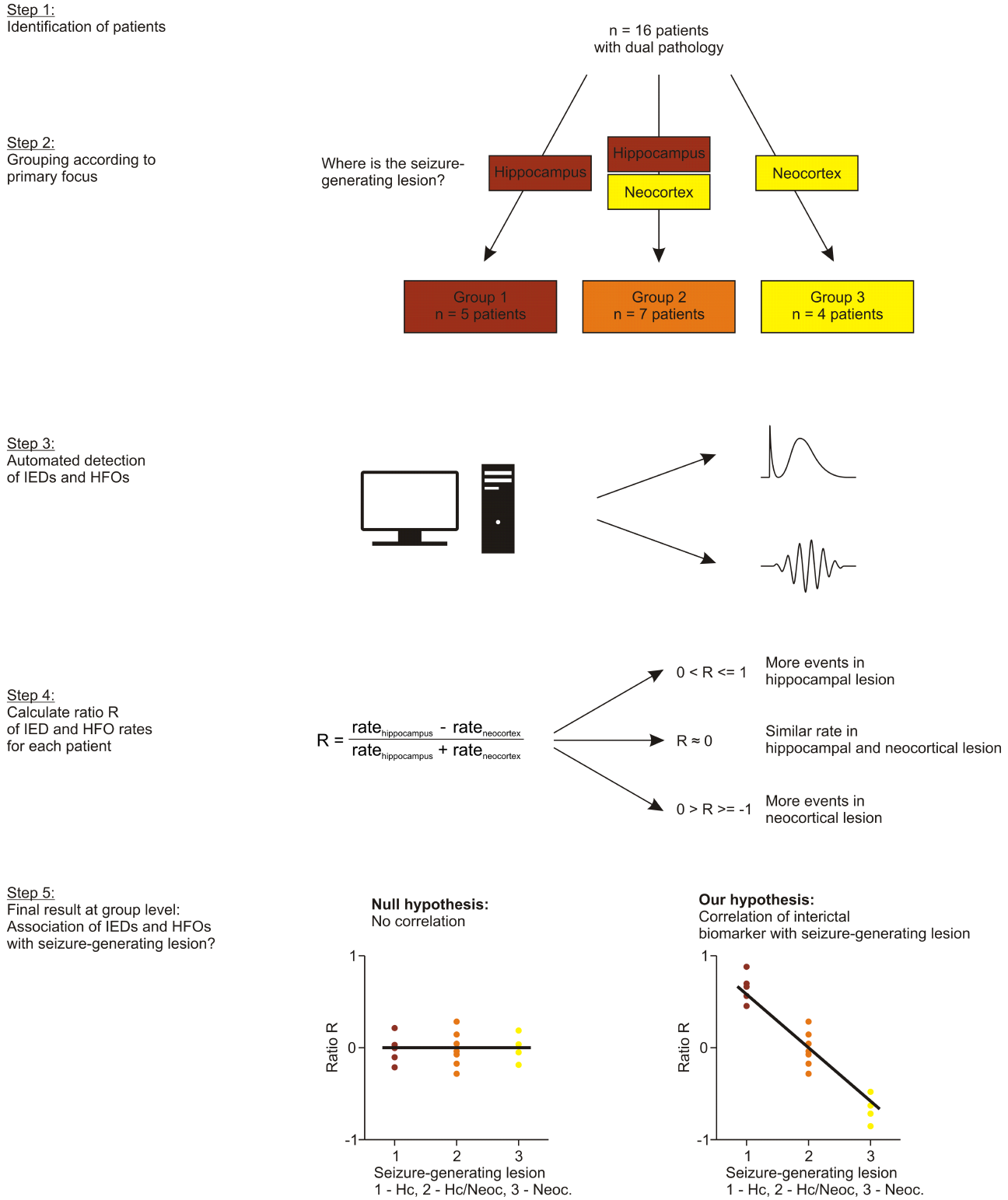


**FIGURE 1 |** Study design. Patients with dual pathology were identified (step 1) and grouped according their seizure-generating lesion, as revealed by ictal SEEG (step 2). We then performed automated detection of interictal spikes and HFOs (step 3) and computed a ratio of rates R to obtain an indicator of whether events were more frequent in the hippocampal lesion (R close to 1), more or less similar (R close to 0) or more frequent in the neocortical lesion (R close to −1) (step 4). Finally, we examined if this ratio R, i.e., occurrence of our interictal biomarkers, was associated with the group that the patients had been assigned to, i.e., their seizure-generating lesion (step 5).

**TABLE 1** | Clinical data.

| ID | Hemisphere | Hippocampal lesion | Neocortical lesion | Surgery | 12-month outcome (Engel class) | Seizure-generating lesion (group) |
|---|---|---|---|---|---|---|
| 1 | L | HS | FCD | / | / | 1 |
| 2 | R | HS | FCD | ATL | IIB | 1 |
| 3 | R | HS | Gliotic area/gray-white blurring | ATL | IA | 2 |
| 4 | R | HS | FCD | ATL | IA | 1 |
| 5 | L | Hc malformation | FCD | / | / | 2 |
| 6 | L | HS | FCD | EL + Hc resection | IB | 2 |
| 7 | R | HS | FCD | ATL | IIIA | 2 |
| 8 | R | HS | FCD | ATL | IIA[a] | 1 |
| 9 | R | HS | FCD | ATL | IA | 3 |
| 10 | R | HS | Gliotic area/gray-white blurring | ATL | IVB | 2 |
| 11 | L | Hc malformation | Meningoencephalocele | Temporal pole resection | IA | 3 |
| 12 | L | HS | Mild MCD | ATL | IA | 1 |
| 13 | R | Hc gliosis | FCD | ATL | IA | 3 |
| 14 | R | Hc gliosis | Meningoencephalocele | Temporal pole resection + AH | IA[a] | 3 |
| 15 | R | HS | Mild MCD | ATL | IA[b] | 2 |
| 16 | R | Hc gliosis | Mild MCD | ATL | IA[b] | 2 |

*If 12-month outcome was not available, 3-month[a] or 6-month[b] outcome has been specified. AH, amygdalohippocampectomy; ATL, anterior temporal lobectomy; EL, extended lesionectomy; FCD, focal cortical dysplasia; Hc, hippocampus; HS, hippocampal sclerosis; L, left; R, right; y, years.*

To explore the diagnostic value of fast ripple analysis in individual patients, those were finally ranked according to their $R_{fast\ ripples}$. If $R_{fast\ ripples}$ was an ideal biomarker, group 1 patients would have the top 5 values, group 3 patients the bottom 4 values, and group 2 patients would have values in between. For each subject, we thus determined retrospectively which primary focus might have been "predicted" as follows:

- $R_{fast\ ripples}$ among top 5: Seizures generated exclusively in the hippocampal lesion (group 1)
- $R_{fast\ ripples}$ among bottom 4: Seizures generated exclusively in the neocortical lesion (group 3)
- $R_{fast\ ripples}$ in between (i.e., not among top 5 or bottom 4): Seizures generated in both lesions (group 2).

## Statistical Analysis

A significance level of 5% was chosen. The data was considered to be not normally distributed. We therefore specified the median as a measure of central tendency and the range as a measure of dispersion. The two-sided Mann-Whitney-*U*-test was applied to compare unpaired data. We performed Spearman's rank order correlation to examine the relationship between the group to which our patients had been assigned, i.e., their seizure-generating lesion, and the ratio R, i.e., the proportion of interictal epileptic spikes or HFOs detected in this lesion. These analyses were performed using SPSS (IBM, Armonk, NY).

A permutation test was conducted to examine whether $R_{fast\ ripples}$ might have predicted the seizure-generating lesion in individual patients significantly better than chance [see e.g., (25, 26) for other examples of a permutation test]. To this end, we randomly shuffled the three group labels (5 × "1", 7 × "2", and 4 × "3") between our 16 patients and then determined the number of correct "predictions," which was between zero (no patient assigned correctly) and 16 (all patients assigned correctly). This procedure was repeated 100,000 times to compute a distribution of "surrogate" correct predictions. Finally, we compared our "empiric" number of correct predictions to this distribution to estimate the probability of obtaining such a result by chance. This part of our analysis was implemented in Matlab (Mathworks, Natick, MA).

# RESULTS

## Patients and Their Seizure-Generating Lesions

We reviewed 115 patients with drug-resistant focal epilepsy who, as part of their evaluation for epilepsy surgery, had undergone SEEG recordings. Sixteen subjects (8 females, 8 males; age: median 39 years, range 12–53 years, see **Table 1** for more clinical data) fulfilled inclusion criteria. The mesial temporal lesion was usually hippocampal sclerosis ($n = 11$), while the most frequent neocortical pathology was focal cortical dysplasia ($n = 9$) or a mild malformation of cortical development ($n = 3$). Most of our patients were treated by anterior temporal lobectomy, a minority received selective surgery of the hippocampal or neocortical lesion. We then grouped our patients according to their primarily seizure-generating lesion, as suggested by ictal SEEG: Seizures originated exclusively from the hippocampal lesion in five patients (group 1), from both hippocampus and neocortex in 7 patients (group 2) and exclusively from the neocortical lesion in four patients (group 3).

## Spike and HFO Rates in Hippocampal vs. Neocortical Lesions

First, we compared the rates of interictal epileptic spikes and HFOs between the two lesions. Spikes, ripples, ripples co-occurring with spikes (IES-ripples) and fast ripples occurred significantly more often in electrode contacts located in the hippocampal lesion as compared to the neocortical lesion (**Figure 2**; $p < 0.001$; hippocampus: $n = 60$, neocortex: $n = 124$ channels; Mann-Whitney-$U$-test). When seizure onset zone (SOZ) and non-SOZ channels were analyzed separately, a significant difference was found inside the SOZ (Spikes: $p < 0.05$, ripples: $p < 0.05$, IES-ripples: $p$

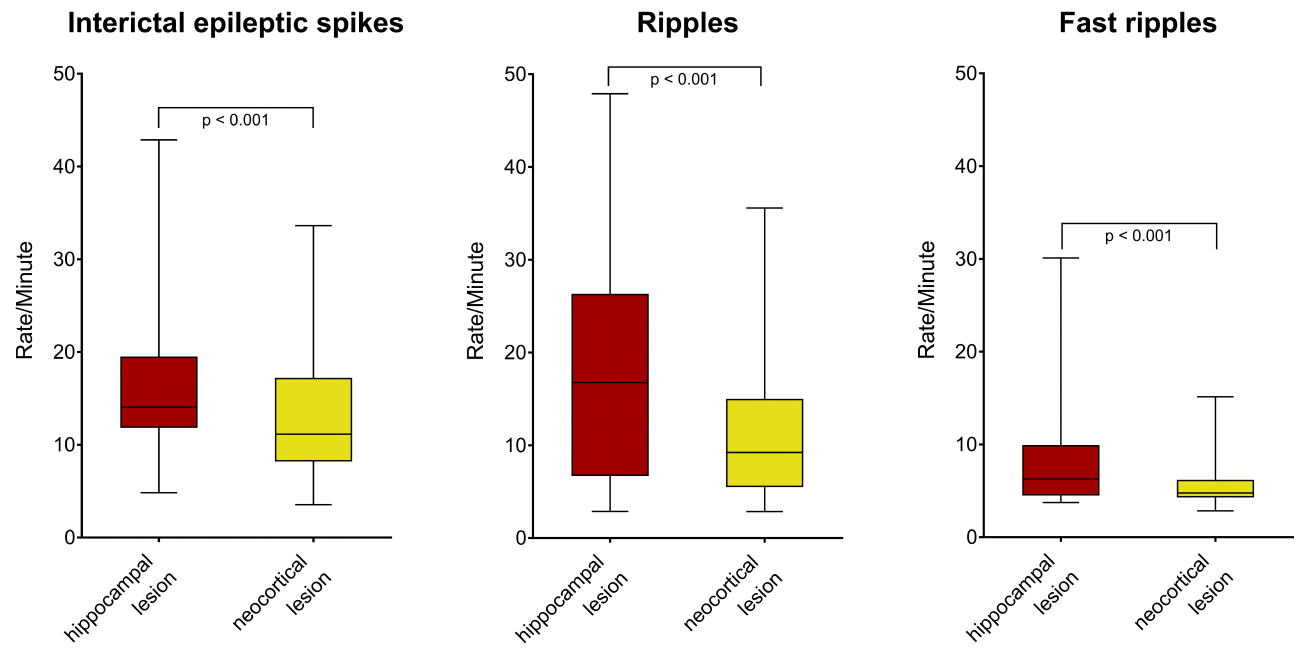


**FIGURE 2 |** Rates of interictal spikes and HFOs in hippocampal vs. neocortical lesion. Note that spikes **(left)**, ripples **(middle)**, and fast ripples **(right)** occurred more often in channels located in the hippocampal lesion.

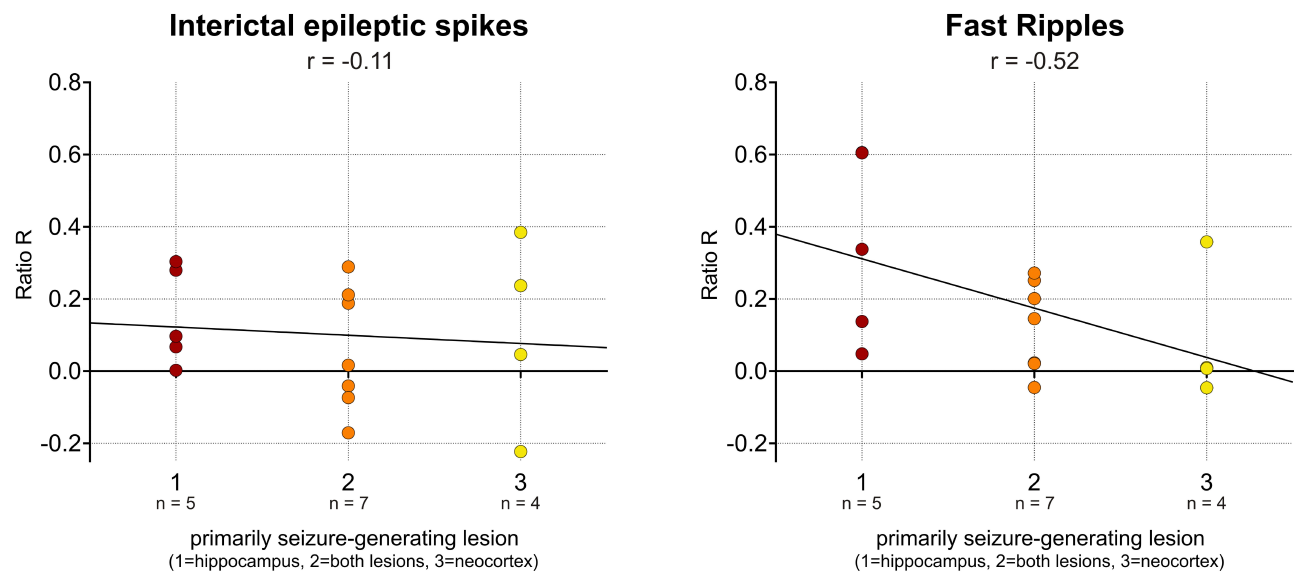


**FIGURE 3 |** Association of interictal fast ripples with seizure-generating lesion. No significant correlation was observed for interictal spikes **(left)**. Note the significant correlation between ratio R, i.e., the proportion of fast ripples detected in a lesion, and the group that the patient had been assigned to, i.e., its seizure-generating potential **(right)**.

$< 0.001$, fast ripples: $p < 0.01$; hippocampus: $n = 47$, neocortex $n = 46$ channels; Mann-Whitney-*U*-test), but not for non-SOZ contacts (Spikes: $p = 0.20$, ripples: $p = 0.93$, IES-ripples: $p = 0.61$, fast ripples: $p = 0.39$; hippocampus: $n = 13$, neocortex $n = 78$ channels). Hippocampal lesions thus tend to generate more spikes and HFOs than neocortical lesions—and this difference seems to be specific to SOZ channels.

## Correlation of Spike and HFO Rates With Seizure-Generating Lesion

Keeping in mind this finding, it seemed rather unlikely that finding a higher spike or HFO rate in a patient's hippocampal lesion would indicate that this lesion also generates seizures. We therefore calculated the ratio R for each subject and examined if R, i.e., the proportion of spikes or HFOs detected in a lesion, correlates with the group to which the patient had been assigned, i.e., seizure genesis in this lesion. Such a correlation was found for interictal fast ripples (**Figure 3**; $r = -0.52$; $p < 0.05$; Spearman's rank order correlation), but not for spikes ($r = -0.11$; $p = 0.69$), ripples ($r = -0.14$; $p = 0.60$), or IES-ripples ($r = -0.17$; $p = 0.54$). Of note, these analyses were performed on interictal data from all electrode contacts located in either of the two lesions—thus, R was calculated independent from any information on the patient's seizures. In summary, our findings suggest that $R_{fast\ ripples}$ is a biomarker which is specifically associated with the seizure-generating lesion.

## Diagnostic Value for Individual Patients

Finally, we aimed to explore whether an analysis of interictal fast ripples could be of diagnostic value for individual patients. If fast ripples were a good biomarker, $R_{fast\ ripples}$ would be high in most subjects with seizures originating from the hippocampal lesion and low in those with neocortical onset (**Figure 4**). As we retrospectively estimated performance by a data-based approach, we obtained correct "predictions" in 11 of our patients (69%; $p < 0.01$, permutation test; **Table 2**). Correct or incorrect predictions were not obviously linked to a distinct pathology. Thus, fast ripple analysis might classify above chance, but performance would be impaired due to the overlap between different groups.

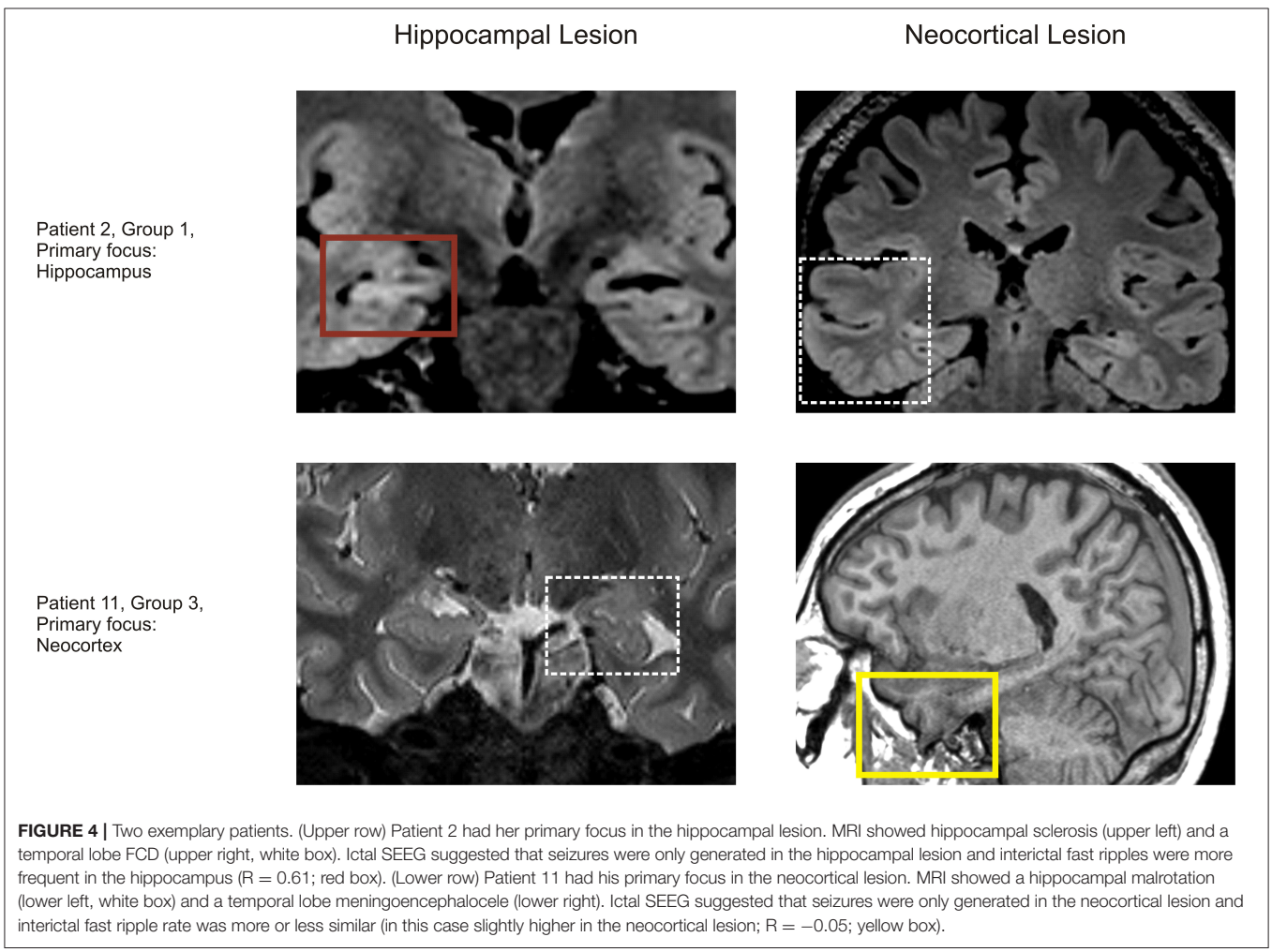


**FIGURE 4 |** Two exemplary patients. (Upper row) Patient 2 had her primary focus in the hippocampal lesion. MRI showed hippocampal sclerosis (upper left) and a temporal lobe FCD (upper right, white box). Ictal SEEG suggested that seizures were only generated in the hippocampal lesion and interictal fast ripples were more frequent in the hippocampus (R = 0.61; red box). (Lower row) Patient 11 had his primary focus in the neocortical lesion. MRI showed a hippocampal malrotation (lower left, white box) and a temporal lobe meningoencephalocele (lower right). Ictal SEEG suggested that seizures were only generated in the neocortical lesion and interictal fast ripple rate was more or less similar (in this case slightly higher in the neocortical lesion; R = −0.05; yellow box).

**TABLE 2 |** Interictal fast ripple analysis and seizure-generating lesion in individual patients.

| Ratio $R_{fast\ ripples}$ | Patient ID | Seizure-generating lesion (group), as revealed by ictal SEEG | Seizure-generating lesion (group), as "predicted" by ratio $R_{fast\ ripples}$ | Prediction correct? |
|---|---|---|---|---|
| 0.61 | 2 | 1 | 1 | Yes |
| 0.60 | 12 | 1 | 1 | Yes |
| 0.36 | 13 | 3 | 1 | No |
| 0.34 | 1 | 1 | 1 | Yes |
| 0.27 | 10 | 2 | 1 | No |
| 0.25 | 3 | 2 | 2 | Yes |
| 0.20 | 5 | 2 | 2 | Yes |
| 0.15 | 15 | 2 | 2 | Yes |
| 0.14 | 4 | 1 | 2 | No |
| 0.05 | 8 | 1 | 2 | No |
| 0.02 | 7 | 2 | 2 | Yes |
| 0.02 | 16 | 2 | 2 | Yes |
| 0.01 | 9 | 3 | 3 | Yes |
| 0.01 | 14 | 3 | 3 | Yes |
| −0.05 | 6 | 2 | 3 | No |
| −0.05 | 11 | 3 | 3 | Yes |

*To estimate the performance value of our tool, we ranked our subjects according to their ratio of rates R. For each individual, we then retrospectively determined if $R_{fast\ ripples}$ would have correctly "predicted" the seizure-generating lesion. An ideal biomarker would sort group 1 patients to the top of this table, group 3 patients to its bottom and group 2 patients in between. 11 patients (69%) were assigned correctly ($p < 0.01$). See Methods section for a detailed description of our approach.*

# DISCUSSION

The main novel findings of this study are that in patients with dual pathology (1) interictal spikes and HFOs are more frequent in the hippocampal pathology, particularly in seizure onset zone channels, (2) fast ripples are associated with the seizure-generating lesion, and (3) might have some diagnostic value for individual patients.

## Hippocampal Lesions Generate More Spikes and HFOs

We report that spike and HFO rates were higher in hippocampal than in neocortical lesions—and that this difference is specific to the seizure-onset zone (SOZ). This result is consistent with a previous study suggesting that HFOs are primarily an indicator of epileptogenicity (27, 28). Analyzing subjects with dual pathology, we could now directly compare biomarker occurrence between the two lesions. Most of our patients had hippocampal sclerosis and focal cortical dysplasia. Therefore, our results may not be representative of other pathologic entities, such as e.g., post-ischemic alterations or tumors. At the end, we can only speculate on the main reasons for which the seizure-generating portion of lesions in the hippocampus might generate more HFOs: Its complex architecture, with several distinct three-layered sub-regions, contrasts with six-layered neocortex in healthy individuals. Hippocampal sclerosis and focal cortical dysplasia are furthermore due to a fundamentally different pathogenesis. In some patients, it was hard to clearly delineate the neocortical lesion; it could thus be hypothesized that sometimes our electrodes did not record from tissue with maximum pathogenicity. Finally, the hippocampus is suited best for generation of physiological HFOs (29–31), and network alterations associated with epilepsy might exploit this machinery—a concept that has also been proposed e.g., for spike-wave seizures (32).

## Association Between Interictal Fast Ripples and Seizure-Generating Lesion

Since the hippocampus in general (31, 33), and hippocampal lesions in particular, tend to generate more HFOs than the neocortex, it is not trivial to compare the epileptogenicity of these two regions—observing slightly higher rates in the hippocampus e.g., does not indicate that this is the primary focus. Nevertheless, we report that in patients with dual pathology, the potential of a lesion to be seizure-generating correlates with its potential to generate fast ripples. This conclusion was based on calculations of the ratio R, which adjusts for the fact that hippocampal lesions have in general higher fast ripple rates. Such a correlation was not found for interictal spikes, ripples, or ripples co-occurring with spikes (IES-ripples). These findings are in line with previous work suggesting that HFOs might identify epileptogenic tissue better than spikes (9, 34). It is still subject to debate which of the HFO subgroups is suited best as a biomarker, but a popular notion is that ripples lack specificity, possibly because some of the events are physiological. One strategy to overcome this problem could be to analyze ripples associated with spikes, which may perform better in distinct clinical scenarios (23, 34). The other main approach has been to focus on fast (10) and very fast ripples (35, 36): Those might only rarely be physiological (31), thus be more specific, and also be involved in seizure generation (15, 16, 37). Our present study clearly supports this view of fast ripples as a biomarker with unique properties—at least in distinct clinical scenarios.

## Value for Clinical Decision-Making in Individual Patients

We report that two variables correlate at the group level. But from a clinician's point of view, the question is: Could this biomarker be useful for decision-making in individual patients? Presurgical workup in dual pathology aims to evaluate whether both lesions can generate seizures—if so, anterior temporal lobectomy is often recommended, whereas more restrictive surgery might be considered if concordant findings suggest that only one lesions has seizure-generating potential and even more if the second lesion is not clearly visible on MRI. Based on data obtained in this study, we estimated that interictal fast ripples might have correctly predicted the seizure-generating lesion in 69% of the patients. This approach permits only to crudely estimate the value of our tool, which seems to perform better than chance, but no better than traditional elements of presurgical evaluation. At

present, HFOs are rarely studied in a clinical routine setting, but we hope that application of a publicly available detector will promote such analyses. In summary, interictal fast ripples could be considered to obtain complementary information on seizure-generating networks—especially in cases with few or no recorded seizures.

### Limitations and Outlook

The current study has some limitations and additional work is needed to fully investigate the role of HFOs in patients with dual pathology. A sample size of 16 subjects only permits to detect pronounced differences. Besides, our study is purely retrospective. Especially when it comes to estimating the value of fast ripples in individual patients, we would have needed more subjects for a thorough analysis and our tool might have performed worse if tested in another sample of patients. Finally, it should be considered that the reference to which we compared our HFO data was the seizure-generating lesion, as determined by SEEG, and not post-surgical outcome because most of our patients were treated by anterior temporal lobectomy. This implies that patients grouped as "hippocampal" or "neocortical" could have seizures originating from the other lesion that had just not been captured—or that, after resection of the primary focus, the "secondary" lesion might start to generate seizures. These limitations can only be overcome by a larger, if possible prospective, study that relates HFO data to post-surgical seizure outcome. Before we move on to this step, it may be interesting to analyze additional aspects of HFOs, e.g., the temporal relationship between events from the two lesions. Such an approach could not only yield a diagnostic tool for dual pathology—it might in general delineate the role of HFOs in epileptogenic networks further.

## DATA AVAILABILITY STATEMENT

The data analyzed in this study is available on reasonable request. Requests to access these datasets should be directed to jan.schoenberger@yahoo.de.

## ETHICS STATEMENT

The studies involving human participants were reviewed and approved by Ethics Commission, University Medical Center Freiburg. Written informed consent to participate in this study was provided by the participants' legal guardian/next of kin.

## AUTHOR CONTRIBUTIONS

JS and JJ designed the study and wrote the manuscript. JS, CH, DL-P, KK, MD, AS-B, and JJ acquired and analyzed data and edited and approved the final version of the manuscript. JS, CH, AS-B, and JJ drafted the figures and tables. All authors contributed to the article and approved the submitted version.

## FUNDING

JS and KK were supported by the Berta-Ottenstein-Program for Clinician Scientists from the Faculty of Medicine, University of Freiburg. JJ was supported by the German Research Foundation (DFG; JA 1725/4-1).

## REFERENCES

1. Semah F, Picot MC, Adam C, Broglin D, Arzimanoglou A, Bazin B, et al. Is the underlying cause of epilepsy a major prognostic factor for recurrence? *Neurology.* (1998) 51:1256–62. doi: 10.1212/WNL.51.5.1256
2. Wiebe S, Blume WT, Girvin JP, Eliasziw M. A randomized, controlled trial of surgery for temporal-lobe epilepsy. *N Engl J Med.* (2001) 345:311–18. doi: 10.1056/NEJM200108023450501
3. Engel JJ, McDermott MP, Wiebe S, Langfitt JT, Stern JM, Dewar S, et al. Early surgical therapy for drug-resistant temporal lobe epilepsy: a randomized trial. *JAMA.* (2012) 307:922–30. doi: 10.1001/jama.2012.220
4. Berkovic SF, McIntosh AM, Kalnins RM, Jackson GD, Fabinyi GC, Brazenor GA, et al. Preoperative MRI predicts outcome of temporal lobectomy: an actuarial analysis. *Neurology.* (1995) 45:1358–63. doi: 10.1212/WNL.45.7.1358
5. Téllez-Zenteno JF, Ronquillo LH, Moien-Afshari F, Wiebe S. Surgical outcomes in lesional and non-lesional epilepsy: a systematic review and meta-analysis. *Epilepsy Res.* (2010) 89:310–18. doi: 10.1016/j.eplepsyres.2010.02.007
6. Lévesque MF, Nakasato N, Vinters HV, Babb TL. Surgical treatment of limbic epilepsy associated with extrahippocampal lesions: the problem of dual pathology. *J Neurosurg.* (1991) 75:364–70. doi: 10.3171/jns.1991.75.3.0364
7. Cook MJ, O'Brien TJ, Berkovic SF, Murphy M, Morokoff A, Fabinyi G, et al. Prediction of seizure likelihood with a long-term, implanted seizure advisory system in patients with drug-resistant epilepsy: a first-in-man study. *Lancet Neurol.* (2013) 12:563–71. doi: 10.1016/S1474-4422(13)70075-9
8. Bautista RE, Cobbs MA, Spencer DD, Spencer SS. Prediction of surgical outcome by interictal epileptiform abnormalities during intracranial EEG monitoring in patients with extrahippocampal seizures. *Epilepsia.* (1999) 40:880–90. doi: 10.1111/j.1528-1157.1999.tb00794.x
9. Jacobs J, Zijlmans M, Zelmann R, Chatillon C-E, Hall J, Olivier A, et al. High-frequency electroencephalographic oscillations correlate with outcome of epilepsy surgery. *Ann Neurol.* (2010) 67:209–20. doi: 10.1002/ana.21847
10. Wu JY, Sankar R, Lerner JT, Matsumoto JH, Vinters HV, Mathern GW. Removing interictal fast ripples on electrocorticography linked with seizure freedom in children. *Neurology.* (2010) 75:1686–94. doi: 10.1212/WNL.0b013e3181fc27d0
11. Höller Y, Kutil R, Klaffenböck L, Thomschewski A, Höller PM, Bathke AC, et al. High-frequency oscillations in epilepsy and surgical outcome. a meta-analysis. *Front Hum Neurosci.* (2015) 9:574. doi: 10.3389/fnhum.2015.00574
12. Jacobs J, Wu JY, Perucca P, Zelmann R, Mader M, Dubeau F, et al. Removing high-frequency oscillations. *Neurology.* (2018) 91:e1040–52. doi: 10.1212/WNL.0000000000006158
13. Zijlmans M, Jacobs J, Zelmann R, Dubeau F, Gotman J. High-frequency oscillations mirror disease activity in patients with epilepsy. *Neurology.* (2009) 72:979–86. doi: 10.1212/01.wnl.0000344402.20334.81
14. Perucca P, Dubeau F, Gotman J. Intracranial electroencephalographic seizure-onset patterns: effect of underlying pathology. *Brain.* (2014) 137:183–96. doi: 10.1093/brain/awt299
15. Weiss SA, Alvarado-Rojas C, Bragin A, Behnke E, Fields T, Fried I, et al. Ictal onset patterns of local field potentials, high frequency oscillations, and unit activity in human mesial temporal lobe epilepsy. *Epilepsia.* (2016) 57:111–21. doi: 10.1111/epi.13251
16. Schönberger J, Frauscher B, von Ellenrieder N, Avoli M, Dubeau F, Gotman J. Fast ripple analysis in human mesial temporal lobe epilepsy suggests two different seizure-generating mechanisms. *Neurobiol Dis.* (2019) 127:374–81. doi: 10.1016/j.nbd.2019.03.030

17. Schönberger J, Birk N, Lachner-Piza D, Dümpelmann M, Schulze-Bonhage A, Jacobs J. High-frequency oscillations mirror severity of human temporal lobe seizures. *Ann Clin Transl Neurol.* (2019) 6:2479–88. doi: 10.1002/acn3.50941
18. Staba RJ, Wilson CL, Bragin A, Fried I, Engel JJ. Quantitative analysis of high-frequency oscillations (80-500 Hz) recorded in human epileptic hippocampus and entorhinal cortex. *J Neurophysiol.* (2002) 88:1743–52. doi: 10.1152/jn.2002.88.4.1743
19. Zelmann R, Mari F, Jacobs J, Zijlmans M, Dubeau F, Gotman J. A comparison between detectors of high frequency oscillations. *Clin Neurophysiol.* (2012) 123:106–16. doi: 10.1016/j.clinph.2011.06.006
20. von Ellenrieder N, Andrade-Valenca LP, Dubeau F, Gotman J. Automatic detection of fast oscillations (40-200 Hz) in scalp EEG recordings. *Clin Neurophysiol.* (2012) 123:670–80. doi: 10.1016/j.clinph.2011.07.050
21. Dümpelmann M, Jacobs J, Kerber K, Schulze-Bonhage A. Automatic 80–250Hz "ripple" high frequency oscillation detection in invasive subdural grid and strip recordings in epilepsy by a radial basis function neural network. *Clin Neurophysiol.* (2012) 123:1721–31. doi: 10.1016/j.clinph.2012.02.072
22. Roehri N, Lina J-M, Mosher JC, Bartolomei F, Benar C-G. Time-frequency strategies for increasing high-frequency oscillation detectability in intracerebral EEG. *IEEE Trans Biomed Eng.* (2016) 63:2595–606. doi: 10.1109/TBME.2016.2556425
23. Lachner-Piza D, Jacobs J, Bruder JC, Schulze-Bonhage A, Stieglitz T, Dumpelmann M. Automatic detection of high-frequency-oscillations and their sub-groups co-occurring with interictal-epileptic-spikes. *J Neural Eng.* (2020) 17:16030. doi: 10.1088/1741-2552/ab4560
24. Roehri N, Pizzo F, Bartolomei F, Wendling F, Benar C-G. What are the assets and weaknesses of HFO detectors? A benchmark framework based on realistic simulations. *PLoS ONE.* (2017) 12:e0174702. doi: 10.1371/journal.pone.0174702
25. Fisher RA. *The Design of Experiments*. New York, NY: Hafner Publishing Company (1971).
26. Oostenveld R, Fries P, Maris E, Schoffelen J-M. FieldTrip: open source software for advanced analysis of MEG, EEG, and invasive electrophysiological data. *Comput Intell Neurosci.* (2011) 2011:1–9. doi: 10.1155/2011/156869
27. Jacobs J, Levan P, Chatillon C-E, Olivier A, Dubeau F, Gotman J. High frequency oscillations in intracranial EEGs mark epileptogenicity rather than lesion type. *Brain.* (2009) 132:1022–37. doi: 10.1093/brain/awn351
28. Jacobs J, Banks S, Zelmann R, Zijlmans M, Jones-Gotman M, Gotman J. Spontaneous ripples in the hippocampus correlate with epileptogenicity and not memory function in patients with refractory epilepsy. *Epilepsy Behav.* (2016) 62:258–66. doi: 10.1016/j.yebeh.2016.05.025
29. Buzsaki G, Horvath Z, Urioste R, Hetke J, Wise K. High-frequency network oscillation in the hippocampus. *Science.* (1992) 256:1025–7. doi: 10.1126/science.1589772
30. Foster DJ, Wilson MA. Reverse replay of behavioural sequences in hippocampal place cells during the awake state. *Nature.* (2006) 440:680–83. doi: 10.1038/nature04587
31. Frauscher B, von Ellenrieder N, Zelmann R, Rogers C, Nguyen DK, Kahane P, et al. High-frequency oscillations in the normal human brain. *Ann Neurol.* (2018) 84:374–85. doi: 10.1002/ana.25304
32. Blumenfeld H. Cellular and network mechanisms of spike-wave seizures. *Epilepsia.* (2005) 46(Suppl. 9):21–33. doi: 10.1111/j.1528-1167.2005.00311.x
33. Jacobs J, Vogt C, LeVan P, Zelmann R, Gotman J, Kobayashi K. The identification of distinct high-frequency oscillations during spikes delineates the seizure onset zone better than high-frequency spectral power changes. *Clin Neurophysiol.* (2016) 127:129–42. doi: 10.1016/j.clinph.2015.04.053
34. Kramer MA, Ostrowski LM, Song DY, Thorn EL, Stoyell SM, Parnes M, et al. Scalp recorded spike ripples predict seizure risk in childhood epilepsy better than spikes. *Brain.* (2019) 142:1296–309. doi: 10.1093/brain/awz059
35. Usui N, Terada K, Baba K, Matsuda K, Nakamura F, Usui K, et al. Very high frequency oscillations (over 1000 Hz) in human epilepsy. *Clin Neurophysiol.* (2010) 121:1825–31. doi: 10.1016/j.clinph.2010.04.018
36. Brázdil M, Pail M, Halamek J, Plesinger F, Cimbalnik J, Roman R, et al. Very high-frequency oscillations: novel biomarkers of the epileptogenic zone. *Ann Neurol.* (2017) 82:299–310. doi: 10.1002/ana.25006
37. Jirsch JD, Urrestarazu E, LeVan P, Olivier A, Dubeau F, Gotman J. High-frequency oscillations during human focal seizures. *Brain.* (2006) 129:1593–608. doi: 10.1093/brain/awl085

**Conflict of Interest:** The authors declare that the research was conducted in the absence of any commercial or financial relationships that could be construed as a potential conflict of interest.

The handling editor is currently organizing a Research Topic with one of the authors JJ.

*Copyright © 2020 Schönberger, Huber, Lachner-Piza, Klotz, Dümpelmann, Schulze-Bonhage and Jacobs. This is an open-access article distributed under the terms of the Creative Commons Attribution License (CC BY). The use, distribution or reproduction in other forums is permitted, provided the original author(s) and the copyright owner(s) are credited and that the original publication in this journal is cited, in accordance with accepted academic practice. No use, distribution or reproduction is permitted which does not comply with these terms.*

frontiers in Neurology

ORIGINAL RESEARCH
published: 19 October 2020
doi: 10.3389/fneur.2020.563577

# Automatic vs. Manual Detection of High Frequency Oscillations in Intracranial Recordings From the Human Temporal Lobe

*Aljoscha Thomschewski[1,2,3]*, Nathalie Gerner[1], Patrick B. Langthaler[1,2], Eugen Trinka[1], Arne C. Bathke[2,4], Jürgen Fell[5] and Yvonne Höller[6]*

*[1] Department of Neurology, Christian-Doppler Medical Center, Paracelsus Medical University, Salzburg, Austria, [2] Department of Mathematics, Paris-Lodron University of Salzburg, Salzburg, Austria, [3] Department of Psychology, Paris-Lodron University of Salzburg, Salzburg, Austria, [4] Intelligent Data Analytics Lab Salzburg, Paris-Lodron University of Salzburg, Salzburg, Austria, [5] Department of Epileptology, University Hospital Bonn, Bonn, Germany, [6] Faculty of Psychology, University of Akureyri, Akureyri, Iceland*

**Background:** High frequency oscillations (HFOs) have attracted great interest among neuroscientists and epileptologists in recent years. Not only has their occurrence been linked to epileptogenesis, but also to physiologic processes, such as memory consolidation. There are at least two big challenges for HFO research. First, detection, when performed manually, is time consuming and prone to rater biases, but when performed automatically, it is biased by artifacts mimicking HFOs. Second, distinguishing physiologic from pathologic HFOs in patients with epilepsy is problematic. Here we automatically and manually detected HFOs in intracranial EEGs (iEEG) of patients with epilepsy, recorded during a visual memory task in order to assess the feasibility of the different detection approaches to identify task-related ripples, supporting the physiologic nature of HFOs in the temporal lobe.

**Methods:** Ten patients with unclear seizure origin and bilaterally implanted macroelectrodes took part in a visual memory consolidation task. In addition to iEEG, scalp EEG, electrooculography (EOG), and facial electromyography (EMG) were recorded. iEEG channels contralateral to the suspected epileptogenic zone were inspected visually for HFOs. Furthermore, HFOs were marked automatically using an RMS detector and a Stockwell classifier. We compared the two detection approaches and assessed a possible link between task performance and HFO occurrence during encoding and retrieval trials.

**Results:** HFO occurrence rates were significantly lower when events were marked manually. The automatic detection algorithm was greatly biased by filter-artifacts. Surprisingly, EOG artifacts as seen on scalp electrodes appeared to be linked to many HFOs in the iEEG. Occurrence rates could not be associated to memory performance, and we were not able to detect strictly defined "clear" ripples.

**Conclusion:** Filtered graphoelements in the EEG are known to mimic HFOs and thus constitute a problem. So far, in invasive EEG recordings mostly technical artifacts and filtered epileptiform discharges have been considered as sources for these "false" HFOs.

OPEN ACCESS

***Edited by:***
*Julia Jacobs,*
*University of Freiburg Medical Center, Germany*

***Reviewed by:***
*Giovanni Pellegrino,*
*McGill University, Canada*
*Xiaofeng Yang,*
*Beijing Institute for Brain Disorders, China*

****Correspondence:***
*Aljoscha Thomschewski*
*a.thomschewski@salk.at*

***Specialty section:***
*This article was submitted to Epilepsy, a section of the journal Frontiers in Neurology*

***Received:*** *22 May 2020*
***Accepted:*** *26 August 2020*
***Published:*** *19 October 2020*

***Citation:***
*Thomschewski A, Gerner N, Langthaler PB, Trinka E, Bathke AC, Fell J and Höller Y (2020) Automatic vs. Manual Detection of High Frequency Oscillations in Intracranial Recordings From the Human Temporal Lobe. Front. Neurol. 11:563577. doi: 10.3389/fneur.2020.563577*

The data at hand suggests that even ocular artifacts might bias automatic detection in invasive recordings. Strict guidelines and standards for HFO detection are necessary in order to identify artifact-derived HFOs, especially in conditions when cognitive tasks might produce a high amount of artifacts.

**Keywords: high-frequency oscillations, visual memory, invasive EEG, electroencephalography, epilepsy**

# 1. INTRODUCTION

High frequency oscillations (HFOs) have gained considerable interest amongst neurologists and neuroscientists in the last decade. These relatively new electroencephalographic (EEG) markers are defined as single events of at least four oscillations with a frequency above 80 Hz that clearly stand out from the background EEG (1). Classically, HFOs have further been divided into two subgroups: ripples (80–250 Hz) and fast ripples (250–500 Hz; 2). Given these criteria, a high signal-to-noise ratio is key when attempting to detect HFOs. Hence, the first findings of HFOs stem from invasive EEG (iEEG) recordings with micro- or macroelectrodes (2–7).

As these recordings are only performed during presurgical evaluation in patients with drug resistant epilepsies, their occurrence has naturally been studied and linked to epilepsy and many findings indicate a link between HFOs and epileptogenity, both during ictal (8, 9) and interictal states (10–12). Besides there association with epilepsy, several studies also suggested an existence of a second HFO population, reflecting physiologic processes (3, 13–17). Especially entorhinal and hippocampal ripples have been associated with memory consolidation in animals (18, 19) and humans (20–23).

Albeit these numerous investigations, the detection of HFOs remains a highly debatable subject, and many aspects need to be considered. Besides technical considerations regarding the signal-to-noise ratio and data sampling (24–26), choosing the actual method of detection can be difficult. Considering the mentioned criteria (1), visual inspection requires enlarging the signal both in time scale and amplitude in order to discern these discrete events from the background EEG (27). Screening the data in such a way is highly time-consuming and visual detection can further be biased by the raters' subjective assessment of what "clearly stands out from the background EEG" (28, 29).

In contrast, automatic HFO detection is fast and objective. In facts, there exist a plethora of automatic detection algorithms for HFOs (30–34). Though considerably minimizing the time necessary to perform HFO detection, automatic detectors are prone to biases from signal artifacts (35–39), and they are seldom accurate on datasets they have not been trained on (24, 40). Furthermore, automatic detection algorithms are unable to differentiate between HFOs occurring as single elements and HFOs that are coupled with epileptiform discharges.

Given its more adaptive and strict results, manual detection may thus be necessary when dealing with data containing different (physiologic and pathologic) HFO populations and artifacts. For instance, when wanting to detect physiologic HFOs that are evoked by cognitive paradigms in patients with epilepsy. In the study at hand, we analyzed such a dataset. Using a dataset described by Axmacher et al. (20), we investigated stimulus-induced HFOs during encoding and retrieval to demonstrate possible differences between the two approaches of HFO detection, as well as to take advantage of the high sensitivity of automatic detectors and the specificity of a manual review when trying to link ripple occurrence to memory performance.

For this purpose, we assessed for both detection approaches: (1) whether ripple occurrence rates during encoding or retrieval phases differed between correct and incorrect responses in the memory task; (2) whether the event rates detected during encoding were predictive for the performance in the subsequent retrieval trials on a trial level; and (3) whether the amount of detected events was related to the response times in the memory task. We hypothesized the results to differ between automatically detected and manually detected events. Assuming that automatic detection results in less valid detections, we hypothesized that event rates revealed no or less of an association with memory performance as compared to events detected visually. Confirming our hypothesis would emphasize the importance for an accurate detection in order to differentiate physiologic, e.g., memory-related, from pathologic HFOs.

# 2. METHODS

## 2.1. Subjects and Experimental Procedure

Ten patients with pharmacoresistant temporal lobe epilepsies (five women, mean age = 39.4 years, SD = 10.83), enrolled in a study that took place at the University Hospital Bonn between 2004 and 2006, were retrospectively analyzed. All patients received bilateral intracranial EEG (iEEG) recordings for presurgical evaluation. Patients enrolled in the study were asked to perform a visual memory task on a recording day previous to which no seizures had been experienced for 24 h. Detailed information on the patient sample may be found in **Table 1**. The study was approved by the local ethics committee, and all patients gave written informed consent before participating.

The visual working memory task contained two encoding as well as one retrieval phase, intertwined by a nap time. During encoding, patients were presented with 80 pictures of either landscapes or houses. Each image was presented for 1,200 ms with a variable interstimulus interval of 1,800 $\pm$ 200 ms. In order to ensure that patients stayed focused they were asked to indicate via button press whether they saw an image depicting a house or landscape. After this initial encoding phase, patients were asked to rest in a darkened room for 60 min and try to nap. Following a pause of 15 min after this period of resting there was another encoding phase with 80 novel images. After another break of 15 min, patients were presented with all 160 images they

**TABLE 1 |** Patient information.

| Subject | Age (years) | Gender | Structural lesion | Seizure type(s) | Onset age | SOZ (iEEG) | Further remarks |
|---|---|---|---|---|---|---|---|
| P1 | 45 | f | Hippocampal sclerosis right | Focal non-motor impaired awareness seizures | 13 | Right temporo-mesial | |
| P2 | 34 | m | Hippocampal sclerosis right | Focal non-motor impaired awareness seizures + ftbTCS | n\a | Right temporo-mesial | |
| P3 | 54 | m | Hippocampal sclerosis left | Focal aware non-motor seizures + focal motor impaired awareness seizures + ftbTCS | 9 | Left temporo-mesial | |
| P4 | 33 | f | Hippocampal sclerosis + hypometabolism (FDG) temporal left | Focal non-motor impaired awareness seizures + ftbTCS | n\a | Left temporo-mesial | Left sided speech dominance (WADA) |
| P5 | 44 | f | MRI negative; hypometabolism (FDG) temporo-polar left | Focal aware non-motor seizures | 18 | Left temporo-polar | Right handed |
| P6 | 46 | m | Hippocampal sclerosis + hypometabolism (FDG) temporal mesial and polar left | Focal motor and non-motor impaired awareness seizures | 11 | Left temporo-mesial | Right handed, bilateral speech (WADA) |
| P7 | 47 | m | Hippocampal sclerosis right; discrete hypometabolism (FDG) temporo-polar left | Focal aware motor seizures + ftbTCS | n\a | Right temporo-mesial | |
| P8 | 45 | m | Hippocampal sclerosis and hypometabolism (FDG) temporal right | Focal non-motor impaired awareness seizures | 6 | Bitemporal | |
| P9 | 18 | f | Hippocampal sclerosis left | Focal motor and non-motor impaired awareness seizures | n\a | Most prominently left temporo-mesial | Hint of right-sided hippocampal sclerosis |
| P10 | 28 | f | Hippocampal sclerosis and temporo-polar dysplasia right | Focal motor impaired awareness seizures | n\a | Right temporo-mesial | Ictal aphasia |

*SOZ, seizure onset zone; iEEG, intracranial electroencephalography; f, female; m, male; ftbTCS, focal to bilateral tonic clonic seizures; FDG, fluorodeoxyglucose; MRI, magnetic resonance imaging.*

had learned previously plus an addition of 80 unlearned images. During this retrieval phase, patients were asked to indicate whether they recognized the presented images from the encoding phases before.

## 2.2. iEEG Recordings and HFO Detection

Invasive EEG recordings were performed via inserted multicontact depth electrodes (AD-Tech; 10 platinum-iridium contacts each). Depth electrodes were inserted from a posterior approach into the hippocampus and rhinal cortex, and electrode locations were documented via post-implantation MRI scans. Furthermore, six patients (patients 1, 4, 5, 6, 8, and 10) received also ECoG (24–102 channels, mean = 45.67) recordings, covering additional temporal lobe areas. In all of these cases, strips covered at least the anterior temporal cortex as well as the lateral temporal cortex. Patients 6 and 10 only received unilateral depth electrode implantations, but had additional large ECoG grids over the respective other hemisphere. In patient 10, depth electrodes were implanted in the left hemisphere and thus could be included in the analyses. In addition to the described invasive EEG recordings, 3–7 scalp electrodes, vertical and horizontal eye movements, an ECG, as well as a facial electromyogram were recorded in each patient during the experiment. Invasive EEG channels were recorded at a sampling rate of 1,000 Hz, and a linked mastoid signal served as reference.

For each patient one encoding and the respective retrieval session were exported to .edf format and then imported to an in-house built software called MEEGIPS (41), for HFO detection. The individual encoding recordings lasted between 305 and 387 s (mean = 329.3 s), whereas the retrieval phase lasted between 903 and 1,011 s (mean = 927 s). On average, HFO analysis was performed on 21 min of EEG data for each participant. The imported EEG data was then analyzed in two ways. First, events of interest were marked visually by one experienced rater, and second, another person conducted an automatic HFO detection.

For visual inspection, the EEG data, as well as additional EMG, ECG, and EOG channels, were prepared in two ways: First, the data was high-pass filtered at 0.1 Hz, and a FIR multiline band reject filter was applied in order to filter out the powerline noise at 50 Hz as well as its respective harmonics. This data was considered the "raw signal." Second, the data was filtered between 80 and 250 Hz to extract the ripple-band signal, which will be referred to hereafter as the "filtered EEG." For inspection, both of these signals were displayed next to each other on a screen, and the time cursor was synchronized. Up to eight iEEG channels at a time and the additional EMG, ECG, and EOG channels were visually inspected. In addition to the EEG signals, small windows for the empirical mode decomposition, the discrete Fourier transform, the discrete wavelet power density, and the continuous wavelet transform, calculated from any marked

segment of the raw signal, were displayed on the right of the screen. iEEG channels with continuous artifacts corrupting the signal and channels with a generally poor signal-to-noise ratio were excluded.

Ripples were then marked according to the following criteria: (1) consisting of at least four consecutive oscillations both seen in the filtered signal and in the empirical mode decomposition; (2) displaying a regular morphology clearly discernable from the background EEG; (3) revealing an isolated "blob" either in the discrete wavelet power density (DWPD) or in the continuous wavelet transformed signal (CWT; 37); (4) showing a superimposed fast activity in the raw data; and (5) not directly linked to artifacts observed in the EEG, EMG, ECG or EOG channels. Based on these criteria three event categories were identified and marked: (i) ripples, fulfilling all criteria; (ii) unclear HFOs (uHFO), events that did not meet all criteria based on signal quality or unclear evidence of artifacts; and (iii) artifacts, generating ripples meeting the described criteria except the last one. All detected ripples and uHFOs were additionally discussed in the team in order to rigorously exclude all false positive events.

For the automatic detection, the data was decomposed into empirical mode functions (two intrinsic mode functions with a maximum of 100 iterations; 42). Events of interest were detected using an RMS detector with a sliding window size of 10 samples and 1-s-sized statistics segments. The properties for events of interest were fixed as follows: minimum duration of $\geq$12 ms; RMS transition threshold of 2SD and a peak threshold of 3SD. Events separated by $<$30 ms were combined taken into account a standard deviation square root. The detected events were then classified based on Stockwell's S-transformation (43) for the frequency range of 80–250 Hz, and a Tukey window was applied to segments 1 s around the center of each event of interest. Events of interest were classified as ripples (autoR) based on a maximum power ratio between the trough and the high-frequency peak of 90%, and a minimum high-frequency to low-frequency peak ratio of 20%. The process of automated HFO detection using these methods has been described in detail by Burnos et al. (44).

## 2.3. Statistical Analysis

The events, detected automatically and visually, were then exported together with the experimental markers and analyzed using MATLAB (release R2019a, The Mathworks, Massachusetts, USA). Rates for all autoR, ripples, uHFO, artifacts, as well as all events detected manually in cumulation were summarized for each encoding and retrieval trial and for each individual patient. Trials were defined as segments starting with stimulus onset and lasting until either patients responded via button press or the next stimulus was presented. In a next step, retrieval trials were paired with their respective encoding trials and grouped into trials with correctly and incorrectly retrieved items (i.e., correct "old" vs. incorrect "new" decisions for previously presented items). Finally, the event rates were related to the respective number of trials and iEEG channels per patient as well as to the lengths of each trial. Thus, we ended up with relative event rates for encoding and retrieval trials corrected for the trial lengths in seconds and for the number of iEEG channels analyzed. For statistical analysis, only events from temporal sites within the hemisphere contralateral to the suspected epileptic zone were considered. In patient 8, we considered the right hemisphere to contain the epileptogenic zone due to the imaging findings, despite seizure onset zones observed in both temporal lobes.

The resulting event matrices were imported into R (45). Statistical analysis aimed at answering three questions to test the general hypothesis. First, we wanted to investigate whether there was a general difference between correct and incorrect trials for the rates of detected events during the retrieval phase. For this purpose, the mean event rates for correct and incorrect trials during retrieval for each patient were entered into a rank-based ANOVA-type test from the package "nparLD" (46) with the two within-subject factors response accuracy (correct vs. incorrect) and event type (all manual events, artifacts, uHFOs, ripples, autoR).

Second, we analyzed whether the rate of events detected during encoding was predictive for the correctness in the subsequent retrieval trials on a trial level. For this purpose, we calculated a generalized linear model with the retrieval trial accuracy as dependent variable and the event rates as predictive factor. Patients were considered as a random factor, in order to take into account variations in baseline events across subjects. Furthermore, we calculated Kendall's correlation between the number of correct trials and the mean event rates per second and estimated a confidence interval using the bias corrected and accelerated bootstrap method with 10,000 bootstrap samples to assess an effect at the group level.

Third, we tested whether the amount of detected events during encoding or retrieval impacted the response time in the retrieval phase. For this we calculated Kendall's correlation between response times and event occurrence rates for each patient individually. We then tested the null hypothesis that the median of these correlations was zero, using a sign test/binomial test: The fact that under the null hypothesis, the number of correlations smaller than zero follows a binomial distribution with probability 0.5 allows for an easy calculation of $p$-values. Correcting for multiple comparisons (13 statistically significance tests) using the Bonferroni method, the adjusted p-threshold was set at 0.0038, in order to avoid an increased family wise error rate.

# 3. RESULTS

All event rates per second for both encoding and the corresponding correct or incorrect retrieval trials are presented in **Table 2**. No events fulfilled all five criteria to being marked as ripples in the channels of interest. We did detect a small number of unclear HFOs in some of the patients that adhered to most criteria, but could potentially be connected to non-cerebral electrophysiological origins. **Figure 1** shows such an uHFO, whereas a clear ripple detected on the ipsilateral site of the suspected epileptic focus in patient 6 is depicted in **Figure 2**. Notably, not all trials could be taken into consideration, as there were some missing responses during retrieval in patients 1, 2, 5, and 8.

Regarding possible differences in event occurrence rates during retrieval, we did not observe a difference between correct

**TABLE 2 |** Event rates per second and iEEG channel, detected during encoding and retrieval in correct (top rows) and incorrect (bottom rows) trials.

| Subject | Chans. | Trials | Resp. time | Encoding events/sec. | | | | Retrieval events/sec. | | | |
|---|---|---|---|---|---|---|---|---|---|---|---|
| | | | | autoR | Man. events | Artifact | uHFOs | autoR | Man. events | Artifact | uHFOs |
| P1 | 24 | 36 | 1.312 | 0.657 | 0.017 | 0.017 | 0 | 0.735 | 0 | 0 | 0 |
| | | 43 | 1.428 | 0.657 | 0.021 | 0.021 | 0 | 0.682 | 0.018 | 0.018 | 0 |
| P2 | 10 | 35 | 1.208 | 0.353 | 0.188 | 0.188 | 0 | 0.376 | 0.071 | 0.071 | 0 |
| | | 41 | 1.2 | 0.261 | 0.065 | 0.065 | 0 | 0.258 | 0 | 0 | 0 |
| P3 | 10 | 28 | 0.99 | 0.544 | 0.089 | 0.053 | 0.035 | 0.711 | 0 | 0 | 0 |
| | | 28 | 1.032 | 0.605 | 0.051 | 0.019 | 0.033 | 0.696 | 0.049 | 0.042 | 0.007 |
| P4 | 24 | 44 | 0.953 | 0.535 | 0.061 | 0.058 | 0.004 | 0.633 | 0.014 | 0.014 | 0 |
| | | 36 | 0.943 | 0.668 | 0.077 | 0.069 | 0.009 | 0.656 | 0.023 | 0.023 | 0 |
| P5 | 24 | 47 | 0.931 | 0.247 | 0.032 | 0.029 | 0.003 | 0.531 | 0.012 | 0.012 | 0 |
| | | 32 | 1.101 | 0.295 | 0.011 | 0.01 | 0.001 | 0.498 | 0.024 | 0.024 | 0 |
| P6 | 40 | 17 | 0.915 | 1.048 | 0.077 | 0.055 | 0.022 | 0.904 | 0.127 | 0.122 | 0.005 |
| | | 63 | 0.851 | 0.992 | 0.112 | 0.09 | 0.023 | 0.816 | 0.059 | 0.057 | 0.002 |
| P7 | 10 | 29 | 0.965 | 0.32 | 0.127 | 0.127 | 0 | 0.55 | 0.072 | 0.072 | 0 |
| | | 27 | 0.923 | 0.362 | 0.191 | 0.191 | 0 | 0.417 | 0.04 | 0.04 | 0 |
| P8 | 22 | 2 | 0.997 | 0.521 | 0 | 0 | 0 | 0.365 | 0.023 | 0.023 | 0 |
| | | 42 | 1.152 | 0.448 | 0.077 | 0.077 | 0 | 0.512 | 0.015 | 0.015 | 0 |
| P9 | 10 | 30 | 1.044 | 0.447 | 0 | 0 | 0 | 0.444 | 0 | 0 | 0 |
| | | 26 | 1.082 | 0.525 | 0 | 0 | 0 | 0.555 | 0 | 0 | 0 |
| P10 | 24 | 17 | 1.221 | 0.211 | 0.124 | 0.124 | 0 | 0.55 | 0.114 | 0.144 | 0 |
| | | 63 | 1.139 | 0.239 | 0.25 | 0.25 | 0 | 0.37 | 0.071 | 0.071 | 0 |

**Chans., Nr. of channels; Trials, Nr. of trials; Resp. time, mean response time during retrieval; autoR, automatically detected ripples; man. events, all manually detected events; uHFOs, unclear HFOs.*

and incorrect trials ($F_{1,\infty}$ = 0.108, $p$ = 0.743). There was, however, a main effect for the event type ($F_{1.291,\infty}$ = 81.514, $p < 0.001$). As can be seen in **Figure 3**, automatic ripple detection resulted in higher rates across all subjects, regardless of trials being correct or incorrect. Finally, we did not observe an interaction effect between response type and event type ($F_{1.138,\infty}$ = 0.135, $p$ = 0.746). This difference between event types, to some degree, possibly stems from artifactual HFO-like events being marked as ripples. In fact, we have observed plenty of artifacts to mimic HFOs even in the iEEG channels. Especially eye-movements often resulted in such artifactual ripples (see **Figure 4** for an example).

A higher event rate for automatically detected events was also observed when looking at event rates during encoding. Considering single encoding trials in relation to performance in the corresponding retrieval trials later on, one does not detect an effect for correct vs. incorrect responses (see **Figure 5**). As such, analysis revealed no predictive values for any of the event types detected during encoding with regards to the later response: autoR ($z = -0.767$, $p = 0.443$), manual events ($z = -0.515$, $p = 0.607$), artifacts ($z = -0.475$, $p = 0.635$), uHFOs ($z = -0.337$, $p = 0.736$). Different baseline rates for patients were taken into account for this analysis, as we expected general differences across patients (see **Figure 6**). However, in none of the patients the event rate during encoding seemed to affect the response in the respective retrieval trials.

Estimated group correlations between event rates and the number of correct trials corrected for the overall number of trials per patient was weak for all event types. Automatically detected event rates revealed no direction of correlation ($\tau = 0$; CI: −0.684–0.563). Ripple-mimicking artifacts were, however, slightly negatively correlated ($\tau = -0.27$; CI: −0.73–0.15), which also is mirrored in the correlation of all manual events ($\tau = -0.18$; CI: −0.537–0.373). In contrast, uHFOs did not reveal a negative correlation with the number of correct trials ($\tau = 0.083$; CI: −0.462–0.632).

Finally, we analyzed a relationship between response times and event rates during retrieval trials as well as during the respective encoding trials. The median correlation coefficients for each patient are depicted in **Figure 7**. Probability testing suggested a trend for retrieval trials with more artifacts and respectively more overall manual events to be longer (both with $Md\ \tau$ = 0.094, $p$ = 0.039). Other than that, no relationships between event rates and response times for any of the event occurrence rates more extreme than the random binomial probability of 0.5 have been found.

## 4. DISCUSSION

In the present study we aimed at assessing a relationship between the occurrence of stimulus-induced ripples and performance in a visual memory task in order to evaluate two detection approaches for HFOs. We incorporated both, automatic and manual ripple detection and analyzed the iEEG during encoding and retrieval periods of a task, that had previously been reported

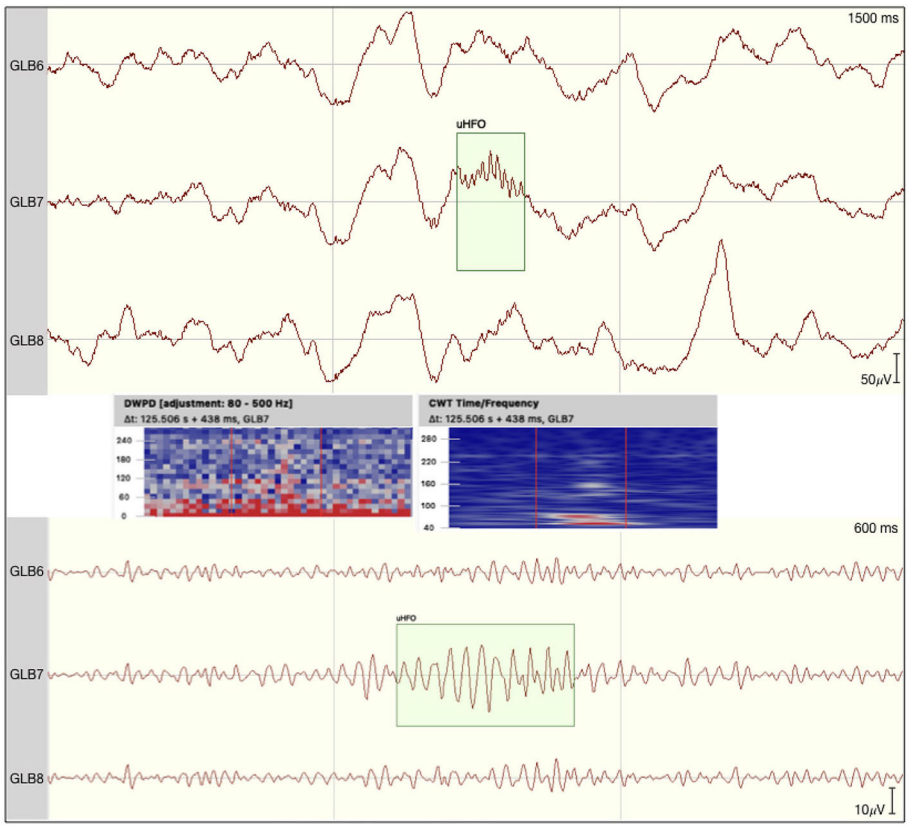


**FIGURE 1 |** Event of interest defined as unclear HFO by the team as morphology was not regular. Time frequency analyses revealed no clear blob suggesting the potential ripple to be nested in an equally high-frequency noise. The raw signal is depicted at the top with the discrete wavelet power density and the continuous wavelet transformation plotted underneath. At the bottom the signal is filtered between 80 and 250 Hz.

to induce meaningful HFOs in the resting period between the task phases (20).

Importantly, manual detection did not reveal any events to occur in the iEEG channels contralateral to the suspected epileptogenic zone fulfilling all strict criteria defined for ripples. In contrast, automatic detection revealed significantly higher numbers of events detected in the chosen segments. This discrepancy seems to be caused by a high number of artifacts falsely detected as ripples. In any case, statistical analysis, did not reveal a relationship between task performance and event occurrence rates derived from either detection approach. There was no significant difference between correct and incorrect trials, and also event occurrence during encoding was not predictive of the accuracy in the respective retrieval trials. Furthermore, analyses did not suggest an association between event rates and the time needed to respond during retrieval, either.

In the first part of this section we will elaborate on the incorporated detection strategies, and discuss discrepancies in the detected ripple rates, taking into account important sources of falsely detected events. In the second part, we will briefly discuss physiologic explanations for our findings, especially the lack of manually detected ripple events. Finally, we will consider some limitations to this investigation before drawing an overall conclusion.

## 4.1. Manual vs. Automatic Detection of HFOs

Ever since the first examinations of HFOs, the exact way of detection has left room for debate. The gold standard of visual data inspection and manual marking by one or more raters is highly uneconomic in terms of time and resources needed (12). Furthermore, detecting events that are defined as clearly discernible from the background EEG is subjective, introducing a bias that can be well-appreciated when considering the high variability in events detected by different raters on the same data (29).

Several automatic detection algorithms have been developed to overcome these problems (25, 30–34), making it easier than ever to conduct HFO analyses. However, automatic detection algorithms are not without flaws in their own respect. First of all, algorithms are usually developed and trained on specific data sets, leading to them offering good results in optimal conditions, i.e., a high signal-to-noise ratio and relatively clean data (24, 40). Furthermore, for each algorithm there are numerous settings,

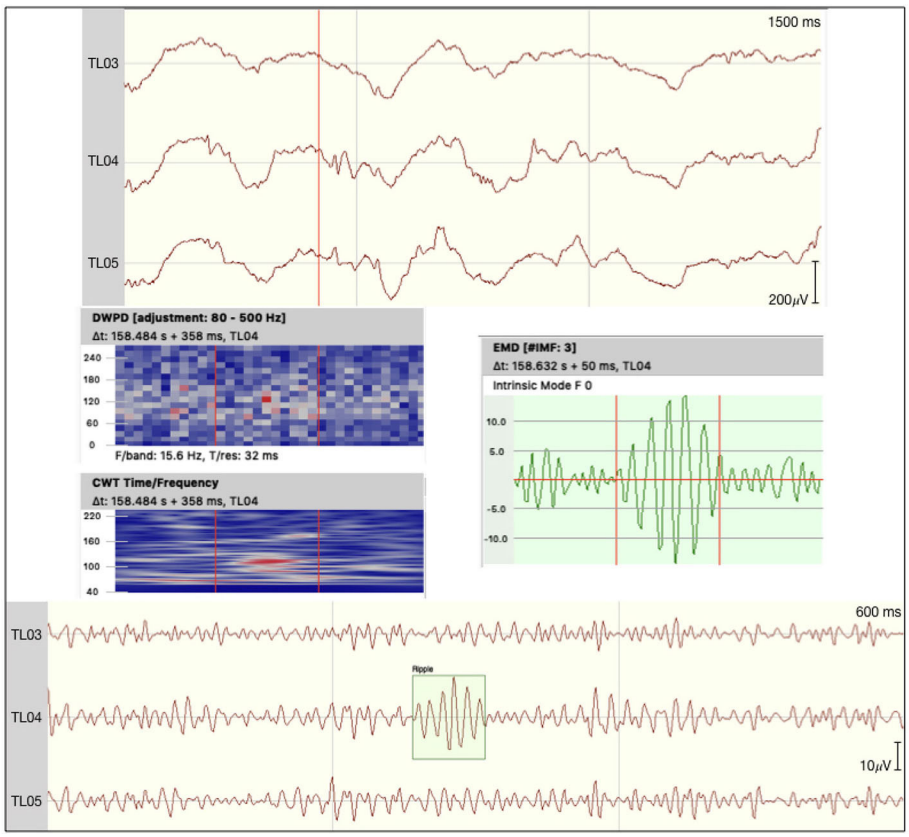


**FIGURE 2 |** Ripple detected on the epileptogenic site of patient 6. The raw signal is depicted at the top with the discrete wavelet power density, the continuous wavelet transformation, and an empirical mode decomposition (F0) plotted underneath. At the bottom the signal is filtered between 80 and 250 Hz.

that can be altered, making it difficult to compare findings derived from the use of different algorithms and settings.

Second, and more importantly, automatic detection is prone to false-positive detections, resulting from artifacts and sharp transients, that can mimic HFOs after filtering (24, 36, 37), as wells as from a high-frequency noise in the data (24, 35, 38, 39). Even in invasive EEG recordings, which are considered to seldom contain biological artifacts, automatic HFO detection seems to produce a (comparably) high number of false positives.

There have been reports of muscle contractions, body movements and ocular artifacts to corrupt EEG data recorded from deep in the brain (39, 47). Furthermore, eye movements have also been shown to elicit artifacts in brain regions close to extra-ocular muscles (35, 48), appearing as HFO-like events. In line with these reports, we also found ripple-like events to coincide with eye-movements and, when filtered, EOG revealed similar HFO-like derivates as iEEG channels, suggesting eye movement-related ripples to also appear in the iEEG. Taking into account additional channels, such as EOG and EMG, highly increased the number of events defined as artifact-derived HFOs in our data.

Comparing both detection approaches, manual detection led to only few events being considered as possible ripples in our data. Taking into account additional channels, such as EOG and EMG, highly increased the number of events defined as artifact-derived HFOs. Considering these additional channels may be crucial when opting for HFO detection, even in intracranial EEG data. While the strict visual detection led to a high specificity, automatic detection appeared to produce a very high number of false positives. These findings underline the pitfalls of automated HFO detection. Preprocessing the data with special emphasis on reducing artifacts or training algorithms to acknowledge artificial HFOs might prove helpful to increase the specificity of detection algorithms (49, 50).

Given the lack of visually detected clear ripples, and the extreme discrepancy between the detection approaches, further point to a need for a more precise definition of what truly constitutes an HFO. While a very strict definition, as applied in our manual detection, leads to very few or even no clear HFOs to be detected, it may serve as a basis to align detection strategies between different rater, research groups, and different detection algorithms. Besides, the methodological and technical interpretation of our findings, there are also some physiologic explanations for the lack of manually detected ripples in our data.

## 4.2. Memory Task-Related HFO Occurrence

Neither of the two incorporated HFO detection approaches yielded event rates, that could be linked to performance during

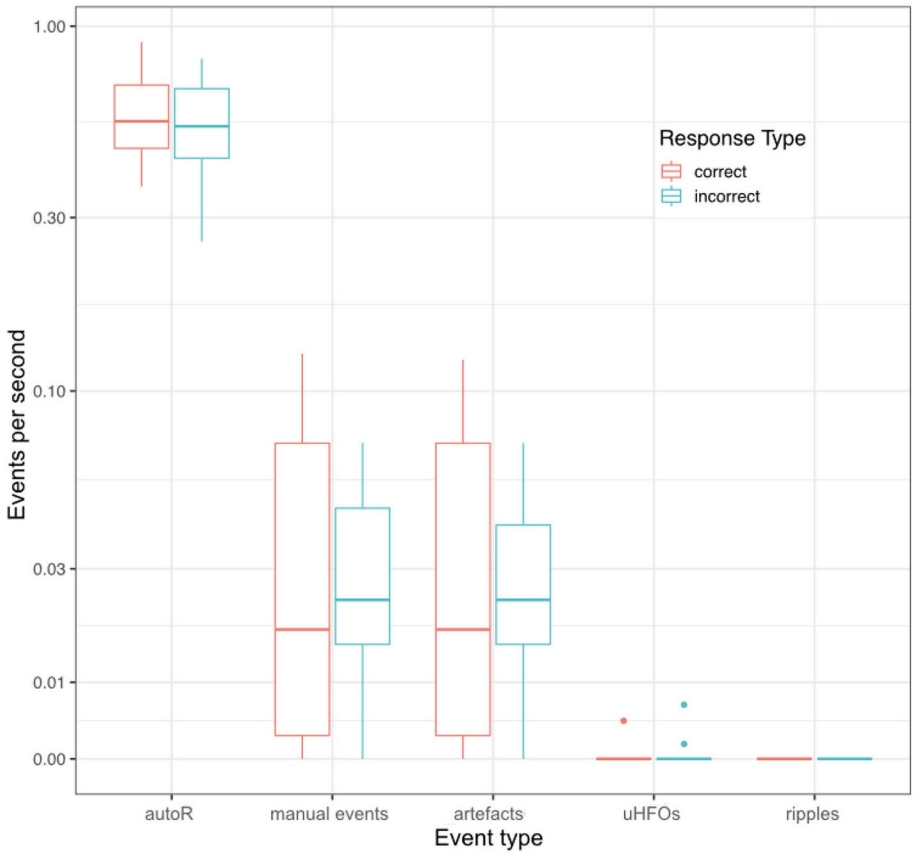


**FIGURE 3 |** Mean event rates per second during retrieval for all different event types and for correct and incorrect retrieval trials. Each data point corresponds to one patient.

encoding or retrieval in the visual memory task. It should be noted, however, that we correlated event rates across all analyzed channels with memory performance and did not subselect specific channels. Furthermore, we were unable to manually detect clear ripples in the data. This finding is notable, given the numerous notions of spontaneous HFO occurrence in memory-related brain areas (3, 14, 15, 20). One explanation for the incompatible findings could be that our manual detection criteria were extremely strict (maybe too strict) and missed physiologic ripples that did not conform to the ideal pattern. Another explanation could lie in the fact, that these studies all investigated HFOs during periods of rest and sleep.

Sleep has been suggested to offer a unique window into memory consolidation via hippocampal reactivation (18, 51–53), and thus might offer an increased probability to record memory-related HFOs. Especially hippocampal ripples being nested in sleep spindles have been suggested to be crucial for long-term potentiation and memory consolidation (22, 54, 55). Furthermore, resting and sleep EEG may provide data with a higher signal-to-noise ratio. Especially, high background noise and artifacts, that might have also been induced by the task, can lead to a number of false-positives for automatic detectors (24, 56). This would explain the discrepancy between the automatic and manual detection, as visual inspection would not have considered events embedded within a noisy background.

On another note, continuous high frequency activity in the background EEG has been suggested to reflect physiological activity distinctive for certain brain regions (57). This is in line with reports of high gamma band activity (including frequencies that fall into the ripple band) being related to memory (58, 59). These studies further point to a weakness in detecting single HFO events, as ripple band activity might be not only easier to detect during memory tasks, but also reveal important links to memory processes. Thus, a shift in focus from single oscillatory events to frequency band characteristics when studying cognition may be promising. Distinguishing HFOs from high frequency activity in this context may have the further benefit of ruling out epilepsy-related HFOs confounding the events of interest (60, 61).

## 4.3. Limitations

There are some limitations to the study at hand, some of which have already been outlined in the discussion. First, performing a manual detection with one rater only may result in very

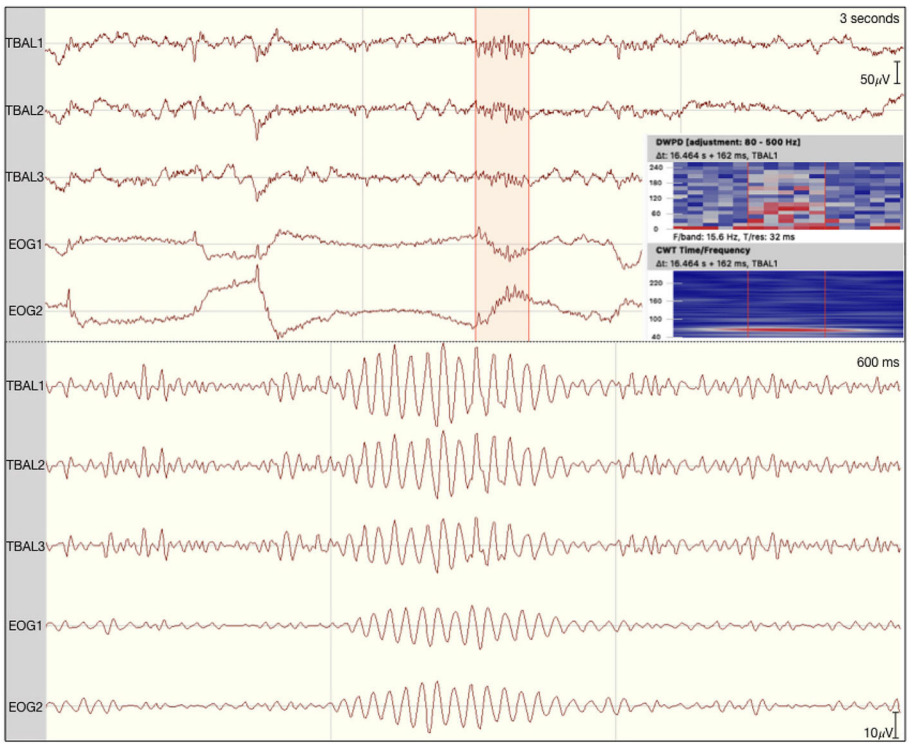


**FIGURE 4 |** Eye movement-related ripple-like event on the left temporal lobe of patient 1. The raw signal is depicted at the top with the discrete wavelet power density and the continuous wavelet transformation plotted on the side. At the bottom the signal is filtered between 80 and 250 Hz.

stable event detections across recordings, however multiple raters might have increased the sensitivity of visual detection. Since all unclear events and marked ripples were discussed in the team, specificity would not have changed with multiple raters, though. Second, differences between the two detection strategies have to be interpreted with caution, bearing in mind that we chose two very extreme approaches. The visual detection was performed strictly, with events of interest only being marked as ripples in case of no doubt. In contrast, the automatic detection algorithm's settings were chosen to increase sensitivity in order to make the differences between both detection strategies as visible as possible.

Third, the external reference used (linked mastoids) may have contributed to the artifact contamination of our iEEG data. The impact of the reference electrodes have already been described, and to this end a bipolar montage might have resulted in less artifactual events (24, 35, 62), which would have impacted the data for both detection strategies, however. Finally, numbers of trials between patients differed, especially with respect to correct and incorrect trials. Thus, the statistical sample was small for some analyses. This fact in connection with the small number of events for some types likely led to a low statistical power, which even carefully selected statistical tests may not have been able to compensate. Regardless of these limitations, there are some conclusions that can be drawn from the obtained results.

## 4.4. Conclusion

Our findings suggest grave differences between automatically and manually detected events. Our analysis suggests automatic detection to be highly affected by false ripples derived not only from technical but also from physiologic artifacts. Recording additional facial EMG as well as EOG channels seems beneficial for the identification of false ripples even in iEEG data. Future automated detection algorithms should implement artifact matching in these additional channels, in order to improve specificity. Also developing a preprocessing pipeline in order to clean the data of artifacts before automatic algorithms detect HFOs could be a potential aim for future studies. Until then, guidelines for a more strict and careful visual inspection are needed to ensure comparable results, especially when dealing with conditions that seldom offer ideal data, for instance when performing cognitive paradigms.

Finally, we were not able to visually detect clear ripples, and other event types, including automatically detected ripples, could not be related to memory processes. Therefor, it remains questionable whether HFOs as single events can be exclusively identified as physiologic biomarkers. For now high frequency activity rather than single high frequency events may present a more suitable surrogate marker for cognition. Being also less affected by epileptogenity as well as artifacts,

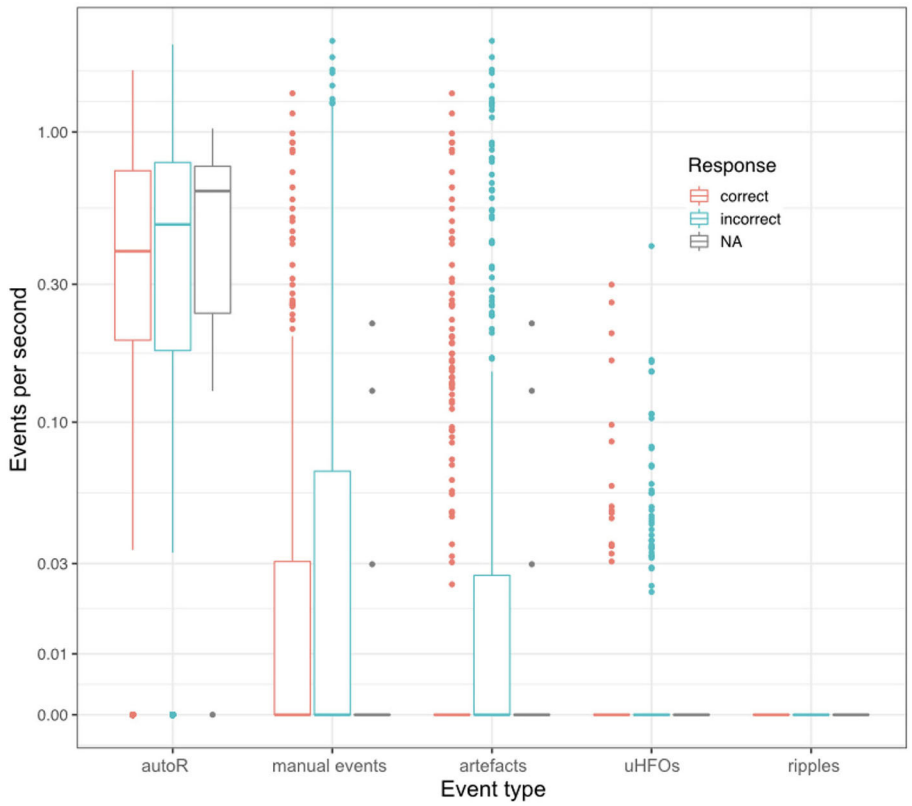


**FIGURE 5 |** Event rates per second for each encoding trial in relation to the respective response during the corresponding retrieval trial. NA refers to missed responses during retrieval.

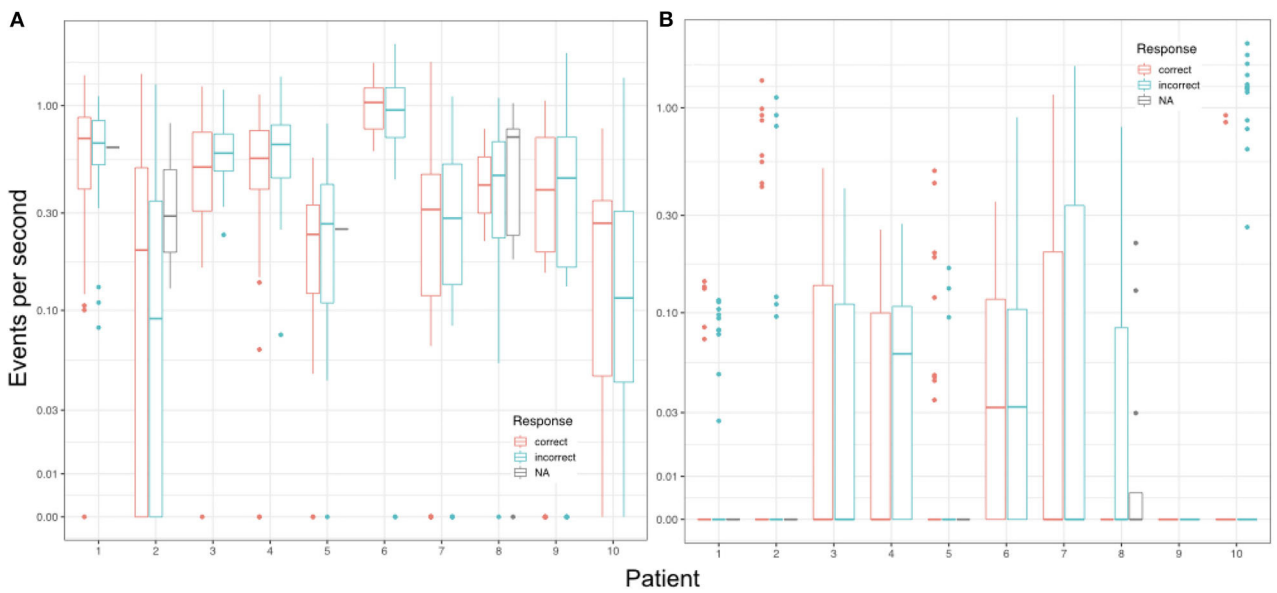


**FIGURE 6 |** Mean event rates per second during encoding trials in relation to the respective response during the corresponding retrieval trial for each individual patient. **(A)** Shows the results for automatically detected ripples (autoR) and **(B)** depicts all manually detected events. NA refers to missed responses during retrieval.

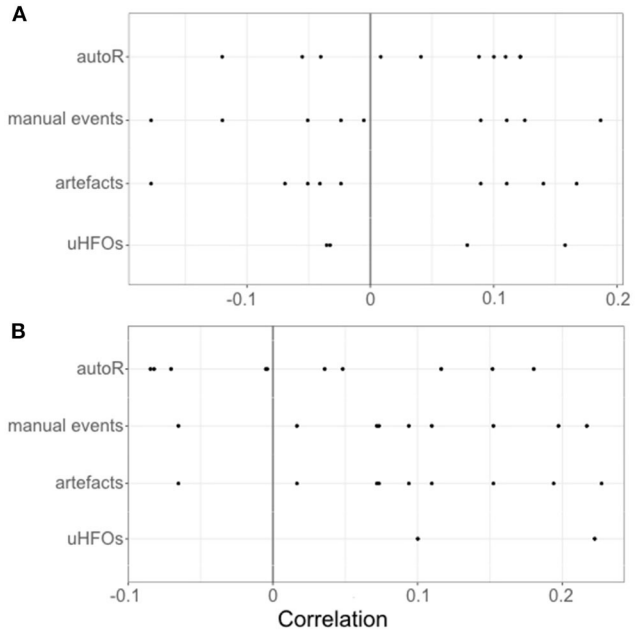


**FIGURE 7 |** Individual correlations for each patients' event occurrence rates per second during encoding **(A)** and retrieval **(B)** with the response times during the respective retrieval trials.

it is also less time-consuming to investigate high frequency band activity, thus offering another promising approach for future studies.

## DATA AVAILABILITY STATEMENT

The raw data supporting the conclusions of this article will be made available by the authors, without undue reservation.

## ETHICS STATEMENT

The studies involving human participants were reviewed and approved by local ethics committee: Ethikkommission an der Medizinischen Fakultät der Rheinischen Friedrich-Wilhelms-Universität Bonn, Venusberg Campus 1 (Geb. 02), 53127 Bonn. The patients/participants provided their written informed consent to participate in this study. Written informed consent was obtained from the individual(s) for the publication of any potentially identifiable images or data included in this article.

## AUTHOR CONTRIBUTIONS

AT wrote the initial manuscript and performed the automatic event detection. NG manually detected the events and developed the marking strategy in correspondence with AT and YH. PL performed the marker statistics supervised by AB. JF prepared the EEG data for analysis and conducted the initial study. ET and YH supervised the event detection strategies and general data analysis. All authors read and critically revised the manuscript before submission.

## FUNDING

The presented research was supported by the Austrian Science Fund (FWF): KLI657-B31 and T 798-B27, and by the Research Fund of the Paracelsus Medical University Salzburg (PMU-FFF): A-16/02/021-HÖL and A-18/01/029-HÖL.

## ACKNOWLEDGMENTS

We would like to thank the staff at the Department of Epileptology of the University Hospital Bonn, who took part in conducting this study, as well as Hui Zhang and Nikolai Axmacher from the Dept. of Psychology of the University of Bochum.

## REFERENCES

1. Jacobs J, Staba R, Asano E, Otsubo H, Wu J, Zijlmans M, et al. High-frequency oscillations (HFOs) in clinical epilepsy. *Prog Neurobiol.* (2012) 98:302–15. doi: 10.1016/j.pneurobio.2012.03.001
2. Bragin A, Engel J Jr., Wilson CL, Fried I, Buzsáki G. High-frequency oscillations in human brain. *Hippocampus.* (1999) 9:137–42. doi: 10.1002/(SICI)1098-1063(1999)9:2<137::AID-HIPO5>3.0.CO;2-0
3. Bragin A, Engel J, Wilson CL, Fried I, Mathern GW. Hippocampal and entorhinal cortex high-frequency oscillations (100–500 Hz) in human epileptic brain and in kainic acid-treated rats with chronic seizures. *Epilepsia.* (1999) 40:127–37. doi: 10.1111/j.1528-1157.1999.tb02065.x
4. Bragin A, Wilson CL, Staba RJ, Reddick M, Fried I, Engel J Jr. Interictal high-frequency oscillations (80–500 Hz) in the human epileptic brain: entorhinal cortex. *Ann Neurol.* (2002) 52:407–15. doi: 10.1002/ana.10291
5. Staba RJ, Wilson CL, Bragin A, Jhung D, Fried I, Engel J Jr. High-frequency oscillations recorded in human medial temporal lobe during sleep. *Ann Neurol.* (2004) 56:108–15. doi: 10.1002/ana.20164
6. Jirsch J, Urrestarazu E, LeVan P, Olivier A, Dubeau F, Gotman J. High-frequency oscillations during human focal seizures. *Brain.* (2006) 129:1593–608. doi: 10.1093/brain/awl085
7. Urrestarazu E, Jirsch JD, LeVan P, Hall J. High-frequency intracerebral EEG activity (100–500 Hz) following interictal spikes. *Epilepsia.* (2006) 47:1465–76. doi: 10.1111/j.1528-1167.2006.00618.x
8. Allen P, Fish D, Smith S. Very high-frequency rhythmic activity during sEEG suppression in frontal lobe epilepsy. *Electroencephalogr Clin Neurophysiol.* (1992) 82:155–9. doi: 10.1016/0013-4694(92)90160-J
9. Fisher RS, Webber W, Lesser RP, Arroyo S, Uematsu S. High-frequency EEG activity at the start of seizures. *J Clin Neurophysiol.* (1992) 9:441–8. doi: 10.1097/00004691-199207010-00012
10. Urrestarazu E, Chander R, Dubeau F, Gotman J. Interictal high-frequency oscillations (100–500 Hz) in the intracerebral EEG of epileptic patients. *Brain.* (2007) 130:2354–66. doi: 10.1093/brain/awm149
11. Wang S, Wang IZ, Bulacio JC, Mosher JC, Gonzalez-Martinez J, Alexopoulos AV, et al. Ripple classification helps to localize the seizure-onset zone in neocortical epilepsy. *Epilepsia.* (2013) 54:370–6. doi: 10.1111/j.1528-1167.2012.03721.x
12. Frauscher B, Bartolomei F, Kobayashi K, Cimbalnik J, Klooster MA, Rampp S, et al. High-frequency oscillations: the state of clinical research. *Epilepsia.* (2017) 58:1316–29. doi: 10.1111/epi.13829
13. Buzsáki G, da Silva FL. High frequency oscillations in the intact brain. *Prog Neurobiol.* (2012) 98:241–9. doi: 10.1016/j.pneurobio.2012.02.004

14. Worrell GA, Gardner AB, Stead SM, Hu S, Goerss S, Cascino GJ, et al. High-frequency oscillations in human temporal lobe: simultaneous microwire and clinical macroelectrode recordings. *Brain.* (2008) 131:928–37. doi: 10.1093/brain/awn006
15. Staba RJ, Wilson CL, Bragin A, Fried I, Engel J Jr. Quantitative analysis of high-frequency oscillations (80–500 Hz) recorded in human epileptic hippocampus and entorhinal cortex. *J Neurophysiol.* (2002) 88:1743–52. doi: 10.1152/jn.2002.88.4.1743
16. Frauscher B, von Ellenrieder N, Zelmann R, Doležalová I, Minotti L, Olivier A, et al. Atlas of the normal intracranial electroencephalogram: neurophysiological awake activity in different cortical areas. *Brain.* (2018) 141:1130–44. doi: 10.1093/brain/awy035
17. Frauscher B, von Ellenrieder N, Zelmann R, Rogers C, Nguyen DK, Kahane P, et al. High-frequency oscillations in the normal human brain. *Ann Neurol.* (2018) 84:374–85. doi: 10.1002/ana.25304
18. Wilson MA, McNaughton BL. Reactivation of hippocampal ensemble memories during sleep. *Science.* (1994) 265:676–9. doi: 10.1126/science.8036517
19. Chrobak JJ, Buzsáki G. High-frequency oscillations in the output networks of the hippocampal-entorhinal axis of the freely behaving rat. *J Neurosci.* (1996) 16:3056–66. doi: 10.1523/JNEUROSCI.16-09-03056.1996
20. Axmacher N, Elger CE, Fell J. Ripples in the medial temporal lobe are relevant for human memory consolidation. *Brain.* (2008) 131:1806–17. doi: 10.1093/brain/awn103
21. Clemens Z, Mölle M, Erőss L, Barsi P, Halász P, Born J. Temporal coupling of parahippocampal ripples, sleep spindles and slow oscillations in humans. *Brain.* (2007) 130:2868–78. doi: 10.1093/brain/awm146
22. Siapas AG, Wilson MA. Coordinated interactions between hippocampal ripples and cortical spindles during slow-wave sleep. *Neuron.* (1998) 21:1123–8. doi: 10.1016/S0896-6273(00)80629-7
23. Sirota A, Csicsvari J, Buhl D, Buzsáki G. Communication between neocortex and hippocampus during sleep in rodents. *Proc Natl Acad Sci USA.* (2003) 100:2065–9. doi: 10.1073/pnas.0437938100
24. Worrell GA, Jerbi K, Kobayashi K, Lina JM, Zelmann R, Le Van Quyen M. Recording and analysis techniques for high-frequency oscillations. *Prog Neurobiol.* (2012) 98:265–78. doi: 10.1016/j.pneurobio.2012.02.006
25. Navarrete M, Pyrzowski J, Corlier J, Valderrama M, Le Van Quyen M. Automated detection of high-frequency oscillations in electrophysiological signals: methodological advances. *J Physiol.* (2016) 110:316–26. doi: 10.1016/j.jphysparis.2017.02.003
26. Zijlmans M, Worrell GA, Dümpelmann M, Stieglitz T, Barborica A, Heers M, et al. How to record high-frequency oscillations in epilepsy: a practical guideline. *Epilepsia.* (2017) 58:1305–15. doi: 10.1111/epi.13814
27. Zelmann R, Zijlmans M, Jacobs J, Châtillon CE, Gotman J. Improving the identification of high frequency oscillations. *Clin Neurophysiol.* (2009) 120:1457–64. doi: 10.1016/j.clinph.2009.05.029
28. Roehri N, Pizzo F, Bartolomei F, Wendling F, Bénar CG. What are the assets and weaknesses of HFO detectors? A benchmark framework based on realistic simulations. *PLoS ONE.* (2017) 12:e0174702. doi: 10.1371/journal.pone.0174702
29. Spring AM, Pittman DJ, Aghakhani Y, Jirsch J, Pillay N, Bello-Espinosa LE, et al. Interrater reliability of visually evaluated high frequency oscillations. *Clin Neurophysiol.* (2017) 128:433–41. doi: 10.1016/j.clinph.2016.12.017
30. Liu S, Sha Z, Sencer A, Aydoseli A, Bebek N, Abosch A, et al. Exploring the time-frequency content of high frequency oscillations for automated identification of seizure onset zone in epilepsy. *J Neural Eng.* (2016) 13:026026. doi: 10.1088/1741-2560/13/2/026026
31. Migliorelli C, Alonso JF, Romero S, Nowak R, Russi A, Mañanas MA. Automated detection of epileptic ripples in MEG using beamformer-based virtual sensors. *J Neural Eng.* (2017) 14:046013. doi: 10.1088/1741-2552/aa684c
32. Quitadamo LR, Foley E, Mai R, De Palma L, Specchio N, Seri S. EPINETLAB: a software for seizure-onset zone identification from intracranial EEG signal in epilepsy. *Front Neuroinform.* (2018) 12:45. doi: 10.3389/fninf.2018.00045
33. Ren GP, Yan JQ, Yu ZX, Wang D, Li XN, Mei SS, et al. Automated detector of high frequency oscillations in epilepsy based on maximum distributed peak points. *Int J Neural Syst.* (2018) 28:1750029. doi: 10.1142/S0129065717500290
34. Shimamoto S, Waldman ZJ, Orosz I, Song I, Bragin A, Fried I, et al. Utilization of independent component analysis for accurate pathological ripple detection in intracranial EEG recordings recorded extra-and intra-operatively. *Clin Neurophysiol.* (2018) 129:296–307. doi: 10.1016/j.clinph.2017.08.036
35. Jerbi K, Freyermuth S, Dalal S, Kahane P, Bertrand O, Berthoz A, et al. Saccade related gamma-band activity in intracerebral EEG: dissociating neural from ocular muscle activity. *Brain Topogr.* (2009) 22:18–23. doi: 10.1007/s10548-009-0078-5
36. Amiri M, Lina JM, Pizzo F, Gotman J. High frequency oscillations and spikes: separating real HFOs from false oscillations. *Clin Neurophysiol.* (2016) 127:187–96. doi: 10.1016/j.clinph.2015.04.290
37. Bénar CG, Chauviére L, Bartolomei F, Wendling F. Pitfalls of high-pass filtering for detecting epileptic oscillations: a technical note on 'false' ripples. *Clin Neurophysiol.* (2010) 121:301–10. doi: 10.1016/j.clinph.2009.10.019
38. Kovach CK, Tsuchiya N, Kawasaki H, Oya H, Howard III MA, Adolphs R. Manifestation of ocular-muscle EMG contamination in human intracranial recordings. *Neuroimage.* (2011) 54:213–33. doi: 10.1016/j.neuroimage.2010.08.002
39. Otsubo H, Ochi A, Imai K, Akiyama T, Fujimoto A, Go C, et al. High-frequency oscillations of ictal muscle activity and epileptogenic discharges on intracranial EEG in a temporal lobe epilepsy patient. *Clin Neurophysiol.* (2008) 119:862–8. doi: 10.1016/j.clinph.2007.12.014
40. Zelmann R, Mari F, Jacobs J, Zijlmans M, Dubeau F, Gotman J. A comparison between detectors of high frequency oscillations. *Clin Neurophysiol.* (2012) 123:106–16. doi: 10.1016/j.clinph.2011.06.006
41. Höller P, Trinka E, Höller Y. MEEGIPS-a modular EEG investigation and processing system for visual and automated detection of high frequency oscillations. *Front Neuroinform.* (2019) 13:20. doi: 10.3389/fninf.2019.00020
42. Flandrin P, Rilling G, Goncalves P. Empirical mode decomposition as a filter bank. *IEEE Signal Process Lett.* (2004) 11:112–4. doi: 10.1109/LSP.2003.821662
43. Stockwell RG, Mansinha L, Lowe R. Localization of the complex spectrum: the S transform. *IEEE Trans Signal Process.* (1996) 44:998–1001. doi: 10.1109/78.492555
44. Burnos S, Hilfiker P, Sürücü O, Scholkmann F, Krayenbühl N, Grunwald T, et al. Human intracranial high frequency oscillations (HFOs) detected by automatic time-frequency analysis. *PLoS ONE.* (2014) 9:e94381. doi: 10.1371/journal.pone.0094381
45. R Core Team. *R: A Language and Environment for Statistical Computing.* Vienna (2018). Available online at: https://www.R-project.org/
46. Noguchi K, Gel YR, Brunner E, Konietschke F. nparLD: an R software package for the nonparametric analysis of longitudinal data in factorial experiments. *J Stat Softw.* (2012) 50:1–23. doi: 10.18637/jss.v050.i12
47. Worrell G. High-frequency oscillations recorded on scalp EEG. *Epilepsy Curr.* (2012) 12:57–8. doi: 10.5698/1535-7511-12.2.57
48. Yuval-Greenberg S, Tomer O, Keren AS, Nelken I, Deouell LY. Transient induced gamma-band response in EEG as a manifestation of miniature saccades. *Neuron.* (2008) 58:429–41. doi: 10.1016/j.neuron.2008.03.027
49. Jiang C, Li X, Yan J, Yu T, Wang X, Ren Z, et al. Determining the quantitative threshold of high-frequency oscillation distribution to delineate the epileptogenic zone by automated detection. *Front Neurol.* (2018) 9:889. doi: 10.3389/fneur.2018.00889
50. Ren S, Gliske SV, Brang D, Stacey WC. Redaction of false high frequency oscillations due to muscle artifact improves specificity to epileptic tissue. *Clin Neurophysiol.* (2019) 130:976–85. doi: 10.1016/j.clinph.2019.03.028
51. Davidson TJ, Kloosterman F, Wilson MA. Hippocampal replay of extended experience. *Neuron.* (2009) 63:497–507. doi: 10.1016/j.neuron.2009.07.027
52. Gais S, Albouy G, Boly M, Dang-Vu TT, Darsaud A, Desseilles M, et al. Sleep transforms the cerebral trace of declarative memories. *Proc Natl Acad Sci USA.* (2007) 104:18778–83. doi: 10.1073/pnas.0705454104
53. Ji D, Wilson MA. Coordinated memory replay in the visual cortex and hippocampus during sleep. *Nat Neurosci.* (2007) 10:100–7. doi: 10.1038/nn1825
54. Buzsáki G. Long-term changes of hippocampal sharp-waves following high frequency afferent activation. *Brain Res.* (1984) 300:179–82. doi: 10.1016/0006-8993(84)91356-8
55. Staresina BP, Bergmann TO, Bonnefond M, Van Der Meij R, Jensen O, Deuker L, et al. Hierarchical nesting of slow oscillations, spindles and ripples

in the human hippocampus during sleep. *Nat Neurosci.* (2015) 18:1679. doi: 10.1038/nn.4119
56. von Ellenrieder N, Andrade-Valença LP, Dubeau F, Gotman J. Automatic detection of fast oscillations (40–200 Hz) in scalp EEG recordings. *Clin Neurophysiol.* (2012) 123:670–80. doi: 10.1016/j.clinph.2011.07.050
57. Melani F, Zelmann R, Dubeau F, Gotman J. Occurrence of scalp-fast oscillations among patients with different spiking rate and their role as epileptogenicity marker. *Epilepsy Res.* (2013) 106:345–56. doi: 10.1016/j.eplepsyres.2013.06.003
58. Kunii N, Kawai K, Kamada K, Ota T, Saito N. The significance of parahippocampal high gamma activity for memory preservation in surgical treatment of atypical temporal lobe epilepsy. *Epilepsia.* (2014) 55:1594–601. doi: 10.1111/epi.12764
59. Pu Y, Cornwell BR, Cheyne D, Johnson BW. High-gamma activity in the human hippocampus and parahippocampus during inter-trial rest periods of a virtual navigation task. *Neuroimage.* (2018) 178:92–103. doi: 10.1016/j.neuroimage.2018.05.029
60. Liu S, Parvizi J. Cognitive refractory state caused by spontaneous epileptic high-frequency oscillations in the human brain. *Sci Transl Med.* (2019) 11:eaax7830. doi: 10.1126/scitranslmed.aax7830
61. Waldman ZJ, Camarillo-Rodriguez L, Chervenova I, Berry B, Shimamoto S, Elahian B, et al. Ripple oscillations in the left temporal neocortex are associated with impaired verbal episodic memory encoding. *Epilepsy Behav.* (2018) 88:33–40. doi: 10.1016/j.yebeh.2018.08.018
62. Nagasawa T, Matsuzaki N, Juhász C, Hanazawa A, Shah A, Mittal S, et al. Occipital gamma-oscillations modulated during eye movement tasks: simultaneous eye tracking and electrocorticography recording in epileptic patients. *Neuroimage.* (2011) 58:1101–9. doi: 10.1016/j.neuroimage.2011.07.043

**Conflict of Interest:** The authors declare that the research was conducted in the absence of any commercial or financial relationships that could be construed as a potential conflict of interest.

*Copyright © 2020 Thomschewski, Gerner, Langthaler, Trinka, Bathke, Fell and Höller. This is an open-access article distributed under the terms of the Creative Commons Attribution License (CC BY). The use, distribution or reproduction in other forums is permitted, provided the original author(s) and the copyright owner(s) are credited and that the original publication in this journal is cited, in accordance with accepted academic practice. No use, distribution or reproduction is permitted which does not comply with these terms.*

frontiers in Neurology

ORIGINAL RESEARCH
published: 27 October 2020
doi: 10.3389/fneur.2020.578571

# Cognitive Processing Impacts High Frequency Intracranial EEG Activity of Human Hippocampus in Patients With Pharmacoresistant Focal Epilepsy

*Jan Cimbalnik[1*†], Martin Pail[2], Petr Klimes[1,3], Vojtech Travnicek[1,3], Robert Roman[2,4], Adam Vajcner[2,5] and Milan Brazdil[2,4]*

*[1] International Clinical Research Center, St. Anne's University Hospital, Brno, Czechia, [2] Department of Neurology, Faculty of Medicine, Brno Epilepsy Center, St. Anne's University Hospital, Masaryk University, Brno, Czechia, [3] Institute of Scientific Instruments, The Czech Academy of Sciences, Brno, Czechia, [4] Behavioral and Social Neuroscience Research Group, CEITEC - Central European Institute of Technology, Masaryk University, Brno, Czechia, [5] Department of Sports Medicine and Rehabilitation, Faculty of Medicine, St. Anne's University Hospital, Masaryk University, Brno, Czechia*

OPEN ACCESS

**Edited by:**
*Maeike Zijlmans, University Medical Center Utrecht, Netherlands*

**Reviewed by:**
*Luiz E. Mello, Federal University of São Paulo, Brazil*
*Dinesh Upadhya, Manipal Academy of Higher Education, India*

***Correspondence:**
*Jan Cimbalnik*
*jan.cimbalnik@fnusa.cz*

**†ORCID:**
*Jan Cimbalnik*
*orcid.org/0000-0001-6670-6717*

**Specialty section:**
*This article was submitted to Epilepsy, a section of the journal Frontiers in Neurology*

**Received:** *10 July 2020*
**Accepted:** *18 September 2020*
**Published:** *27 October 2020*

**Citation:**
*Cimbalnik J, Pail M, Klimes P, Travnicek V, Roman R, Vajcner A and Brazdil M (2020) Cognitive Processing Impacts High Frequency Intracranial EEG Activity of Human Hippocampus in Patients With Pharmacoresistant Focal Epilepsy. Front. Neurol. 11:578571. doi: 10.3389/fneur.2020.578571*

The electrophysiological EEG features such as high frequency oscillations, spikes and functional connectivity are often used for delineation of epileptogenic tissue and study of the normal function of the brain. The epileptogenic activity is also known to be suppressed by cognitive processing. However, differences between epileptic and healthy brain behavior during rest and task were not studied in detail. In this study we investigate the impact of cognitive processing on epileptogenic and non-epileptogenic hippocampus and the intracranial EEG features representing the underlying electrophysiological processes. We investigated intracranial EEG in 24 epileptic and 24 non-epileptic hippocampi in patients with intractable focal epilepsy during a resting state period and during performance of various cognitive tasks. We evaluated the behavior of features derived from high frequency oscillations, interictal epileptiform discharges and functional connectivity and their changes in relation to cognitive processing. Subsequently, we performed an analysis whether cognitive processing can contribute to classification of epileptic and non-epileptic hippocampus using a machine learning approach. The results show that cognitive processing suppresses epileptogenic activity in epileptic hippocampus while it causes a shift toward higher frequencies in non-epileptic hippocampus. Statistical analysis reveals significantly different electrophysiological reactions of epileptic and non-epileptic hippocampus during cognitive processing, which can be measured by high frequency oscillations, interictal epileptiform discharges and functional connectivity. The calculated features showed high classification potential for epileptic hippocampus (AUC = 0.93). In conclusion, the differences between epileptic and non-epileptic hippocampus during cognitive processing bring new insight in delineation between pathological and physiological processes. Analysis of computed iEEG features in rest and task condition can improve the functional mapping during

pre-surgical evaluation and provide additional guidance for distinguishing between epileptic and non-epileptic structure which is absolutely crucial for achieving the best possible outcome with as little side effects as possible.

**Keywords: pharmacoresistant epilepsy, high frequency oscillation (HFO), interictal epileptiform discharge, functional connectivity, hippocampus, cognitive processing**

## INTRODUCTION

Epilepsy is one of the mostcommon chronic neurological diseases (1) and approximately one third of epileptic patients suffer from a medically intractable form. Those patients are candidates for intracranial EEG (iEEG) monitoring and subsequent surgical treatment of their condition.

The hippocampus is a brain structure that is often involved in temporal lobe epilepsy (TLE). In particular, hippocampal sclerosis is often found in TLE, even though it is not clear whether it is the primary cause of epilepsy, its alteration or consequence (2). Nonetheless, its surgical removal often leads to improvement of the epileptic condition and substantial reduction of seizures (3). The correct determination of epileptic hippocampus and whether the particular hippocampus or its part should be removed can improve the outcome of epileptic surgeries and reduce the unnecessary removal of possible healthy tissue.

In the end of the last millennium, high frequency oscillations (HFO) emerged as a marker of normal function of the brain and epileptic activity (4, 5). Since then, numerous studies have been conducted to evaluate their potential for localization of epileptogenic tissue from iEEG signals (6–11). The distinction of pathological HFO and normal HFO based on their features has been investigated but the results never showed that their separation is possible (12, 13).

The hippocampus is the brain structure where the first HFO were described (4). Physiological HFO in the hippocampus are often studied as markers of cognitive processes and as part of memory formation (14). On the other hand, epileptic hippocampus is often abundant with pathologic HFO (15). It is, therefore, likely that both types of HFO occur simultaneously in epileptic hippocampus and physiological HFO are likely to interfere with the interpretation of the pathological HFO occurrence.

Another iEEG phenomenon connected to epileptogenic tissue and the hippocampus are interictal epileptic discharges (IEDs). They have been proven to be insufficiently specific for the pathological tissue (16), they propagate across multiple brain structures or are generated in zones not generating seizures (green spikes) (17) and can even occur in non epileptic hippocampus (6).

Apart from distinct electrophysiological events such as IEDs and HFO, high frequency functional brain connectivity in ripple and fast ripple frequency range has been used both for studying normal function of the brain and epileptogenic areas (18, 19).

**Abbreviations:** iEEG, intracranial EEG; TLE, temporal lobe epilepsy; HFO, high frequency oscillation; IED, interictal epileptiform discharge; EH, epileptic hippocampus; NEH, non- epileptic hippocampus; SEEG, stereo EEG.

The mentioned high frequency iEEG features represent different underlying electrophysiology. In recent years, the use of machine learning algorithms that combine the diverse information carried by the iEEG features have been shown to outperform the single feature approaches in localization tasks (20–23).

In this study we investigated iEEG features during resting state and task performance to elucidate the impact of cognitive processing on underlying brain electrophysiology under the hypothesis that HFO, IEDs and functional connectivity are modulated differently by cognitive processes in epileptic (EH) and non-epileptic (NEH) hippocampus. The secondary goal of this study was to provide evidence whether these modulations can contribute to better classification of epileptic and non-epileptic hippocampus.

## MATERIALS AND METHODS

### Subjects

The study was carried out on the data of 36 patients (17 females) with age ranging from 22 to 58 (mean: 37.4 ± 11.3) suffering from medically intractable focal epilepsies. All patients provided a written consent to participate in the study approved by the Ethics Committee of St. Anne's University Hospital in Brno and Masaryk University. Patient information is summarized in **Table 1**. In most patients, chronic anticonvulsant medication was reduced slightly for the purposes of video-EEG monitoring. All methods were performed in accordance with the relevant guidelines and regulations.

### Recordings

All patients participating in this study underwent stereotactic depth electrode implantation as part of their presurgical evaluation for treatment of pharmacoresistant focal epilepsy. The localization of the electrodes was determined solely by clinical needs. Used electrodes were either DIXI or ALCIS (diameter = 0.8 mm; inter-contact distance = 1.5 mm, contact surface area = 5 $mm^2$; contact length = 2 mm). All used electrodes were MRI compatible. The acquired iEEG was low-pass filtered and downsampled from 25 kHz to 5,000 Hz for subsequent storage and analysis. The used recording reference was the average of all intracranial signals. We analyzed hippocampal stereo EEG (SEEG) during an awake resting interictal period and various simple cognitive tasks.

### Behavioral Tasks

#### Oddball Task

The oddball task was performed similarly to the previous study by Polich (24). Subjects were seated in a moderately lit room with a

**TABLE 1 |** Study subjects overview with regard to individual hippocampi.

| Analyzed hippocampus | Epilepsy side | Epilepsy type | Engel outcome | MRI | Histopathology |
|---|---|---|---|---|---|
| Epileptic $N = 22$ | Left $N = 8$<br>Right $N = 9$<br>Bilateral $N = 5$ | Temporal $N = 22$ | Engel IA $N = 12$<br>Engel II-III $N = 6$<br>NA $N = 4$ | Normal $N = 6$<br>Abnormal $N = 16$ | FCD $N = 3$<br>HS $N = 8$<br>Negative $N = 5$<br>NA $N = 6$ |
| Non-epileptic $N = 23$ | Left $N = 12$<br>Right $N = 11$ | Temporal $N = 16$<br>Extratemporal $N = 7$ | Engel IA $N = 10$<br>Engel II-III $N = 12$<br>NA $N = 1$ | Normal $N = 5$<br>Abnormal $N = 18$ | AVM $N = 1$<br>FCD $N = 9$<br>HS $N = 5$<br>Heterotophy $N = 1$<br>Negatvie $N = 4$<br>NA $N = 3$ |

*FCD, focal cortical dysplasia; AVM, arteriovenous malformation; HS, hippocampal sclerosis; NA, not available.*
*Some subjects had both epileptic and non-epileptic hippocampi.*

monitor screen positioned approximately 100 cm in front of their eyes. During the task, they were requested to focus their eyes on the small fixation point in the center of the screen. A standard visual oddball task was performed: three types of stimuli (target, frequent, and distractor) at a ratio of 1:4.6:1, were presented in the center of the screen in random order. The number of targets was 50. Clearly visible yellow capital letters X (target), O (frequent), and various other capital letters (distractor) on a black background were used as experimental stimuli that were presented for 500 ms. The task was divided into four blocks, each block consisted of 12 or 13 target stimuli. The interstimulus interval randomly varied between 4 and 6 s. Each subject was instructed to count the target stimuli in their mind and to report the calculated number after each block.

## Go/NoGo Task

The Go/NoGo task was replicated from work of Albares et al. (25). Experimental stimuli, i.e., white capital letters A and B, were displayed in the center of the black screen for 0.2 s, followed by a black screen for 2 s. Each letter was preceded by a red or green fixation cross presented with a random duration of 2–6 s. The red fixation cross was followed by the letter A (Go stimulus) or B (NoGo stimulus) with an equal probability. The green fixation cross was always followed by the letter A (Go stimulus). The red cross was twice as common as the green one. In total, 72 NoGo stimuli and 144 Go stimuli were presented, divided into four blocks of the experiment. Participants were instructed to press a button as quickly as possible on Go stimuli and to suppress this action when a NoGo stimulus appeared. Before the experiment, participants completed a short practice.

## Ultimatum Game Task

The Ultimatum Game task was previously used in an fMRI study by Shaw et al. (26). It presents a simple paradigm to investigate dyadic interaction. The patient was randomly assigned to the role of a Proposer or a Responder. The opposite role was assigned to a nurse willing to participate in the game. Roles were fixed for all rounds.

Each round of the ultimatum game started with the Proposer being given 4 s to choose one of two divisions of a sum of money (of 100 CZK, i.e.,∼€4) that differed in the degree of inequity, between themselves and the Responder. After this fixed period, the Proposer's offer was highlighted for 4 s, during which the Responder could either accept or reject the proposal. If they accepted it, then the money was divided accordingly, but if they rejected it, then neither player received any payoff. After this 4-s period, the Responder's decision was then presented for a final 4 s.

The exact same procedure was followed on control rounds, but the choice set comprised two alternative divisions of different colors between the players; rather than dividing a sum of money, Proposers were required to choose the color they preferred for themselves and the color that should go to the Responder, and the Responder then accepted or rejected that offer. Both players were instructed that control rounds had no monetary consequence. Each round ended with a jittered inter-trial interval, with a fixation cross presented pseudo-randomly for 2–4 s. All stimuli were presented to both players simultaneously—Responders saw the initial choice set from which Proposers selected their offer, and Proposers saw the Responder's accept/reject decision. Players were instructed at the start that they would receive the outcome of six rounds selected at random. At no point was any information given to participants on the number of rounds remaining in the task. The whole experiment consisted of two functional runs performed successively in a single session. The two runs together comprised 120 rounds of the experimental condition and 60 rounds of a control condition.

## Mismatch Negativity

Mismatch negativity (MMN) protocol was based on studies of (27–29).

We recorded a passive task of attention called MMN protocol to find out the presence of MMN/MMN-like response in aiming structures. Each patient lay on the bed in a semi-sitting position with eyes opened. Patient's task was to concentrate voluntary selective attention on watching a self-selected movie and ignore the tones of auditory stimulation, no further information was received. Simultaneously, auditory stimulation was presented binaurally through loudspeakers (∼2 m far from ears) in parameters of roving paradigm (frequent and infrequent stimuli).

Frequent and infrequent stimuli (standard and deviant tones of 50/100 ms duration) were randomly presented with the presentation probability of 0.8/0.2. Interstimulus intervals' (ITS)

duration was 2,000 ms. All tones were 54 dB (SD ± 4, adjusted subjectively for patient's comfort) SPL, frequency 1,000 Hz, and with jump increase and gradual decrease of the tones' course. The experiment protocol lasted 17 min. This part of investigation was focused on the preattentive detection mechanism on the unconscious level for auditory stimuli which is illustrated by Mismatch negativity.

## Determination of Anatomical Location

To localize the MRI compatible electrode contacts in patients' brains the preoperative MRI was coregistered with postoperative MRI/CT using a custom made Matlab (The MathWorks, Inc.) based on Statistical Parametric Mapping module. After the software coregistration the brain volume was transformed to MNI space and the MNI coordinates of individual contacts were determined. The coregistered volume was used to estimate he anatomical location of each contact by two clinical neurologists using Co-Planar Stereotaxic Atlas of the Human Brain (Talairach-Tournoux system). Only the contacts clearly located in the hippocampus were included in the analysis of iEEG.

## Selection of Hippocampi

The hippocampi in individual patients were classified as epileptic or non-epileptic specifically, according to the results of a standard visual analysis of interictal and ictal SEEG recordings. If contacts implanted in the hippocampus were included in seizure onset zone (SOZ) the hippocampus was classified as epileptic. Conversely, if all contacts implanted in the hippocampus were outside of SOZ and did not exhibit excessive spiking (<50 per 10 min) they were classified as putative non-epileptic hippocampi. The putative non-epileptic hippocampi with spiking above the threshold were visually reviewed whether the IEDs were propagated from other brain structures. The putative non-epileptic hippocampi that generated IEDs were excluded from the analysis.

## Data Processing and Feature Extraction

The iEEG data were processed by automated algorithms that were already used in other published studies. The Python codes of these algorithms are part of the ElectroPhYsiology Computation Module (EPYCOM) and can be found online at https://gitlab.com/icrc-bme/epycom.

### HFO Detection

The automated detection of HFO was performed by an algorithm used in our previous studies (30, 31). A statistical window of 10 s was used to compute z-scored amplitude envelopes using Hilbert transforms in a series of logarithmically spaced frequency bands (300 bands between 60 and 800 Hz). The detection of putative HFO was done by thresholding the amplitude envelopes by three standard deviations above the mean in each frequency band. The detections overlapping in temporal domain in adjacent frequency bands were joined into one HFO detection obtaining temporal and spectral span of the putative HFO. Final detections were obtained by selecting HFO that have time span >4 cycles at their peak frequency and HFO with minimal frequency at 60 Hz were discarded to remove false positive detections of spikes. HFO amplitude, peak frequency and duration were extracted along with the HFO detections. The detector thresholds were chosen to achieve high sensitivity in order to detect physiological HFO which were shown to have smaller amplitude than pathological HFO (12).

Detected HFO were split into broadband ripple (R; 80–250 Hz) and fast ripple (FR; 250–600 Hz) HFO based on their dominant frequency. Subsequently, HFO rate, mean relative amplitude, duration and dominant frequency per 10 min was calculated for each channel and R/FR and used as features.

### IED Detection

IED detection was done using the spike detector developed by Barkmeier et al. (32). The detector utilizes filtration in two frequency bands. 20–50 Hz band to detect putative spikes and 1–35 Hz band to determine scaling factor which is used to scale the data in all iEEG channels and to determine amplitude and slope thresholds for final spike detections.

The spike rate and mean spike amplitude per 10 min was calculated for each channel.

### Functional Connectivity Calculation

Recorded signals were filtered in ripple (80–250 Hz) and fast ripple (250–600 Hz) frequency bands and non-overlapping 1-s sliding windows were used to calculate linear correlation and relative entropy to estimate functional connectivity between iEEG signals recorded by adjacent contacts on an electrode implanted in the hippocampus. For iEEG signals X and Y, the linear correlation was calculated as $corr(X,Y) = cov(X,Y)/std(X)\cdot std(Y)$, where cov stands for covariance and std for standard deviation. The relative entropy was calculated as $REN(X,Y) = sum[pX\cdot log(pX/pY)]$, where pX is a probability distribution of investigated signal and pY is a probability distribution of expected signal.

The connectivity metrics were calculated for R and FR frequency bands and mean value per channel was used in subsequent processing as an iEEG feature.

## Statistical Analysis and Machine Learning

All statistical analyzes and machine learning tasks in this study were performed using custom-made Python scripts, open-source statistical libraries (scipy, statsmodels) and machine learning libraries (scikit-learn).

### Statistical Analysis

Paired *t*-tests were carried out to evaluate the changes in iEEG features between resting state and during task performance when the patients were under cognitive load for EH and NEH. The statistical difference between EH and NEH during rest and cognitive processing was tested with Mann-Whitney test.

To assess the potential of individual signal features for discrimination of epileptic and non-epileptic hippocampi the receiver operating curve (ROC) and its area under the curve (AUC) was calculated for values during resting state, task performance and for difference of values between resting state

**TABLE 2 |** Mean values and standard deviations of iEEG features per channel in EH and NEH channels during rest and cognitive task performance.

| Hippocampus type | EH | NEH | EH | NEH |
|---|---|---|---|---|
| **Task** | **Rest** | | **Cognitive task** | |
| R/10 min | 120.1 ± 141.92 | 44.94 ± 37.07 | 64.84 ± 79.77 | 21.13 ± 14.71 |
| FR/10 min | 214.16 ± 327.25 | 44.28 ± 50.18 | 137.15 ± 176.33 | 35.39 ± 24.36 |
| R amplitude [–] | 6.87 ± 1.26 | 5.35 ± 0.93 | 6.28 ± 1.06 | 4.95 ± 0.81 |
| FR amplitude [–] | 6.62 ± 1.26 | 5.15 ± 0.86 | 6.12 ± 0.93 | 5.05 ± 0.54 |
| R frequency [Hz] | 176.75 ± 13.83 | 153.99 ± 17.42 | 175.69 ± 11.37 | 156.96 ± 18.25 |
| FR frequency [Hz] | 399.6 ± 28.81 | 400.05 ± 30.43 | 412.24 ± 29.2 | 412.36 ± 22.14 |
| R duration [ms] | 34.56 ± 4.13 | 38.09 ± 4.2 | 34.41 ± 3.61 | 35.78 ± 4.19 |
| FR duration [ms] | 18.19 ± 2.68 | 15.11 ± 3.35 | 17.11 ± 2.69 | 14.07 ± 1.86 |
| IED/10 min | 158.84 ± 154.96 | 44.81 ± 54.86 | 105.03 ± 127.74 | 16.27 ± 31.74 |
| IED amplitude [μV] | 378.61 ± 152.44 | 339.8 ± 172.27 | 370.88 ± 139.48 | 320.24 ± 214.9 |
| R linear correlation [–] | 0.43 ± 0.21 | 0.43 ± 0.26 | 0.44 ± 0.21 | 0.44 ± 0.27 |
| FR linear correlation [–] | 0.49 ± 0.22 | 0.44 ± 0.2 | 0.51 ± 0.24 | 0.48 ± 0.17 |
| R relative entropy [–] | 0.29 ± 0.26 | 0.1 ± 0.05 | 0.19 ± 0.15 | 0.08 ± 0.04 |
| FR relative entropy [–] | 0.15 ± 0.15 | 0.06 ± 0.03 | 0.1 ± 0.08 | 0.05 ± 0.02 |

*The statistical evaluation of differences between the values in this table are shown in **Figure 1**.*

and task performance. Hanley-McNeil test was used to determine the ROCs significantly different from chance (AUC = 0.5).

The statistical tests were carried out per channel for each task individually as well as for all the tasks grouped together. In case one subject performed multiple tasks, the mean value of iEEG features across all performed tasks was calculated for statistical testing. To verify that the statistics are not influenced by a subgroup of channels with outlying iEEG features we performed the same analysis per hippocampus where the median of iEEG features from all hippocampal channels was used.

The chosen significance level for all statistical tests was $\alpha = 0.05$.

### Machine Learning

The iEEG features with ROC significantly different from chance (AUC = 0.5) either for resting state, task performance or difference between the two states were used to create an SVM model for classification of EH and NEH channels. Only the grouped task ROC values were used for this analysis. To decorrelate the features we used principal component analysis (PCA) during training and testing of the model.

The SVM model was trained and tested in a similar fashion as in our previous work (22) where we performed leave-one-patient-out cross validation for localization of contacts in epileptogenic tissue. Here we use leave-one-hippocampus-out cross validation. The SVM model was trained on all data apart from one hippocampus which was used for classification by the trained model. To optimize the SVM performance, linear and radial basis function kernels were tested and their hyperparameters were tuned by an iterative grid search approach. The performance of the model was evaluated by mean ROC and corresponding AUC calculated from ROCs of each leave-one-hippocampus-out iteration. The evaluated hippocampus was classified as pathologic if the mean probability for classification of the channels as pathologic exceeded 50%. To assess whether iEEG features during rest, cognitive task or the difference between the two states carry different information the SVM model was created separately for each group and for all groups joined.

## RESULTS

### Statistical Analysis

The total number of analyzed channels was 254 (140 EH, 114 NEH) in 45 analyzed hippocampi (22 EH, 23 NEH). The numerical results for all iEEG features are summarized in **Table 2** while the results of individual statistical tests are visualized in **Figure 1**.

### HFO

The influence of cognitive processing on HFO was evaluated by comparing the difference in HFO features during resting state and cognitive task performance (**Figure 1A**). The rate of R was significantly reduced both in EH and NEH as a result of cognitive processing while FR rate was reduced only in EH and remained practically unchanged in NEH. The HFO amplitude was significantly reduced by cognitive processing in EH for both explored HFO groups but in NEH this trend was observed only in the R range. The evaluation of cognitive task influence on HFO duration revealed that the duration was significantly shorter in R band only in NEH and in FR in both NEH and EH. The frequency of HFO in EH and NEH was significantly higher during cognitive stimulation in FR while in R band the significant change occurred only in NEH.

To inspect how HFO features are different between EH and NEH the analysis during resting state and cognitive tasks was performed (**Figure 1B**).

During resting state, the rate and amplitude of HFO was significantly lower in NEH than in EH in both frequency bands.

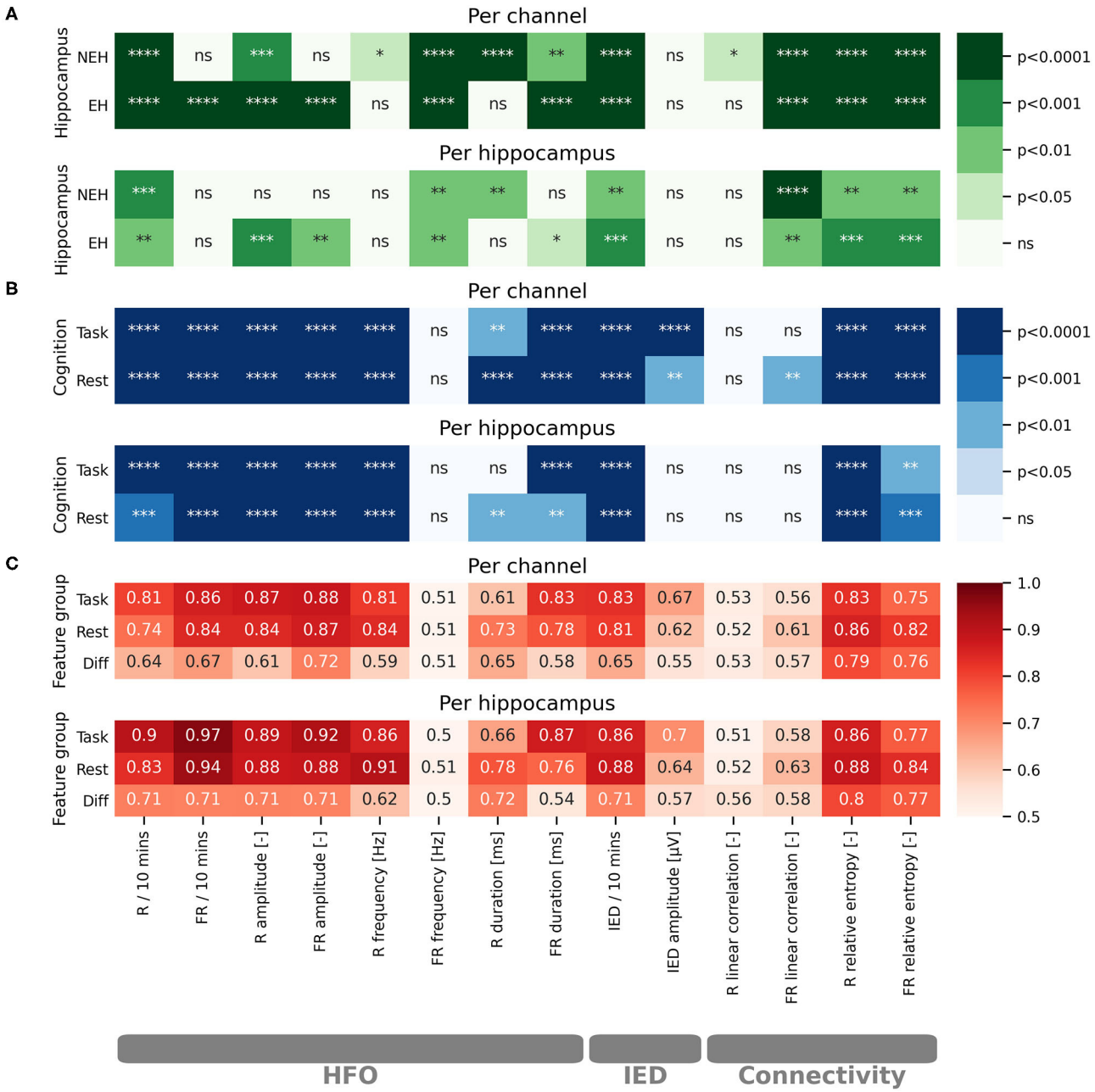


**FIGURE 1 |** Statistical evaluation of the impact of cognitive processing on iEEG features and evaluation of iEEG feature potential for classification of EH and NEH. The results are visualized for per channel and per hippocampus evaluations. The stars represent the level of significance as marked on the colorbars. Non significant results are marked by "ns." **(A)** Color-coded paired *t*-test significance level of iEEG features in EH and NEH as a result of cognitive stimulation. **(B)** Color-coded significance between EH and NEH during resting state period and cognitive task. **(C)** Color-coded values of ROC-AUC for classification of EH. ****($p < 0.0001$), ***($p < 0.001$), **($p < 0.01$), *($p < 0.05$), ns ($p < 1$).

The duration of HFO in EH compared to NEH was significantly longer in the R band but significantly shorter in the FR band. Significantly lower HFO frequencies in NEH were observed for R band but the difference in FR band was insignificant. During task performance, the HFO rate and amplitude changed similarly to resting state where they were significantly lower in NEH both for R and FR. The duration of R was significantly increased in NEH and, conversely, decreased in FR. HFO frequency during cognitive task was significantly different only in R band, where the NEH exhibited lower HFO frequencies.

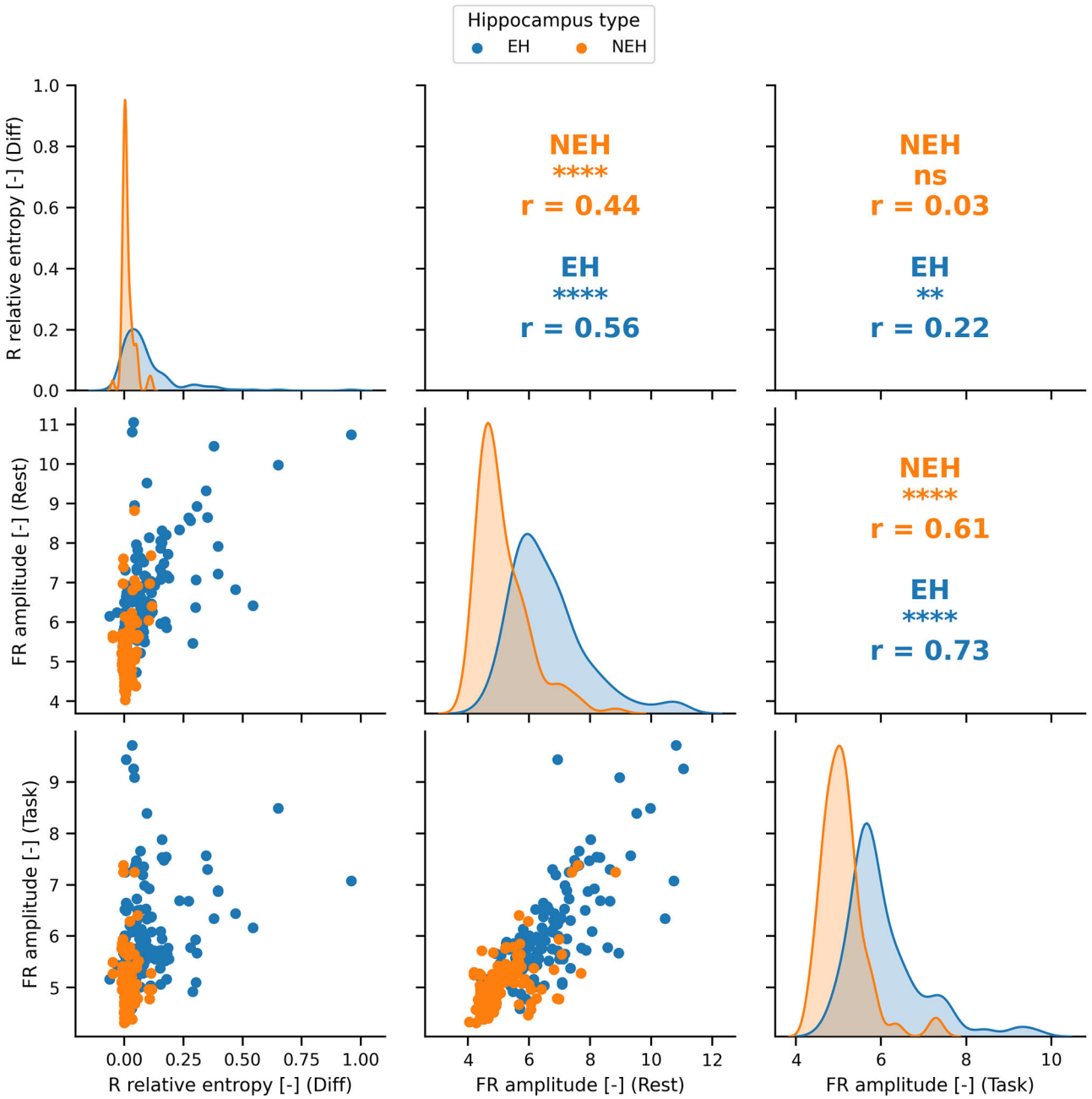


**FIGURE 2 |** The distributions and Pearson correlation coefficient (*r*) of the best performing features in rest, cognition and the difference between the two states. The best performing features are significantly correlated (significance denoted by stars) in most cases apart from FR amplitude during task and R relative entropy difference in NEH. PCA was therefore used to obtain uncorrelated principal components. ****($p < 0.0001$), ***($p < 0.001$), **($p << 0.01$), *($p < 0.05$), ns($p < 1$).

The analysis of HFO features utility for classification of EH and NEH was assessed by ROC-AUC during rest, during cognitive task and by the change between the two states (**Figure 1C**). More than half of the explored HFO features were significantly better than chance (14 out of 24). The HFO rate and amplitude along with R frequency and FR duration showed the highest classification potential both during resting state and task performance.

## IED

The changes in IED occurrence and amplitude as a result of cognitive task performance was evaluated in a similar fashion as HFO. IED rate was significantly reduced during task in EH and NEH. Conversely, the amplitude of spikes was not influenced neither in EH nor in NEH.

The rate of IED, and IED amplitude were significantly higher in EH during resting state and task performance.

While IED amplitude did not exhibit an ROC significantly better than chance, IED rate reached similar values of AUC as HFO rate and amplitude and was significant for resting state and task performance.

### Functional Connectivity

The changes in functional connectivity resulting from cognitive stimulation were estimated by linear correlation and relative entropy in the R and FR band. Linear correlation significantly increased during cognitive task in NEH in the R band. In the FR band the significant increase was observed in EH and NEH. The effect on relative entropy was reversed as it was significantly decreased in both bands and hippocampus types.

During resting state, linear correlation was significantly increased in EH compared to NEH only in the FR band while relative entropy was increased in both frequency bands. During cognitive task, relative entropy remained significantly increased in EH but linear correlation did non exhibit any significant difference between EH and NEH.

Hippocampus classification ROC-AUC of linear correlation was slightly higher in FR range but the ROCs were not significantly different from chance. On the other hand, relative entropy showed similar performance as HFO rate and amplitude with highly significant ROCs.

Per hippocampus analysis yielded similar results to per channel bases (**Figure 1**) with some tests showing nonsignificant results where per channel results were significant. This is a natural effect of performing statistical tests on fewer samples.

## Machine Learning

The features with ROC significantly different than chance during rest, task or the difference between the two states were chosen for the SVM model creation (**Figure 1C**). The top performing features and their correlation is presented in **Figure 2**.

The best performing SVM model hyperparameters were determined by an iterative grid search approach (**Table 3**). This approach was performed for iEEG features during rest, during task performance, the difference between the two states and for all feature groups joined.

ROC-AUC for classification of EH and NEH channels was calculated for each feature group. The lowest AUC was revealed for rest-task feature differences, followed by features during resting state and task performance. Combination of all features resulted in the highest AUC.

**TABLE 3 |** Best performing SVM hyperparameters for individual groups of features and for their aggregate.

| Group | Kernel | C | Gamma | AUC |
|---|---|---|---|---|
| Only rest | Linear | 0.001 | – | 0.90 |
| Only task | Linear | 0.001 | – | 0.92 |
| Only diff | rbf | 0.1 | 10 | 0.79 |
| All | rbf | 0.1 | 0.01 | 0.93 |

# DISCUSSION

Functional brain connectivity is commonly characterized by activity synchronization of neuronal subpopulations. Widespread neuronal networks including studied hippocampus are thought to be coordinated into synchronous oscillations, HFO during cognitive phenomena but also pathologic epileptic processes. In the presented study we investigated how the iEEG features are influenced by cognitive processing in EH and NEH. We subsequently used the results of this analysis to create an SVM model for classification of channels as EH and NEH.

The higher HFO rate and amplitude in EH during rest and task suggest the possible absence of pathological HFO in NEH and corroborates the results of previous studies (6, 12, 13, 33, 34). Higher resting state R frequency in EH compared to NEH is likely the result of imperfect labeling of FR as R due to the strict frequency boundary of 250 Hz and thus reflects the presence of pathological FR in EH. Some authors have put forward a hypothesis that pathological ripples are only slower fast ripples (11). In NEH, the longer R duration during rest and task performance is not surprising (35, 36). Nevertheless, these results contradict other previously published results (6, 12). This discrepancy might be caused by the fact that the work of Matsumoto et al. was mainly focused on motor cortex which might produce physiological HFO exhibiting disparate features from those in the hippocampus due to histologically different underlying tissue. Conversely to R, FR were longer in EH both during resting state and cognitive task performance reflecting the presence of pathological oscillations (12).

Cognitive processing induced reduction of HFO rates in EH and NEH across all explored frequency bands apart from FR in NEH. The observation that cognitive processing causes R rate decrease and no change in FR in NEH could be the result of decrease in number of R and increase of FR rates observed by Kucewicz et al. (30) in multiple structures including the hippocampus. As other studies previously suggested (37, 38), we hypothesize that the decrease of HFO rate and amplitude in EH as a result of cognitive processing is caused by suppression of epileptic activity in this structure. HFO changes within affected structures may suggest an increased involvement of the preserved normal hippocampal neurons that are active in some physiological cognitive processing and a reduced involvement of the synchronously bursting neurons within the epileptic network that are generating pathological HFO (38). The same explanation can be applied to similar results of possible pathologic ripple reduction in EH. In contrast to EH, the suppression of R rates and amplitude in NEH might be caused by shift of general HFO frequency toward FR band and, therefore, reduction of HFO amplitude and rate. This shift is further supported by the increased R and FR frequency along with shorter R and FR duration in NEH. It is likely that some residual physiological function remains in EH and the effect of reduction of epileptic activity is mingled with the shift observed in NEH.

IED rate was influenced in a similar way as R, being significantly higher in EH during rest as well as during cognitive task and decreased during cognitive task in both types of hippocampus which might reflect the suppression in epileptic activity not only in the hippocampus but also in non hippocampal structures from which the IEDs propagated to NEH. As was shown, specific tasks can suppress focal discharges over the brain regions that mediate the cognitive activity in question (37). IED amplitude was higher in EH than in NEH for both states which is an expected result.

Increased FR linear correlation in resting state EH could be ascribed to functional isolation of epileptic tissue as previously reported (18, 39). The increase in local FR linear correlation during cognitive task likely reflects high neuronal synchronization which is manifested through increased rate of FR HFO (30). Conversely to linear correlation, relative entropy was shown in our previous studies to reflect pathological processes (22, 23). This effect is further confirmed by the results in this study. Decrease in relative entropy during cognitive task further supports the hypothesis that cognitive processing suppresses pathological activity in the brain.

The AUC for classification of NEH and EH using resting state features in an SVM showed good performance. The task performance shower slightly higher AUC suggesting that the changes occurring during cognitive stimulation might carry unique information for localization of hippocampal epileptogenic tissue. The highest AUC was achieved when the SVM model was created with a combination of rest, task and difference features.

We show statistically different electrophysiological reactions of epileptic and non-epileptic hippocampus, which can be measured by HFO, IED and functional connectivity. We propose a hypothesis that cognitive processing reduces pathological electrophysiological activity in EH. Whether this effect is tied directly to stimuli presented to the patient and whether it is present in other brain structures remains to be explored. Analysis of the computed iEEG features in rest and task condition can improve functional mapping during pre-surgical evaluation and provide additional guidance for distinguishing between epileptic and non-epileptic structure which is absolutely crucial for achieving the best possible outcome with as little side effects as possible.

## LIMITATIONS OF THE STUDY

The NEH classification is problematic because even though such hippocampus is outside of the epileptogenic zone it is still likely influenced by epileptic networks and might exhibit traces of pathological behavior. The influence of different anti-epileptic drugs on the results could not be analyzed due to many variations in medication of individual patients.

## DATA AVAILABILITY STATEMENT

The datasets generated for this study are available on request to the corresponding author.

## ETHICS STATEMENT

The studies involving human participants were reviewed and approved by Ethics Committee of St. Anne's University Hospital in Brno. The patients/participants provided their written informed consent to participate in this study.

## AUTHOR CONTRIBUTIONS

JC carried out the statistical analyses and result visualizations. JC, MP, PK, VT, and MB participated on collection of metadata, writing of the manuscript and interpretation of the results. RR and AV provided data and metadata for cognitive task and assisted in interpretation of the cognitive task results. All authors contributed to the article and approved the submitted version.

## FUNDING

This work was supported by Ministry of Education, Youth and Sports of the Czechia Republic project no. LTAUSA18056 (programme INTER-EXCELLENCE). This study was also supported by the project no. LQ1605 from the National Program of Sustainability II (MEYS CR).

## REFERENCES

1. Leonardi M, Ustun TB. The global burden of epilepsy. *Epilepsia.* (2002) 43 (Suppl. 6):21–5. doi: 10.1046/j.1528-1157.43.s.6.11.x
2. Jefferys JGR. Hippocampal sclerosis and temporal lobe epilepsy: cause or consequence? *Brain.* (1999) 122:1007–8. doi: 10.1093/brain/122.6.1007
3. Wiebe S, Blume WT, Girvin JP, Eliasziw M. A randomized, controlled trial of surgery for temporal-lobe epilepsy. *N Engl J Med.* (2001) 345:311–8. doi: 10.1056/NEJM200108023450501
4. Buzsaki G, Horvath Z, Urioste R, Hetke J, Wise K. High-frequency network oscillation in the hippocampus. *Science.* (1992) 256:1025–7. doi: 10.1126/science.1589772
5. Bragin A, Engel J Jr, Wilson CL, Fried I, Mathern GW. Hippocampal and entorhinal cortex high-frequency oscillations (100–500 Hz) in human epileptic brain and in kainic acid–treated rats with chronic seizures. *Epilepsia.* (1999) 40:127–37. doi: 10.1111/j.1528-1157.1999.tb02065.x
6. Jacobs J, LeVan P, Chander R, Hall J, Dubeau F, Gotman J. Interictal high-frequency oscillations (80-500 Hz) are an indicator of seizure onset areas independent of spikes in the human epileptic brain. *Epilepsia.* (2008) 49:1893–907. doi: 10.1111/j.1528-1167.2008.01656.x
7. Worrell G, Gotman J. High-frequency oscillations and other electrophysiological biomarkers of epilepsy: clinical studies. *Biomark Med.* (2011) 5:557–66. doi: 10.2217/bmm.11.74
8. Zijlmans M, Jacobs J, Kahn YU, Zelmann R, Dubeau F, Gotman J. Ictal and interictal high frequency oscillations in patients with focal epilepsy. *Clin Neurophysiol.* (2011) 122:664–71. doi: 10.1016/j.clinph.2010.09.021
9. Engel J Jr, da Silva FL. High-frequency oscillations - where we are and where we need to go. *Prog Neurobiol.* (2012) 98:316–8. doi: 10.1016/j.pneurobio.2012.02.001
10. Fedele T, Burnos S, Boran E, Krayenbühl N, Hilfiker P, Grunwald T, et al. Resection of high frequency oscillations predicts seizure outcome in the individual patient. *Sci Rep.* (2017) 7:13836. doi: 10.1038/s41598-017-13064-1

11. Frauscher B, Bartolomei F, Kobayashi K, Cimbalnik J, van't Klooster MA, Rampp S, et al. High-frequency oscillations: the state of clinical research. *Epilepsia*. (2017) 58:1316–29. doi: 10.1111/epi.13829
12. Matsumoto A, Brinkmann BH, Matthew Stead S, Matsumoto J, Kucewicz MT, Marsh WR, et al. Pathological and physiological high-frequency oscillations in focal human epilepsy. *J Neurophysiol.* (2013) 110:1958–64. doi: 10.1152/jn.00341.2013
13. Cimbalnik J, Brinkmann B, Kremen V, Jurak P, Berry B, Van Gompel J, et al. Physiological and pathological high frequency oscillations in focal epilepsy. *Ann Clin Transl Neurol.* (2018) 5:1062–76. doi: 10.1002/acn3.618
14. Buzsáki G, da Silva FL. High frequency oscillations in the intact brain. *Prog Neurobiol.* (2012) 98:241–9. doi: 10.1016/j.pneurobio.2012.02.004
15. Bragin A, Engel J, Staba RJ. High-frequency oscillations in epileptic brain. *Curr Opin Neurol.* (2010) 23:151–6. doi: 10.1097/WCO.0b013e3283373ac8
16. Jacobs J, Zijlmans M, Zelmann R, Chatillon C-É, Hall J, Olivier A, et al. High-frequency electroencephalographic oscillations correlate with outcome of epilepsy surgery. *Ann Neurol.* (2010) 67:209–20. doi: 10.1002/ana.21847
17. Serafini R. Similarities and differences between the interictal epileptiform discharges of green-spikes and red-spikes zones of human neocortex. *Clin Neurophysiol.* (2019) 130:396–405. doi: 10.1016/j.clinph.2018.12.011
18. Klimes P, Duque JJ, Brinkmann B, Van Gompel J, Stead M, St Louis EK, et al. The functional organization of human epileptic hippocampus. *J Neurophysiol.* (2016) 115:3140–5. doi: 10.1152/jn.00089.2016
19. Zweiphenning WJEM, van't Klooster MA, van Diessen E, van Klink NEC, Huiskamp GJM, Gebbink TA, et al. High frequency oscillations and high frequency functional network characteristics in the intraoperative electrocorticogram in epilepsy. *Neuroimage Clin.* (2016) 12:928–39. doi: 10.1016/j.nicl.2016.09.014
20. Chen D, Wan S, Bao FS. Epileptic focus localization using discrete wavelet transform based on interictal intracranial EEG. *IEEE Trans Neural Syst Rehabil Eng.* (2017) 25:413–25. doi: 10.1109/TNSRE.2016.2604393
21. Varatharajah Y, Berry B, Cimbalnik J, Kremen V, Van Gompel J, Stead M, et al. Integrating artificial intelligence with real-time intracranial EEG monitoring to automate interictal identification of seizure onset zones in focal epilepsy. *J Neural Eng.* (2018) 15:046035. doi: 10.1088/1741-2552/aac960
22. Cimbalnik J, Klimes P, Sladky V, Nejedly P, Jurak P, Pail M, et al. Multi-feature localization of epileptic foci from interictal, intracranial EEG. *Clin Neurophysiol.* (2019) 130:1945–53. doi: 10.1016/j.clinph.2019.07.024
23. Klimes P, Cimbalnik J, Brazdil M, Hall J, Dubeau F, Gotman J, et al. NREM sleep is the state of vigilance that best identifies the epileptogenic zone in the interictal electroencephalogram. *Epilepsia*. (2019) 60:2404–15. doi: 10.1111/epi.16377
24. Polich J. Updating P300: an integrative theory of P3a and P3b. *Clin Neurophysiol*. (2007) 118:2128–48. doi: 10.1016/j.clinph.2007.04.019
25. Albares M, Lio G, Criaud M, Anton JL, Desmurget M, Boulinguez P. The dorsal medial frontal cortex mediates automatic motor inhibition in uncertain contexts: evidence from combined fMRI and EEG studies. *Hum Brain Mapp*. (2014) 35:5517–31. doi: 10.1002/hbm.22567
26. Shaw DJ, Czekóová K, Staněk R, Mareček R, Urbánek T, Špalek J, et al. A dual-fMRI investigation of the iterated Ultimatum Game reveals that reciprocal behaviour is associated with neural alignment. *Sci Rep*. (2018) 8:10896. doi: 10.1038/s41598-018-29233-9
27. Näätänen R, Paavilainen P, Rinne T, Alho K. The mismatch negativity (MMN) in basic research of central auditory processing: a review. *Clin Neurophysiol.* (2007) 118:2544–90. doi: 10.1016/j.clinph.2007.04.026
28. Duncan CC, Barry RJ, Connolly JF, Fischer C, Michie PT, Näätänen R, et al. Event-related potentials in clinical research: guidelines for eliciting, recording, and quantifying mismatch negativity, P300, and N400. *Clin Neurophysiol.* (2009) 120:1883–908. doi: 10.1016/j.clinph.2009.07.045
29. Higuchi Y, Seo T, Miyanishi T, Kawasaki Y, Suzuki M, Sumiyoshi T. Mismatch negativity and p3a/reorienting complex in subjects with schizophrenia or at-risk mental state. *Front Behav Neurosci.* (2014) 8:172. doi: 10.3389/fnbeh.2014.00172
30. Kucewicz MT, Cimbalnik J, Matsumoto JY, Brinkmann BH, Bower MR, Vasoli V, et al. High frequency oscillations are associated with cognitive processing in human recognition memory. *Brain.* (2014) 137:2231–44. doi: 10.1093/brain/awu149
31. Rehulka P, Cimbálník J, Pail M, Chrastina J, Hermanová M, Brázdil M. Hippocampal high frequency oscillations in unilateral and bilateral mesial temporal lobe epilepsy. *Clin Neurophysiol.* (2019) 130:1151–9. doi: 10.1016/j.clinph.2019.03.026
32. Barkmeier DT, Shah AK, Flanagan D, Atkinson MD, Agarwal R, Fuerst DR, et al. High inter-reviewer variability of spike detection on intracranial EEG addressed by an automated multi-channel algorithm. *Clin Neurophysiol.* (2012) 123:1088–95. doi: 10.1016/j.clinph.2011.09.023
33. Urrestarazu E, Chander R, Dubeau F, Gotman J. Interictal high-frequency oscillations (100-500 Hz) in the intracerebral EEG of epileptic patients. *Brain.* (2007) 130:2354–66. doi: 10.1093/brain/awm149
34. Jacobs J, Levan P, Châtillon C-E, Olivier A, Dubeau F, Gotman J. High frequency oscillations in intracranial EEGs mark epileptogenicity rather than lesion type. *Brain.* (2009) 132:1022–37. doi: 10.1093/brain/awn351
35. Nagasawa T, Juhász C, Rothermel R, Hoechstetter K, Sood S, Asano E. Spontaneous and visually driven high-frequency oscillations in the occipital cortex: intracranial recording in epileptic patients. *Hum Brain Mapp.* (2012) 33:569–83. doi: 10.1002/hbm.21233
36. Pail M, Rehulka P, Cimbálník J, DoleŽalová I, Chrastina J, Brázdil M. Frequency-independent characteristics of high-frequency oscillations in epileptic and non-epileptic regions. *Clin Neurophysiol.* (2017) 128:106–14. doi: 10.1016/j.clinph.2016.10.011
37. Binnie CD. Cognitive impairment during epileptiform discharges: is it ever justifiable to treat the EEG? *Lancet Neurol.* (2003) 2:725–30. doi: 10.1016/S1474-4422(03)00584-2
38. Brázdil M, Cimbálník J, Roman R, Shaw DJ, Stead MM, Daniel P, et al. Impact of cognitive stimulation on ripples within human epileptic and non-epileptic hippocampus. *BMC Neurosci.* (2015) 16:47. doi: 10.1186/s12868-015-0184-0
39. Warren CP, Hu S, Stead M, Brinkmann BH, Bower MR, Worrell GA. Synchrony in normal and focal epileptic brain: the seizure onset zone is functionally disconnected. *J Neurophysiol.* (2010) 104:3530–9. doi: 10.1152/jn.00368.2010


**Conflict of Interest:** The authors declare that the research was conducted in the absence of any commercial or financial relationships that could be construed as a potential conflict of interest.

*Copyright © 2020 Cimbalnik, Pail, Klimes, Travnicek, Roman, Vajcner and Brazdil. This is an open-access article distributed under the terms of the Creative Commons Attribution License (CC BY). The use, distribution or reproduction in other forums is permitted, provided the original author(s) and the copyright owner(s) are credited and that the original publication in this journal is cited, in accordance with accepted academic practice. No use, distribution or reproduction is permitted which does not comply with these terms.*

frontiers in Human Neuroscience

REVIEW
published: 12 January 2021
doi: 10.3389/fnhum.2020.612024

# The Oscillatory Basis of Working Memory Function and Dysfunction in Epilepsy

*Olivia N. Arski[1,2], Julia M. Young[2,3], Mary-Lou Smith[2,3,4] and George M. Ibrahim[1,2,5,6]**

[1] Institute of Medical Science, University of Toronto, Toronto, ON, Canada, [2] Program in Neuroscience and Mental Health, Hospital for Sick Children Research Institute, Toronto, ON, Canada, [3] Department of Psychology, Hospital for Sick Children, Toronto, ON, Canada, [4] Department of Psychology, University of Toronto Mississauga, Mississauga, ON, Canada, [5] Institute of Biomaterials and Biomedical Engineering, University of Toronto, Toronto, ON, Canada, [6] Division of Neurosurgery, Department of Surgery, Hospital for Sick Children, University of Toronto, Toronto, ON, Canada

Working memory (WM) deficits are pervasive co-morbidities of epilepsy. Although the pathophysiological mechanisms underpinning these impairments remain elusive, it is thought that WM depends on oscillatory interactions within and between nodes of large-scale functional networks. These include the hippocampus and default mode network as well as the prefrontal cortex and frontoparietal central executive network. Here, we review the functional roles of neural oscillations in subserving WM and the putative mechanisms by which epilepsy disrupts normative activity, leading to aberrant oscillatory signatures. We highlight the particular role of interictal epileptic activity, including interictal epileptiform discharges and high frequency oscillations (HFOs) in WM deficits. We also discuss the translational opportunities presented by greater understanding of the oscillatory basis of WM function and dysfunction in epilepsy, including potential targets for neuromodulation.

**Keywords: working memory, epilepsy, neural networks, high frequency oscillations, hippocampus**

OPEN ACCESS

***Edited by:***
*Johannes Sarnthein, University of Zurich, Switzerland*

***Reviewed by:***
*Vasileios S. Dimakopoulos, University Hospital Zürich, Switzerland*
*pierre-pascal Lenck-Santini, Institut National de la Santé et de la Recherche Médicale (INSERM), France*

***Correspondence:**
*George M. Ibrahim*
*george.ibrahim@sickkids.ca*

***Specialty section:***
*This article was submitted to Health, a section of the journal Frontiers in Human Neuroscience*

***Received:*** *30 September 2020*
***Accepted:*** *10 December 2020*
***Published:*** *12 January 2021*

***Citation:***
*Arski ON, Young JM, Smith M-L and Ibrahim GM (2021) The Oscillatory Basis of Working Memory Function and Dysfunction in Epilepsy. Front. Hum. Neurosci. 14:612024. doi: 10.3389/fnhum.2020.612024*

## INTRODUCTION

Epilepsy is a serious neurological condition that affects millions worldwide (Guerrini, 2006). While epilepsy is characterized by seizures, deficits in working memory (WM) are also pervasive (Motamedi and Meador, 2003; Holmes, 2013; Nickels et al., 2016) and associated with significant morbidity and diminished quality of life (Danguecan and Smith, 2017). The burden of WM impairment in epilepsy is underscored by the ubiquitous need for WM in adaptive functioning and cognition. In particular, WM encompasses the capacity to transiently retain information to guide goal-directed behavior (Baddeley, 1992). As such, WM is implicated in a host of higher cognitive processes and skills. Indeed, WM impairment has been associated with difficulties in academic outcomes, attention deficits, and memory impairment in children and adults with epilepsy (Fastenau et al., 2004; van Rijckevorsel, 2006; Fuentes and Kerr, 2016).

**Abbreviations:** AEDs, anti-epileptic drugs; AI, anterior insula; dACC, dorsal anterior cingulate cortex; DAN, dorsal attention network; dlPFC, dorsolateral prefrontal cortex; DMN, default mode network; EEG, electroencephalography; fMRI, functional magnetic resonance imaging; FP-CEN, frontoparietal central executive network; FLE, frontal lobe epilepsy; HFOs, high frequency oscillations; IEDs, interictal epileptiform discharges; IPL, inferior parietal lobe; IPS, intraparietal sulcus; IQ, intelligence quotient; LEV, levetiracetam; LTD, long-term depression; LTM, long-term memory; LTP, long-term potentiation; MFG, middle frontal gyrus; mPFC, medial prefrontal cortex; MS-DBB, medial septum-diagonal band of Broca; MTL, medial temporal lobe; PCC, posterior cingulate cortex; PFC, prefrontal cortex; PPC, posterior parietal cortex; rs-MRI, resting-stating magnetic resonance imaging; SFG, superior frontal gyrus; SN, salience network; SV2A, synaptic vesicle protein 2A; TCI, transient cognitive impairment; TLE, temporal lobe epilepsy; TPM, topiramate, WM, working memory.

Notably, epilepsy surgery can render an individual seizure-free, but may not improve WM (Helmstaedter and Kurthen, 2001). Therefore, there is an unmet need to better understand these impairments and to develop treatments targeting WM function in individuals with epilepsy. Translational opportunities are afforded greater understanding of first, the neural substrates underlying WM function, and second, the pathophysiological mechanisms by which epileptic activity disrupts these dynamics.

Converging evidence from multiple modalities including resting-state and functional magnetic resonance imaging (rs-MRI and fMRI) and intracranial electroencephalography (EEG) demonstrates that WM relies on oscillatory interactions within and between nodes of canonical, large-scale functional networks, including the frontoparietal central executive network (FP-CEN), salience network (SN), and default mode network (DMN) (Liang et al., 2016). These oscillatory interactions occur in various frequencies, including the theta, alpha, and gamma bands. Importantly, the activity of each functional network and oscillatory frequency is specialized to subserve different subprocesses of WM (Von Stein and Sarnthein, 2000). In particular, theta oscillations in the hippocampus and prefrontal cortex (PFC) are thought to be critical to WM function, mediating the encoding, maintenance, and retrieval of stimuli as well as their governing central executive processes (Kahana et al., 2001; Sauseng et al., 2010).

The causes of WM impairment in epilepsy remain elusive and likely multifactorial. There may be primary dysfunction of underlying brain circuitry comorbid with epilepsy. Indeed, neurocognitive deficits often predate the onset of seizures and the diagnosis of epilepsy (Austin et al., 2001). Conversely, recurrent seizures, epileptiform discharges, and transient epilepsy-related events, such as high frequency oscillations (HFOs) may affect coordinated functional interactions between and within cortical regions subserving WM (Holmes and Lenck-Santini, 2006; Ewell et al., 2019). In addition, anti-epileptic drugs (AEDs), and particularly topiramate (TPM), have also been implicated in WM impairment (Kockelmann et al., 2003; Lee et al., 2003; Jansen et al., 2006; Ciantis et al., 2008; Szaflarski and Allendorfer, 2012; Yasuda et al., 2013; Tang et al., 2016; Wandschneider et al., 2017; Hu et al., 2019; Callisto et al., 2020).

The current review maps the literature pertaining to the oscillatory and large-scale network basis of WM and its impairment in epilepsy. We describe the current literature linking regional and spectral specificity to WM function. The mechanisms by which epilepsy may interfere with normative network function are summarized and explored. The current work provides a framework for WM function and dysfunction in epilepsy with a view toward expanding understanding of this fundamental process and informing future research into better treatments for affected individuals.

## WORKING MEMORY

Working memory is a cognitive system that subsumes the ability to encode, maintain, manipulate, and retrieve information in a transient manner (Roux and Uhlhaas, 2014). This system is limited in capacity and operates across a range of cognitive tasks to facilitate goal-oriented behavior (Baddeley, 1992). The conceptual underpinnings of WM have been described in several models (**Table 1**; Baddeley and Hitch, 1974; Cowan, 1988; Ericsson and Delaney, 1999; Shah and Miyake, 1999; Repovš and Baddeley, 2006; Lovett et al., 2012). A particularly influential framework of WM is described in the multi-component model, proposed by Baddeley and Hitch (1974) and later revised by Repovš and Baddeley (2006). The multi-component model of WM assumes four functional components: the central executive, the phonological loop, the visuospatial sketchpad, and the episodic buffer (Baddeley and Hitch, 1974; Repovš and Baddeley, 2006; **Figure 1**).

The central executive serves as the attentional component of WM, supervising and coordinating the two subsidiary storage systems: the phonological loop and the visuospatial sketchpad. These systems are domain-specific, enabling the temporary storage and rehearsal of verbal and visuospatial information, respectively. The phonological loop and the visuospatial sketchpad are both comprised of a passive limited-capacity store (e.g., phonological store, visual cache), which holds information for a few seconds before the memory trace fades, and an active rehearsal process (e.g., articulatory control process, inner scribe), which rehearses and manipulates information (Baddeley, 1992; Logie, 2011). The episodic buffer is responsible for integrating information across domains and serves as the intermediary system between WM and long-term memory (LTM) (Baddeley and Hitch, 1974; Repovš and Baddeley, 2006).

The importance of WM is indexed by its role in supporting higher cognitive processes, including learning, memory, planning, reasoning, language comprehension, mathematical abilities, and spatial processing (Baddeley, 2003; Raghubar et al., 2010; Logie, 2011). Given the ubiquity of WM in cognitive processes, impairment in WM is debilitating and underlies a host of learning and developmental difficulties in children and can lead to functional challenges in adults (Jeffries and Everatt, 2004).

## LARGE-SCALE NETWORKS SUBSERVING WM

Working memory is mediated by a distributed network of cortical and subcortical regions (Wager and Smith, 2003; Owen et al., 2005; Rottschy et al., 2012). A core WM network, comprised of frontal and parietal cortices, has been identified by several meta-analyses of neuroimaging studies (Wager and Smith, 2003; Owen et al., 2005; Rottschy et al., 2012). This frontoparietal network is associated with the central executive of WM and is known as the FP-CEN (Collette et al., 1999; Kondo et al., 2004; Li et al., 2004; Osaka et al., 2004; Sauseng et al., 2005; Palva et al., 2010). The function of the FP-CEN includes resource allocation during the simultaneous execution of two tasks (e.g., dual task coordination), modification of WM contents according to internal or external inputs (e.g., updating processes), and decision-making in the context of goal-directed behavior (Miller and Cohen, 2001; Collette and Van Der Linden, 2002). Cortical regions that are consistently implicated in the FP-CEN

**TABLE 1 |** Summary of prominent WM models.

| Models of WM | Authors | Components | Access to WM information | Description |
|---|---|---|---|---|
| Multi-component | Baddeley and Hitch, 1974; Repovš and Baddeley, 2006 | Central executive<br>Phonological loop<br>Visuospatial sketchpad<br>Episodic buffer | Modality-specific buffers<br>Long-term memory activation | Central executive supervises stored information in modality-specific buffers (e.g., verbal in phonological loop and visuospatial in visuospatial sketchpad)<br>Episodic buffer integrates information across modalities and activates long-term memory information |
| Embedded-processes | Cowan, 1988; Shah and Miyake, 1999 | Central executive<br>Active memory<br>Focus of attention | Long-term memory activation | Central executive activates long-term memory information (e.g., active memory)<br>Subset of active memory becomes focus of attention |
| Adaptive Control of Thought – Rational (ACT-R) | Lovett et al., 2012 | Central executive<br>Task goal | Long-term memory activation | Central executive activates long-term memory information relevant to task goals |
| Long-term Working Memory (LT-WM) | Ericsson and Delaney, 1999 | Experience-related retrieval cues | Long-term memory activation | Experience-related retrieval cues in short term memory activate long-term memory information |

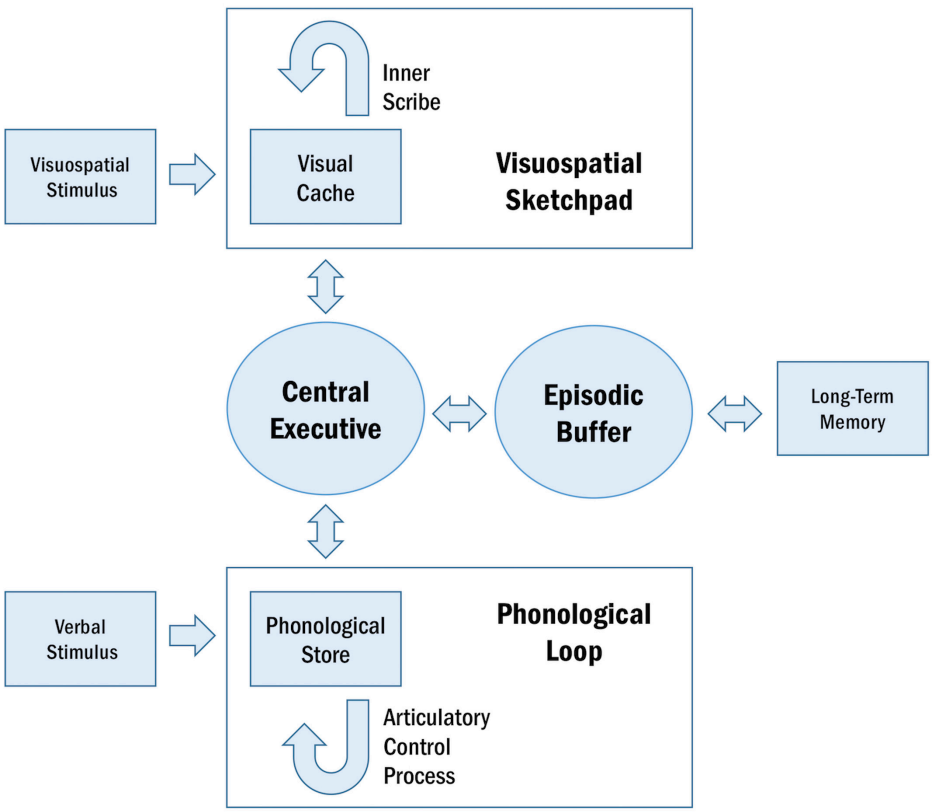


**FIGURE 1 |** Schematic representation of the multi-component model of WM. The central executive supervises the two domain-specific subsystems, the phonological loop and the visuospatial sketchpad. Within these sub-systems, the phonological store and visual cache serve as limited-capacity stores and the articulatory control process and inner scribe rehearse information. The episodic buffer integrates information across domains and enables interactions between WM and long-term memory.

include the dorsolateral prefrontal cortex (dlPFC) and posterior parietal cortex (PPC)/intraparietal sulcus (IPS) (Baddeley, 2003; Seeley et al., 2007; Braunlich et al., 2015).

The FP-CEN interacts with other functional networks during WM tasks, including the SN, the dorsal attention network (DAN), and the DMN. WM demands modulate these interactions, mediating between the internally oriented activity of the DMN and the externally oriented activities of the FP-CEN, the SN, and the DAN (Liang et al., 2016).

The SN comprises the anterior insula (AI)/frontoinsular cortex and dorsal anterior cingulate cortex (dACC)/middle frontal gyrus (Braunlich et al., 2015). The SN is responsible for the detection of salient stimuli (Seeley et al., 2007). Notably, salience detection by the SN is not engendered in a task-specific manner and can encompass cognitive, homeostatic, or emotional salience (White et al., 2010). It is postulated that the FP-CEN selectively operates on salient stimuli detected by the SN (Seeley et al., 2007). These FP-CEN-mediated operations are task-specific

and include maintaining and manipulating relevant stimulus representations in WM (Braunlich et al., 2015). Braunlich et al. (2015) demonstrated these dissociable WM functions of the SN and the FP-CEN using principal components analysis and fMRI during delayed-match-to-category and delayed-match-to-sample tasks. The authors identified a network comprising regions of the SN, which demonstrated a pattern of activity consistent with orienting to and processing of complex information. These regions of the SN exhibited rapid hemodynamic response peaks following stimulus onset and increased activity during conditions requiring item processing. The authors also identified a network comprising regions of the FP-CEN, which demonstrated a pattern of activity consistent with decision-making. These regions of the FP-CEN exhibited slower responses following stimulus onset and increased activity during categorization, which relies on stimulus maintenance and manipulation (Braunlich et al., 2015). Conceivably, integration of the FP-CEN and the SN is necessary for these WM-related processes, which encompass both stimulus detection and selective maintenance and manipulation of relevant stimuli (Gong et al., 2016). Indeed, resting-state coupling between core regions within the FP-CEN and the SN contributes to WM performance (Fang et al., 2016).

The DAN is comprised of important nodes in the frontal eye fields, premotor cortex, and superior parietal lobe (Braunlich et al., 2015). The DAN is closely associated with sensorimotor regions and is characterized by externally oriented activity, playing a key role in visuospatial perceptual attention (Dixon et al., 2018). The FP-CEN co-activates with the DAN during externally oriented WM tasks. Here, both networks attend to relevant stimuli in the environment (Elton and Gao, 2014).

The DMN is primarily comprised of the medial prefrontal cortex (mPFC), posterior cingulate cortex (PCC), and inferior parietal lobe (IPL) (Liang et al., 2016). The DMN is characterized by internally oriented activity and is involved in mentalizing, spontaneous cognition, and self-referential processing (Dixon et al., 2018). The DMN is negatively correlated with FP-CEN activity during WM (Clare Kelly et al., 2008) and opposing patterns of connectivity can be observed within these two networks during WM processing (Liang et al., 2016). For instance, connectivity within the FP-CEN increases with WM load, whereas connectivity within the DMN decreases with WM load (Liang et al., 2016). Interestingly, the SN facilitates switching between the FP-CEN and the DMN during WM. This switching enables the SN to allocate attentional and WM-related resources to the most salient stimuli among internal (i.e., DMN-related) and external (i.e., FP-CEN-related) events (Sridharan et al., 2008; Menon and Uddin, 2010). Notably, the SN becomes more integrated with both the FP-CEN and the DMN as WM load increases (Liang et al., 2016).

The DMN and the FP-CEN are further divided into sub-systems that are relevant to WM. The DMN is comprised of two sub-systems, the dorsal medial sub-system and the medial temporal sub-system (Andrews-Hanna et al., 2014). The dorsal medial sub-system is involved in mentalizing and social cognition and comprises the dorsal medial PFC, the temporoparietal junction, the lateral temporal cortex, and the temporal pole (Andrews-Hanna et al., 2014). The medial temporal sub-system is involved in past and future autobiographical thought, episodic memory, and contextual retrieval, and comprises the hippocampus, the parahippocampal cortex, the retrosplenial cortex, the posterior IPL and the ventromedial PFC (Andrews-Hanna et al., 2014). The medial temporal sub-system, and particularly the hippocampus, is implicated in WM.

The hippocampus plays an important role in novelty detection (Knight, 1996) and associative binding (Wallenstein et al., 1998; Yonelinas, 2013) and is consistently recruited during the encoding, maintenance, and retrieval of novel or complex information in WM (Karlsgodt et al., 2005; Cashdollar et al., 2009; Leszczynski, 2011). The activity of hippocampal neurons is thought to represent a conjunction of task-relevant features in WM, including those of a non-spatial origin (Deadwyler et al., 1996). Notably, recent findings demonstrate that hippocampal firing during WM could differentiate between success and error trials during stimulus encoding, predict workload during WM maintenance, and predict behavioral response during retrieval (Boran et al., 2019). Further evidence for the role of the hippocampus in WM derives from anatomical and behavioral dissociations, which demonstrate that lesions of the hippocampus or its extrinsic connections adversely affect WM performance (Olton and Feustle, 1981; Deadwyler et al., 1996). Additionally, the hippocampus serves as a locus of interaction between WM and LTM, supporting the encoding of information from WM into LTM and the retrieval of information from LTM into WM. Indeed, activation of the hippocampus during the maintenance of information in WM is predictive of subsequent LTM performance (Ranganath et al., 2005). Given the role of the hippocampus in associative binding and WM-LTM interactions, it is thought that the hippocampus contributes to the underlying substrate of the episodic buffer in WM.

The FP-CEN also comprises two subnetworks, FP-CEN subnetwork A and FP-CEN subnetwork B. Each subnetwork is associated with either the DAN or the DMN (Elton and Gao, 2014; Dixon et al., 2018; Murphy et al., 2020). FP-CEN subnetwork A is preferentially associated with the DMN and mainly consists of the rostrolateral PFC, middle frontal gyrus (MFG), and superior frontal gyrus (SFG) (Kam et al., 2019). During internally oriented WM tasks, the FP-CEN subnetwork A disengages with the DAN and engages with the DMN. Conversely, the FP-CEN subnetwork B is preferentially associated with the DAN and mainly encompasses the inferior frontal sulcus and the posterior aspect of the superior frontal sulcus (Kam et al., 2019). During externally oriented WM tasks, the FP-CEN subnetwork B disengages with the DMN and engages with the DAN. Together, the complementary processes of the FP-CEN subnetworks are thought to segregate external stimuli from internal trains of thought during WM (Elton and Gao, 2014; Dixon et al., 2018; Murphy et al., 2020).

In addition to the WM trends that emerge with specialization of the functional networks, material-specific lateralization has previously been demonstrated in the WM network as a collective (Sauseng et al., 2005), although these effects are less robust in children. The phonological loop is associated with left hemispheric activation (Smith et al., 1996; Sarnthein et al., 1998;

Clark et al., 2001), and neuroimaging studies have identified the supramarginal gyrus (BA 40) as the phonological store and Broca's area in the left IFG (BA 6/44) as the articulatory control process (Paulesu et al., 1993; Baddeley, 2003; Papagno et al., 2017). Conversely, the visuospatial sketchpad is associated with right hemispheric activation (Smith et al., 1996), and neuroimaging studies have identified the right inferior parietal cortex (BA 40) as the visual cache and the right premotor cortex (BA 6) and right inferior frontal cortex (BA 47) (Baddeley, 2003) as regions of the inner scribe (Baddeley, 2003; **Figure 2**).

## NEURAL OSCILLATIONS

Working memory processing depends on interactions between neuronal ensembles within WM networks (Klimesch et al., 2010). These interactions are subserved by the intrinsic oscillatory character of neuronal ensembles (Fries, 2005). As neuronal ensembles oscillate, they undergo rhythmic changes in neuronal excitability, which enable and suppress their ability to send and receive information (Buzsáki and Draguhn, 2004). For information to be propagated from one neuronal ensemble to another, the two ensembles must be excitable in the same temporal window (Fries, 2005). Neuronal coherence, the synchronization of the oscillating ensembles, facilitates information propagation by establishing a transient network with shared temporal windows for communication (Fries, 2005).

Neural oscillations are subdivided into canonical bands based on frequency. These frequency bands include delta (1–4 Hz), theta (4–7 Hz), alpha (8–12 Hz), beta (15–30 Hz), and gamma (>30 Hz). Neural oscillations serve specialized functions in WM according to their frequency (**Figure 3**). Low frequency synchronization is observed between distant brain regions and is thought to underlie context-driven, top-down WM processes including executive control (Von Stein and Sarnthein, 2000). Conversely, high frequency synchronization is observed between local brain regions and is thought to underlie stimulus-driven, bottom-up WM processes including perception (Von Stein and Sarnthein, 2000).

Certain properties of neural oscillations can be modulated by WM, including the oscillatory amplitude and phase. The oscillatory amplitude is related to the power, which is the squared amplitude of the oscillation. Power reflects the number of neuronal units that are synchronously active and indicates the extent of task involvement: task-relevant oscillations exhibit increased amplitudes, whereas task-irrelevant oscillations exhibit decreased amplitudes (Klimesch et al., 2008). The oscillatory phase refers to the timing of neuronal excitability and is an important mechanism determining whether information is propagated within the task-relevant network. A neuron is unlikely to generate action potentials during the phase of low excitability, whereas a neuron is very likely to generate action potentials during the phase of high excitability (Fries, 2005). By extension, oscillating

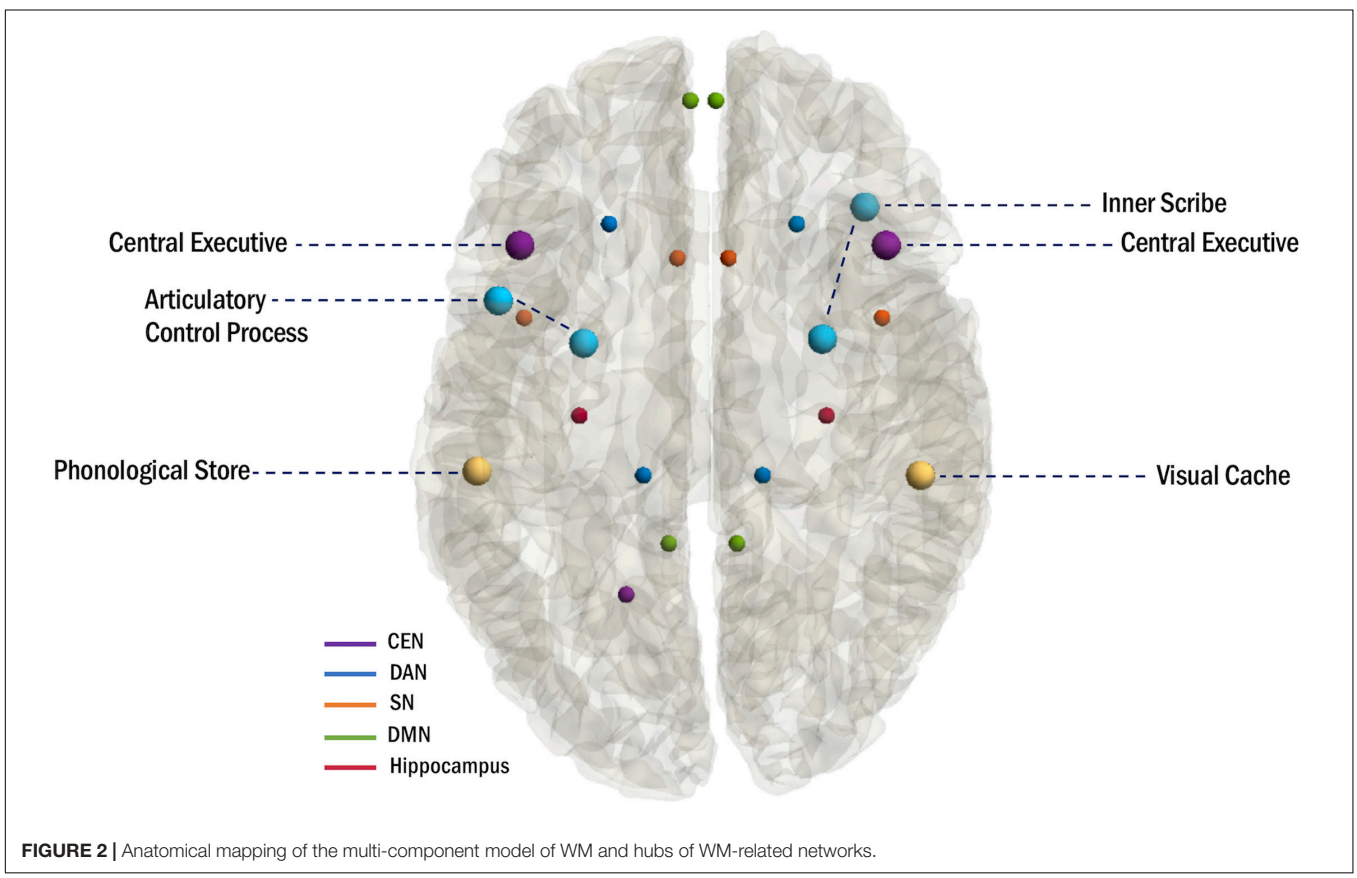


**FIGURE 2 |** Anatomical mapping of the multi-component model of WM and hubs of WM-related networks.

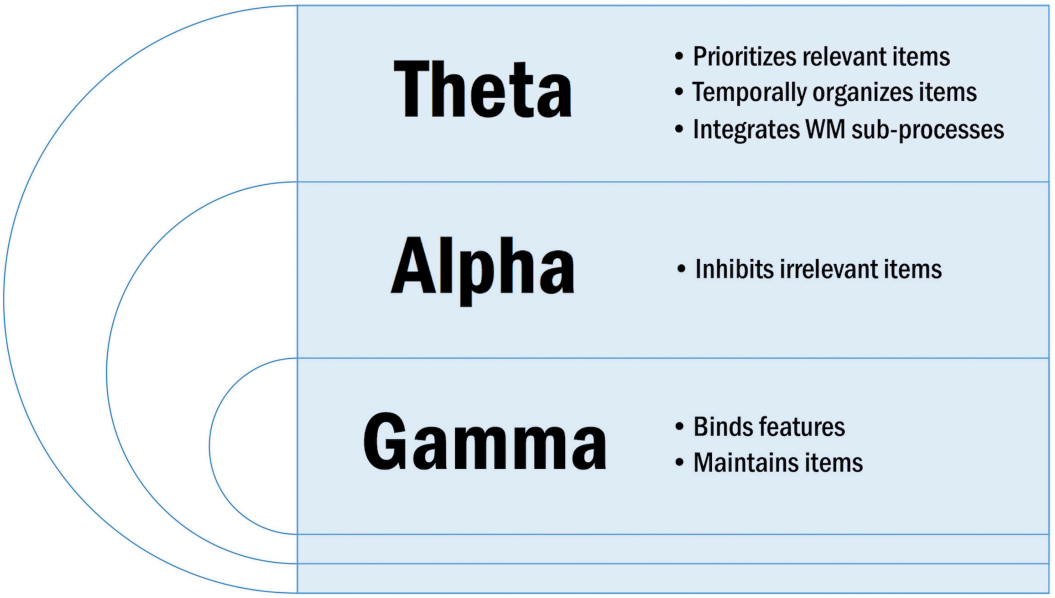


**FIGURE 3 |** Overview of specialized oscillatory functions in WM.

neuronal ensembles fire synchronously during the excitatory phase. Consequently, targeted neuronal ensembles receive the information synchronously, and information is propagated throughout the network (Klimesch et al., 2010).

In a similar vein, oscillatory phase can synchronize over large distance or modulate local oscillatory amplitude to facilitate the integration of information into WM. It is posited that phase synchronization among task-relevant brain regions can serve to integrate information across multiple spatial scales (Fries, 2005). Phase-amplitude cross-frequency coupling, wherein the amplitude of a fast oscillation is modulated by the phase of a low-frequency oscillation, is thought to integrate information across multiple temporal scales within local cortical networks (Fell and Axmacher, 2011).

## OSCILLATORY BASIS OF WM

### Theta

Theta oscillations are well-studied in the rodent brain, where they are particularly prominent in the hippocampus (Kahana et al., 2001). Hippocampal theta emerges when the rodent engages in exploratory behavior (Vanderwolf, 1969). Studies probing the medial septum-diagonal band of Broca (MS-DBB), a generator of the hippocampal theta rhythm, additionally suggest that theta oscillations in the rodent hippocampus are associated with WM function (Kahana et al., 2001). Their findings demonstrate that lesions of the MS-DBB eliminate the hippocampal theta rhythm and induce WM impairment (Olton et al., 1979; Mizumori et al., 1990), whereas addition of cholinergic agonists to the MS-DBB increases the hippocampal theta rhythm (Lawson and Bland, 1993) and enhances WM performance (Markowska et al., 1995).

The discovery of hippocampal place cells, which fire when a specific location of the environment is traversed, further facilitated investigations into the role of hippocampal theta in WM (O'Keefe and Recce, 1993). Several experiments demonstrated that theta sequences, which compress the behavioral order of place cells within a theta cycle, represent trajectories or spatial paths in the environment (Gupta et al., 2012; Wikenheiser and Redish, 2015; Kay et al., 2020). These theta sequences can vary considerably in their individual trajectory representations, wherein some sequences are confined to a narrow range around the rat's current position while others project further beyond. It is postulated that these modulations occur according to the behavioral demands of WM. Indeed, in rats performing a value-guided decision-making task, the extent to which theta sequences projected ahead of the rat's current position varied on a moment-by-moment basis depending on the rat's goals (Wikenheiser and Redish, 2015). These results challenge the notion that place cells represent simple aspects of spatial and episodic memories. Conversely, it could be suggested that place cells comprise a complex system that is involved in behaviorally relevant transitions between WM and LTM.

Evidence for the functional relevance of theta oscillations in WM has since been extended to the human brain, where theta is thought to underlie WM processing in both local circuits and distributed neuronal ensembles. Previous findings demonstrate that local modulations in theta power and phase contribute to the processing and organization of WM contents, whereas long-range theta coherence integrates WM sub-processes (Sauseng et al., 2010).

#### Local Theta Activity

In local circuits, theta oscillations provide optimal neuronal ambiance for the processing of WM-related information

(Sauseng et al., 2010). Notably, cortical theta power increases during WM encoding and is sustained during the retention period until retrieval (Raghavachari et al., 2001; Raghavachari et al., 2006). Theta activity additionally increases parametrically with WM load in prominent nodes of the WM network, including frontal regions of the FP-CEN and the hippocampus (Jensen and Tesche, 2002). Collectively, these synchronous theta signatures have been interpreted as a gating mechanism, enhancing attention and prioritizing relevant information during WM processing (Gevins et al., 1997; Raghavachari et al., 2001; Riddle et al., 2020).

Converging evidence suggests that local instantaneous theta phase in the hippocampus organizes WM contents. First, hippocampal theta plays a role in phase-dependent plasticity, essentially determining the likelihood of a stimulus to undergo long-term potentiation (LTP). Importantly, LTP is theorized to strengthen the connectivity between neurons and is considered a synaptic mechanism for the encoding of a stimulus into WM (Klimesch and Doppelmayr, 1996). Previously, it has been demonstrated that LTP is preferentially induced at theta rhythm periodicity (Greenstein et al., 1988) and particularly at the positive phase of the theta rhythm (Pavlides et al., 1988). Indeed, in region CA1 of the hippocampus, LTP can be induced by stimulation on the peak, but not the trough, of the theta rhythm recorded in stratum radiatum in slice preparations, urethane-anesthetized rats, and awake rats (Hölscher et al., 1997; Hyman et al., 2003).

Second, hippocampal theta plays a role in phase-dependent coding of information. In rodents, spatial WM information is represented by the alignment of hippocampal place cell firing to specific phases of theta band activity (O'Keefe and Recce, 1993). In humans, Hasselmo et al. (2002) have proposed a model wherein hippocampal theta phase segregates encoding and retrieval phases in WM. In this model, WM encoding is associated with the trough of theta recorded at the hippocampal fissure – equivalent to the peak of theta recorded in stratum radiatum – when there is strong synaptic input from the entorhinal cortex into the stratum lacunosum-moleculare. Here, there is weak synaptic input from region CA3 of the hippocampus, however these same synapses show a strong capacity for LTP. Collectively, these phenomena enable the encoding of afferent information from the entorhinal cortex, while preventing interference from previously encoded information arising from region CA3 of the hippocampus. Conversely, retrieval is associated with the peak of theta recorded at the hippocampal fissure – equivalent to the trough of theta recorded in stratum radiatum – when there is relatively weak synaptic input from the entorhinal cortex into the stratum lacunosum-moleculare (Hasselmo et al., 2002). Here, there is strong synaptic input from region CA3 of the hippocampus, however these same synapses show a weaker capacity for LTP and tend to undergo long-term depression (LTD). Collectively, these phenomena enable retrieval of previously encoded information, while preventing further encoding of retrieval activity. The model proposed by Hasselmo et al. (2002) has been corroborated by evidence which demonstrates that theta oscillations exhibit a phase difference of 180° between WM encoding and retrieval (Rizzuto et al., 2006).

Third, hippocampal theta is phase-locked to WM-related stimuli (Givens, 1997; Tesche and Karhu, 2000; Rizzuto et al., 2003). Phase-locking occurs when the presentation of a WM-related stimulus causes the phases of an ongoing hippocampal theta oscillation to re-align or reset. In a seminal study, Givens (1997) demonstrated that phase resetting of the hippocampal theta rhythm in rodents occurs exclusively in response to WM-related stimuli, which are actively processed in the hippocampus, and not in response to reference memory-related stimuli. Givens (1997) hypothesized that this resetting phenomenon allows the hippocampus to experience a wave of depolarization at precisely the time that relevant sensory stimuli arrive in the hippocampus from the entorhinal cortex. Specifically, the phase-locking of theta oscillations would allow for later arriving and more highly processed sensory information to be potentiated or reverberated through several autoassociative theta cycles, which would ultimately facilitate the encoding of sensory information into WM. McCartney et al. (2004) corroborated this hypothesis, demonstrating that phase resetting of the hippocampal theta rhythm promotes optimal conditions for WM-related stimuli to be encoded and potentiated into memory.

Phase resetting has since been demonstrated in humans with similar manifestations, wherein the presentation of a behaviorally relevant stimulus in WM, such as a list item or probe, is followed by phase-locking in neocortical (Rizzuto et al., 2003) and hippocampal (Tesche and Karhu, 2000; Kleen et al., 2016) oscillations. This phase-locking has been reported in various frequencies, including delta, theta, and alpha bands (Rizzuto et al., 2003; Kleen et al., 2016). Notably, Kleen et al. (2016) observed that the degree of phase resetting in delta, theta, and alpha bands correlated with WM performance.

Interestingly, emerging evidence suggests that the properties of phase-locking in the theta band during WM are dependent on item content and load (Kamiński et al., 2020). In low loads, neurons phase-lock to the theta rhythm only when their preferred item is in WM, whereas in higher loads, the phase of the theta rhythm that neurons phase-lock to depends on whether the preferred item is in WM (Kamiński et al., 2020). These findings describe a putative mechanism by which theta phase could orchestrate hippocampal neural activity to successfully maintain multiple items in WM (Kamiński et al., 2020).

### Long-Range Theta Coherence

Long-range theta coherence is thought to integrate WM sub-processes (Sauseng et al., 2010). Synchronous theta activity is consistently reported between frontal and temporo-parietal regions during the encoding, maintenance, and retrieval of WM information (Sarnthein et al., 1998; Sauseng et al., 2004; Wu et al., 2007). Furthermore, this oscillatory phenomenon has material-specific manifestations. For instance, Sauseng et al. (2004) reported that the encoding of visual information is characterized by theta coupling between the dlPFC and right posterior temporal regions, whereas during retrieval of verbal and visuospatial information, theta coupling occurs between prefrontal and bilateral temporo-parietal regions.

Sarnthein et al. (1998) reported similar findings during the retention of verbal and visuospatial information, wherein theta coupling was observed between the PFC and posterior association cortex. Notably, interregional theta synchronization could play a role in integrating multi-modal information. Wu et al. (2007) used EEG to investigate phase synchronization in a WM task, wherein participants retained verbal information (e.g., letters), visuospatial information (e.g., locations), or bound information from both modalities (e.g., letters and locations). The authors found that theta phase synchronization increased between bilateral frontal regions and between the left frontal and right temporal-parietal regions during the maintenance of bound verbal and visuospatial information relative to segregated information (Wu et al., 2007). In these collective findings, long-range theta coherence between frontal and temporo-parietal regions likely serves to integrate processes that underly the storage of sensory information (e.g., temporo-parietal activity) and processes that underly the maintenance and updating of current relevant information (e.g., frontal activity) (Sarnthein et al., 1998).

Experiments in rodents support the postulation that theta coherence between the PFC and the hippocampus supports WM performance (Hyman et al., 2005; Jones and Wilson, 2005a,b; Kleen et al., 2011). In particular, mPFC neurons can be entrained to the hippocampal theta rhythm, and this entrainment is implicated in learning and memory during WM processing. In fact, mPFC cells that are actively involved in behavioral tasks are predisposed to fire entrained to the hippocampal theta rhythm (Hyman et al., 2005). Indeed, it has previously been demonstrated that a subset of neurons in the mPFC that predict the turn choices of a rat during a WM task are more strongly phase-locked to hippocampal theta than non-predicting cells (Fujisawa and Buzsáki, 2011). Furthermore, it has been observed that the most robust instances of mPFC phase precession coincide with enhanced CA1-mPFC coherence and occur during behavioral epochs, which demand the transfer of information from CA1 to mPFC (Jones and Wilson, 2005a).

Moreover, long-range theta synchronization between frontal and temporo-parietal regions could reflect central executive functions mastering WM sub-components (Sauseng et al., 2010). In this framework, theta coupling would enable the frontal central executive to access posterior, modality-specific storage sub-systems during WM (Sauseng et al., 2010). In line with this postulation, Sauseng et al. (2005) reported increased theta coupling between fronto-parietal regions with increasing central executive demands. Furthermore, there is substantial evidence for long-range theta coherence during attentionally demanding, central executive-dependent tasks, including between the FP-CEN subnetwork A and the DMN during internal attention (Kam et al., 2019) and within the FP-CEN during mental arithmetic, which requires mental manipulation of information and continuous updating of the WM store (Sauseng et al., 2010). Further support for this postulation derives from recent evidence which demonstrates that communication between the medial temporal lobe (MTL) and the PFC is bi-directional (Johnson et al., 2018). This bi-directional communication is facilitates central executive functions in WM by coordinating PFC-guided parallel processing of incoming information and MTL-dependent information prioritization in space and time (Johnson et al., 2018).

## Alpha

Alpha oscillations are prominent in sensory regions and the thalamus (Roux and Uhlhaas, 2014). Alpha synchronization is consistently observed in posterior regions during the maintenance of WM (Jensen et al., 2002; Klimesch et al., 2010; Bonnefond and Jensen, 2012; Riddle et al., 2020), and this activity increases parametrically with WM load (Jensen and Tesche, 2002). Recently, these findings have been recapitulated in a larger-scale WM network, wherein load-dependent alpha-theta coupling was observed between the hippocampus and parietal scalp electrodes during WM maintenance (Boran et al., 2019). It is posited that these collective alpha signatures reflect functional inhibition of task-irrelevant brain regions (Jensen et al., 2002; Jokisch and Jensen, 2007; Klimesch et al., 2010; Bonnefond and Jensen, 2012; Roux and Uhlhaas, 2014; Riddle et al., 2020). Indeed, studies probing visuospatial attention and WM demonstrate that attention directed toward one visual hemifield is expressed as an ipsilateral increase and/or a contralateral decrease of posterior alpha power (Medendorp et al., 2007). Interestingly, recent evidence suggests that the inhibitory function of alpha applies to both exogenous and endogenous information; irrelevant exogenous information is suppressed from being encoded into WM, whereas endogenous information that is already encoded into memory is suppressed when it is no longer relevant to guide future behavior (Riddle et al., 2020).

Conversely, alpha desynchronization reflects a release from functional inhibition and is often associated with activation processes related to attention (Michels et al., 2008). For instance, stimulus monitoring during WM is characterized by alpha desynchronization in nodes of the DAN. This desynchronization facilitates external attention, allowing regions of the DAN to engage in neural processing that enables the detection of relevant stimuli in the environment (Cona et al., 2020). On a similar vein, alpha desynchronization is thought to support the attentional demands of the WM central executive (Michels et al., 2008). Indeed, short-range alpha coherence between frontal regions in the FP-CEN decreases with central executive needs, allowing these regions to fulfill increased attentional demands (Sauseng et al., 2005).

## Gamma

Gamma oscillations are detectable in cortical regions and some subcortical regions (Roux and Uhlhaas, 2014). Gamma synchronization occurs in local circuits and has previously been associated with perception and feature integration (Singer and Gray, 1995; Von Stein and Sarnthein, 2000). It is further posited that these gamma signatures could reflect the neuronal correlate of maintained WM representations (Jokisch and Jensen, 2007). In line with this postulation, sustained gamma oscillatory activity has been reported during the retention of various domains of stimuli, including visual, visuospatial, auditory, and somatosensory information (Roux and Uhlhaas, 2014). Moreover, gamma oscillations synchronize with increasing WM

load, and this activity occurs in the hippocampus and key nodes of the FP-CEN that are integral to WM maintenance (Howard et al., 2003; Palva et al., 2010, 2011; Van Vugt et al., 2010; Roux et al., 2012).

Importantly, gamma oscillations can couple with theta or alpha oscillations to form a distinct oscillatory code that is specialized for a type of WM information. A theta-gamma code is thought to underlie the maintenance of sequential WM items and be related to a frontohippocampal network (Axmacher et al., 2010; Roux and Uhlhaas, 2014). In a framework proposed by Lisman and Idiart, individual WM items are represented by single gamma periods, which are nested into a single theta period. Here, the sequence of WM items is coded via the phase relationship between theta and gamma. Corroborating evidence of a theta-gamma code has been reported by Axmacher et al. (2010), who demonstrate that the maintenance of multiple items in WM is accompanied by load-dependent theta-gamma coupling in the hippocampus.

Additionally, an alpha-gamma code is thought to underlie the maintenance of sensory-spatial WM items. Roux and Uhlhaas (2014) propose that this oscillatory code is related to a thalamocortical network, comprising the PFC, parietal cortex, and thalamus. In this framework, gamma oscillations underlie the maintenance and read-out of relevant WM items, whereas alpha oscillations are involved in the inhibition of task-irrelevant WM items. In contrast to theta-gamma interactions, there is little evidence that directly portrays this alpha-gamma activity. However, Roux et al. (2012) review convincing evidence, which demonstrates that if WM contents are changed from multiple sequentially ordered items to discrete visual or spatial information, theta activity is replaced by alpha activity.

## WM IN EPILEPSY

Working memory impairment is well-documented in both children (Hernandez et al., 2002; Myatchin and Lagae, 2011; Sherman et al., 2012; Braakman et al., 2013; Longo et al., 2013) and adults (Hermann and Seidenberg, 1995; Black et al., 2010; Mwangala et al., 2018) with epilepsy. WM impairment is common across epilepsy types, manifesting in primary generalized epilepsies (Swartz et al., 1994), temporal lobe epilepsy (TLE) (Stretton and Thompson, 2012), and frontal lobe epilepsy (FLE) (Swartz et al., 1994). In both childhood and adulthood epilepsies, several factors are associated with greater risk of WM impairment, including younger age at seizure onset, longer duration of epilepsy, higher seizure frequency, and AED polytherapy (Meador, 2002; Black et al., 2010; MacAllister et al., 2012; Sherman et al., 2012; Fuentes and Kerr, 2016). Nonetheless, individuals with recently diagnosed epilepsies or well-controlled, benign epilepsies are also vulnerable to WM impairment (Myatchin and Lagae, 2011). In childhood epilepsies, WM impairment is a key feature distinguishing the cognitive profiles of children with epilepsy from healthy controls on formal intelligence tests (Sherman et al., 2012). Furthermore, WM impairment is implicated in all areas of academic achievement (Fastenau et al., 2004; Fuentes and Kerr, 2016). In adulthood epilepsies, the most frequently reported cognitive complaints are related to WM processing as well as mental slowness, attention deficits, and memory impairment (van Rijckevorsel, 2006). Notably, subjective cognitive impairment is associated with objective measures in WM and no other cognitive domains (Feldman et al., 2018).

## WM NETWORKS IN EPILEPSY

Normative WM networks are perturbed in epilepsy. These perturbations are marked by changes in functional connectivity between regions in the WM network. It is posited that hypoconnectivity within the epileptic WM network indicates network dysfunction, whereas hyperconnectivity has previously been interpreted as an indicator of network dysfunction, network reorganization, or a compensatory mechanism (Gutierrez-Colina et al., 2020). In the literature, studies probing network changes in epilepsy report heterogenous findings.

In resting-state fMRI, hypoconnectivity has been observed between the FP-CEN and the SN, as well as within the FP-CEN, the SN, and cerebellar regions (Gutierrez-Colina et al., 2020). Conversely, hyperconnectivity has been reported within frontal regions and also between interhemispheric frontal and parietal regions in the same modality (Gutierrez-Colina et al., 2020). In task-based measures, hypoconnectivity has been observed in a specific subset of frontal lobe connections in children with FLE, including local connections (e.g., within the frontal lobe) and distant connections (e.g., between the anterior cingulate cortex of the SN and the superior parietal lobe of the DAN) (Braakman et al., 2013). Additionally, children with TLE show less activation in the FP-CEN (Oyegbile et al., 2018) and less de-activation in the DMN relative to healthy controls (Oyegbile et al., 2019). Importantly, these collective resting-state and task-based signatures have been associated with worse measures of WM, suggesting that aberrant connectivity may underpin WM deficits in epilepsy.

## PATHOPHYSIOLOGICAL MECHANISMS OF WM IMPAIRMENT IN EPILEPSY

A multitude of factors likely contributes to WM impairment in epilepsy, including the epileptogenic substrate, recurrent seizures, interictal epileptic activity, and AED therapy (Motamedi and Meador, 2003; Sherman et al., 2012; Ibrahim et al., 2014). Here, the putative contributions of interictal epileptic activity and AED therapy will be reviewed.

### Interictal Epileptiform Discharges

Interictal epileptiform discharges (IEDs) are spikes, sharp waves, or spike-wave complexes that occur without observed clinical seizures (Noachtar and Rémi, 2009). IEDs can induce a phenomenon known as transient cognitive impairment (TCI). In TCI, the occurrence of an IED is accompanied by a transient disturbance in neural processing and cognitive function (Aarts et al., 1984; Binnie, 1993). Previous works

suggest that WM is particularly vulnerable to IED-induced TCI (Hutt and Gilbert, 1980; Aarts et al., 1984; Binnie et al., 1987). This increased vulnerability could be attributed to the characteristically high information processing demands of WM (Aldenkamp and Arends, 2004).

Transient cognitive impairment is demonstrable in 50% of patients who exhibit IEDs during a WM task (Binnie, 1993). The nature of the WM impairment is dependent upon where the IED occurs in the brain (Holmes, 2014). Material-specific deficits have previously been reported, wherein right-hemispheric IEDs are associated with errors in non-verbal WM tasks and left-hemispheric IEDs are associated with errors in verbal WM tasks (Aarts et al., 1984; Binnie et al., 1987). Interestingly, IEDs occurring in the mesial temporal lobe have been associated with a 6% decline in WM performance (Krauss et al., 1997). However, it is to be noted that even the occurrence of local IEDs could have widespread effects in the brain. For instance, IEDs could propagate from the hippocampus to the PFC and prevent synchronization between these structures during key WM steps (Corkin, 2001). In a similar vein, it has recently been demonstrated that hippocampal IEDs induce spindles in the mPFC and that both IED frequency and coupling with mPFC spindles are correlated with the degree of memory impairment (Gelinas et al., 2016).

Working memory impairment is additionally dependent upon the timing of the IED during WM. For instance, Kleen et al. (2010, 2013) observed that hippocampal IEDs were related to decrements in WM retrieval, but not encoding, in both rats and humans. Given that WM retrieval is dependent upon the functioning and integrity of intrahippocampal circuitry, this WM sub-process could be particularly sensitive to disruption following hippocampal IED. Conversely, WM encoding could be buffered by other cortical structures, such as the PFC or primary sensory areas, the latter of which could hold lingering stimulus representations (Kleen et al., 2013).

Studies leveraging intracranial EEG have helped elucidate putative mechanisms of IED-induced WM impairment. The occurrence of an IED in the hippocampus is followed by a sustained reduction of action potentials for a period of up to 2 s. Moreover, when IEDs occur in flurries, action potential firing could be reduced for a period of up to 6 s (Zhou et al., 2007). This IED-induced inhibitory wave disrupts WM-related oscillatory signatures in the hippocampus, resulting in reductions of hippocampal gamma (Urrestarazu et al., 2006) and theta power (Fu et al., 2018). By extension, IEDs could conceivably disrupt the organization and functioning of WM networks. Indeed, large-scale network changes precede (Ibrahim et al., 2014) and follow IEDs (Lengler et al., 2007; Ibrahim et al., 2014; Dahal et al., 2019). Moreover, the vulnerability of network topologies to IEDs has previously been associated with worse neurocognitive outcomes (Ibrahim et al., 2014).

## High Frequency Oscillations

Pathological high frequency oscillations (HFOs) are transient events detectable in the interictal EEG (Engel et al., 2009). These phenomena have recently emerged as biomarkers of epileptogenicity (Jacobs et al., 2012). Further evidence suggests that HFOs may perturb neural processing that is critical to WM, akin to the effects of IEDs (Ewell et al., 2019; Liu and Parvizi, 2019; Sun et al., 2020). The neurophysiological underpinnings of HFO-induced WM impairment remain elusive. However, it is conceivable that their pathophysiological mechanisms resemble those of IEDs, encompassing disruptions of oscillatory network activity (Brennan and Ahmed, 2019).

Indeed, HFOs have been shown to disrupt hippocampal network function in a rodent model of epilepsy (Ewell et al., 2019). To probe the effects of HFOs on the hippocampal network, Ewell et al. (2019) leveraged high-density single unit and local field potential recordings from the hippocampi of behaving rats with and without chronic epilepsy. The authors reported that the occurrence of HFOs in the epileptic hippocampus impaired spatial coding during foraging behavior via the induction of spurious, uninformative action potentials and the transient reduction of hippocampal theta power (Ewell et al., 2019).

Evidence of HFO-induced TCI has recently been extended to humans, where it has been demonstrated that the occurrence of HFOs in epileptic tissue results in a cognitive refractory state (Liu and Parvizi, 2019). Liu and Parvizi (2019) leveraged intracranial EEG recordings from non-lesional epileptic tissue to probe the effects of HFOs on stimulus-locked physiological activity. The authors observed normative physiological responses to relevant cognitive stimuli in epileptic tissue. However, these physiological responses were more likely to be "seized" (i.e., delayed or missed) when HFOs occurred around the onset of the relevant cognitive stimulus (850–1050 ms prior to stimulus onset, until 150–250 ms following stimulus onset). Furthermore, HFOs in the MTL affected memory performance. The authors concluded that a relevant cognitive stimulus will fail to activate epileptic tissue if it arrives within a shared temporal window as an HFO; this failure to activate the tissue is the pathophysiological mechanism underlying the impaired memory performance (Liu and Parvizi, 2019).

Notably, it has recently been demonstrated that the removal of HFO-generating tissue is associated with post-operative cognitive improvement in children with epilepsy (Sun et al., 2020). To probe whether the number of HFOs in pre- and post-resection intracranial EEG was associated with clinically relevant cognitive improvement, Sun et al. (2020) retrospectively reviewed intracranial EEG data and neuropsychological scores from children who were seizure free after epilepsy surgery. The authors found that children with clinically relevant, improved intelligence quotients (IQ) had significantly more HFOs in the resected tissue and fewer HFOs in the post-resection intracranial EEG relative to children with clinically irrelevant improvements (Sun et al., 2020).

## AEDs

Another potential cause of impaired WM in patients with epilepsy is treatment with AEDs. AED treatment in epilepsy protects against seizures by modulating neuronal excitability (Rogawski and Löscher, 2004). AEDs generally provide satisfactory control of seizures for most patients (Rogawski and Löscher, 2004), however AED tolerability within the cognitive domain is variable: some agents result in psychomotor slowing,

reduced vigilance, and WM impairment (Motamedi and Meador, 2004), whereas others are associated with enhanced WM (Eddy et al., 2011). Two AEDs that have consistently been implicated in WM function are TPM and levetiracetam (LEV).

Topiramate is an AED with multiple mechanisms of action, including the potentiation of GABAergic neurotransmission, inhibition of voltage-dependent sodium and calcium currents, blockage of AMPA/KA receptors, and enhancement of potassium currents (Czapinski et al., 2005). TPM therapy has previously been associated with WM impairment (Kockelmann et al., 2003; Lee et al., 2003; Jansen et al., 2006; Ciantis et al., 2008; Szaflarski and Allendorfer, 2012; Yasuda et al., 2013; Tang et al., 2016; Wandschneider et al., 2017; Hu et al., 2019; Callisto et al., 2020). WM performance deteriorates following initiation of TPM therapy (Hyman et al., 2003), and discontinuation of TPM therapy is associated with significant improvements in WM (Kockelmann et al., 2003; Lee et al., 2003). Functional neuroimaging studies report that TPM therapy is associated with decreased activation in FP-CEN frontal regions (Jansen et al., 2006; Ciantis et al., 2008; Szaflarski and Allendorfer, 2012; Wandschneider et al., 2017) and impaired deactivation of regions in the DMN during WM (Szaflarski and Allendorfer, 2012; Yasuda et al., 2013; Tang et al., 2016; Wandschneider et al., 2017). Recent evidence suggests that the severity of TPM-related WM impairment is modulated by TPM plasma concentration and WM capacity (Callisto et al., 2020). Interestingly, WM capacity is negatively associated with the WM-load modulation of alpha power, and the administration of TPM weakens this association (Hu et al., 2019).

Levetiracetam is an AED with a unique mechanism of action, which involves binding a protein known as synaptic vesicle protein 2A (SV2A) (Lynch et al., 2004), which mediates calcium-dependent vesicular neurotransmitter release (Nowack et al., 2010). LEV is derived from piracetam, a drug that seems to improve learning, memory, and attention (Genton and Van Vleymen, 2000). Piracetam has previously been used to treat memory disturbances in age-related cognitive function or decline (Israel et al., 1994) and aphasia (Huber et al., 1997). It is posited that piracetam derivatives could influence the metabolism of cortical regions responsible for language and attention (Piazzini et al., 2006). Indeed, LEV therapy has previously been associated with improvement in verbal fluency (Piazzini et al., 2006) and WM (López-Góngora et al., 2008; Operto et al., 2019). Interestingly, LEV treatment decreases centrotemporal spike-associated activation in Rolandic epilepsy (Zhang et al., 2018), and neuroimaging findings demonstrate that LEV therapy is associated with restoration of normative activation patterns during WM (Wandschneider et al., 2014).

The mechanism by which LEV supports WM function is unclear. Notably, both LEV and piracetam belong to the pyrrolidine class of drugs, which exhibit low toxicity, protect against brain insults, and enhance the efficacy of higher integration mechanisms in the brain (Schindler, 1989). Conceivably, LEV could enhance the capacity of functionally compromised cortical regions to be reintegrated into the WM network (Piazzini et al., 2006).

## DISCUSSION

In summary, WM is a critical component of cognition that is supported by dynamic oscillatory interactions between distributed cortical and subcortical regions. WM impairment is a pervasive co-morbidity of epilepsy that is likely influenced by pathological disturbances in WM network function. As reviewed, converging evidence suggests that there are disturbances to the FP-CEN, the SN, and the DMN (i.e., "the triple network") in epilepsy. Notably, disturbances of the triple network have been associated with several psychiatric and learning disorders that are characterized by WM impairment, including depression, ADHD, schizophrenia, autism, and frontotemporal dementia (Gürsel et al., 2018). These findings lend credence to the notion that these disorders, and their cognitive co-morbidities, are underpinned by disturbances in widespread networks.

The current clinical benchmark of successful treatment of epilepsy is seizure-freedom. However, individuals may continue to suffer from WM impairments after being rendered seizure-free. IEDs and HFOs are putative pathophysiological mechanisms by which WM networks and their oscillatory signatures continue to be perturbed. Future work should aim to further elucidate the neurophysiological underpinnings of these disturbances, as these findings would provide insight for interventions that could target WM function in epilepsy. Neuromodulatory treatments aimed at suppressing these aberrant signatures and restoring normative network dynamics could be especially promising in this objective. Furthermore, IEDs and HFOs recorded in intracranial EEG could serve as biomarkers in the prediction and understanding of cognitive outcome after epilepsy surgery (Sun et al., 2020).

## AUTHOR CONTRIBUTIONS

OA and GI prepared and revised the manuscript. JY and M-LS revised the manuscript. All authors contributed to the article and approved the submitted version.

## FUNDING

The work was supported by the Canadian Institutes of Health Research.

## REFERENCES

Aarts, J. H. P., Binnie, C. D., Smit, A. M., and Wilkins, A. J. (1984). Selective cognitive impairment during focal and generalized epileptiform eeg activity. *Brain* 107, 293–308. doi: 10.1093/brain/107.1.293

Aldenkamp, A. P., and Arends, J. (2004). Effects of epileptiform EEG discharges on cognitive function: is the concept of 'transient cognitive impairment' still valid? *Epilepsy Behav.* 5, 25–34. doi: 10.1016/j.yebeh.2003.11.005

Andrews-Hanna, J. R., Smallwood, J., and Spreng, R. N. (2014). The default network and self-generated thought: component processes, dynamic control,

and clinical relevance. *Ann. N. Y. Acad. Sci.* 1316, 29–52. doi: 10.1111/nyas.12360

Austin, J. K., Harezlak, J., Dunn, D. W., Huster, G. A., Rose, D. F., and Ambrosius, W. T. (2001). Behavior problems in children before first recognized seizures. *Pediatrics* 107, 115–122. doi: 10.1542/peds.107.1.115

Axmacher, N., Henseler, M. M., Jensen, O., Weinreich, I., Elger, C. E., Fell, J., et al. (2010). Cross-frequency coupling supports multi-item working memory in the human hippocampus. *Proc. Natl. Acad. Sci. U.S.A.* 107, 3228–3233. doi: 10.1073/pnas.0911531107

Baddeley, A. (1992). Working memory. *Science* 255, 556–559.

Baddeley, A. (2003). Working memory: looking back and looking forward. *Nat. Rev. Neurosci.* 4, 829–839.

Baddeley, A. D., and Hitch, G. (1974). Working memory. *Psychol. Learn. Motiv. Adv. Res. Theory* 8, 47–89.

Binnie, C. D. (1993). Significance and management of transitory cognitive impairment due to subclinical EEG discharges in children. *Brain Dev.* 15:30.

Binnie, C. D., Kasteleijn-Nolst Trenité, D. G. A., Smit, A. M., and Wilkins, A. J. (1987). Interactions of epileptiform EEG discharges and cognition. *Epilepsy Res.* 1, 239–245. doi: 10.1016/0920-1211(87)90031-3

Black, L. C., Schefft, B., Howe, S., Szaflarski, J. P., Yeh, H. S., and Privitera, M. D. (2010). The effect of seizures on working memory and executive functioning performance. *Epilepsy Behav.* 17, 412–419. doi: 10.1016/j.yebeh.2010.01.006

Bonnefond, M., and Jensen, O. (2012). Alpha oscillations serve to protect working memory maintenance against anticipated distracters. *Curr. Biol.* 22, 1969–1974. doi: 10.1016/j.cub.2012.08.029

Boran, E., Fedele, T., Klaver, P., Hilfiker, P., Stieglitz, L., Grunwald, T., et al. (2019). Persistent hippocampal neural firing and hippocampal-cortical coupling predict verbal working memory load. *Sci. Adv.* 5:eaav3687. doi: 10.1126/sciadv.aav3687

Braakman, H. M. H., Vaessen, M. J., Jansen, J. F. A., Debeij-van Hall, M. H. J. A., de Louw, A., Hofman, P. A. M., et al. (2013). Frontal lobe connectivity and cognitive impairment in pediatric frontal lobe epilepsy. *Epilepsia* 54, 446–454. doi: 10.1111/epi.12044

Braunlich, K., Gomez-Lavin, J., and Seger, C. A. (2015). Frontoparietal networks involved in categorization and item working memory. *Neuroimage* 107, 146–162. doi: 10.1016/j.neuroimage.2014.11.051

Brennan, E. K. W., and Ahmed, O. J. (2019). Ripple while you walk, and you may get lost: pathological high-frequency activity can alter spatial navigation circuits. *Epilepsy Curr.* 19, 344–346. doi: 10.1177/1535759719871275

Buzsáki, G., and Draguhn, A. (2004). Neuronal oscillations in cortical networks. *Science* 304, 1926–1930. doi: 10.1126/science.1099745

Callisto, S. P., Illamola, S. M., Birnbaum, A. K., Barkley, C. M., Bathena, S. P. R., Leppik, I. E., et al. (2020). Severity of topiramate-related working memory impairment is modulated by plasma concentration and working memory capacity. *J. Clin. Pharmacol.* 60, 1166–1176. doi: 10.1002/jcph.1611

Cashdollar, N., Malecki, U., Rugg-Gunn, F. J., Duncan, J. S., Lavie, N., Duzel, E., et al. (2009). Hippocampus-dependent and-independent theta-networks of active maintenance. *Proc. Natl. Acad. Sci. U.S.A.* 106, 20493–20498. doi: 10.1073/pnas.0904823106

Ciantis, A., Muti, M., Piccolini, C., Principi, M., Renzo, A Di, De Ciantis, R., et al. (2008). A functional MRI study of language disturbances in subjects with migraine headache during treatment with topiramate. *Neurol. Sci.* 29, 141–143. doi: 10.1007/s10072-008-0906-5

Clare Kelly, A. M., Uddin, L. Q., Biswal, B. B., Castellanos, F. X., and Milham, M. P. (2008). Competition between functional brain networks mediates behavioral variability. *Neuroimage* 39, 527–537. doi: 10.1016/j.neuroimage.2007.08.008

Clark, C. R., Moores, K. A., Lewis, A., Weber, D. L., Fitzgibbon, S., Greenblatt, R., et al. (2001). Cortical network dynamics during verbal working memory function. *Int. J. Psychophysiol.* 42, 161–176. doi: 10.1016/s0167-8760(01)00164-7

Collette, F., Salmon, E., Van der Linden, M., Chicherio, C., Belleville, S., Degueldre, C., et al. (1999). Regional brain activity during tasks devoted to the central executive of working memory. *Cogn. Brain Res.* 7, 411–417. doi: 10.1016/s0926-6410(98)00045-7

Collette, F., and Van Der Linden, M. (2002). Brain imaging of the central executive component of working memory. *Neurosci. Biobehav. Rev.* 26, 105–125. doi: 10.1016/s0149-7634(01)00063-x

Cona, G., Chiossi, F., Di Tomasso, S., Pellegrino, G., Piccione, F., and Bisiacchi, P. S. (2020). Theta and alpha oscillations as signatures of internal and external attention to delayed intentions: a magnetoencephalography (MEG) study. *Neuroimage* 205:116295. doi: 10.1016/j.neuroimage.2019.116295

Corkin, S. (2001). Beware of frontal lobe deficits in hippocampal clothing. *Trends Cogn. Sci.* 5, 321–323. doi: 10.1016/s1364-6613(00)01709-5

Cowan, N. (1988). Evolving conceptions of memory storage, selective attention, and their mutual constraints within the human information-processing system. *Psychol. Bull.* 104, 163–191. doi: 10.1037/0033-2909.104.2.163

Czapinski, P., Blaszczyk, B., and Czuczwa, S. J. (2005). Mechanisms of action of antiepileptic drugs. *Curr. Top. Med. Chem.* 5, 3–14.

Dahal, P., Ghani, N., Flinker, A., Dugan, P., Friedman, D., Doyle, W., et al. (2019). Interictal epileptiform discharges shape large-scale intercortical communication. *Brain* 142, 3502–3513. doi: 10.1093/brain/awz269

Danguecan, A. N., and Smith, M. L. (2017). Academic outcomes in individuals with childhood-onset epilepsy: mediating effects of working memory. *J. Int. Neuropsychol. Soc.* 23, 594–604. doi: 10.1017/s135561771700008x

Deadwyler, S. A., Bunn, T., and Hampson, R. E. (1996). Hippocampal ensemble activity during spatial delayed-nonmatch-to-sample performance in rats. *J. Neurosci.* 16, 354–372. doi: 10.1523/jneurosci.16-01-00354.1996

Dixon, M. L., De La Vega, A., Mills, C., Andrews-Hanna, J., Spreng, R. N., Cole, M. W., et al. (2018). Heterogeneity within the frontoparietal control network and its relationship to the default and dorsal attention networks. *Proc. Natl. Acad. Sci. U.S.A.* 115, E1598–E1607.

Eddy, C. M., Rickards, H. E., and Cavanna, A. E. (2011). The cognitive impact of antiepileptic drugs. *Ther. Adv. Neurol. Disord.* 4, 385–407.

Elton, A., and Gao, W. (2014). Divergent task-dependent functional connectivity of executive control and salience networks. *Cortex* 51, 56–66. doi: 10.1016/j.cortex.2013.10.012

Engel, J., Bragin, A., Staba, R., and Mody, I. (2009). High-frequency oscillations: What is normal and what is not? *Epilepsia* 50, 598–604. doi: 10.1111/j.1528-1167.2008.01917.x

Ericsson, K. A., and Delaney, P. F. (1999). "Long-term working memory as an alternative to capacity models of working memory in everyday skilled performance," in *Models of Working Memory*, eds A. Miyake and P. Shah (Cambridge: Cambridge University Press), 257–297. doi: 10.1017/cbo9781139174909.011

Ewell, L. A., Fischer, K. B., Leibold, C., Leutgeb, S., and Leutgeb, J. K. (2019). The impact of pathological high-frequency oscillations on hippocampal network activity in rats with chronic epilepsy. *eLife* 8:e42148.

Fang, X., Zhang, Y., Zhou, Y., Cheng, L., Li, J., Wang, Y., et al. (2016). Resting-state coupling between core regions within the central-executive and salience networks contributes to working memory performance. *Front. Behav. Neurosci.* 10:27.

Fastenau, P. S., Shen, J., Dunn, D. W., Perkins, S. M., Hermann, B. P., and Austin, J. K. (2004). Neuropsychological predictors of academic underachievement in pediatric epilepsy: moderating roles of demographic, seizure, and psychosocial variables. *Epilepsia* 45, 1261–1272. doi: 10.1111/j.0013-9580.2004.15204.x

Feldman, L., Lapin, B., Busch, R. M., and Bautista, J. F. (2018). Evaluating subjective cognitive impairment in the adult epilepsy clinic: effects of depression, number of antiepileptic medications, and seizure frequency. *Epilepsy Behav.* 81, 18–24. doi: 10.1016/j.yebeh.2017.10.011

Fell, J., and Axmacher, N. (2011). The role of phase synchronization in memory processes. *Nat. Rev. Neurosci.* 12, 105–118. doi: 10.1038/nrn2979

Fries, P. (2005). A mechanism for cognitive dynamics: Neuronal communication through neuronal coherence. *Trends Cogn. Sci.* 9, 474–480. doi: 10.1016/j.tics.2005.08.011

Fu, X., Wang, Y., Ge, M., Wang, D., Gao, R., Wang, L., et al. (2018). Negative effects of interictal spikes on theta rhythm in human temporal lobe epilepsy. *Epilepsy Behav.* 87, 207–212. doi: 10.1016/j.yebeh.2018.07.014

Fuentes, A., and Kerr, E. N. (2016). Maintenance effects of working memory intervention (Cogmed) in children with symptomatic epilepsy. *Epilepsy Behav.* 67, 51–59. doi: 10.1016/j.yebeh.2016.12.016

Fujisawa, S., and Buzsáki, G. (2011). A 4 Hz oscillation adaptively synchronizes prefrontal, VTA, and hippocampal activities. *Neuron* 72, 153–165. doi: 10.1016/j.neuron.2011.08.018

Gelinas, J. N., Khodagholy, D., Thesen, T., Devinsky, O., and Buzsáki, G. (2016). Interictal epileptiform discharges induce hippocampal-cortical coupling in temporal lobe epilepsy. *Nat. Med.* 22, 641–648. doi: 10.1038/nm.4084

Genton, P., and Van Vleymen, B. (2000). Piracetam and levetiracetam: close structural similarities but different pharmacological and clinical profiles. *Epileptic Disord.* 2, 99–105.

Gevins, A., Smith, M., McEvoy, L., and Yu, D. (1997). High-resolution EEG mapping of cortical activation related to working memory: Effects of task difficulty, type of processing, and practice. *Cereb. Cortex* 7, 374–385. doi: 10.1093/cercor/7.4.374

Givens, B. (1997). Stimulus-evoked resetting of the dentate theta rhythm: Relation to working memory. *Neuroreport* 8, 159–163. doi: 10.1097/00001756-199612200-00032

Gong, D., He, H., Ma, W., Liu, D., Huang, M., Dong, L., et al. (2016). Functional integration between salience and central executive networks: A role for action video game experience. *Neural Plast* 2016:9803165.

Greenstein, Y. J., Pavlides, C., and Winson, J. (1988). Long-term potentiation in the dentate gyrus is preferentially induced at theta rhythm periodicity. *Brain Res.* 438, 331–334. doi: 10.1016/0006-8993(88)91358-3

Guerrini, R. (2006). Epilepsy in children. *Lancet* 367:499.

Gupta, A. S., Van Der Meer, M. A. A., Touretzky, D. S., and Redish, A. D. (2012). Segmentation of spatial experience by hippocampal theta sequences. *Nat. Neurosci.* 15, 1032–1039. doi: 10.1038/nn.3138

Gürsel, D. A., Avram, M., Sorg, C., Brandl, F., and Koch, K. (2018). Frontoparietal areas link impairments of large-scale intrinsic brain networks with aberrant fronto-striatal interactions in OCD: a meta-analysis of resting-state functional connectivity. *Neurosci. Biobehav. Rev.* 87, 151–160. doi: 10.1016/j.neubiorev.2018.01.016

Gutierrez-Colina, A. M., Vannest, J., Maloney, T., Wade, S. L., Combs, A., Horowitz-Kraus, T., et al. (2020). The neural basis of executive functioning deficits in adolescents with epilepsy: a resting-state fMRI connectivity study of working memory. *Brain Imaging Behav.* 1–11. doi: 10.1007/s11682-019-00243-z

Hasselmo, M. E., Bodelón, C., and Wyble, B. P. (2002). A proposed function for hippocampal theta rhythm: separate phases of encoding and retrieval enhance reversal of prior learning. *Neural Comput.* 14, 793–817. doi: 10.1162/089976602317318965

Helmstaedter, C., and Kurthen, M. (2001). Memory and epilepsy: characteristics, course, and influence of drugs and surgery. *Curr. Opin. Neurol.* 14, 211–216. doi: 10.1097/00019052-200104000-00013

Hermann, B., and Seidenberg, M. (1995). Executive system dysfunction in temporal lobe epilepsy: Effects of nociferous cortex versus hippocampal pathology. *J. Clin. Exp. Neuropsychol.* 17, 809–819. doi: 10.1080/01688639508402430

Hernandez, M., Sauerwein, H. C., Jambaqué, I., De Guise, E., Lussier, F., Lortie, A., et al. (2002). Deficits in executive functions and motor coordination in children with frontal lobe epilepsy. *Neuropsychologia* 40, 384–400. doi: 10.1016/s0028-3932(01)00130-0

Holmes, G. L. (2013). EEG abnormalities as a biomarker for cognitive comorbidities in pharmacoresistant epilepsy. *Epilepsia* 54, 60–62. doi: 10.1111/epi.12186

Holmes, G. L. (2014). What is more harmful, seizures or epileptic EEG abnormalities? Is there any clinical data? *Epileptic Disord.* 16, 12–22. doi: 10.1684/epd.2014.0686

Holmes, G. L., and Lenck-Santini, P. P. (2006). Role of interictal epileptiform abnormalities in cognitive impairment. *Epilepsy Behav.* 8, 504–515. doi: 10.1016/j.yebeh.2005.11.014

Hölscher, C., Anwyl, R., and Rowan, M. J. (1997). Stimulation on the positive phase of hippocampal theta rhythm induces long-term potentiation that can be depotentiated by stimulation on the negative phase in area CA1 in vivo. *J. Neurosci.* 17, 6470–6477. doi: 10.1523/jneurosci.17-16-06470.1997

Howard, M. W., Rizzuto, D. S., Caplan, J. B., Madsen, J. R., Lisman, J., Aschenbrenner-Scheibe, R., et al. (2003). Gamma oscillations correlate with working memory load in humans. *Cereb. Cortex* 13, 1369–1374. doi: 10.1093/cercor/bhg084

Hu, Z., Barkley, C. M., Marino, S. E., Wang, C., Rajan, A., Bo, K., et al. (2019). Working memory capacity is negatively associated with memory load modulation of alpha oscillations in retention of verbal working memory. *J. Cogn. Neurosci.* 31, 1933–1945. doi: 10.1162/jocn_a_01461

Huber, W., Willmes, K., Poeck, K., Van Vleymen, B., and Deberdt, W. (1997). Piracetam as an adjuvant to language therapy for aphasia: A randomized double-blind placebo-controlled pilot study. *Arch. Phys. Med. Rehabil.* 78, 245–250. doi: 10.1016/s0003-9993(97)90028-9

Hutt, S. J., and Gilbert, S. (1980). Effects of evoked spike-wave discharges upon short term memory in patients with epilepsy. *Cortex* 16, 445–457. doi: 10.1016/s0010-9452(80)80045-1

Hyman, J. M., Wyble, B. P., Goyal, V., Rossi, C. A., and Hasselmo, M. E. (2003). Stimulation in hippocampal region CA1 in behaving rats yields long-term potentiation when delivered to the peak of theta and long-term depression when delivered to the trough. *J. Neurosci.* 23, 11725–11731. doi: 10.1523/jneurosci.23-37-11725.2003

Hyman, J. M., Zilli, E. A., Paley, A. M., and Hasselmo, M. E. (2005). Medial prefrontal cortex cells show dynamic modulation with the hippocampal theta rhythm dependent on behavior. *Hippocampus* 15, 739–749. doi: 10.1002/hipo.20106

Ibrahim, G. M., Cassel, D., Morgan, B. R., Smith, M. L., Otsubo, H., Ochi, A., et al. (2014). Resilience of developing brain networks to interictal epileptiform discharges is associated with cognitive outcome. *Brain* 137, 2690–2702. doi: 10.1093/brain/awu214

Israel, L., Melac, M., Milinkevitch, D., and Dubos, G. (1994). Drug therapy and memory training programs: a double-blind randomized trial of general practice patients with age-associated memory impairment. *Int. Psychogeriatrics* 6, 155–170. doi: 10.1017/s1041610294001729

Jacobs, J., Staba, R., Asano, E., Otsubo, H., Wu, J. Y., Zijlmans, M., et al. (2012). High-frequency oscillations (HFOs) in clinical epilepsy. *Prog. Neurobiol.* 98, 302–315.

Jansen, J. F. A., Aldenkamp, A. P., Majoie, H. J. M., Reijs, R. P., de Krom, M. C. T. F. M., Hofman, P. A. M., et al. (2006). Functional MRI reveals declined prefrontal cortex activation in patients with epilepsy on topiramate therapy. *Epilepsy Behav.* 9, 181–185. doi: 10.1016/j.yebeh.2006.05.004

Jeffries, S., and Everatt, J. (2004). Working memory: Its role in dyslexia and other specific learning difficulties. *Dyslexia* 10, 196–214. doi: 10.1002/dys.278

Jensen, O., Gelfand, J., Kounios, J., and Lisman, J. E. (2002). Oscillations in the alpha band (9-12 Hz) increase with memory load during retention in a short-term memory task. *Cereb. Cortex* 12, 877–882. doi: 10.1093/cercor/12.8.877

Jensen, O., and Tesche, C. D. (2002). Frontal theta activity in humans increases with memory load in a working memory task. *Eur. J. Neurosci.* 15, 1395–1399. doi: 10.1046/j.1460-9568.2002.01975.x

Johnson, E. L., Adams, J. N., Solbakk, A. K., Endestad, T., Larsson, P. G., Ivanovic, J., et al. (2018). Dynamic frontotemporal systems process space and time in working memory. *PLoS Biol.* 16:e2004274. doi: 10.1371/journal.pbio.2004274

Jokisch, D., and Jensen, O. (2007). Modulation of gamma and alpha activity during a working memory task engaging the dorsal or ventral stream. *J. Neurosci.* 27, 3244–3251. doi: 10.1523/jneurosci.5399-06.2007

Jones, M. W., and Wilson, M. A. (2005a). Phase precession of medial prefrontal cortical activity relative to the hippocampal theta rhythm. *Hippocampus* 15, 867–873. doi: 10.1002/hipo.20119

Jones, M. W., and Wilson, M. A. (2005b). Theta rhythms coordinate hippocampal-prefrontal interactions in a spatial memory task. *PLoS Biol.* 3:e402. doi: 10.1371/journal.pbio.0030402

Kahana, M. J., Seelig, D., and Madsen, J. R. (2001). Theta returns. *Curr. Opin. Neurobiol.* 11, 739–744. doi: 10.1016/s0959-4388(01)00278-1

Kam, J. W. Y., Lin, J. J., Solbakk, A. K., Endestad, T., Larsson, P. G., and Knight, R. T. (2019). Default network and frontoparietal control network theta connectivity supports internal attention. *Nat. Hum. Behav.* 3, 1263–1270. doi: 10.1038/s41562-019-0717-0

Kamiński, J., Brzezicka, A., Mamelak, A. N., and Rutishauser, U. (2020). Combined phase-rate coding by persistently active neurons as a mechanism for maintaining multiple items in working memory in humans. *Neuron* 106, 256–264.e3.

Karlsgodt, K. H., Shirinyan, D., Van Erp, T. G. M., Cohen, M. S., and Cannon, T. D. (2005). Hippocampal activations during encoding and retrieval in a verbal working memory paradigm. *Neuroimage* 25, 1224–1231. doi: 10.1016/j.neuroimage.2005.01.038

Kay, K., Chung, J. E., Sosa, M., Schor, J. S., Karlsson, M. P., Larkin, M. C., et al. (2020). Constant sub-second cycling between representations of possible futures in the hippocampus. *Cell* 180, 552–567.e25.

Kleen, J. K., Scott, R. C., Holmes, G. L., and Lenck-Santini, P. P. (2010). Hippocampal interictal spikes disrupt cognition in rats. *Ann. Neurol.* 67, 250–257. doi: 10.1002/ana.21896

Kleen, J. K., Scott, R. C., Holmes, G. L., Roberts, D. W., Rundle, M. M., Testorf, M., et al. (2013). Hippocampal interictal epileptiform activity disrupts cognition in humans. *Neurology* 81, 18–24. doi: 10.1212/wnl.0b013e318297ee50

Kleen, J. K., Testorf, M. E., Roberts, D. W., Scott, R. C., Jobst, B. J., Holmes, G. L., et al. (2016). Oscillation phase locking and late ERP components of intracranial hippocampal recordings correlate to patient performance in a working memory task. *Front. Hum. Neurosci.* 10:287.

Kleen, J. K., Wu, E. X., Holmes, G. L., Scott, R. C., and Lenck-Santini, P. P. (2011). Enhanced oscillatory activity in the hippocampal-prefrontal network is related to short-term memory function after early-life seizures. *J. Neurosci.* 31, 15397–15406. doi: 10.1523/jneurosci.2196-11.2011

Klimesch, W., and Doppelmayr, M. (1996). Theta band power in the human scalp EEG and the encoding of new information. *Neuroreport* 7, 1235–1240. doi: 10.1097/00001756-199605170-00002

Klimesch, W., Freunberger, R., and Sauseng, P. (2010). Oscillatory mechanisms of process binding in memory. *Neurosci. Biobehav. Rev.* 34, 1002–1014. doi: 10.1016/j.neubiorev.2009.10.004

Klimesch, W., Freunberger, R., Sauseng, P., and Gruber, W. (2008). A short review of slow phase synchronization and memory: evidence for control processes in different memory systems? *Brain Res.* 1235, 31–44. doi: 10.1016/j.brainres.2008.06.049

Knight, R. T. (1996). Contribution of human hippocampal region to novelty detection. *Lett. Nat.* 383, 256–259. doi: 10.1038/383256a0

Kockelmann, E., Elger, C. E., and Helmstaedter, C. (2003). Significant improvement in frontal lobe associated neuropsychological functions after withdrawal of Topiramate in epilepsy patients. *Epilepsy Res.* 54, 171–178. doi: 10.1016/s0920-1211(03)00078-0

Kondo, H., Morishita, M., Osaka, N., Osaka, M., Fukuyama, H., and Shibasaki, H. (2004). Functional roles of the cingulo-frontal network in performance on working memory. *Neuroimage* 21, 2–14. doi: 10.1016/j.neuroimage.2003.09.046

Krauss, G., Summerfield, M., Brandt, J., Breiter, S., and Ruchkin, D. (1997). Mesial temporal spikes interfere with working memory. *Neurology* 49, 975–980. doi: 10.1212/wnl.49.4.975

Lawson, V. H., and Bland, B. H. (1993). The role of the septohippocampal pathway in the regulation of hippocampal field activity and behavior: analysis by the intraseptal microinfusion of carbachol, atropine, and procaine. *Exp. Neurol.* 120, 132–144. doi: 10.1006/exnr.1993.1047

Lee, S., Sziklas, V., Andermann, F., Farnham, S., Risse, G., Gustafson, M., et al. (2003). The effects of adjunctive topiramate on cognitive function in patients with epilepsy. *Epilepsia* 44, 339–347. doi: 10.1046/j.1528-1157.2003.27402.x

Lengler, U., Kafadar, I., Neubauer, B. A., and Krakow, K. (2007). fMRI correlates of interictal epileptic activity in patients with idiopathic benign focal epilepsy of childhood. A simultaneous EEG-functional MRI study. *Epilepsy Res.* 75, 29–38. doi: 10.1016/j.eplepsyres.2007.03.016

Leszczynski, M. (2011). How does hippocampus contribute to working memory processing? *Front. Hum. Neurosci.* 5:168.

Li, Z. H., Sun, X. W., Wang, Z. X., Zhang, X. C., Zhang, D. R., He, S., et al. (2004). Behavioral and functional MRI study of attention shift in human verbal working memory. *Neuroimage* 21, 181–191. doi: 10.1016/j.neuroimage.2003.08.043

Liang, X., Zou, Q., He, Y., and Yang, Y. (2016). Topologically reorganized connectivity architecture of default-mode, executive-control, and salience networks across working memory task loads. *Cereb. Cortex* 26, 1501–1511. doi: 10.1093/cercor/bhu316

Liu, S., and Parvizi, J. (2019). Cognitive refractory state caused by spontaneous epileptic high-frequency oscillations in the human brain. *Sci. Transl. Med.* 11, 1–14.

Logie, R. H. (2011). The functional organization and capacity limits of working memory. *Curr. Dir. Psychol. Sci.* 20, 240–245. doi: 10.1177/0963721411415340

Longo, C. A., Kerr, E. N., and Smith, M. L. (2013). Executive functioning in children with intractable frontal lobe or temporal lobe epilepsy. *Epilepsy Behav.* 26, 102–108. doi: 10.1016/j.yebeh.2012.11.003

López-Góngora, M., Martínez-Domeño, A., García, C., and Escartín, A. (2008). Effect of levetiracetam on cognitive functions and quality of life: a one-year follow-up study. *Epileptic Disord.* 10, 297–305.

Lovett, M. C., Reder, L. M., and Lebiere, C. (2012). "Modeling working memory in a unified architecture: An ACT-R perspective," in *Models of Working Memory*, eds A. Miyake and P. Shah (Cambridge: Cambridge University Press), 135–182. doi: 10.1017/cbo9781139174909.008

Lynch, B. A., Lambeng, N., Nocka, K., Kensel-Hammes, P., Bajjalieh, S. M., Matagne, A., et al. (2004). The synaptic vesicle is the protein SV2A is the binding site for the antiepileptic drug levetiracetam. *Proc. Natl. Acad. Sci. U.S.A.* 101, 9861–9866. doi: 10.1073/pnas.0308208101

MacAllister, W. S., Vasserman, M., Vekaria, P., Miles-Mason, E., Hochsztein, N., and Bender, H. A. (2012). Neuropsychological endophenotypes in ADHD with and without epilepsy. *Appl. Neuropsychol. Child* 1, 121–128. doi: 10.1080/21622965.2012.709421

Markowska, A. L., Olton, D. S., and Givens, B. (1995). Cholinergic manipulations in the medial septal area: age-related effects on working memory and hippocampal electrophysiology. *J. Neurosci.* 15(3 Pt 1), 2063–2073. doi: 10.1523/jneurosci.15-03-02063.1995

McCartney, H., Johnson, A. D., Weil, Z. M., and Givens, B. (2004). Theta reset produces optimal conditions for long-term potentiation. *Hippocampus* 14, 684–687. doi: 10.1002/hipo.20019

Meador, K. J. (2002). Cognitive outcomes and predictive factors in epilepsy. *Neurology* 58(8 Suppl. 5), S21–S26.

Medendorp, W. P., Kramer, G. F., Jensen, O., Oostenveld, R., Schoffelen, J. M., and Fries, P. (2007). Oscillatory activity in human parietal and occipital cortex shows hemispheric lateralization and memory effects in a delayed double-step saccade task. *Cereb. Cortex* 17, 2364–2374. doi: 10.1093/cercor/bhl145

Menon, V., and Uddin, L. Q. (2010). Saliency, switching, attention and control: a network model of insula function. *Brain Struct. Funct.* 214, 655–667. doi: 10.1007/s00429-010-0262-0

Michels, L., Moazami-Goudarzi, M., Jeanmonod, D., and Sarnthein, J. (2008). EEG alpha distinguishes between cuneal and precuneal activation in working memory. *Neuroimage* 40, 1296–1310. doi: 10.1016/j.neuroimage.2007.12.048

Miller, E. K., and Cohen, J. D. (2001). An integrative theory of prefrontal cortex function. *Annu. Rev. Neurosci.* 24, 167–202. doi: 10.1146/annurev.neuro.24.1.167

Mizumori, S. J. Y., Perez, G. M., Alvarado, M. C., Barnes, C. A., and McNaughton, B. L. (1990). Reversible inactivation of the medial septum differentially affects two forms of learning in rats. *Brain Res.* 528, 12–20. doi: 10.1016/0006-8993(90)90188-h

Motamedi, G., and Meador, K. (2003). Epilepsy and cognition. *Epilepsy Behav.* 7, 1–6.

Motamedi, G. K., and Meador, K. J. (2004). Antiepileptic drugs and memory. *Epilepsy Behav.* 5, 435–439.

Murphy, A. C., Bertolero, M. A., Papadopoulos, L., Lydon-Staley, D. M., and Bassett, D. S. (2020). Multimodal network dynamics underpinning working memory. *Nat. Commun.* 11, 1–13.

Mwangala, P. N., Kariuki, S. M., Nyongesa, M. K., Mwangi, P., Chongwo, E., Newton, C. R., et al. (2018). Cognition, mood and quality-of-life outcomes among low literacy adults living with epilepsy in rural Kenya: a preliminary study. *Epilepsy Behav.* 85, 45–51. doi: 10.1016/j.yebeh.2018.05.032

Myatchin, I., and Lagae, L. (2011). Impaired spatial working memory in children with well-controlled epilepsy: an event-related potentials study. *Seizure* 20, 143–150. doi: 10.1016/j.seizure.2010.11.005

Nickels, K. C., Zaccariello, M. J., Hamiwka, L. D., and Wirrell, E. C. (2016). Cognitive and neurodevelopmental comorbidities in paediatric epilepsy. *Nat. Rev. Neurol.* 12, 465–476. doi: 10.1038/nrneurol.2016.98

Noachtar, S., and Rémi, J. (2009). The role of EEG in epilepsy: a critical review. *Epilepsy Behav.* 15, 22–33. doi: 10.1016/j.yebeh.2009.02.035

Nowack, A., Yao, J., Custer, K. L., and Bajjalieh, S. M. (2010). SV2 regulates neurotransmitter release via multiple mechanisms. *Am. J. Physiol. Cell Physiol.* 299, C960–C967.

O'Keefe, J., and Recce, M. L. (1993). Phase relationship between hippocampal place units and the EEG theta rhythm. *Hippocampus* 3, 317–330. doi: 10.1002/hipo.450030307

Olton, D. S., Becker, J. T., and Handelmann, G. E. (1979). Hippocampus, space, and memory. *Behav. Brain Sci.* 2, 313–322.

Olton, D. S., and Feustle, W. A. (1981). Hippocampal function required for nonspatial working memory. *Exp. Brain Res.* 41, 380–389.

Operto, F. F., Pastorino, G. M. G., Mazza, R., Roccella, M., Carotenuto, M., Verrotti, A., et al. (2019). Cognitive profile in BECTS treated with levetiracetam: a 2-year follow-up. *Epilepsy Behav.* 97, 187–191. doi: 10.1016/j.yebeh.2019.05.046

Osaka, N., Osaka, M., Kondo, H. M., Morishita, M., Fukuyama, H., and Shibasaki, H. (2004). The neural basis of executive function in working memory: An fMRI study based on individual differences. *Neuroimage* 21, 623–631. doi: 10.1016/j.neuroimage.2003.09.069

Owen, A. M., McMillan, K. M., Laird, A. R., and Bullmore, E. (2005). N-back working memory paradigm: A meta-analysis of normative functional neuroimaging studies. *Hum. Brain Mapp.* 25, 46–59. doi: 10.1002/hbm.20131

Oyegbile, T. O., VanMeter, J. W., Motamedi, G., Zecavati, N., Santos, C., Chun, C. L. E., et al. (2018). Executive dysfunction is associated with an altered executive control network in pediatric temporal lobe epilepsy. *Epilepsy Behav.* 86, 145–152. doi: 10.1016/j.yebeh.2018.04.022

Oyegbile, T. O., VanMeter, J. W., Motamedi, G. K., Bell, W. L., Gaillard, W. D., and Hermann, B. P. (2019). Default mode network deactivation in pediatric temporal lobe epilepsy: relationship to a working memory task and executive function tests. *Epilepsy Behav.* 94, 124–130. doi: 10.1016/j.yebeh.2019.02.031

Palva, J. M., Monto, S., Kulashekhar, S., and Palva, S. (2010). Neuronal synchrony reveals working memory networks and predicts individual memory capacity. *Proc. Natl. Acad. Sci. U.S.A.* 107, 7580–7585. doi: 10.1073/pnas.0913113107

Palva, S., Kulashekhar, S., Hämäläinen, M., and Palva, J. M. (2011). Localization of cortical phase and amplitude dynamics during visual working memory encoding and retention. *J. Neurosci.* 31, 5013–5025. doi: 10.1523/jneurosci.5592-10.2011

Papagno, C., Comi, A., Bizzi, A., Vernice, M., Casarotti, A., Fava, E., et al. (2017). Mapping the brain network of the phonological loop. *Hum. Brain Mapp.* 38, 3011–3024. doi: 10.1002/hbm.23569

Paulesu, E., Frith, C. D., and Frackowiak, R. S. (1993). The neural correlates of the verbal component of working memory. *Nature* 362, 342–345. doi: 10.1038/362342a0

Pavlides, C., Greenstein, Y. J., Grudman, M., and Winson, J. (1988). Long-term potentiation in the dentate gyrus is induced preferentially on the positive phase of θ-rhythm. *Brain Res.* 439, 383–387. doi: 10.1016/0006-8993(88)91499-0

Piazzini, A., Chifari, R., Canevini, M. P., Turner, K., Fontana, S. P., and Canger, R. (2006). Levetiracetam: An improvement of attention and of oral fluency in patients with partial epilepsy. *Epilepsy Res.* 68, 181–188. doi: 10.1016/j.eplepsyres.2005.10.006

Raghavachari, S., Kahana, M. J., Rizzuto, D. S., Caplan, J. B., Kirschen, M. P., Bourgeois, B., et al. (2001). Gating of human theta oscillations by a working memory task. *J. Neurosci.* 21, 3175–3183. doi: 10.1523/jneurosci.21-09-03175.2001

Raghavachari, S., Lisman, J. E., Tully, M., Madsen, J. R., Bromfield, E. B., and Kahana, M. J. (2006). Theta oscillations in human cortex during a working-memory task: evidence for local generators. *J. Neurophysiol.* 95, 1630–1638. doi: 10.1152/jn.00409.2005

Raghubar, K. P., Barnes, M. A., and Hecht, S. A. (2010). Working memory and mathematics: a review of developmental, individual difference, and cognitive approaches. *Learn. Individ. Differ.* 20, 110–122. doi: 10.1016/j.lindif.2009.10.005

Ranganath, C., Cohen, M. X., and Brozinsky, C. J. (2005). Working memory maintenance contributes to long-term memory formation: neural and behavioral evidence. *J. Cogn. Neurosci.* 17, 994–1010. doi: 10.1162/0898929054475118

Repovš, G., and Baddeley, A. (2006). The multi-component model of working memory: Explorations in experimental cognitive psychology. *Neuroscience* 139, 5–21. doi: 10.1016/j.neuroscience.2005.12.061

Riddle, J., Scimeca, J. M., Cellier, D., Dhanani, S., and D'Esposito, M. (2020). Causal evidence for a role of theta and alpha oscillations in the control of working memory. *Curr. Biol.* 30, 1748–1754. doi: 10.1016/j.cub.2020.02.065

Rizzuto, D. S., Madsen, J. R., Bromfield, E. B., Schulze-Bonhage, A., and Kahana, M. J. (2006). Human neocortical oscillations exhibit theta phase differences between encoding and retrieval. *Neuroimage* 31, 1352–1358. doi: 10.1016/j.neuroimage.2006.01.009

Rizzuto, D. S., Madsen, J. R., Bromfield, E. B., Schulze-Bonhage, A., Seelig, D., Aschenbrenner-Scheibe, R., et al. (2003). Reset of human neocortical oscillations during a working memory task. *Proc. Natl. Acad. Sci. U.S.A.* 100, 7931–7936. doi: 10.1073/pnas.0732061100

Rogawski, M. A., and Löscher, W. (2004). The neurobiology of antiepileptic drugs. *Nat. Rev. Neurosci.* 5, 553–564. doi: 10.1038/nrn1430

Rottschy, C., Langner, R., Dogan, I., Reetz, K., Laird, A. R., Schulz, J. B., et al. (2012). Modelling neural correlates of working memory: a coordinate-based meta-analysis. *Neuroimage* 60, 830–846. doi: 10.1016/j.neuroimage.2011.11.050

Roux, F., and Uhlhaas, P. J. (2014). Working memory and neural oscillations: alpha-gamma versus theta-gamma codes for distinct WM information? *Trends Cogn. Sci.* 18, 16–25. doi: 10.1016/j.tics.2013.10.010

Roux, F., Wibral, M., Mohr, H. M., Singer, W., and Uhlhaas, P. J. (2012). Gamma-band activity in human prefrontal cortex codes for the number of relevant items maintained in working memory. *J. Neurosci.* 32, 12411–12420. doi: 10.1523/jneurosci.0421-12.2012

Sarnthein, J., Petsche, H., Rappelsberger, P., Shaw, G. L., and Von Stein, A. (1998). Synchronization between prefrontal and posterior association cortex during human working memory. *Proc. Natl. Acad. Sci. U.S.A.* 95, 7092–7096. doi: 10.1073/pnas.95.12.7092

Sauseng, P., Griesmayr, B., Freunberger, R., and Klimesch, W. (2010). Control mechanisms in working memory: a possible function of EEG theta oscillations. *Neurosci. Biobehav. Rev.* 34, 1015–1022.

Sauseng, P., Klimesch, W., Doppelmayr, M., Hanslmayr, S., Schabus, M., and Gruber, W. R. (2004). Theta coupling in the human electroencephalogram during a working memory task. *Neurosci. Lett.* 354, 123–126. doi: 10.1016/j.neulet.2003.10.002

Sauseng, P., Klimesch, W., Schabus, M., and Doppelmayr, M. (2005). Fronto-parietal EEG coherence in theta and upper alpha reflect central executive functions of working memory. *Int. J. Psychophysiol.* 57, 97–103. doi: 10.1016/j.ijpsycho.2005.03.018

Schindler, U. (1989). Pre-clinical evaluation of cognition enhancing drugs. *Neuro Psychophormacol. Biol. Psychiot.* 13:993115.

Seeley, W. W., Menon, V., Schatzberg, A. F., Keller, J., Glover, G. H., Kenna, H., et al. (2007). Dissociable intrinsic connectivity networks for salience processing and executive control. *J. Neurosci.* 27, 2349–2356. doi: 10.1523/jneurosci.5587-06.2007

Shah, P., and Miyake, A. (1999). *Models of Working Memory: Mechanisms of Active Maintenance and Executive Control*, Vol. 21. Cambridge: Cambridge University Press.

Sherman, E. M. S., Brooks, B. L., Fay-Mcclymont, T. B., and MacAllister, W. S. (2012). Detecting epilepsy-related cognitive problems in clinically referred children with epilepsy: is the WISC-IV a useful tool? *Epilepsia* 53, 1060–1066. doi: 10.1111/j.1528-1167.2012.03493.x

Singer, W., and Gray, C. M. (1995). Visual feature integration and the temporal correlation hypothesis. *Annu. Rev. Neurosci.* 18, 555–586. doi: 10.1146/annurev.ne.18.030195.003011

Smith, E. E., Jonides, J., and Koeppe, R. A. (1996). Dissociating verbal and spatial working memory using PET. *Cereb. Cortex* 6, 11–20. doi: 10.1093/cercor/6.1.11

Sridharan, D., Levitin, D. J., and Menon, V. (2008). A critical role for the right fronto-insular cortex in switching between central-executive and default-mode networks. *Proc. Natl. Acad. Sci. U.S.A.* 105, 12569–12574. doi: 10.1073/pnas.0800005105

Stretton, J., and Thompson, P. J. (2012). Frontal lobe function in temporal lobe epilepsy. *Epilepsy Res.* 98, 1–13. doi: 10.1016/j.eplepsyres.2011.10.009

Sun, D., van 't Klooster, M., van Schooneveld, M. M. J., Zweiphenning, W., van Klink, N., Ferrier, C., et al. (2020). High frequency oscillations relate to cognitive improvement after epilepsy surgery in children. *Clin. Neurophysiol.* 131, 1134–1141. doi: 10.1016/j.clinph.2020.01.019

Swartz, B. E., Halgren, E., Simpkins, F., and Syndulko, K. (1994). Primary memory in patients with frontal and primary generalized epilepsy. *J. Epilepsy* 7, 232–241. doi: 10.1016/0896-6974(94)90034-5

Szaflarski, J. P., and Allendorfer, J. B. (2012). Topiramate and its effect on fMRI of language in patients with right or left temporal lobe epilepsy. *Epilepsy Behav.* 24, 74–80. doi: 10.1016/j.yebeh.2012.02.022

Tang, Y., Xia, W., Yu, X., Zhou, B., Wu, X., Lui, S., et al. (2016). Altered cerebral activity associated with topiramate and its withdrawal in patients with epilepsy with language impairment: An fMRI study using the verb generation task. *Epilepsy Behav.* 59, 98–104. doi: 10.1016/j.yebeh.2016.03.013

Tesche, C. D., and Karhu, J. (2000). Theta oscillations index human hippocampal activation during a working memory task. *Proc. Natl. Acad. Sci. U.S.A.* 97, 919–924. doi: 10.1073/pnas.97.2.919

Urrestarazu, E., Jirsch, J. D., LeVan, P., Hall, J., and Gotman, J. (2006). High-frequency intracerebral EEG activity (100-500 Hz) following interictal spikes. *Epilepsia* 47, 1465–1476. doi: 10.1111/j.1528-1167.2006.00618.x

van Rijckevorsel, K. (2006). Cognitive problems related to epilepsy syndromes, especially malignant epilepsies. *Seizure* 15, 227–234. doi: 10.1016/j.seizure.2006.02.019

Van Vugt, M. K., Schulze-Bonhage, A., Litt, B., Brandt, A., and Kahana, M. J. (2010). Hippocampal gamma oscillations increase with memory load. *J. Neurosci.* 30, 2694–2699. doi: 10.1523/jneurosci.0567-09.2010

Vanderwolf, C. H. (1969). Hippocampal electrical activity and voluntary movement in the rat. *Electroencephalogr. Clin. Neurophysiol.* 26, 407–418. doi: 10.1016/0013-4694(69)90092-3

Von Stein, A., and Sarnthein, J. (2000). Different frequencies for different scales of cortical integration: from local gamma to long range alphartheta synchronization. *Int. J. Psychophysiol.* 38:301313.

Wager, T. D., and Smith, E. E. (2003). Neuroimaging studies of working memory: A meta-analysis. *Cogn. Affect. Behav. Neurosci.* 3, 255–274.

Wallenstein, G. V., Eichenbaum, H., and Hasselmo, M. E. (1998). The hippocampus as an associator of discontiguous events. *Trends Neurosci.* 21, 317–323. doi: 10.1016/s0166-2236(97)01220-4

Wandschneider, B., Burdett, J., Townsend, L., Hill, A., Thompson, P. J., Duncan, J. S., et al. (2017). Effect of topiramate and zonisamide on fMRI cognitive networks. *Neurology* 88, 1165–1171. doi: 10.1212/wnl.0000000000003736

Wandschneider, B., Stretton, J., Sidhu, M., Centeno, M., Kozák, L. R., Symms, M., et al. (2014). Levetiracetam reduces abnormal network activations in temporal lobe epilepsy. *Neurology* 83, 1508–1512. doi: 10.1212/wnl.0000000000000910

White, T. P., Joseph, V., Francis, S. T., and Liddle, P. F. (2010). Aberrant salience network (bilateral insula and anterior cingulate cortex) connectivity during information processing in schizophrenia. *Schizophr. Res.* 123, 105–115. doi: 10.1016/j.schres.2010.07.020

Wikenheiser, A. M., and Redish, A. D. (2015). Hippocampal theta sequences reflect current goals. *Nat. Neurosci.* 18, 289–294. doi: 10.1038/nn.3909

Wu, X., Chen, X., Li, Z., Han, S., and Zhang, D. (2007). Binding of verbal and spatial information in human working memory involves large-scale neural synchronization at theta frequency. *Neuroimage* 35, 1654–1662. doi: 10.1016/j.neuroimage.2007.02.011

Yasuda, C. L., Centeno, M., Vollmar, C., Stretton, J., Symms, M., Cendes, F., et al. (2013). The effect of topiramate on cognitive fMRI. *Epilepsy Res.* 105, 250–255. doi: 10.1016/j.eplepsyres.2012.12.007

Yonelinas, A. P. (2013). The hippocampus supports high-resolution binding in the service of perception, working memory and long-term memory. *Behav. Brain Res.* 254, 34–44. doi: 10.1016/j.bbr.2013.05.030

Zhang, Q., Yang, F., Hu, Z., Xu, Q., Bernhardt, B. C., Quan, W., et al. (2018). Antiepileptic drug of levetiracetam decreases centrotemporal spike-associated activation in rolandic epilepsy. *Front. Neurosci.* 12:796. doi: 10.3389/fnins.2018.00796

Zhou, J.-L., Lenck-Santini, P.-P., Zhao, Q., and Holmes, G. L. (2007). Effect of interictal spikes on single-sell firing patterns in the hippocampus. *Epilepsia* 48, 720–731. doi: 10.1111/j.1528-1167.2006.00972.x

**Conflict of Interest:** The authors declare that the research was conducted in the absence of any commercial or financial relationships that could be construed as a potential conflict of interest.

*Copyright © 2021 Arski, Young, Smith and Ibrahim. This is an open-access article distributed under the terms of the Creative Commons Attribution License (CC BY). The use, distribution or reproduction in other forums is permitted, provided the original author(s) and the copyright owner(s) are credited and that the original publication in this journal is cited, in accordance with accepted academic practice. No use, distribution or reproduction is permitted which does not comply with these terms.*

frontiers in Human Neuroscience

ORIGINAL RESEARCH
published: 28 January 2021
doi: 10.3389/fnhum.2020.612899

# Viability of Preictal High-Frequency Oscillation Rates as a Biomarker for Seizure Prediction

*Jared M. Scott*[1,2], *Stephen V. Gliske*[3,4], *Levin Kuhlmann*[5] *and William C. Stacey*[1,2,3]*

[1] *Department of Biomedical Engineering, University of Michigan, Ann Arbor, MI, United States,* [2] *Biointerfaces Institute, University of Michigan, Ann Arbor, MI, United States,* [3] *Department of Neurology, University of Michigan Hospitals, Ann Arbor, MI, United States,* [4] *Department of Neurosurgery, University of Nebraska Medical Center, Omaha, NE, United States,* [5] *Department of Data Science and AI, Faculty of Information Technology, Monash University, Clayton, VIC, Australia*

**Motivation:** There is an ongoing search for definitive and reliable biomarkers to forecast or predict imminent seizure onset, but to date most research has been limited to EEG with sampling rates <1,000 Hz. High-frequency oscillations (HFOs) have gained acceptance as an indicator of epileptic tissue, but few have investigated the temporal properties of HFOs or their potential role as a predictor in seizure prediction. Here we evaluate time-varying trends in preictal HFO rates as a potential biomarker of seizure prediction.

**Methods:** HFOs were identified for all interictal and preictal periods with a validated automated detector in 27 patients who underwent intracranial EEG monitoring. We used LASSO logistic regression with several features of the HFO rate to distinguish preictal from interictal periods in each individual. We then tested these models with held-out data and evaluated their performance with the area-under-the-curve (AUC) of their receiver-operating curve (ROC). Finally, we assessed the significance of these results using non-parametric statistical tests.

**Results:** There was variability in the ability of HFOs to discern preictal from interictal states across our cohort. We identified a subset of 10 patients in whom the presence of the preictal state could be successfully predicted better than chance. For some of these individuals, average AUC in the held-out data reached higher than 0.80, which suggests that HFO rates can significantly differentiate preictal and interictal periods for certain patients.

**Significance:** These findings show that temporal trends in HFO rate can predict the preictal state better than random chance in some individuals. Such promising results indicate that future prediction efforts would benefit from the inclusion of high-frequency information in their predictive models and technological architecture.

**Keywords: epilepsy, seizure prediction, preictal identification, high frequency oscillation, ROC analysis**

OPEN ACCESS

***Edited by:***
*Johannes Sarnthein,*
*University of Zurich, Switzerland*

***Reviewed by:***
*Jan Cimbalnik,*
*International Clinical Research Center (FNUSA-ICRC), Czechia*
*Eishi Asano,*
*Children's Hospital of Michigan, United States*

***Correspondence:**
*William C. Stacey*
*william.stacey@umich.edu*

***Specialty section:***
*This article was submitted to Health, a section of the journal Frontiers in Human Neuroscience*

***Received:*** *01 October 2020*
***Accepted:*** *09 December 2020*
***Published:*** *28 January 2021*

***Citation:***
*Scott JM, Gliske SV, Kuhlmann L and Stacey WC (2021) Viability of Preictal High-Frequency Oscillation Rates as a Biomarker for Seizure Prediction. Front. Hum. Neurosci. 14:612899. doi: 10.3389/fnhum.2020.612899*

## INTRODUCTION

One of the most debilitating aspects of epilepsy is the uncertainty patients feel, not knowing when the next seizure will occur. Though seizures themselves account for an extremely small percentage of an individual's time (Cook et al., 2013), the constant threat of a seizure can make the planning of normal day-to-day activities an impossibility for some (Bishop and Allen, 2003). This has led many investigators to search for methods to predict when seizure might occur (Mormann et al., 2005; Freestone et al., 2015, 2017; Gadhoumi et al., 2016; Kuhlmann et al., 2018a).

While "seizure prediction" has been an attractive research subject for decades, early efforts had many unforeseen challenges. While there was evidence that EEG changed in the minutes or hours before seizures (Mormann et al., 2005), it was difficult to prove that these measures could work prospectively. A major breakthrough occurred when rigorous statistics were developed—the key was to show that a given algorithm could outperform random chance (Mormann et al., 2007; Snyder et al., 2008). Several studies then followed using this method and were able to show that intracranial EEG signals could predict the preictal state better than chance (Cook et al., 2013; Karoly et al., 2017; Kuhlmann et al., 2018b). Critical in that work was the unprecedented collection of months of continuous EEG in a clinical trial in Australia, which allowed for rigorous long-term statistics (Cook et al., 2013; Kuhlmann et al., 2018b). That dataset has become a crucial tool in later work, including international competitions (Kuhlmann et al., 2018b), as prediction algorithms have made many further improvements (Alexandre Teixeira et al., 2014; Karoly et al., 2017; Truong et al., 2018; Stojanović et al., 2020). However, the data also have two important limitations: the data were acquired at low sampling rate (200 Hz) that does not allow analysis of high-resolution EEG signals, and more importantly, since the trial ended no similar chronic recordings have been collected.

Thus, while there have been many very promising results in the field of seizure prediction, most work has been focused on a single dataset of long-term, low-resolution intracranial EEG. The results have proven that seizure prediction is possible in many patients but clearly are far from optimal. One potential avenue for further improvement is the possibility that higher-resolution EEG could hold greater information. In particular, over the past 20 years it has become increasingly apparent that high-frequency oscillations (HFOs) are a powerful biomarker of epilepsy (Jacobs et al., 2012; Zijlmans et al., 2012; Frauscher et al., 2017; Jacobs and Zijlmans, 2020). HFOs consist of short (<100 ms) oscillations in the 80–500-Hz frequency band and require sampling rates of at least 2,000 Hz for accurate identification (Gliske et al., 2016a). HFOs are more likely to occur in the epileptogenic zone (Jacobs et al., 2012) and may help guide surgical decisions (Cho et al., 2014; Höller et al., 2015; Fedele et al., 2017; van 't Klooster et al., 2017). One relatively unexplored aspect of HFOs is that their characteristics can also change in the 30 min prior to seizure initiation in certain individuals (Jacobs et al., 2009; Pearce et al., 2013). These preliminary studies were constrained by small patient cohorts and datasets that were not as specific as currently available methods (Blanco et al., 2010, 2011). Nevertheless, the evidence from those studies motivate using HFOs to identify the preictal state.

Utilizing population-level inference and a large clinical dataset, our group recently found several features of HFO rates that were highly correlated with the preictal state (Scott et al., 2020). In that work, we averaged the HFO response over all available data per patient and compared the responses during interictal and preictal epochs; several patients had significant results. However, in order to utilize HFOs to identify the preictal state prospectively, a different analysis is necessary. The HFO response in a given segment of data must be compared individually to that of other segments, rather than in aggregate as in that prior work.

Robust implementation of seizure detection algorithms requires several months of continuous recording, as was accomplished by the Neurovista trial in Australia (Cook et al., 2013). Such data with a sufficient sampling rate to detect HFOs is currently impossible to attain. Until such devices are available, the only alternative is to utilize inpatient intracranial EEG monitoring, which lasts <2 weeks. Although such data are vastly inferior, they are also the only current option. Until implantable devices with >1,000 Hz sampling rate are available, the role of HFOs in the specific context of seizure prediction must first be evaluated using only the limited intracranial monitoring data available, which is our goal herein.

With this study, we evaluate the preliminary usefulness of HFOs in patient-specific seizure prediction. We employ state-of-the-art automated HFO detection methods on the entire recorded intracranial EEG data of a clinically diverse cohort of 27 patients. With more than 10 million detected HFOs in this dataset, we use various features of HFO rates as predictors in patient-specific preictal classification models. With robust machine learning methods and statistical techniques to validate our results, we find that 10/27 patients have excellent classifier performance. These results are limited due to the short recording periods but were very promising. While the technology does not yet exist that would allow a full prospective analysis using high-resolution data, these results motivate future studies that incorporate such technology in the next generation of seizure prediction devices.

## METHODS

### Patient Population

To form our patient cohort, we looked at all patients with refractory epilepsy who had undergone intracranial EEG (iEEG) monitoring at the University of Michigan from 2016 to 2018. In order to ensure that sufficient data was available for training and testing our models, we required patients with the following: (1) a defined seizure onset zone, (2) at least three recorded seizures that were each preceded by non-zero HFO rates, and (3) the availability of at least 24 h of data; applying these criteria to the 32 available patients resulted in 27 patients. The study was approved by the local IRB, and all patients in the study consented to have their EEG data de-identified for later analysis. Of note, all data were acquired under standard clinical procedures, and the current work was done retrospectively: no data from this research

**TABLE 1 |** Clinical data.

| Subject | Age | Sex | ILAE outcome | Seizure focus (hemisphere, region) | Pathology/ *implant type* | Number of intracranial channels | | | | Total recorded time (hours) | Total number HFOs | Mean HFO rate (#/min./channel) | | Number of seizures | | | | Responder window subset (window duration, min.) | | |
|---|---|---|---|---|---|---|---|---|---|---|---|---|---|---|---|---|---|---|---|---|
| | | | | | | Total | ECoG | depth | SOZ | | | SOZ | OUT | Total | Used | Training | Testing | 30 | 15 | 10 |
| UMHS-0018 | 41 | M | Ib | L F | CD | 32 | 0 | 32 | 4 | 59.8 | 108,510 | 4.18 | 0.54 | 3 | 3 | 2 | 1 | | | |
| UMHS-0019 | 59 | F | II | R T | Gliosis | 106 | 106 | 0 | 2 | 168.8 | 170,946 | 2.30 | 0.19 | 5 | 3 | 2 | 1 | | | |
| UMHS-0020 | 45 | F | II | R T | MTS | 25 | 0 | 25 | 9 | 171.2 | 54,254 | 0.38 | 0.12 | 7 | 7 | 5 | 2 | | | |
| UMHS-0021 | 30 | M | II | R T | Gliosis, PVNH, PMG | 46 | 0 | 46 | 13 | 179.5 | 394,398 | 1.98 | 0.50 | 9 | 7 | 5 | 2 | | | |
| UMHS-0023 | 29 | M | NR | L T, P | PVNH/*Neuropace* | 69 | 41 | 28 | 29 | 164.3 | 390,134 | 0.86 | 0.37 | 20 | 9 | 6 | 3 | | | |
| UMHS-0024 | 31 | M | NR | L, R T | *Neuropace* | 75 | 55 | 20 | 16 | 177.2 | 1,649,380 | 3.40 | 1.71 | 28 | 11 | 7 | 4 | | | |
| UMHS-0025 | 17 | F | II | L T | Gliosis | 20 | 0 | 20 | 5 | 207.7 | 270,125 | 1.75 | 0.86 | 10 | 5 | 3 | 2 | | | |
| UMHS-0026 | 22 | F | NR | R T | PVNH | 52 | 0 | 52 | 3 | 246.2 | 382,201 | 1.28 | 0.45 | 40 | 10 | 7 | 3 | X | X | X |
| UMHS-0027 | 26 | M | NR | L Diffuse | *VNS* | 91 | 81 | 10 | 3 | 205.2 | 1,601,359 | 1.90 | 1.41 | 97 | 11 | 7 | 4 | | | |
| UMHS-0028 | 14 | F | I | R T | Tumor: Glioma | 53 | 47 | 6 | 5 | 79.7 | 140,782 | 2.95 | 0.42 | 7 | 6 | 4 | 2 | X | X | X |
| UMHS-0029 | 48 | M | NR | L T, Occ. | *Neuropace* | 91 | 91 | 0 | 22 | 226.3 | 847,560 | 0.60 | 0.71 | 14 | 7 | 5 | 2 | | | |
| UMHS-0030 | 5 | M | III | L T | MTS, Gliosis | 100 | 100 | 0 | 2 | 146 | 330,614 | 0.98 | 0.56 | 33 | 21 | 14 | 7 | X | | X |
| UMHS-0031 | 13 | M | I | L T | Gliosis, Tumor: NF1 | 99 | 99 | 0 | 6 | 180 | 263,676 | 1.17 | 0.39 | 9 | 4 | 3 | 1 | | | |
| UMHS-0032 | 41 | F | I | R F | CD | 32 | 0 | 32 | 3 | 184.3 | 295,865 | 3.79 | 0.96 | 8 | 6 | 4 | 2 | | | |
| UMHS-0033 | 5 | F | II | R Ins. | CD, Gliosis | 74 | 0 | 74 | 4 | 120.7 | 233,883 | 1.40 | 0.38 | 28 | 8 | 5 | 3 | | X | X |
| UMHS-0034 | 33 | F | I | R F | Gliosis | 32 | 0 | 32 | 11 | 136.3 | 448,718 | 2.58 | 1.26 | 17 | 16 | 11 | 5 | X | | |
| UMHS-0035 | 50 | F | I | L T | Gliosis | 57 | 57 | 0 | 2 | 162.7 | 108,147 | 0.73 | 0.21 | 7 | 4 | 3 | 1 | | X | |
| UMHS-0036 | 43 | M | NR | L, R T | CD/*Neuropace* | 54 | 0 | 54 | 2 | 172.5 | 347,928 | 1.34 | 0.60 | 18 | 12 | 8 | 4 | | | |
| UMHS-0039 | 47 | M | NR | R P | CD/*Neuropace* | 90 | 0 | 90 | 10 | 155.2 | 266,422 | 1.02 | 0.23 | 19 | 9 | 6 | 3 | | | |
| UMHS-0040 | 14 | F | I | L P | CD, Gliosis | 63 | 55 | 8 | 8 | 196.7 | 323,180 | 0.38 | 0.66 | 7 | 7 | 5 | 2 | | X | |
| UMHS-0041 | 32 | F | I | R F | CD | 71 | 0 | 71 | 9 | 176.5 | 43,350 | 0.27 | 0.04 | 36 | 3 | 2 | 1 | | | |
| UMHS-0043 | 28 | M | II | R T | Gliosis | 86 | 0 | 86 | 9 | 182.2 | 386,967 | 1.34 | 0.42 | 46 | 16 | 11 | 5 | | X | X |
| UMHS-0044 | 45 | F | NR | L T, P | *Neuropace* | 76 | 0 | 76 | 6 | 170.2 | 414,195 | 1.29 | 0.47 | 13 | 5 | 3 | 2 | | | |
| UMHS-0045 | 17 | F | NR | L, R T | *Neuropace* | 94 | 0 | 94 | 15 | 331.5 | 631,551 | 0.79 | 0.25 | 6 | 6 | 4 | 2 | | X | |
| UMHS-0046 | 23 | F | I | L F | CD | 30 | 0 | 30 | 9 | 139.3 | 16,575 | 0.15 | 0.04 | 17 | 5 | 3 | 2 | | | |
| UMHS-0048 | 22 | F | NR | L, R T | *Neuropace* | 86 | 0 | 86 | 8 | 141.8 | 404,972 | 2.76 | 0.33 | 23 | 8 | 5 | 3 | X | X | X |
| UMHS-0049 | 53 | F | NR | L, R T | *Neuropace* | 94 | 0 | 94 | 15 | 176.8 | 287,303 | 0.98 | 0.16 | 17 | 5 | 3 | 2 | | | |
| | | | | | **Totals/ averages** | 1,798 | 732 | 1,066 | 230 | 4658.6 | 10,812,995 | 1.58 | 0.53 | 544 | 214 | 143 | 71 | 5 | 8 | 6 |
| | | | | | | | | | | 172.5 | 400,481 | | | 20 | 8 | 5 | 3 | | | |

*Number of unique responders: 10 (37%).*

*M/F, male, female; L/R, left/right; T, temporal; P, parietal; F, frontal; Occ, occipital; NR, not resected; CD, cortical dysplasia; MTS, medial temporal sclerosis; PVNH, periventricular nodular heterotopia; PMG, polymicrogyria; VNS, vagal nerve stimulator; DNET, dysembryoplastic neuroepithelial tumor; NF1, neurofibromatosis type 1.*

had any effect on the clinical care. Further summary of the patient population is found in **Table 1**.

## Data Acquisition

All intracranial recordings were sampled at 4,096 Hz with a Quantum amplifier (Natus Medical Inc., Pleasanton, CA); the electrodes implanted for monitoring consisted of subdural grid, depth, and stereo-EEG electrodes, as deemed appropriate for each patient during standard clinical care. All recordings were referenced to a lab-standard instrument reference placed midway between Fz and Cz when first recorded and then were re-referenced for HFO detection using common average referencing (Gliske et al., 2016b), which was applied to all electrodes of the same type, e.g., all depths or all grids or strips together. The treating epileptologist determined which channels comprised the seizure onset zone (SOZ channels), as well as the onset and offset times of all seizures; we obtained these metadata through the official clinical report for a given patient. Channels within the resected volume of tissue (RV channels) were identified and labeled through consultation with the neurosurgeon and by pre- and post-op imaging comparisons if available. Any channel that was not labeled as an SOZ or RV channel was labeled as an OUT channel. Note that a seizure prediction algorithm should have knowledge of the SOZ and OUT channels available, as it must be trained on previous seizures and would be implemented after these studies are completed. It is also important to note that the SOZ is what was determined by the reading clinician and does not depend upon being the true epileptogenic zone. We incorporated the analysis of OUT channels as a conservative way to account for diagnostic uncertainty and see if other channels also had useful information. Channels labeled as RV that did not overlap with the SOZ were not used in our analysis, in order to maintain a more conservative analysis.

## Data Analysis

All data analysis was conducted with custom MATLAB (Mathworks, Natick, MA) and C++ functions and scripts. As described in detail below and shown in the block process diagram of **Figure 1**, this analysis consisted of several steps: first, automated HFO detection was performed on all patient data. Then, several features across consecutive time windows of varying duration were computed from HFO rates. These features were used to train a logistic regression model to distinguish preictal vs. interictal states. The algorithm was cross validated with held-out data and compared vs. random chance. Model performance was quantified using ROC curves.

## Automated HFO Detection

All HFOs were identified with a validated automated detector (Gliske et al., 2016b) with additional modifications described further below. In summary, this detector is based upon the original "Staba" RMS-based detector (Staba et al., 2002) which then increases the specificity by redacting detections that overlap in time with several EEG artifacts such as sharp transients, electrical interference and noise, and artifacts from signal filtering. To further increase HFO specificity, we excluded detected events with waveforms consistent with features of muscle (EMG) artifact, using another validated algorithm (Ren et al., 2019) as in our previous work (Scott et al., 2020). Of note, these algorithms have previously been shown to be similar to human reviewers (Gliske et al., 2016b, 2020).

We also modified the data processing pipeline of our automated detector to ensure that it functioned appropriately within the unique constraints of seizure prediction. Most automated detectors operate by processing incoming EEG data in successive epochs of fixed length, e.g., 10 min, and then assess the background activity of the entire epoch to determine a threshold for detecting HFOs within that epoch. That process cannot happen in real-time nor (pseudo)prospectively, because evaluating a potential HFO at a specific point in time requires knowledge of background activity that has yet to occur. Such a process would not be possible for prospective seizure prediction, in which there should be no knowledge of the future. To address this constraint, we modified the detection algorithm to work prospectively. First, we approximated real-time detection by only detecting HFOs for 30 s at time. Second, we still used 10 min of EEG to calculate the background, but use the *previous* 10 min of EEG data, relative to the end of each of data segment. In effect, the algorithm is identical to the previous one except it only reports the HFOs that are detected during the final 30 s of a 10 min segment, and the same process is repeated by sliding the 10-min window forward 30 s. One outcome of this is that the first HFOs detected in any given data file start after the first 10 min of recording. With these adaptations, our automated HFO detection was better suited to the constraints of seizure prediction and more closely resembled a real-time process. Further—and perhaps most importantly for preictal HFO detection—these changes also prevented seizure activity from influencing the detector (see section Feature Data Labeling and Exclusion). We compared these results to those of the original detector, and there was no appreciable difference in HFO rate (data not shown), which is expected since there were no changes inherent to the detector itself, but rather how it was fed data.

## Computation of HFO Rate

In order to investigate temporal variations in HFO rate with sufficient resolution, we approximated HFO rate (which we define as the number of HFOs per minute per channel) in both SOZ and OUT channel groups as a continuous function of time (cHFO rate). The cHFO rate was obtained by calculating the estimated HFO rate during 1 min of data, then sliding the 1-min window forward 1 s and recalculating. This sliding window method approximates a continuous HFO rate with a 1-s time resolution. The sliding window was applied to all SOZ or OUT channels, which were grouped separately. For a given window segment and channel group, the HFO rate was computed by summing the number of HFOs occurring across all channels of the same group; this value was then divided by the total number of channels in that respective group, which resulted in an estimate of the average cHFO per channel within each group (SOZ or OUT).

## Features of HFO Rate

The advantage to using cHFO rate as computed above—rather than averaging it over longer periods—is that the temporal resolution of cHFO rates can reveal fluctuations and patterns in

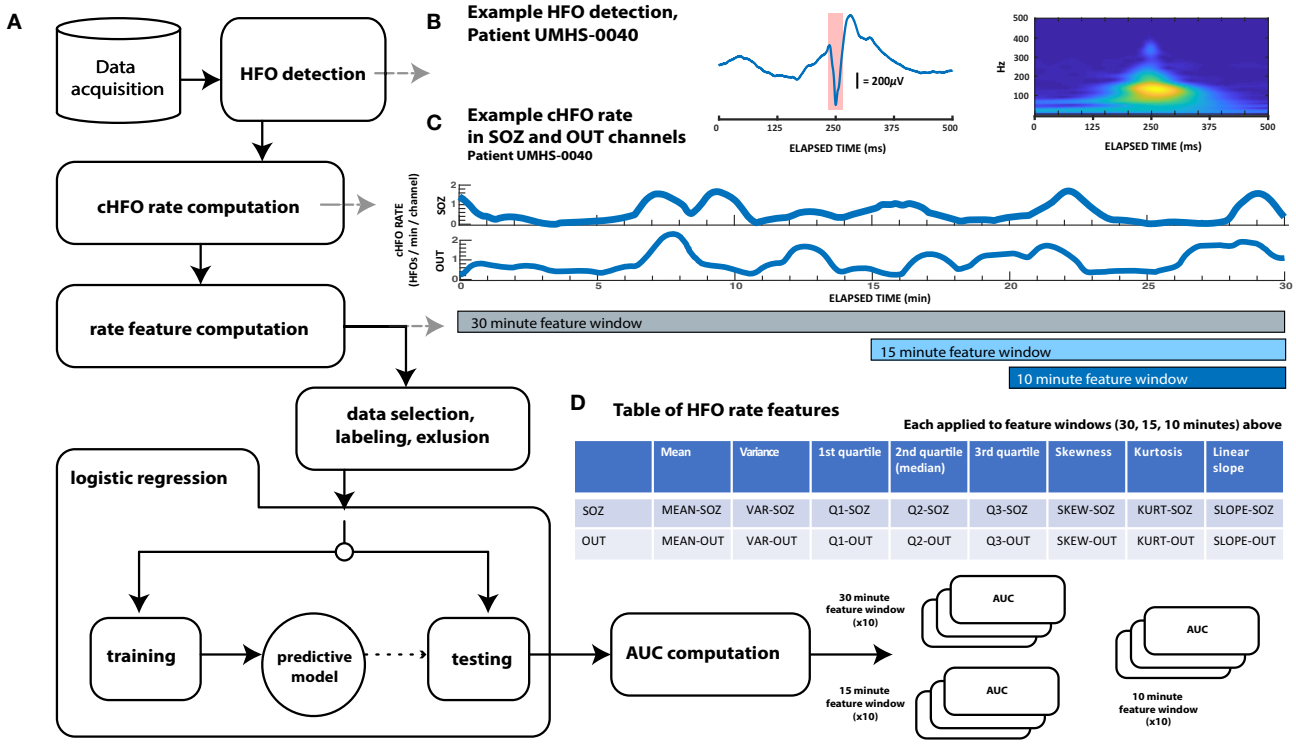


**FIGURE 1 |** Schematic diagram showing overall data analysis workflow. **(A)** General analysis workflow. After automated HFO detection, continuous HFO rates (cHFO rate) are computed in both the SOZ and OUT channel groups. Next, several statistical quantities (features of HFO rate) are computed from cHFO rates in three "feature windows" of different durations: 30-, 15-, and 10-min feature windows. After labeling this feature data as either preictal or interictal, observations that remain after an exclusion process are randomly divided into training and test data sets. Training data is used to train predictive LASSO logistic regression models, which are then tested with unseen testing data. The performance of each model with this testing data is assessed by computing the test AUC value, which, when averaged over 10× cross-validation runs for each of the three feature windows, are finally compared across patients; these results are visualized in **Figure 3**. **(B)** Example HFO detection, "responder" patient UMHS-0040. The HFO waveform is displayed on the left, while its time–frequency decomposition (computed with the Morse wavelet) is visualized on the right. **(C)** Example of cHFO rates computed for patient UMHS-0040. Continuous HFO rates (cHFO rate—defined as HFOs/min/channel) are computed in both the SOZ and OUT channel groups separately. The rate features used in the proceeding Table **(D)** are computed from these cHFO trajectories in 30-, 15-, and 10-min segments. **(D)** Table of rate features. Eight features are applied to cHFO rates per channel group (SOZ and OUT channel groups), which yields a total of 16 rate features. Abbreviations shown in this table are used throughout the text.

HFOs down to the scale of a second—which could be important in characterizing preictal trends. We quantified the temporal variation of cHFO rates with several descriptive statistics, including mean, variance, linear slope, quartiles, skewness, and kurtosis across a given epoch of time. We also compared linear trends in cHFO rates using the slope extracted from linear regression applied to cHFO rates for a given epoch of time. All these values were computed separately in SOZ and OUT channel groups across three different epochs of time: 30, 15, and 10 min, which we call "feature windows." The feature windows were designed to account for possible differences in seizure horizons between patients, as we hypothesized that the duration of any preictal state would not be constant across the entire cohort. All features were computed from the start of a given data file in consecutive 1-min intervals. Each feature window was analyzed independently of the others throughout the entirety of the study.

## Feature Data Labeling and Exclusion

In machine learning, classification algorithms used in prediction need labeled observations of data in order to train their models. In this case, we label data as either interictal or preictal. Based on our prior data showing HFO features changing up to 30 min prior to seizures (Pearce et al., 2013; Scott et al., 2020), we defined the "preictal period" as the 31 min prior to the start of the seizure. The extra minute occurs because we inserted a buffer of 1 min just prior to seizure onset, which accounts for some interrater variability in seizure onset time (Abend et al., 2011).

For each of the feature windows (10, 15, or 30 min), the "preictal" windows were defined as the last window immediately prior to the seizure, but not including any of the 1 min just before seizure onset. Because the calculations slide forward in 1-min steps, this means each "preictal" feature window ends between 1 and 2 min prior to the clinician-determined seizure onset time. For each feature window length, we only included the one "preictal" window immediately before the seizure. Because our prior data suggested up to 30 min could be considered as the physiological preictal period, to be conservative we ignored data during that period that was not in the "preictal" feature window. Data from those times (the two previous 10-min windows and one previous 15-min window) were discarded from both the preictal and interictal analysis.

"Interictal" was defined as all data starting 11 min after a seizure until 31 min prior to the next seizure, which allows a 1-min buffer for uncertainties in the start/stop times of the seizure. We note that some research has shown that the preictal state may extend beyond 30 min (Litt et al., 2001; Stacey et al., 2011), so this definition is conservative and may not capture all differences. We calculated an "interictal" feature window for every consecutive epoch (i.e., every 30 min for the 30-min feature window; every 10 min for the 10-min feature window).

There were other limited circumstances that we excluded from analysis. To ensure that seizures were evaluated independently of other seizures, such as when multiple seizures occur sequentially, we redacted preictal observations falling within peri-ictal extent (11 min postictal or 31 min preictal) of other seizures. Further, we also redacted any observation that overlapped with periods of incomplete or missing data, which could result from gaps within a file or from a file's end. Finally, considering our modifications to the HFO detector, any data observation overlapping with the first 10 min of a given data file was also redacted, as HFOs are not detected for the first 10 min.

## Logistic Regression Model

We used a logistic regression model to classify preictal vs. interictal data. Logistic regression determines the probability that given data is from a specific labeled class and has been used in seizure prediction studies previously (Mirowski et al., 2009). It also has the advantage of allowing us to analyze the relative contributions of each feature, rather than being a "black box" approach. We trained models for each of the three feature windows (10, 15, 30 min) using 2/3 of the data and then testing on the remaining 1/3. This process was cross-validated 10 times for each feature window by randomly selecting different interictal and preictal data, and re-running the training and testing step, for a total of 30 models per patient. Random selection, rather than chronological, was used because of the limitations of this dataset: unlike in the Neurovista dataset that had months for the recordings to stabilize (Ung et al., 2017), our data is limited to 2 weeks of inpatient monitoring. This unavoidably leads to some variability over time due to various factors such as medication taper, sleep disturbances, and the settling of electrodes (Zijlmans et al., 2009; Ung et al., 2017; Gliske et al., 2018). Here, we used random selection to reduce the influence of these factors on overall model performance, but this also may reduce the effectiveness of the model.

In order to facilitate the models helping to determine which coefficients were most useful in forecasting seizures, we used LASSO logistic regression (Mirowski et al., 2009; Tibshirani, 2011; Lu et al., 2020) to create the predictive models used in our study. Specifically, in Matlab we used the lassoglm function, with the following general syntax: lassoglm(XTrain, yTrain, "binomial," "CV," k), where XTrain is the feature vector, yTrain is a binary vector with "0" for interictal and "1" for preictal, and k is chosen as the number of seizures within the training data. This function inherently cross-validates the trained model based upon the number of seizures k, which reduces overfitting. In general, LASSO introduces a penalty on the absolute value of the coefficients, and optimizes the model by iterating through different penalty parameters to find the lowest error, while removing coefficients that have minimal effects (Tibshirani, 2011). Thus, one outcome of the training step is to identify which features were the most important for identification of the preictal state.

## Assessing Predictive Performance

Each cross-validation iteration tests whether the predictive model can correctly classify novel preictal vs. interictal data. We computed the ROC curve for each iteration, then computed the arithmetic mean of all the areas under the curve (AUC) across all 10 iterations. A random predictor would have an AUC of 0.5, while a successful predictor should have an AUC higher than 0.5. We chose a nominal threshold of 0.6 to show the minimal improvement above 0.5 that would be meaningful. However, that threshold is subjective so we then tested the significance of each AUC using bootstrapping by randomizing preictal and interictal labels ($n = 1{,}000$). The statistical significance of these average AUC was determined by taking the harmonic mean of the bootstrap $p$-values (Wilson, 2019), a procedure used in meta-analysis to combine $p$-values from multiple tests. Successful tests were those in which the average AUC was $\geq$0.6 and $p < 0.05$. We note that in clinical practice an AUC of 0.6 might be difficult to implement successfully on its own; however, it is comparable with prior seizure prediction work in standard EEG (Mormann et al., 2005; Freestone et al., 2015, 2017; Gadhoumi et al., 2016; Kuhlmann et al., 2018a).

# RESULTS

Our heterogeneous patient cohort was comprised of individuals with a variety of ages, clinical etiologies and pathologies, and seizure foci. Out of 32 original patients in our database, four patients (UMHS-0037,−0038,−0042,−0047) were excluded because of either insufficient recorded seizures or undefined seizure onset zones. One patient in particular (UMHS-0022) had seizures with no HFOs prior to onset; this patient was also excluded, which left a total of 27 patients remaining for further analysis. Across these 27 patients, we detected more than 10 million HFOs across over 190 total days of intracranial EEG recordings. Over 210 seizures and 3,800 h of interictal data (average of 8 seizures and 141 h per patient) were used to train and test our classification models.

## Comparison of Test AUC Values

We first assessed the general responses across all cross validation models in all patients. Over the 27 patients, with 30 models each (810 total), the model successfully converged to a solution in 403 instances (49.8%). The non-converging solutions are easily identified because all coefficients for HFO features are 0, and it is obvious that the model could not be used. In such cases, we conservatively assigned them a testing AUC value of 0.5 (and a bootstrap $p$-value equal to 1)—the same performance as a random predictor. The remaining patient models were composed of linear combinations of HFO rate features. As shown in the histogram of **Figure 2**, the distribution of test AUC values for these models overall showed significant variability and spread

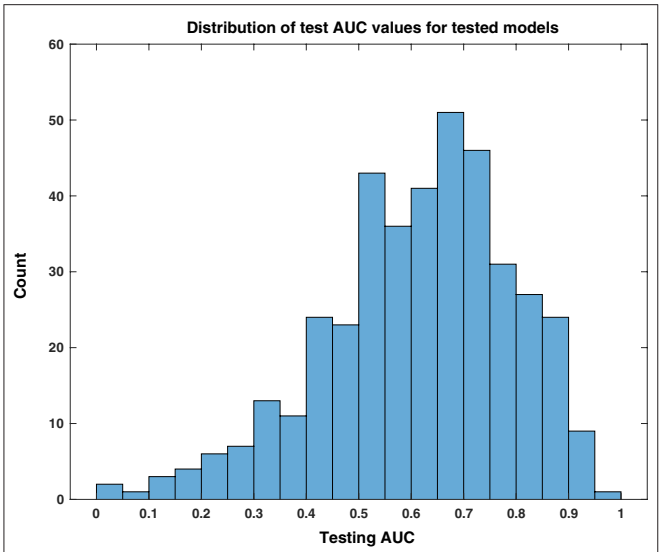


**FIGURE 2 |** Distribution of test AUC values for tested models. This histogram of testing AUC values, computed for all tested models individually over all patients and feature windows, is skewed toward predictive performance that is better than random chance, i.e., values higher than 0.5.

from 0.5 (AUC test—maximum: 0.97, minimum: 0.024, median: 0.64). The skew of this distribution toward values >0.5 suggests that a significant portion of models that used HFO features could perform better than random chance at identifying the preictal period.

We evaluated the consistency and reliability of this result within patients by determining if its average test AUC was at least 0.6 and if the average bootstrapped $p$-value was $< 0.05$. These values are shown with statistical significance noted in the bar plots of **Figure 3**. We found that 10 out of the 27 patients had a significant response in at least one of the feature windows. We denote these 10 patients as "responders," and their average predictive response was robust and consistent. The presence of this subset of patients in our cohort suggests that there are measurable changes in preictal HFO rate preceding epileptic seizures that deviate from interictal trends. This finding shows that HFOs can act as a temporal biomarker of seizure onset in some patients.

Within the responder group, 4 were significant in only one feature window, while the rest had multiple. We compared the three windows (10, 15, 30 min) and found no evidence that the performance of one window was better than any other—either by how frequently it was significant in these patients, or by how high its overall performance was (Chi-square test: $p = 0.61$; Kruskal–Wallis test: $p = 0.737$). All responders and their significant windows are identified in **Figure 3** and in **Table 1**. The $p$-value and associated asterisks indicating statistical significance in **Figure 3** were based on individual bootstrap tests and not corrected for multiple comparisons.

## Significance of Responder Predictors

We investigated which features contributed to the significant predictive response observed in responder patients. Overall, both the combination and relative magnitude of HFO features in responder models varied significantly between patients, feature windows, and even between different cross-validation runs. Considering this variability, we could not evaluate feature importance directly by the raw coefficient values that resulted from LASSO logistic regression. Instead, we calculated how often a given feature was included among models—specifically, how often its corresponding coefficient was non-zero. In this manner, we considered the most commonly used features to be the most important to differentiating the preictal state from other interictal observations—whether its associated output coefficient was positive (which would indicate increased likelihood of an imminent seizure resulting from an increase in the feature's value) or negative (i.e., decreased seizure likelihood from a feature's increase). These frequencies of non-zero model coefficients per feature are shown by a feature window in **Figure 4** and are sorted in order from most to least common within responder models. Though we did not evaluate feature magnitude directly, we note that the medians of all responder SLOPE-SOZ features by patient and feature window were all positive, which reinforces our prior findings that gradually increasing HFO rates anticipate seizure onset (Scott et al., 2020).

While there were some observed differences in which features were the most common between window durations, there were no statistically significant differences in feature frequency across the three feature windows (Kruskal–Wallis: $p = 0.64$). In terms of the most important features, the linear slope of HFO rate in the SOZ (Slope-SOZ) was most important in both the 30- and 15-min windows. Also common among important features were those computed from cHFO rates in OUT channels—channels that might be traditionally considered as less involved in pathological brain networks. Yet, there were no statistical differences in frequency between SOZ and OUT channel features (rank-sum tests: $p = 0.34$, $= 0.24$, $= 0.42$ for 30-, 15-, and 10-min windows, respectively), even though SOZ features were highest ranked across feature windows, with an average cumulative frequency almost 14% greater than that of OUT channel features. This suggests that HFO rates could be used to identify the preictal state regardless of their location.

## Clinical Factors of Responders

Considering the clinical outcomes of responders, four were ILAE class I, two were class II, there was one class III, and the others were not resected. Comparing various clinical factors, there was no statistical evidence for differences in the composition of responder patients compared to the rest of the cohort. The ratio of temporal to extra-temporal seizure foci in responders was similar to other that of other patients (Fisher exact test: $p = 0.68$), and while there appeared to be a difference in the pathology of resected responders favoring gliosis, this was not significant in comparison to the rest of the cohort (Fisher exact test: $p = 0.14$). Despite lacking a clinical factor to differentiate this group from the rest of the population, based on our results, we estimate the relative proportion of responders in a given population is 19–55% of patients (95% binomial confidence

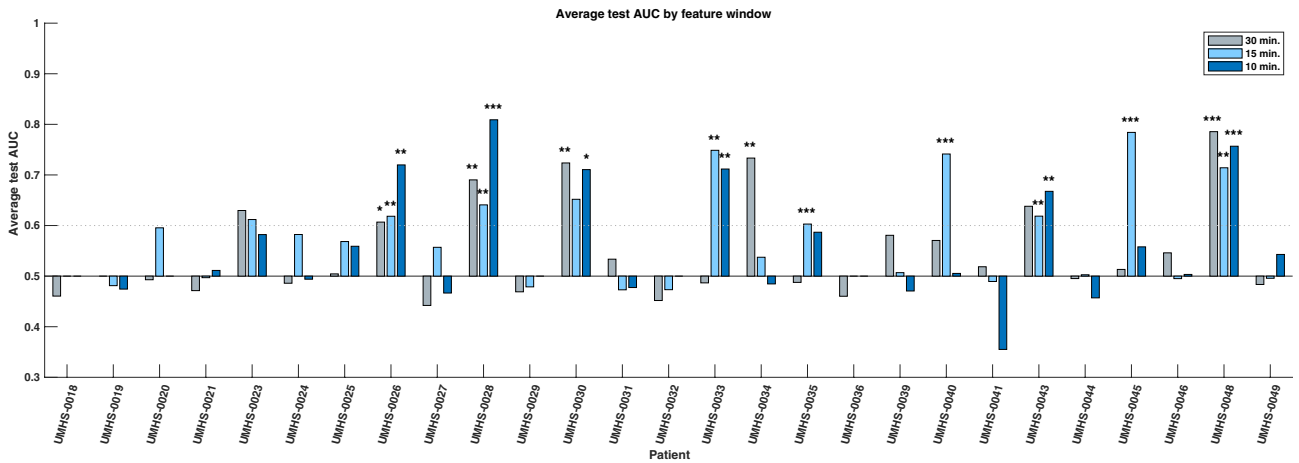


**FIGURE 3 |** Bar chart of average test AUC values by patient and feature window. Ten individual responder patients have significant predictive performance (average test AUC >=0.6, significant average bootstrap test $p < 0.05$) in one or more feature windows. The statistical significance of the bootstrap test per feature window is indicated with asterisks: *$p < 0.05$, **$p < 0.01$, ***$p < 0.001$, respectively. Note that the significance is based upon how likely that patient's data could produce the given AUC by random chance, not whether the magnitude of the AUC itself is high.

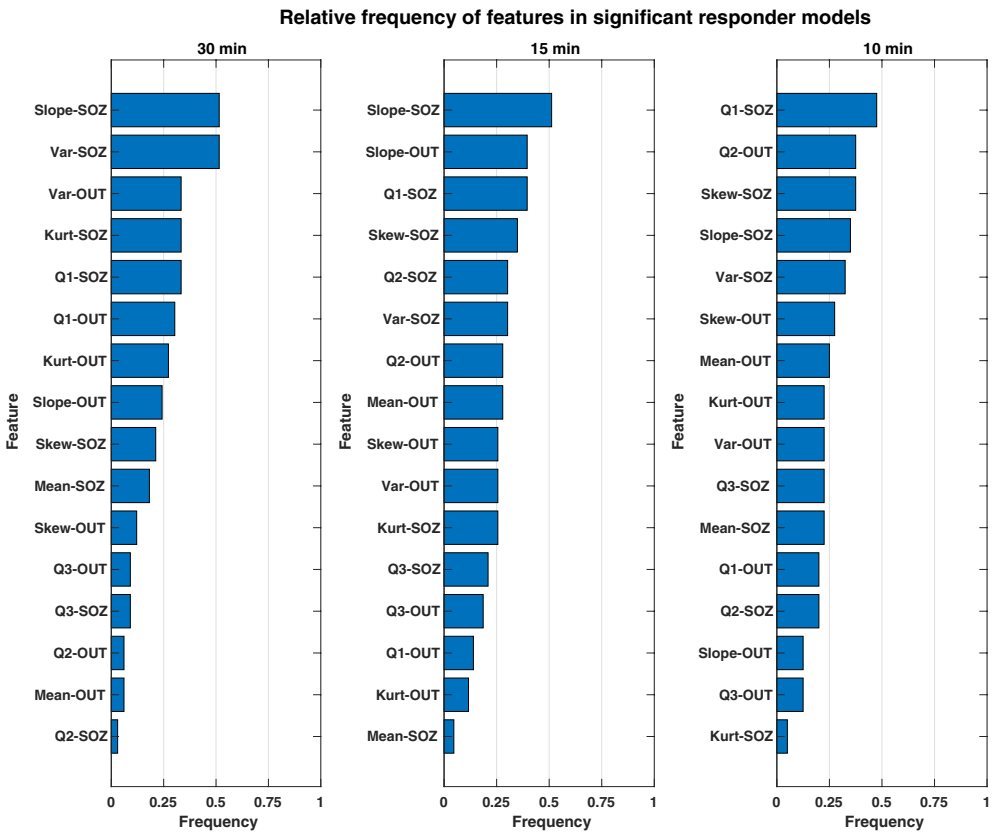


**FIGURE 4 |** Bar chart showing the relative frequency of each rate feature for only significant responder models. The features of HFO rate most important to discerning the preictal HFO response in responders are ranked in descending order (top to bottom) according to how often their respective model coefficients were non-zero for a given feature window. Overall, the most important feature was the SLOPE-SOZ feature, which was ranked first in the both 30- and 15-min feature windows. Also important were features in OUT channels, a novel finding that suggests HFOs outside epileptic tissue could still be involved in the process of seizure generation.

interval with a test sample of 10/27), which demonstrates that patients with potential for significant HFO rate predictive performance could comprise a substantial portion of a large clinical cohort.

## DISCUSSION

In this first-of-its-kind study, we combined advanced automated HFO detection with the intracranial data of a large clinical cohort to investigate the potential use of high-frequency oscillations in seizure prediction. Across patients, we found a significant variation in the ability of time-varying properties of HFO rate to discern a preictal state. After applying a statistical benchmark to the average predictive performance of all models across our cohort, a subset of patient responders was identified that had consistent predictive performance better than random chance. The identification of these 10 individuals represents a novel finding and is our study's most important result. It provides firm support that high-frequency oscillations can function as a temporal biomarker of seizure onset and additionally gives preliminary evidence that seizure prediction using HFOs is not only possible in a clinical context; it can hold significant potential for certain patients.

Another important outcome is the identification of *which* HFO rate features are the most useful. Ranked by their frequency in responder models across multiple windows of time, the most important predictive features of HFO rate included linear slope, variance, and the first quartile cHFO rate within the feature window. The most common feature was the linear slope, which measures gradual changes in HFO rate (either increasing or decreasing), suggesting that these changes are centrally important in determining if a seizure is imminent. One surprising finding was that even HFOs outside the SOZ were useful features. Note that it is not possible to compare relative magnitude of these feature coefficients directly because of the considerable model variability between patients, feature windows, and cross-validation runs. We analyzed the 10 responders and found that three of them had clinical situations in which the OUT channels were likely to be pathological. One patient had a known secondary seizure focus not included in the official SOZ (UMHS-0026), while another had high HFO activity in a non-resected hippocampus that was likely dual pathology from a parietal lesion (UMHS-0040). However, the OUT features were not restricted just to those patients, and thus our finding of predictive value of HFO features outside the SOZ is an intriguing finding. This result suggests that HFOs even outside the SOZ provide important information on identifying impending seizures.

The test AUC values of responder patients we report are within the ranges presented in several seizure prediction studies, notably Brinkmann et al. (2016), Karoly et al. (2017), and Kuhlmann et al. (2018b). There is one caveat to using the AUC metric in seizure prediction, as the inherent imbalance of interictal and preictal data can increase the reported specificity. In order to compare our work with other studies, however, this was an acceptable limitation for our analysis. While no prior work has evaluated HFOs for seizure prediction, there is evidence for a "preictal state" (Stacey et al., 2011). HFOs have been shown to have different signal features (Pearce et al., 2013; Bandarabadi et al., 2019) and changes in rate 30 min before seizures (Scott et al., 2020). Further, some studies have shown distinct changes in high-frequency activity preceding seizure onset; some have also suggested that HFOs could be linked to seizure-generating mechanisms (Worrell et al., 2004).

Despite our positive result, it must be noted that our overall methodology has a number of inherent constraints that limit our findings from being more widely applicable to seizure prediction in general. First, this analysis was based upon processing several minutes of data at a time (10, 15, or 30 min) rather than analyzing features of individual HFOs. There are a wide range of HFO features that could be incorporated into future prediction algorithms. Next, we note that "true" seizure prediction would involve choosing a specific algorithm and testing accuracy prospectively, which was not done here. Second, this method requires HFOs to be present and enough seizures to develop a predictive model; five of our cohort of 32 did not meet this standard. Finally, as stated before these data are limited to only 2 weeks immediately postoperatively during varied medication changes, which is known to be insufficient to have consistent EEG signals and sometimes even atypical seizures. Several of our patients had inconsistent results, but with so few seizures it is impossible to predict whether this would stabilize to an effective solution with more data. A much longer dataset under standard living conditions would be necessary to develop robust algorithms, but such data are not physically possible at present. Future work with a larger dataset could also incorporate additional features of the HFOs themselves (e.g., signal features such as frequency data), as well as previous prediction algorithms using standard EEG. This type of synergistic analysis on larger datasets could have much greater chance at a clinically realizable seizure prediction algorithm.

## CONCLUSION

Our results show that HFOs can function as a temporal biomarker of seizure onset. We show that changes in the HFO rate are capable of identifying the preictal state up to 30 min before a seizure in some patients. As a preliminary study, our findings are a foundation for future work pursuing individualized seizure-specific prediction efforts, which we envision could eventually function as a tool inside advanced implanted neuromodulation devices that utilize patient-specific and seizure-specific prediction methodologies. Advancement of this HFO seizure prediction framework, however, will require the availability of many chronic high-sampling rate intracranial recordings. While this technology does not yet exist, recent technological improvements have brought it closer to realization—which is sufficient impetus to further investigate HFOs both as a temporal biomarker

of epilepsy, and as a potentially powerful predictor of epileptic seizures.

## DATA AVAILABILITY STATEMENT

The raw data supporting the conclusions of this article will be made available by the authors, without undue reservation.

## ETHICS STATEMENT

The studies involving human participants were reviewed and approved by University of Michigan IRB. Written informed consent to participate in this study was provided by the participants' legal guardian/next of kin.

## AUTHOR CONTRIBUTIONS

JS, SG, LK, and WS designed the study and wrote the paper. JS, SG, and WS performed the analyses. SG and WS were responsible for funding. All authors contributed to the article and approved the submitted version.

## FUNDING

This research and publication fees were supported by the National Institutes of Health (grants K01-ES026839 and R01-NS094399) and by the Robbins Family Research Fund and Lucas Family Research Fund at Michigan Medicine.

## REFERENCES

Abend, N. S., Gutierrez-Colina, A., Marsh, E., Clancy, R. R., Dlugos, D. J., Zhao, H., et al. (2011). Interobserver reproducibility of EEG interpretation in critically Ill children. *J. Clin. Neurophysiol.* 28, 333–334. doi: 10.1097/WNP.0b013e31821cac0a

Alexandre Teixeira, C., Direito, B., Bandarabadi, M., Le Van Quyen, M., Valderrama, M., Schelter, B., et al. (2014). Epileptic seizure predictors based on computational intelligence techniques: a comparative study with 278 patients. *Comput. Methods Programs Biomed.* 114, 324–336. doi: 10.1016/j.cmpb.2014.02.007

Bandarabadi, M., Gast, H., Rummel, C., Bassetti, C., Adamantidis, A., Schindler, K., et al. (2019). Assessing epileptogenicity using phase-locked high frequency oscillations: a systematic comparison of methods. *Front Neurol.* 10:1132. doi: 10.3389/fneur.2019.01132

Bishop, M., and Allen, C. A. (2003). The impact of epilepsy on quality of life: a qualitative analysis. *Epilepsy Behav.* 4, 226–233. doi: 10.1016/S1525-5050(03)00111-2

Blanco, J. A., Stead, M., Krieger, A., Stacey, W., Maus, D., Marsh, E., et al. (2011). Data mining neocortical high-frequency oscillations in epilepsy and controls. *Brain* 134, 2948–2959. doi: 10.1093/brain/awr212

Blanco, J. A., Stead, M., Krieger, A., Viventi, J., Marsh, W. R., Lee, K. H., et al. (2010). Unsupervised classification of high-frequency oscillations in human neocortical epilepsy and control patients. *J. Neurophysiol.* 104, 2900–2912. doi: 10.1152/jn.01082.2009

Brinkmann, B. H., Wagenaar, J., Abbot, D., Adkins, P., Bosshard, S. C., Chen, M., et al. (2016). Crowdsourcing reproducible seizure forecasting in human and canine epilepsy. *Brain* 139, 1713–1722. doi: 10.1093/brain/aww045

Cho, J. R., Koo, D. L., Joo, E. Y., Seo, D. W., Hong, S. C., Jiruska, P., et al. (2014). Resection of individually identified high-rate high-frequency oscillations region is associated with favorable outcome in neocortical epilepsy. *Epilepsia* 55, 1872–1883. doi: 10.1111/epi.12808

Cook, M. J., O'Brien, T. J., Berkovic, S. F., Murphy, M., Morokoff, A., Fabinyi, G., et al. (2013). Prediction of seizure likelihood with a long-term, implanted seizure advisory system in patients with drug-resistant epilepsy: a first-in-man study. *Lancet Neurol.* 12, 563–571. doi: 10.1016/S1474-4422(13)70075-9

Fedele, T., Burnos, S., Boran, E., Krayenbühl, N., Hilfiker, P., Grunwald, T., et al. (2017). Resection of high frequency oscillations predicts seizure outcome in the individual patient. *Sci. Rep.* 7, 1–10. doi: 10.1038/s41598-017-13064-1

Frauscher, B., Bartolomei, F., Kobayashi, K., Cimbalnik, J., van 't Klooster, M. A., Rampp, S., et al. (2017). High-frequency oscillations: The state of clinical research. *Epilepsia* 58, 1316–1329. doi: 10.1111/epi.13829

Freestone, D. R., Karoly, P. J., and Cook, M. J. (2017). A forward-looking review of seizure prediction. *Curr. Opin. Neurol.* 30, 167–173. doi: 10.1097/WCO.0000000000000429

Freestone, D. R., Karoly, P. J., Peterson, A. D. H., Kuhlmann, L., Lai, A., Goodarzy, F., et al. (2015). Seizure prediction: science fiction or soon to become reality? *Curr. Neurol. Neurosci. Rep.* 15:73. doi: 10.1007/s11910-015-0596-3

Gadhoumi, K., Lina, J. M., Mormann, F., and Gotman, J. (2016). Seizure prediction for therapeutic devices: a review. *J. Neurosci. Methods* 260, 270–282. doi: 10.1016/j.jneumeth.2015.06.010

Gliske, S. V., Irwin, Z. T., Chestek, C., Hegeman, G. L., Brinkmann, B., Sagher, O., et al. (2018). Variability in the location of high frequency oscillations during prolonged intracranial EEG recordings. *Nat. Commun.* 9:2155. doi: 10.1038/s41467-018-04549-2

Gliske, S. V., Irwin, Z. T., Chestek, C., and Stacey, W. C. (2016a). Clinical Neurophysiology Effect of sampling rate and filter settings on High Frequency Oscillation detections. *Clin. Neurophysiol.* 127, 3042–3050. doi: 10.1016/j.clinph.2016.06.029

Gliske, S. V., Irwin, Z. T., Davis, K. A., Sahaya, K., Chestek, C., and Stacey, W. C. (2016b). Universal automated high frequency oscillation detector for real-time, long term EEG. *Clin. Neurophysiol.* 127, 1057–1066. doi: 10.1016/j.clinph.2015.07.016

Gliske, S. V., Qin, Z. A., Lau, K., Alvarado-Rojas, C., Salami, P., Zelmann, R., et al. (2020). Distinguishing false and true positive detections of high frequency oscillations. *J. Neural. Eng.* 17:056005. doi: 10.1088/1741-2552/abb89b

Höller, Y., Kutil, R., Klaffenböck, L., Thomschewski, A., Höller, P. M., Bathke, A. C., et al. (2015). High-frequency oscillations in epilepsy and surgical outcome. A meta-analysis. *Front. Hum. Neurosci.* 9:574. doi: 10.3389/fnhum.2015.00574

Jacobs, J., Staba, R., Asano, E., Otsubo, H., Wu, J. Y., Zijlmans, M., et al. (2012). High-frequency oscillations (HFOs) in clinical epilepsy. *Prog. Neurobiol.* 98, 302–315. doi: 10.1016/j.pneurobio.2012.03.001

Jacobs, J., Zelmann, R., Jirsch, J., Chander, R., Châtillon, C.-É., Dubeau, F., et al. (2009). High frequency oscillations (80-500 Hz) in the preictal period in patients with focal seizures. *Epilepsia* 50, 1780–1792. doi: 10.1111/j.1528-1167.2009.02067.x

Jacobs, J., and Zijlmans, M. (2020). HFO to measure seizure propensity and improve prognostication in patients with epilepsy. *Epilepsy Curr.* 20, 338–347. doi: 10.1177/1535759720957308

Karoly, P. J., Ung, H., Grayden, D. B., Kuhlmann, L., Leyde, K., Cook, M. J., et al. (2017). The circadian profile of epilepsy improves seizure forecasting. *Brain* 140, 2169–2182. doi: 10.1093/brain/awx173

Kuhlmann, L., Karoly, P., Freestone, D. R., Brinkmann, B. H., Temko, A., Barachant, A., et al. (2018b). Epilepsyecosystem.org: crowd-sourcing reproducible seizure prediction with long-term human intracranial EEG. *Brain* 141, 2619–2630. doi: 10.1093/brain/awy210

Kuhlmann, L., Lehnertz, K., Richardson, M. P., Schelter, B., and Zaveri, H. P. (2018a). Seizure prediction — ready for a new era. *Nat. Rev. Neurol.* 14, 618–630. doi: 10.1038/s41582-018-0055-2

Litt, B., Esteller, R., Echauz, J., D'Alessandro, M., Shor, R., Henry, T., et al. (2001). Epileptic seizures may begin hours in advance of clinical onset: a report of five patients. *Neuron.* 30, 51–64. doi: 10.1016/S0896-6273(01)00262-8

Lu, C. W., Malaga, K. A., Chou, K. L., Chestek, C. A., and Patil, P. G. (2020). High density microelectrode recording predicts span of therapeutic tissue activation volumes in subthalamic deep brain stimulation for Parkinson disease. *Brain Stimul.* 13, 412–419. doi: 10.1016/j.brs.2019.11.013

Mirowski, P., Madhavan, D., LeCun, Y., and Kuzniecky, R. (2009). Classification of patterns of EEG synchronization for seizure prediction. *Clin. Neurophysiol.* 120, 1927–1940. doi: 10.1016/j.clinph.2009.09.002

Mormann, F., Andrzejak, R. G., Elger, C. E., and Lehnertz, K. (2007). Seizure prediction: the long and winding road. *Brain* 130, 314–333. doi: 10.1093/brain/awl241

Mormann, F., Kreuz, T., Rieke, C., Andrzejak, R. G., Kraskov, A., David, P., et al. (2005). On the predictability of epileptic seizures. *Clin. Neurophysiol.* 116, 569–587. doi: 10.1016/j.clinph.2004.08.025

Pearce, A., Wulsin, D., Blanco, J. A., Krieger, A., Litt, B., and Stacey, W. C. (2013). Temporal changes of neocortical high-frequency oscillations in epilepsy. *J. Neurophysiol.* 110, 1167–1179. doi: 10.1152/jn.01009.2012

Ren, S., Gliske, S. V., Brang, D., and Stacey, W. C. (2019). Redaction of false high frequency oscillations due to muscle artifact improves specificity to epileptic tissue. *Clin. Neurophysiol.* 130, 976–985. doi: 10.1016/j.clinph.2019.03.028

Scott, J. M., Ren, S., Gliske, S. V., and Stacey, W. C. (2020). Preictal variability of high-frequency oscillation rates in refractory epilepsy. *Epilepsia* 61, 2521–2533. doi: 10.1111/epi.16680

Snyder, D. E., Echauz, J., Grimes, D. B., and Litt, B. (2008). The statistics of a practical seizure warning system. *J. Neural. Eng.* 5, 392–401. doi: 10.1088/1741-2560/5/4/004

Staba, R. J., Wilson, C. L., Bragin, A., and Fried, I. (2002). Quantitative analysis of high-frequency oscillations (80-500 Hz) recorded in human epileptic hippocampus and entorhinal cortex. *J. Neurophysiol.* 88, 1743–1752. doi: 10.1152/jn.2002.88.4.1743

Stacey, W., Le Van Quyen, M., Mormann, F., and Schulze-Bonhage, A. (2011). What is the present-day EEG evidence for a preictal state? *Epilepsy Res.* 97, 243–251. doi: 10.1016/j.eplepsyres.2011.07.012

Stojanović, O., Kuhlmann, L., and Pipa, G. (2020). Predicting epileptic seizures using nonnegative matrix factorization. *PLoS ONE* 15:e0228025. doi: 10.1371/journal.pone.0228025

Tibshirani, R. (2011). Regression shrinkage and selection via the lasso: a retrospective. *J. R. Stat. Soc. Ser. B Stat. Methodol.* 73, 273–282. doi: 10.1111/j.1467-9868.2011.00771.x

Truong, N. D., Nguyen, A. D., Kuhlmann, L., Bonyadi, M. R., Yang, J., Ippolito, S., et al. (2018). Convolutional neural networks for seizure prediction using intracranial and scalp electroencephalogram. *Neural. Netw.* 105, 104–111. doi: 10.1016/j.neunet.2018.04.018

Ung, H., Baldassano, S. N., Bink, H., Krieger, A. M., Williams, S., Vitale, F., et al. (2017). Intracranial EEG fluctuates over months after implanting electrodes in human brain. *J. Neural. Eng.* 14, 1–25. doi: 10.1088/1741-2552/aa7f40

van 't Klooster, M. A., van Klink, N. E. C., Zweiphenning, W. J. E. M., Leijten, F. S. S., Zelmann, R., Ferrier, C. H., et al. (2017). Tailoring epilepsy surgery with fast ripples in the intraoperative electrocorticogram. *Ann. Neurol.* 81, 664–676. doi: 10.1002/ana.24928

Wilson, D. J. (2019). Erratum: the harmonic mean p-value for combining dependent tests. *Proc Natl Acad Sci USA*. 116:21948. doi: 10.1073/pnas.1914128116

Worrell, G. A., Parish, L., Cranstoun, S. D., Jonas, R., Baltuch, G., and Litt, B. (2004). High-frequency oscillations and seizure generation in neocortical epilepsy. *Brain* 127, 1496–1506. doi: 10.1093/brain/awh149

Zijlmans, M., Jacobs, J., Zelmann, R., Dubeau, F., and Gotman, J. (2009). High-frequency oscillations mirror disease activity in patients with epilepsy. *Neurology* 72, 979–986. doi: 10.1212/01.wnl.0000344402.20334.81

Zijlmans, M., Jiruska, P., Zelmann, R., Leijten, F., Jefferys, J. G. R., and Gotman, J. (2012). High frequency oscillations as a new biomarker in epilepsy. *Ann. Neurol.* 71, 169–178. doi: 10.1002/ana.22548

**Conflict of Interest:** WS and SG have a licensing agreement with Natus Medical, Inc. Natus had no involvement in the study.

The remaining authors declare that the research was conducted in the absence of any commercial or financial relationships that could be construed as a potential conflict of interest.

*Copyright © 2021 Scott, Gliske, Kuhlmann and Stacey. This is an open-access article distributed under the terms of the Creative Commons Attribution License (CC BY). The use, distribution or reproduction in other forums is permitted, provided the original author(s) and the copyright owner(s) are credited and that the original publication in this journal is cited, in accordance with accepted academic practice. No use, distribution or reproduction is permitted which does not comply with these terms.*

frontiers in Neurology

ORIGINAL RESEARCH
published: 10 February 2021
doi: 10.3389/fneur.2021.612293

# Physiological Ripples Associated With Sleep Spindles Can Be Identified in Patients With Refractory Epilepsy Beyond Mesio-Temporal Structures

*Jonas C. Bruder[1]*, Christoph Schmelzeisen[1], Daniel Lachner-Piza[1], Peter Reinacher[2], Andreas Schulze-Bonhage[3] and Julia Jacobs[1,3]*

[1] Department of Neuropediatrics and Muscular Disease, University Medical Center, Freiburg, Germany, [2] Stereotactic & Functional Neurosurgery, University Medical Center, Freiburg, Germany, [3] Epilepsy Center, University Medical Center, Freiburg, Germany

OPEN ACCESS

**Edited by:**
Stefano Seri,
Aston University, United Kingdom

**Reviewed by:**
Lucia Rita Quitadamo,
Aston University, United Kingdom
Christos Papadelis,
Cook Children's Medical Center,
United States

***Correspondence:**
Jonas C. Bruder
jonas.bruder@uniklinik-freiburg.de

**Specialty section:**
This article was submitted to Epilepsy, a section of the journal Frontiers in Neurology

**Received:** 30 September 2020
**Accepted:** 11 January 2021
**Published:** 10 February 2021

**Citation:**
Bruder JC, Schmelzeisen C, Lachner-Piza D, Reinacher P, Schulze-Bonhage A and Jacobs J (2021) Physiological Ripples Associated With Sleep Spindles Can Be Identified in Patients With Refractory Epilepsy Beyond Mesio-Temporal Structures. Front. Neurol. 12:612293. doi: 10.3389/fneur.2021.612293

**Introduction:** High frequency oscillations (HFO) are promising biomarkers of epileptic tissue. While group analysis suggested a correlation between surgical removal of HFO generating tissue and seizure free outcome, HFO could not predict seizure outcome on an individual patient level. One possible explanation is the lack of differentiation between physiological and epileptic HFO. In the mesio-temporal lobe, a proportion of physiological ripples can be identified by their association with scalp sleep spindles. Spike associated ripples in contrast can be considered epileptic. This study investigated whether categorizing ripples by the co-occurrence with sleep spindles or spikes improves outcome prediction after surgery. Additionally, it aimed to investigate whether spindle-ripple association is limited to the mesio-temporal lobe structures or visible across the whole brain.

**Methods:** We retrospectively analyzed EEG of 31 patients with chronic intracranial EEG. Sleep spindles in scalp EEG and ripples and epileptic spikes in iEEG were automatically detected. Three ripple subtypes were obtained: SpindleR, Non-SpindleR, and SpikeR. Rate ratios between removed and non-removed brain areas were calculated. We compared the distinct ripple subtypes and their rates in different brain regions, inside and outside seizure onset areas and between patients with good and poor seizure outcome.

**Results:** SpindleR were found across all brain regions. SpikeR had significantly higher rates in the SOZ than in Non-SOZ channels. A significant positive correlation between removal of ripple-events and good outcome was found for the mixed ripple group ($r_s = 0.43$, $p = 0.017$) and for ripples not associated with spindles ($r_s = 0.40$, $p = 0.044$). Also, a significantly high proportion of spikes associated with ripples were removed in seizure free patients ($p = 0.036$).

**Discussion:** SpindleR are found in mesio-temporal and neocortical structures, indicating that ripple-spindle-coupling might have functional importance beyond

mesio-temporal structures. Overall, the proportion of SpindleR was low and separating spindle and spike associated ripples did not improve outcome prediction in our patient group. SpindleR analysis therefore can be a tool to identify physiological events but needs to be used in combination with other methods to have clinical relevance.

**Keywords: high frequency oscillations, ripples, sleep spindles, epileptic spikes, post-surgical outcome, refractory epilepsy**

## INTRODUCTION

Around 30% of patients continue to suffer from epileptic seizures after optimized medical treatment (1). Their best chance to achieve seizure freedom is epilepsy surgery offering success rates of up to 80% (2). Epilepsy surgery aims to resect all epileptic tissue including the seizure onset zone (SOZ), which is defined as the area of the cortex that generates seizures at a given point in time (3). In patients in whom non-invasive diagnostics cannot securely identify epileptic regions, intracranial video-EEG (iEEG) monitoring is considered the gold standard to localize the primary epileptic focus (4).

High frequency oscillations (HFO, ripples: 80–250 Hz, fast ripples: 250–500 Hz) are promising EEG markers of epileptic tissue (5–9). HFO rates were repeatedly shown to be higher in the SOZ (5, 6, 10, 11) and the resection of HFO-generating areas correlated with a good postsurgical outcome in several studies (9, 12, 13). These findings were confirmed by a meta-analysis of Höller et al. reviewing 11 HFO studies (14). Furthermore, HFO were considered superior to spikes in delineating the SOZ by some studies (6, 15). Nevertheless, the question whether epileptic spikes or HFO are more reliable biomarkers of epileptic tissue is still controversial. For instance, Roehri et al. found no benefits in using HFO instead of spikes for delineating the SOZ, especially on a single patient level. Furthermore, the analysis of HFO co-occurring with spikes could improve the delineation of epileptogenic areas (16–18).

Several retrospective analysis have shown that removing HFO-generating areas correlates well with favorable postsurgical outcome in group analyses (19). In the clinical context outcome prediction is only relevant if it can be performed prospectively and on a single-patient basis. Results show that HFO can correctly predict outcome in some but not all patients (12, 13, 20).

Several pitfalls have been identified when using HFO to delineate epileptic areas. One of the most commonly named challenges is the co-existence of physiological and epileptic HFO. As Engel and co-workers pointed out early on, a simple frequency analysis does not allow us to safely separate physiological HFO. Identification of physiological HFO in the human brain is complicated for two reasons. First of all, for ethical reasons all patients investigated with iEEG are suffering from epilepsy and might have widespread brain abnormalities. Identifying clearly healthy brain regions and certain physiological HFO is challenging but can be accomplished as has been recently demonstrated by Frauscher et al. (19). Their atlas of physiological HFO activity suggests that physiological HFOs are visible over most brain regions in agreement with other recent studies that could show physiological HFO activity originating not only from mesio-temporal regions but also from central and occipital regions (21, 22). Identifying HFO in clearly healthy brain tissue however does not help to overcome the second challenge, which is to separate physiological and epileptic HFO in regions of the SOZ and those with clear epileptic activity. In these regions either advanced analysis of HFO frequency and amplitude characteristics (23–25) or coupling analysis to co-occurring EEG phenomena has been successfully used (26, 27).

One approach for identifying physiological HFO that has been previously explored by our group is the analysis of spindle–ripple coupling (25). At this point, spindle-ripple association has been shown for physiological ripples in mesio-temporal structures (27–29). Clemens and co-workers stated that thalamo-cortical sleep spindles—functionally linked to periods of reduced sensory input—enable a secure timeframe for information transfer from the HC to the neocortex (30, 31). Ripples nested into single troughs of spindles are believed to enable a temporally synchronized memory-transfer from the HC to neocortical areas for long-term storage (30, 32, 33). The formation of spindle–ripple events is thought to be supported by neocortical slow oscillations (<1 Hz) which organize the occurrence of both thalamocortical spindles and hippocampal ripples (as illustrated in **Figure 1**). By analyzing the oscillatory features of a mixed group of ripple-range HFO, our group found that HFO associated with sleep spindles have different amplitude features than those with spikes and in the SOZ. Their lower amplitude could be used to separate mesio-temporal ripples from other ripples (25, 34).

It remains unclear, if spindle associated ripples also occur outside mesio-temporal structures and might support other cognitive functions. In the current paper we therefore aim to investigate ripple-spindle association across the brain including temporal neocortical, frontal, parietal, and occipital areas. We hypothesize that sleep spindle-ripple-links might support information transfer across brain regions for different functional purposes. Moreover, we investigate whether systematic separation of ripples associated with spindles and spikes can improve surgical seizure outcome prediction in our patient population.

## METHODS

### Patient Selection

One hundred and eight patients received chronic intracranial EEG (iEEG) at Freiburg Epilepsy Center between January 2012 and December 2017. The decision for implantation and the exact placement of the invasive electrodes was solely based on the clinical needs and results of a multidisciplinary surgical case

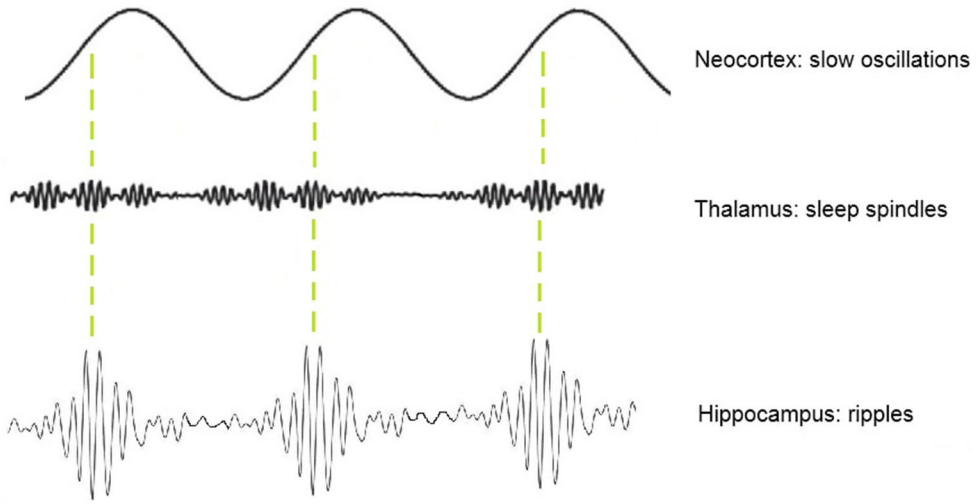


**FIGURE 1 |** Schematic illustration of thalamic sleep-spindles and hippocampal ripples nesting in the depolarizing up-states of neocortical slow oscillations.

conference. All EEG recordings were evaluated independently of this study by experienced neurophysiologists, who also determined the extent of the SOZ (3). HFO were not clinically used for delineating the epileptogenic area. The study was validated by the Ethics Committee of the Freiburg University Medical Center.

For this study, inclusion criteria were: at least one electrode in the mesio-temporal structures, simultaneous scalp EEG for sleep spindle detection and an EEG sampling rate of 2 kHz. For outcome prediction we also only included patients which underwent surgery after iEEG recording.

## Recording Methods

Intracranial depth electrodes with five to 18 contacts and a diameter of 0.8 mm made of Platinum/Iridium (Dixi Medical, Besancon, France) were implanted. Intracranial EEG was recorded with a digital video system called "Profusion EEG Software" (Compumedics Limited, Abbotsford Victoria, Australia) and sampled with a 2 kHz rate using a digital low-pass filtering with a cutoff frequency of 800 Hz. Ten- to twenty-system scalp EEG combined with electrooculogram and electromyogram was installed the second day after iEEG implantation. The different sleep stages were determined independently from this study by experienced EEG technologists according to the American association of sleep medicine (AASM) guidelines (35).

## EEG Segment Selection

As spikes and HFO occur more frequently in slow-wave-sleep (36) and sleep spindles are found predominantly in slow wave sleep stage N2 (37), we chose N2-EEG periods for all analyses. For each patient 30 min of EEG with at least 60 min distance to epileptic seizures were selected.

The EEG data was transformed into a binary format and high-pass-filtered using the "ASA" (ANT Neuro, Enschede, Netherlands) software via 2nd Butterworth filter with a cut-off-frequency of 0.5 Hz. All files were then converted into "edf"-format for automatic detection.

## Detection and Division of Ripple Subtypes

Automatic detection of ripples and spikes was performed on iEEG, while frontal and parietal sleep spindles were detected on the simultaneous scalp EEG. For both analysis previously published detectors were used (38, 39). These detectors are based on the multivariate classification of iEEG epochs using kernelized support-vector-machines. The features used for the multivariate classification described the amplitude, waveform and frequency characteristics of the iEEG epochs and were also based on the raw, filtered and wavelet-transformed signals. The description of the feature calculation and selection is described in the corresponding publications, as well as the procedures followed for the training, validation and testing of the detectors. We used a custom MATLAB 2018b script to determine ripples coinciding with spikes and sleep-spindles.

The first 5 min of each EEG segment were then visually examined to exclude any EEG artifacts i.e., background noise. Ripples were categorized into four subtypes: all ripples, ripples coincident with scalp sleep spindles (SpindleR), ripples not coincident with scalp spindles (Non-SpindleR) and ripples coincident with epileptic spikes in the same iEEG channels (SpikeR). Ripples coincident with both spindles and spikes were excluded as we were not able to categorize them as either epileptic or physiological.

## Clinical Data

Clinical information on lesion, epilepsy type, EEG, imaging results and postsurgical outcome were collected from the electronic patient record system. All patients had at least 12 months of postsurgical seizure follow-up.

All patients received MRI while the electrodes were in place as well as 3 months after epilepsy surgery. MRI with electrodes in place were used to locate channels and assign them to one brain region. Both MRI were co-registered using SPM software to visualize which contacts were located in the surgical cavity. This analysis allowed us to clearly decide whether a contact was located within or outside the surgical area. In <5% of the channels a clear allocation was not possible and these were excluded from analysis. Examples would be contacts directly located at the border of a resection or in brain areas that can be considered as functionally disconnected after the resection. All EEG-contacts were divided into surgically removed channels (RemCh) or channels remaining after surgical intervention (Non-RemCh).

## Statistical Analyses

**Figure 2** summarizes the methodological approach of this study.

## Descriptive Statistics

In our descriptive analysis we examined the rates of the ripple subtypes in mesio-temporal (amygdale, hippocampal, parahippocampal) and neocortical (frontal, parietal, temporal occipital) regions. The rate per minute of the different ripple subtypes for each channel (all Ripples, SpindleR, SpikeR and Non-SpindleR was calculated. Additionally, the rates in SOZ vs. Non-SOZ channels of each subtype were calculated.

## Correlation With Surgical Outcome

First, we performed a Wilcoxon rank sum test to compare rates of different event types in different brain regions and patient outcomes as listed below:

- mesio-temporal vs. neocortical channels
- SOZ vs. Non-SOZ-channels
- patients with a good post-surgical (Engel I) vs. a bad post-surgical outcome (II–IV).

Significance level was set at $\alpha = 0.05$.

To evaluate whether the proportion of removed events correlated with the surgical seizure outcome several ratios were calculated between removed and non-removed areas:

1. Ratios between rates of each ripple subtype (ev) in surgically removed channels (RemCh) vs. non-removed channels (Non-RemCh) were calculated for each ripple-subtype (all Ripples, SpindleR, SpikeR, Non-SpindleR), separately.

$$Ratio\ Rate\ (ev) = \frac{\sum_{RemCh} Rate\ (ev) - \sum_{NonRemCh} Rate(ev)}{\sum_{[RemCh,NonRemCh]} Rate(ev)}$$

   Following the methods of Jacobs et al. (12) a value close to +1 states that the majority of ripples has been removed, and therefore the patient should have a good postsurgical outcome. A value close to −1 states that the majority of ripples remained unchanged, so the postsurgical outcome should be poor. A value around zero indicates that the amount of removed ripples equates approximately the amount of non-removed ripples.

2. Patient-specific thresholds (high-rate ratios) according to the upper-fence-method of Akiyama et al. (40) were calculated to focus on areas with high HFO activity. The-upper-fence-method enabled us to identify channels with high rates of HFO. Ratios for these high-rate channels were calculated in the same way as the ratios for all channels.
3. We calculated if the removal of all SOZ channels (#ChannSOZRem) would result in a better postsurgical outcome than their non-removal (#ChannSOZNonRem).

$$RatioSOZ = \frac{\#ChannSOZRem - \#ChannSOZNonRem}{\#ChannSOZRem + \#ChannSOZNonRem}$$

This ratio increases as the proportion of removed to non-removed channels increases. A value close to +1 indicates, that the majority of ripples lay within the SOZ, so after resection patients with a high SOZ-Ratio should have a good postsurgical outcome, if the SOZ and the HFO-generating tissue overlapped. A value close to −1 states that the majority of ripples lay outside the SOZ, these patients should have a poor postsurgical outcome.

Spearman correlations were performed for all described ratios and the post-surgical outcome (Engel I-IV). The significance level of all analyses was set at $\alpha = 0.05$.

# RESULTS

Thirty one patients met the study inclusion criteria (see **Table 1** for clinical information). All patients showed ripples, spikes and sleep spindles in the automatic detections.

In total 2,291 iEEG channels were analyzed, 187 of these were located in mesio-temporal structures, 2,104 in the neocortex. Overall, 767,763 ripples were detected. Of these 82,717 (10.77%) were SpindleR (Spindle-coincident-ripple), 143,416 (18.68%) SpikeR (Spike Ripples), 572,953 (74.63%) Non-SpindleR (ripples outside spindles) and 511,743 (66.65%) Non-cR (ripples not coincident with spikes or spindles). Ripples coincident with spindles and spikes (29,887; 3.89%) were excluded from the analysis as it was unclear whether to classify them as physiological or epileptic.

In total, 457,995 (59.65%) ripples were found in the temporal neocortex (TNC), followed by the frontal neocortex (FNC: 128688 ripples; 16.76%), the occipital neocortex (ONC: 50,914 ripples; 6.63%), the hippocampus (HC: 46,397 ripples; 6.04%), the parietal neocortex (PNC: 38,642 ripples; 5.03%), the amygdala (A: 31,264 ripples; 4.07%) and the parahippocampal structures (PHC: 13,863 ripples; 1.81%).

## Ripple Distribution Across Brain Regions

**Table 2** shows all rates of the ripple subtypes in different brain regions (see **Table 2** in for detailed information), **Figure 3** additionally illustrates the distribution of SpindleR and SpikeR. **Figure 4** shows the percentage of SpindleR, SpikeR, and Non-CoincidentRipples of the sum of ripples in the specific brain regions, respectively.

Notably none of the ripple subtypes was exclusive to one brain region. Ripples associated with spindles were visible over all brain regions and not exclusively observed in the mesio-temporal structures.

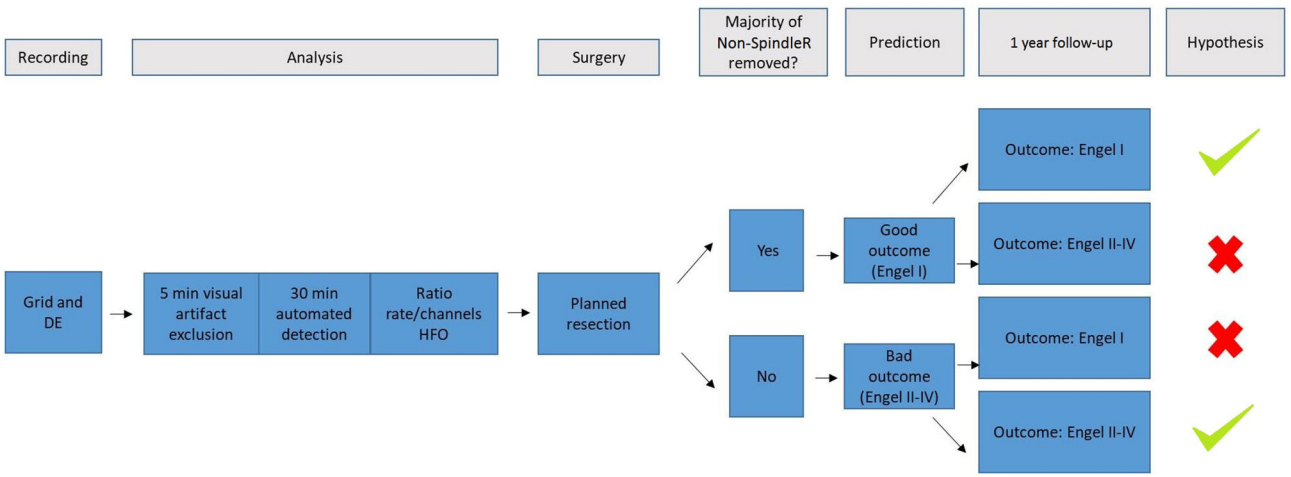


**FIGURE 2 |** It summarizes the methodological approach of this study. We used scalp and intracranial EEG (DE, depth electrodes) of the video-EEG-monitoring of patients with refractory epilepsy. The raw EEG data was then visually examined to exclude channels in white matter or with too many artefacts. Afterwards, sleep spindles were automatically detected in frontal/parietal scalp EEG contacts; ripples and spikes were automatically detected in intracranial EEG. Rate ratios (mirroring the extent of removal of HFO generating tissue) were calculated for All Ripples, ripples outside spindles (Non-SpindleR) and Spike-Ripples. All included patients received surgery and a 1 year-follow-up. We hypothesized, that the removal of brain tissue generating ripples outside spindles would lead to a good postsurgical outcome after 12 months, whereas the remaining of respective tissue would lead to a bad postsurgical outcome.

Mesio-temporal channels showed significantly higher rates in all four ripple subtypes than neocortical channels according to the Wilcoxon rank-sum tests ($p = 0.015$ in SpindleR, $p < 0.001$ in all Ripples, Non-SpindleR and SpikeR) (see **Figure 5**). All four ripple subtypes showed higher rates in the SOZ channels than in Non-SOZ-channels ($p = 0.039$ in SpindleR, $p < 0.001$ in all Ripples, Non-SpindleR, and SpikeR (see **Figure 6**).

The average SOZ ratio over the entire cohort was $0.60 \pm 0.43$. Patients, in which SOZ channels were removed, showed a significantly better outcome than patients with remaining SOZ channels (Wilcoxon rank sum test: $p = 0.024$) (see **Figure 7**).

The Spearman correlation concerning the SOZ channel ratio showed a significant correlation between removal of SOZ channels and good outcome: $r_s = 0.350$, $p = 0.030$.

## Correlation Between Surgical Outcome and Removal of HFO Subtypes

The following average rate ratios were obtained for the different ripple subtypes over the entire cohort: All ripples: $-0.29 \pm 0.33$; Non-SpindleR: $-0.29 \pm 0.33$; SpikeR: $-0.07 \pm 0.46$.

Considering all channels, significantly higher ratios for spike-ripple removal were seen in patients with seizure free vs. poor outcome ($p = 0.04$). No significant differences were seen for the other ripple subtypes (see **Figure 8**).

Considering only channels with high rates of HFO as determined by the upper fence method, a significantly higher proportion of ripples were removed in seizure free patients compared to those with poor outcome. This significant difference was comparable for all ripples ($p = 0.02$), Non-SpindleR ($p = 0.03$) and SpikeR ($p = 0.04$) (see **Figure 9**).

The Spearman correlations between the removal of the different ripple events and a good post-surgical outcome did not show significant correlations when all channels were analyzed: All ripples ($r_s$ = Spearman's rank correlation coefficient = 0.22, $p = 0.24$), Non-SpindleR ($r_s = 0.16$, $p = 0.39$), Spike-ripples ($r_s = 0.33$, $p = 0.07$), ripples not coincident with other events ($r_s = 0.17$, $p = 0.36$), and SpindleR ($r_s = 0.21$, $p = 0.25$).

When only considering high rate channels, the Spearman correlations showed significant correlations between removal of ripple events in high rate ripple channels and seizure free outcome. This was strongest for all ripples ($r_s = 0.43$, $p = 0.02$) and Non-SpindleR ($r_s = 0.40$, $p = 0.03$), but borderline significant for SpikeR ($r_s = 0.35$, $p = 0.05$).

# DISCUSSION

The present study demonstrates that ripples are associated with sleep spindles not only in the mesio-temporal regions but across the brain. Overall, this ripple subtype is rather infrequent and probably only represents a small subpopulation of physiological ripples. As previously described, we could show a correlation between the removal of ripple generating tissue and seizure free outcome. Without restricting the data to areas with frequent ripples, this analysis was only significant for ripples associated with spikes as has been suggested by Roehri et al. (16). Thresholding the data for areas with high ripple rates was highly effective in our population in increasing the correlation between outcome and ripple removal, as has been described previously (40). This correlation was independent of whether we looked at the mixed event group or subpopulations of ripples. Therefore, the separation of spindle associated ripples did not lead to the hypothesized improvement of outcome correlation.

**TABLE 1 |** Summary of clinical and demographic data.

| Pat.Nr. | Age at OP | Gender | Type of Seizure | MRI | Type of surgery |
|---|---|---|---|---|---|
| 1 | 49 | M | FAS | no lesion | R sAHC |
| 2 | 23 | F | FAS, FIAS, FBTCS | R HS | R T-pole resection, AHC |
| 3 | 34 | F | FAS, FIAS, FBTCS | NF1, ganglioglioma WHO°I | L F pall lesionectomy |
| 4 | 44 | F | FAS, FIAS, FBTCS | Bil T P MEC | L T-pole resection |
| 5 | 46 | M | FIAS, FBTCS | FCC | R Ant T-pole resection, AHC |
| 6 | 39 | M | FAS, FIAS, FBTCS | R FCD tmp, L T NC lesion | R F lesionectomy |
| 7 | 60 | F | FAS, FIAS, FBTCS | Bil T P MEC, L T P lesion | L T-pole resection, sphen Enceph resection |
| 8 | 49 | M | FAS, FIAS, FBTCS | R O bas FCD | R O T resection |
| 9 | 51 | F | FAS, FIAS, FBTCS | R HS, T A FCD | R Ant T-pole resection, AHC |
| 10 | 40 | F | FAS, FIAS, FBTCS | R HS | R T-pole resection, AHC |
| 11 | 18 | F | FAS, FIAS | L T FCD, HS | L T-pole part resection, AHC |
| 12 | 25 | M | FAS, FIAS, FBTCS | L T M lesion, possible FCD | L lesionectomy, HC |
| 13 | 12 | M | FAS, FIAS | R T possible FCD | R T-pole resection, AHC |
| 14 | 56 | F | FAS, FIAS | R A GC lesion, possible FCD | R Ant lesionectomy GC |
| 15 | 12 | M | FAS, FIAS | tuber sclerosis, NCN | R pall T-pole resection, AHC |
| 16 | 34 | F | FAS, FIAS, FBTCS | R sphen MEC | R T-pole resection, AHC |
| 17 | 17 | M | FAS, FIAS, FBTCS | R T Pol AC, F B lesions | R F resection, T-pole |
| 18 | 24 | F | FAS, FIAS, FBTCS | no lesion | L sAHC |
| 19 | 52 | F | FAS, FIAS, FBTCS | possible postembolic lesions infratent | L T-pole part resection, AHC |
| 20 | 29 | M | FAS, FIAS, FBTCS | Bil T-pol sphen MEC, L possible FCD | L T-pole resection |
| 21 | 31 | F | FAS, FIAS | Bil HS | R T-pole resection, AHC |
| 22 | 55 | M | FAS, FIAS, FBTCS | L T-pol possible FCD | L T-pole part resection |
| 23 | 27 | M | FAS, FBTCS | R possible TAE | R GTS resection |
| 24 | 55 | M | FIAS, FBTCS | L T P MEC, thal infarct 2008 | L T-pole resection |
| 25 | 22 | M | FAS | R HS | R sAHC |
| 26 | 28 | F | FAS, FIAS | L FCC, Bil white matter lesions | L T-pole resection, AHC |
| 27 | 33 | F | FAS, FIAS, FBTCS | no lesion | R T-pole part resection |
| 28 | 53 | M | FAS, FIAS, FBTCS | R T-pol possible FCD | R T-pole part resection, AHC |
| 29 | 38 | M | FAS, FIAS | Bil HS | L pall sAHC |
| 30 | 22 | F | FAS, FIAS, FBTCS | PCA WHO°I | R T resection, AHC |
| 31 | 13 | M | FAS, FIAS | no lesion | R T-pole resection, AHC |

*AC, arachnoidal cyst; AHC, amygdalohippocampectomy; Ant, anterior; B, basal; Bil, bilateral; Enceph, encephalon; F, frontal; FAS, focal aware seizure; FBTCS, focal to bilateral tonic-clonic seizure; FCC, Fissura choroidea cyst; FCD, focal cortical dysplasia; FIAS, focal impaired awareness seizure; GC, gyrus cinguli; GTS, gyrus temporalis superior; HS, hippocampal sclerosis; infratent, infratentorial; L, left; M, mesial; MEC, meningoencephaloceles; NF1, neurofibromatosis 1; NC, Neocortex; NCN, nevus cell nevi; O, occipital; PCA, pylocytic astrocytoma; pol, polar; R, right; sAHC, selective AHC; sphen, sphenoidal; T, temporal; TAE, teleangieectasia; thal, thalamus; tmp, temporomesiopolar.*

## Occurrence of SpindleR in Different Brain Regions

The first goal of this study was to examine whether spindle associated ripples could be found outside of mesio-temporal structures, as SpindleR have thus far only been reported from mesio-temporal sites (25, 30, 31, 41). Our results suggest that SpindleR can be found across all brain regions. In a second step the anatomic distribution of SpindleR, Non-SpindleR, and SpikeR was assessed.

While it is well-known that the correlation between sleep spindles and ripples in MTL structures is part of the process that allows information transfer from mesio-temporal to neocortical structures (30–32), it remains unclear whether there is a functional spindle-ripple-coupling in neocortical areas. Possibly, neocortical SpindleR fulfill a similar task of information-transfer over wide distances in the brain. However, there is evidence that slow waves, sleep spindles and ripples are functionally connected (42–44). Ellenrieder et al. found a connection of slow waves with mesio-temporal ripples but also with neocortical ripples outside the SOZ (45). Another study showed that neocortical physiological HFO tend to occur with 0.5–1 Hz slow waves, whereas epileptic HFO tend to occur with another type of slow-waves with frequencies between 3 and 4 Hz (22). According to these results it is likely that physiological neocortical ripples may also occur during sleep spindles.

Overall, the proportion of ripples associated with sleep spindles is low. This is the case for contacts inside and outside the SOZ, as well as for contacts with and without epileptic spikes. It is therefore very likely that SpindleR only represent a subtype of physiological ripples expressed in the brain. At this point no study has investigated a correlation between function and SpindleR. It remains therefore an open task to

**TABLE 2 |** Average ripple rate/minute + SD (standard deviation) for All Ripple, SpikeR, SpindleR, and Non-SpindleR.

| Ø Ripple Rate/min | All Ripple (R) | SpikeR | SpindleR | R outside Spindles |
|---|---|---|---|---|
| A | 4.14 ± 2.67 | 1.95 ± 3.44 | 1.20 ± 1.00 | 9.26 ± 7.49 |
| HC | 4.27 ± 2.76 | 2.07 ± 3.53 | 1.19 ± 1.00 | 9.53 ± 7.71 |
| PHC | 4.11 ± 2.73 | 1.97 ± 3.42 | 1.12 ± 0.85 | 9.25 ± 7.48 |
| TNC | 4.28 ± 2.78 | 2.09 ± 3.59 | 1.20 ± 1.00 | 9.54 ± 7.75 |
| FNC | 4.15 ± 2.69 | 1.96 ± 3.43 | 1.19 ± 1.00 | 9.31 ± 7.51 |
| PNC | 3.83 ± 2.60 | 1.83 ± 3.24 | 1.09 ± 0.82 | 8.57 ± 7.13 |
| ONC | 4,32 ± 2,81 | 2.13 ± 3.63 | 1.21 ± 1.01 | 9.63 ± 7.83 |

*A, Amygdala; HC, Hippocampus; PHC, Parahippocampus; TNC, Temporal Neocortex; FNC, Frontal Neocortex; PNC, Parietal Neocortex; ONC, Occipital Neocortex.*

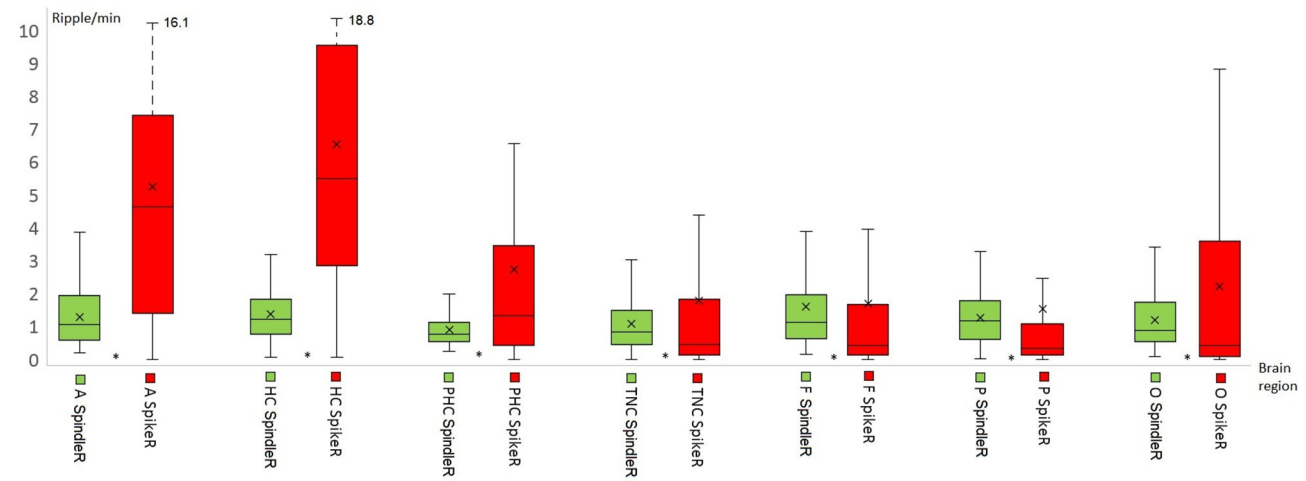


**FIGURE 3 |** Distribution of Spindle-Ripple (SpindleR) and Spike-Ripple (SpikeR) in different brain areas. SpindleR and SpikeR were more frequent in mesio-temporal structures than in neocortical structures. Mesio-temporal lobe: A, amygdala; HC, hippocampus; PHC, parahippocampal; Neocortex: TNC, temporal neocortex; F, frontal neocortex; P, parietal neocortex; O, occipital neocortex.

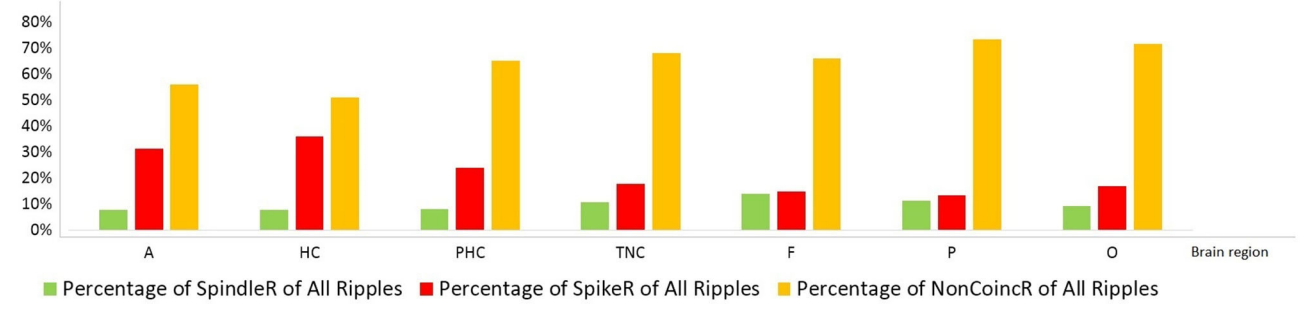


**FIGURE 4 |** Percentage distribution of the three different ripple subtypes in mesio-temporal and neocortical channels. The amount of SpikeR was higher in mesio-temporal structures compared to the amount of SpindleR, whereas the amount of SpikeR and SpindleR was more alike in the neocortex. Mesio-temporal lobe: A, amygdala; HC, hippocampus; PHC, parahippocampal; Neocortex: TNC, temporal neocortex; F, frontal neocortex; P, parietal neocortex; O, occipital neocortex.

correlate specific functions like memory performance with the proportion of SpindleR expressed over a certain brain region. It will also have to be assessed whether SpindleR are somehow linked to other physiological ripples such as those coupled with slow waves. In the present study a very small percentage of ripples co-occurred with spikes and sleep spindles at the same time. This phenomenon is hard to explain but might be an indicator that physiological ripples occur in epileptic regions and might be visible at the same time as epileptic spikes. This is in line with the observation that SpindleR clearly occur over

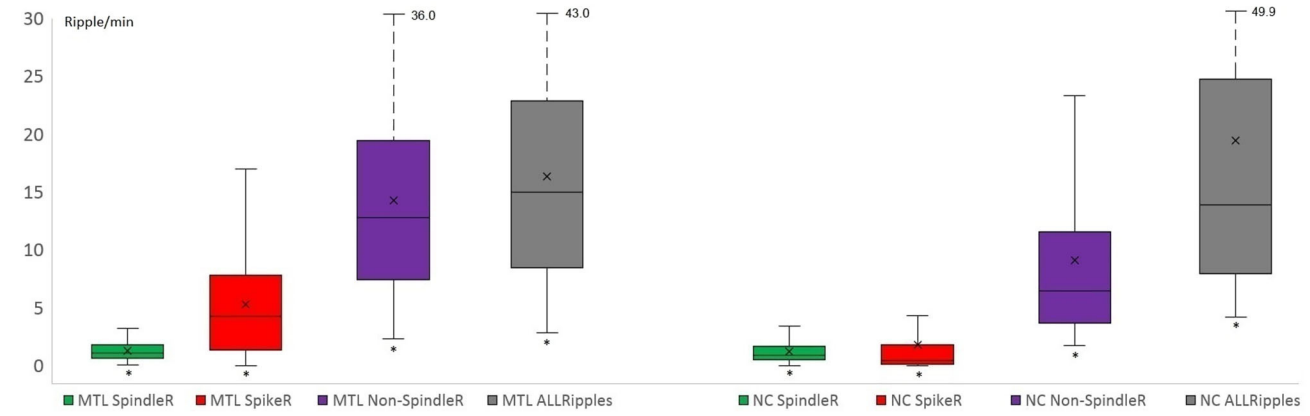


**FIGURE 5 |** Rates of four different ripple subtypes in mesio-temporal and neocortical channels. Mesio-temporal (MTL) channels showed significantly higher rates of all four ripple subtypes than neocortical (NC) channels. The share of likely pathological ripples [Spike-ripple (SpikeR) and ripples outside spindles (Non-SpindleR)] was significantly higher in the mesio-temporal contacts. SpindleR, Spindle-Ripples.

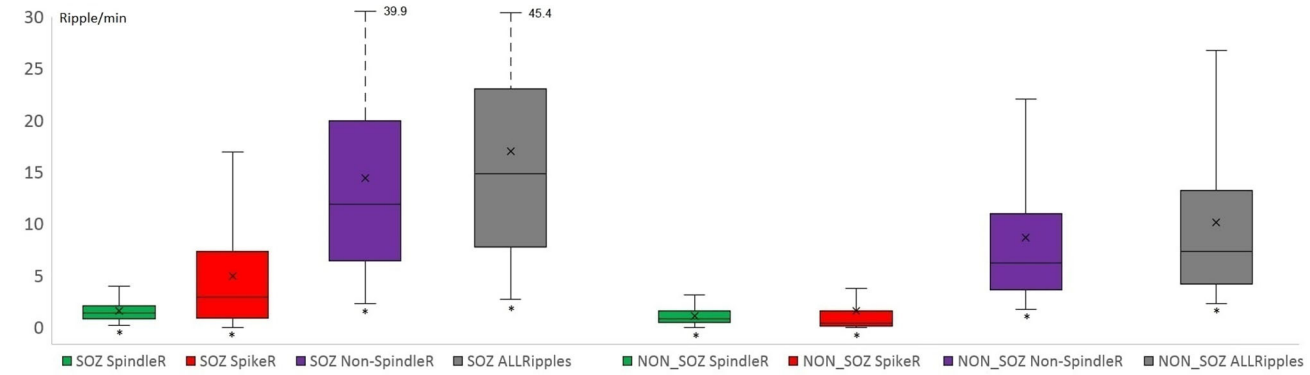


**FIGURE 6 |** Rates of different ripple subtypes in SOZ and Non-SOZ channels. All Ripple subtype rates were significantly higher in SOZ (=seizure onset zone) channels than in Non-SOZ channels. (SpindleR, Spindle-ripples; SpikeR, spike-ripples; Non-SpindleR, ripples outside spindles).

SOZ areas again suggesting that regions generating physiological and epileptic activity have substantial overlap. This has been suggested by other studies (20), which could not show that high rates of epileptic spikes and HFO necessarily correlate with poor cognitive function.

## Ripple Subtypes in the SOZ

The results of this study showed that all ripple types are most frequent in mesio-temporal regions as described before (6, 45). Moreover, our results are similar to many previous studies in regard to ripple rates being significantly higher inside than outside the SOZ (7, 13, 46–50). As expected, SpikeR and Non-SpindleR showed significantly higher rates in the SOZ. Consistent with recent findings, SpikeR were especially more frequent in SOZ channels than in channels outside the SOZ (51). A previous study from our group suggested that physiological ripples occur and can carry function in SOZ areas (52). It might explain why in this study SpindleR were seen slightly more frequently in the SOZ. This underlines the fact that function can take place in brain areas capable of generating seizures. Moreover, it demonstrates the complexity of separating physiological from epileptic HFO. A pure separation by looking at healthy vs. epileptic brain tissue might fall short of describing the actual coexistence of both event types within the same brain region.

## Correlation Between Surgical Removal of Ripple Generating Areas and the Postoperative Seizure Outcome

It was one important goal of this study to see whether the identification of SpindleR as one group of physiological ripples would improve specificity of HFO as a biomarker for epileptic tissue and therefore improve the prediction of postsurgical seizure outcome. This hypothesis was based on several studies suggesting sleep spindle associated ripples being most probable physiological HFO models (25, 30, 31, 34, 41). The results in this study fail to show clear improvement of outcome correlation when only analyzing those HFO that are not linked to sleep spindles.

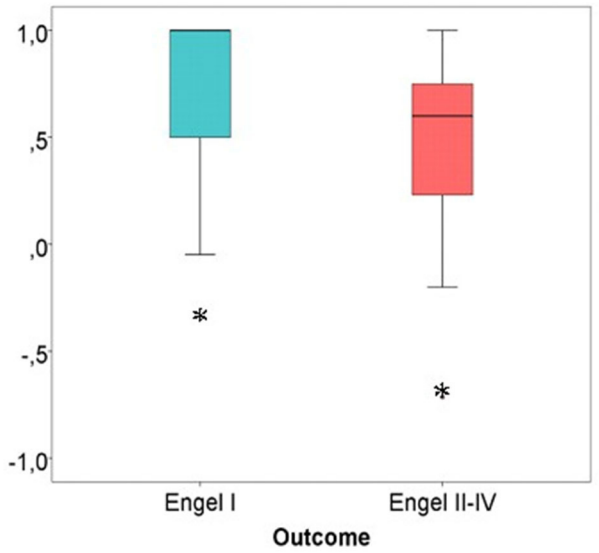


**FIGURE 7 |** SOZ channel ratio in good vs. bad post-surgical outcome. Patients with the majority of SOZ-channels successfully removed showed a significantly better outcome in comparison to patients with SOZ-channels still in place after resection. Significant difference to the correspondent boxplot (same colour).

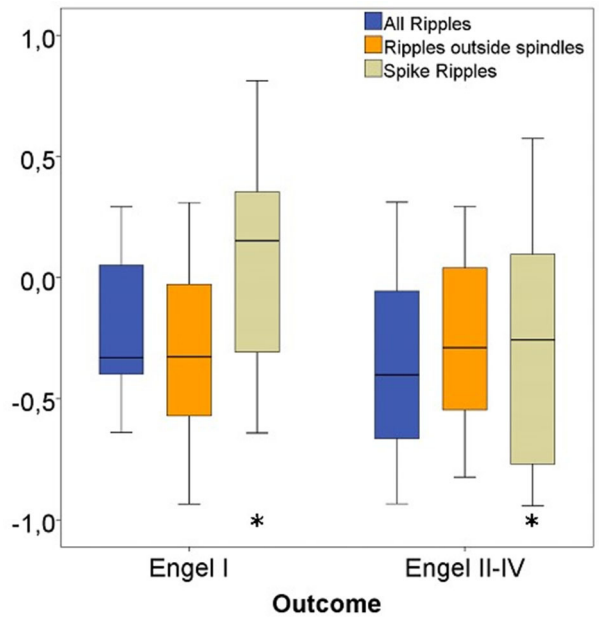


**FIGURE 8 |** Rate ratios of three ripple subgroups with good vs. bad outcome. The ratio of removed Spike-Ripples were significantly higher in patients with a good (Engel I) compared to patients with a bad postsurgical outcome (Engel II-IV). No significant differences in ratios for Ripples outside spindles and All Ripples between both patient groups were seen. Significant difference to the correspondent boxplot (same colour).

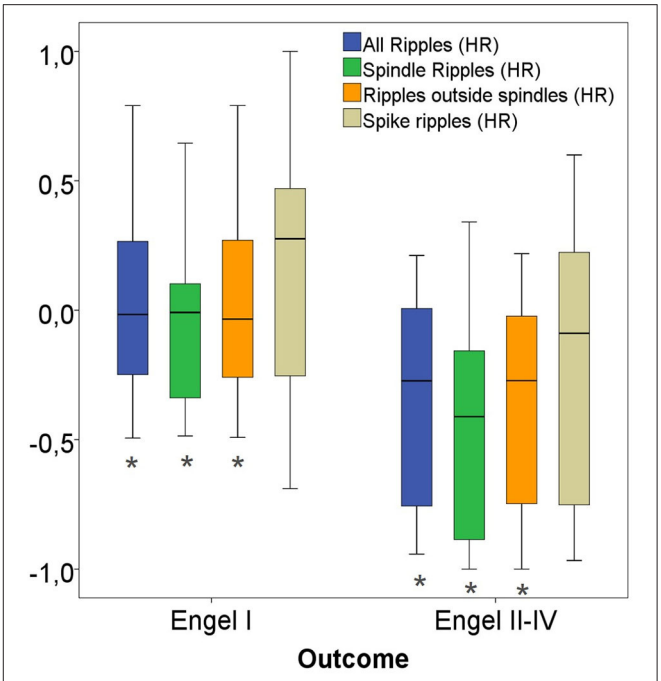


**FIGURE 9 |** High-rate (HR) ratios of four ripple subgroups with good vs. bad outcome. Significant difference to the correspondent boxplot (same colour).

As expected, the correlation between HFO removal and surgical outcome was strongest when focusing on spike associated ripples (16, 51). Moreover, results improved when applying a thresholding technique that allows only considering areas with high rates of HFO (20, 40). The categorization of SpindleR therefore does not allow to sufficiently separate physiological and epileptic ripples in all those events that are not coupled to an epileptic spike. The most likely explanation for this observation is that various types of physiological HFO exist and that their characteristics and coupling to other physiological rhythms largely varies as does their function and location.

To actually improve the outcome correlation, it might therefore be essential to combine several techniques to classify ripples as physiological or epileptic. Previous studies suggested that the timing in which ripples are coupled to slow waves is one way to identify physiological ripples (45). Another way might be to analyze several sleep stages as only epileptic ripples are suppressed during phasic REM sleep. Liu and coworkers additionally suggest that epileptic ripples have more stereotypic characteristics than physiological ones (53). The technique presented in this study can identify ripples associated with spikes and sleep spindles in a fully automated way. If these analyses can be combined with other techniques, separation of more physiological ripples might be possible. Independent of this, further research will have to aim at providing a better understanding of influences such as brain region, structural brain abnormalities and epilepsy duration on the occurrence and shape of physiological HFO. The virtual brain atlas project initiated by Frauscher and co-workers is one step in this direction (19).

## Methodological Considerations

There are several limitations of this study, which might have contributed to the above-discussed findings.

First, we only included patients which had electrodes implanted in the mesio-temporal structures as it was unclear at the beginning of this project whether spindle-ripple-association existed outside the mesio-temporal region. This was not limited to patients with temporal lobe SOZ but results in more patients with temporal lobe epilepsy than others. The predominance of contacts in the mesio-temporal structures might have increased the overall number of ripples detected in this study as HFO in general have highest rates in these structures. It is however unlikely that this selection influenced the correlation analysis between ripple removal and outcome, as predominance of ripples in SOZ and surgical areas was visible independent of the location of the SOZ and resection. Additionally, like many previous studies (14) this study had a retrospective design and did not aim to predict surgical outcome prospectively. This design does not provide strong information for translation into clinical use and if a future method of ripple classification should be more successful it would be mandatory to test this method prospectively.

Our study shows that distinct ripple subtypes can be separated by analyzing co-occurrence with spikes and spindles. The analysis was focused on analyzing subtypes of events in each channel, separately analyzing interactions between neighboring or distant channels. At this point it remains unclear whether these subtypes also show distinct network characteristics. While HFO were considered very focal events in the past, most recent research suggests that they might show propagation similarly to the well-described propagation of epileptic spikes. Recent studies have differentiated ripple-subtypes according to their role as "onset-ripples" and "spread-ripples," suggesting that removing ripples that initiated the propagation (onset-ripples) were associated with a good outcome, whereas removing areas where ripple spread were not (54, 55). Network characteristics and propagation phenomenon of HFO have also been discussed as a result of studies using intraoperative EEG prior and after surgery to analyze HFO. These studies suggest that HFO have network interactions. More specifically HFO visible in the postsurgical EEG might be different in locations from those in the pre-surgical EEG and more relevant for the surgical outcome prediction (50). At this point it is unclear whether HFO networks and propagation is limited to specific anatomical structures and whether network characteristic of HFO are distinct for epileptic and physiological events. Using spindle-ripple analysis could shed future light into this question.

In the present study we focussed on the analysis of scalp sleep spindles using an automated detector that has been modified to application in patients with epilepsy (38, 39). This is important as automated detection tools developed in healthy subjects might not work reliably to detect spindles in scalp EEG that are recorded simultaneous to intracranial EEG in patients with chronic epilepsy. It is well-known that epilepsy influences sleep phenomena and can alter sleep spindle characteristics (56). Epilepsy might reduce the occurrence of sleep spindles. This has been described to be most prominent in times of frequent seizures (57), generalized epilepsies (56), and in those patients with large cortical malformations (58). It can therefore not be excluded that the analyzed patients had reduced sleep spindle occurrence compared to healthy subjects. Most patients however had very focal or no structural abnormalities and we selected EEG periods with the longest time interval away from seizures that could be selected. The fact that we could find sleep spindles and SpindleR in all our patients therefore suggests that SpindleR analysis is possible in patients with chronic refractory focal epilepsy.

## CONCLUSION AND OUTLOOK

The observation that SpindleR occur in brain regions beyond the mesio-temporal areas will be relevant when it comes to understanding functional importance of ripple oscillations as well as using HFO as biomarkers in patients with epilepsy. Extending the questions of this study, spindle-ripple analysis might be useful to identify functionally active brain regions during the pre-surgical diagnostics. A possible correlation of mesio-temporal HFO and memory performance has been examined before (52). An approach for future studies might therefore be the assessment of various cognitive functions and the occurrence of SpindleR.

It has been shown that HFO analysis is not limited to intracranial EEG and that HFO can also be seen in scalp recordings. The identified scalp HFO have a clear intracranial correlate as could be shown in simultaneous scalp-intracranial (59, 60) and EEG-MEG recordings (18). Data suggests that both physiological and epileptic HFO can be seen in scalp EEG (61). Papadelis et al. could show that HFO localization was comparable between invasive and non-invasive methods (62). While scalp HFO clearly co-occur with spikes it is unclear whether there is also a possible temporal coupling with sleep spindles. In the present study no scalp HFO analysis was performed as this is difficult to achieve with automated methods. Moreover, our recordings were too long for visual scalp HFO analysis. Future studies however could focus on scalp HFO spindle correlation and on better understanding which intracranial HFO are visible on the scalp.

Overall, SpindleR are most likely one type of physiological ripple activity generated by the brain. As has been hypothesized, spindle-ripple coupling most likely serves information transfer between brain lobes. Evidence in this study suggests that the value of SpindleR alone to identify physiological ripples on pre-surgical diagnostics is limited. A combination of different methodological approaches including the identification of SpindleR to differentiate between epileptic and physiological HFO is therefore more promising.

## DATA AVAILABILITY STATEMENT

The raw data supporting the conclusions of this article will be made available by the authors, without undue reservation.

## ETHICS STATEMENT

The studies involving human participants were reviewed and approved by Ethik-Kommission der Albert-Ludwigs-Universität Freiburg. Written informed consent to participate in this study

was provided by the participants' legal guardian/next of kin. Written informed consent was obtained from the individual(s), and minor(s)' legal guardian/next of kin, for the publication of any potentially identifiable images or data included in this article.

## AUTHOR CONTRIBUTIONS

JJ and JB have contributed to the conception and design of the study. CS, JB, and DL-P have contributed to the acquisition and analysis of data. JB, CS, and JJ have drafted significant portions of the manuscript and figures. AS-B provided all clinical data and EEG data. PR performed the epilepsy surgeries. All authors contributed to the article and approved the submitted version.

## FUNDING

JB and JJ were supported by grant JA 1725/4-1 of the German Research Foundation.

## REFERENCES


1. Kwan P, Brodie MJ. Early identification of refractory epilepsy. *N Engl J Med.* (2000) 342:314–9. doi: 10.1056/NEJM200002033420503
2. Schmeiser B, Wagner K, Schulze-Bonhage A, Mader I, Wendling A-S, Steinhoff BJ, et al. Surgical treatment of mesiotemporal lobe epilepsy: which approach is favorable? *Neurosurgery*. (2017) 81:992–1004. doi: 10.1093/neuros/nyx138
3. Rosenow F, Lüders H. Presurgical evaluation of epilepsy. *Brain.* (2001) 124:1683–700. doi: 10.1093/brain/124.9.1683
4. Blount JP, Cormier J, Kim H, Kankirawatana P, Riley KO, Knowlton RC. Advances in intracranial monitoring. *Neurosurg Focus.* (2008) 25:E18. doi: 10.3171/FOC/2008/25/9/E18
5. Jacobs J, LeVan P, Châtillon C-É, Olivier A, Dubeau F, Gotman J. High frequency oscillations in intracranial EEGs mark epileptogenicity rather than lesion type. *Brain.* (2009) 132:1022–37. doi: 10.1093/brain/awn351
6. Jacobs J, LeVan P, Chander R, Hall J, Dubeau F, Gotman J. Interictal high-frequency oscillations (80–500 Hz) are an indicator of seizure onset areas independent of spikes in the human epileptic brain. *Epilepsia.* (2008) 49:1893–907. doi: 10.1111/j.1528-1167.2008.01656.x
7. Bragin A, Engel J, Staba RJ. High-frequency oscillations in epileptic brain. *Curr Opin Neurol.* (2010) 23:151–6. doi: 10.1097/WCO.0b013e3283373ac8
8. Akiyama T, McCoy B, Go CY, Ochi A, Elliott IM, Akiyama M, et al. Focal resection of fast ripples on extraoperative intracranial EEG improves seizure outcome in pediatric epilepsy. *Epilepsia*. (2011). 52:1802–11. doi: 10.1111/j.1528-1167.2011.03199.x
9. Wu JY, Sankar R, Lerner JT, Matsumoto JH, Vinters HV, Mathern GW. Removing interictal fast ripples on electrocorticography linked with seizure freedom in children. *Neurology.* (2010) 75:1686–94. doi: 10.1212/WNL.0b013e3181fc27d0
10. Brázdil M, Halámek J, Jurák P, Daniel P, Kuba R, Chrastina J, et al. Interictal high-frequency oscillations indicate seizure onset zone in patients with focal cortical dysplasia. *Epilepsy Res.* (2010). 90:28–32. doi: 10.1016/j.eplepsyres.2010.03.003
11. Andrade-Valença L, Mari F, Jacobs J, Zijlmans M, Olivier A, Gotman J, et al. Interictal high frequency oscillations (HFOs) in patients with focal epilepsy normal MRI. *Clin Neurophysiol.* (2012) 123:100–5. doi: 10.1016/j.clinph.2011.06.004
12. Jacobs J, Zijlmans M, Zelmann R, Chatillon C-É, Hall J, Olivier A, et al. High-frequency electroencephalographic oscillations correlate with outcome of epilepsy surgery. *Ann Neurol.* (2010) 67:209–20. doi: 10.1002/ana.21847
13. Haegelen C, Perucca P, Châtillon C-E, Andrade-Valença L, Zelmann R, Jacobs J, et al. High-frequency oscillations, extent of surgical resection, and surgical outcome in drug-resistant focal epilepsy. *Epilepsia*. (2013) 54:848–57. doi: 10.1111/epi.12075
14. Höller Y, Kutil R, Klaffenböck L, Thomschewski A, Höller PM, Bathke AC, et al. High-frequency oscillations in epilepsy and surgical outcome. A meta-analysis. *Front Hum Neurosci.* (2015) 9:574. doi: 10.3389/fnhum.2015.00574
15. Jacobs J, Kobayashi K, Gotman J. High-frequency changes during interictal spikes detected by time-frequency analysis. *Clin Neurophysiol.* (2011) 122:32–42. doi: 10.1016/j.clinph.2010.05.033
16. Roehri N, Pizzo F, Lagarde S, Lambert I, Nica A, McGonigal A, et al. High-frequency oscillations are NOT better biomarkers of epileptogenic tissues than spikes. *Ann Neurol.* (2018) 83:84–97. doi: 10.1002/ana.25124
17. Roehri N, Bartolomei F. Are high-frequency oscillations better biomarkers of the epileptogenic zone than spikes? *Curr Opin Neurol.* (2019) 32:213–9. doi: 10.1097/WCO.0000000000000663
18. Tamilia E, Dirodi M, Alhilani M, Grant PE, Madsen JR, Stufflebeam SM, et al. Scalp ripples as prognostic biomarkers of epileptogenicity in pediatric surgery. *Ann Clin Transl Neurol.* (2020) 7:329–42. doi: 10.1002/acn3.50994
19. Frauscher B, von Ellenrieder N, Zelmann R, Rogers C, Nguyen DK, Kahane P, et al. High-frequency oscillations in the normal human brain. *Ann Neurol.* (2018) 84:374–85. doi: 10.1002/ana.25304
20. Jacobs J, Wu JY, Perucca P, Zelmann R, Mader M, Dubeau F, et al. Removing high-frequency oscillations: a prospective multicenter study on seizure outcome. *Neurology*. (2018) 91:e1040–52. doi: 10.1212/WNL.0000000000006158
21. Nagasawa T, Juhász C, Rothermel R, Hoechstetter K, Sood S, Asano E. Spontaneous and visually driven high-frequency oscillations in the occipital cortex: intracranial recording in epileptic patients. *Hum Brain Mapp.* (2012) 33:569–83. doi: 10.1002/hbm.21233
22. Nonoda Y, Miyakoshi M, Ojeda A, Makeig S, Juhász C, Sood S, et al. Interictal high-frequency oscillations generated by seizure onset and eloquent areas may be differentially coupled with different slow waves. *Clin Neurophysiol.* (2016) 127:2489–99. doi: 10.1016/j.clinph.2016.03.022
23. Pearce A, Wulsin D, Blanco JA, Krieger A, Litt B, Stacey WC. Temporal changes of neocortical high-frequency oscillations in epilepsy. *J Neurophysiol.* (2013) 110:1167–79. doi: 10.1152/jn.01009.2012
24. Blanco JA, Stead M, Krieger A, Stacey W, Maus D, Marsh E, et al. Data mining neocortical high-frequency oscillations in epilepsy and controls. *Brain.* (2011) 134:2948–59. doi: 10.1093/brain/awr212
25. Bruder JC, Dümpelmann M, Piza DL, Mader M, Schulze-Bonhage A, Jacobs-Le Van J. Physiological ripples associated with sleep spindles differ in waveform morphology from epileptic ripples. *Int J Neural Syst.* (2017) 27:1750011. doi: 10.1142/S0129065717500113
26. Frauscher B, von Ellenrieder N, Ferrari-Marinho T, Avoli M, Dubeau F, Gotman J. Facilitation of epileptic activity during sleep is mediated by high amplitude slow waves. *Brain J Neurol.* (2015) 138(Pt. 6):1629–41. doi: 10.1093/brain/awv073
27. Buzsáki G. Two-stage model of memory trace formation: a role for "noisy" brain states. *Neuroscience.* (1989) 31:551–70. doi: 10.1016/0306-4522(89)90423-5
28. Buzsáki G. The hippocampo-neocortical dialogue. *Cereb Cortex.* (1996) 6:81–92. doi: 10.1093/cercor/6.2.81
29. Diekelmann S, Born J. The memory function of sleep. *Nat Rev Neurosci.* (2010) 11:114–26. doi: 10.1038/nrn2762
30. Clemens Z, Mölle M, Eross L, Jakus R, Rásonyi G, Halász P, et al. Fine-et altuned coupling between human parahippocampal ripples and sleep spindles. *Eur J Neurosci.* (2011) 33:511–20. doi: 10.1111/j.1460-9568.2010.07505.x
31. Clemens Z, Mölle M, Eross L, Barsi P, Halász P, Born J. Temporal coupling of parahippocampal ripples, sleep spindles and slow oscillations in humans. *Brain J Neurol.* (2007) 130(Pt. 11):2868–78. doi: 10.1093/brain/awm146
32. Siapas AG, Wilson MA. Coordinated interactions between hippocampal ripples and cortical spindles during slow-wave sleep. *Neuron.* (1998) 21:1123–8. doi: 10.1016/S0896-6273(00)80629-7
33. Sirota A, Csicsvari J, Buhl D, Buzsáki G. Communication between neocortex and hippocampus during sleep in rodents. *Proc Natl Acad Sci USA.* (2003) 100:2065–9. doi: 10.1073/pnas.0437938100

34. Piza DL, Bruder JC, Jacobs J, Schulze-Bonhage A, Stieglitz T, Dumpelmann M. Differentiation of spindle associated hippocampal HFOs based on a correlation analysis. *Annu Int Conf IEEE Eng Med Biol Soc.* (2016) 2016:5501–4. doi: 10.1109/EMBC.2016.7591972
35. Iber C, Ancoli-Israel S, Chesson AL, Quan S. *The AASM Manual for the Scoring of Sleep and Associated Events: Rules, Terminology and Technical Specifications*. Westchest, IL: American Academy of Sleep Medicine (2007).
36. Staba RJ, Wilson CL, Bragin A, Jhung D, Fried I, Engel J. High-frequency oscillations recorded in human medial temporal lobe during sleep. *Ann Neurol.* (2004) 56:108–15. doi: 10.1002/ana.20164
37. De Gennaro L, Ferrara M. Sleep spindles: an overview. *Sleep Med Rev.* (2003) 7:423–40. doi: 10.1053/smrv.2002.0252
38. Lachner-Piza D, Jacobs J, Bruder JC, Schulze-Bonhage A, Stieglitz T, Dümpelmann M. Automatic detection of high-frequency-oscillations and their sub-groups co-occurring with interictal-epileptic-spikes. *J Neural Eng.* (2020) 17:016030. doi: 10.1088/1741-2552/ab4560
39. Lachner-Piza D, Epitashvili N, Schulze-Bonhage A, Stieglitz T, Jacobs J, Dümpelmann M. A single channel sleep-spindle detector based on multivariate classification of EEG epochs: MUSSDET. *J Neurosci Methods.* (2018) 297:31–43. doi: 10.1016/j.jneumeth.2017.12.023
40. Akiyama T, Otsubo H, Ochi A, Ishiguro T, Kadokura G, Ramachandrannair R, et al. Focal cortical high-frequency oscillations trigger epileptic spasms: confirmation by digital video subdural EEG. *Clin Neurophysiol.* (2005) 116:2819–25. doi: 10.1016/j.clinph.2005.08.029
41. Staresina BP, Bergmann TO, Bonnefond M, van der Meij R, Jensen O, Deuker L, et al. Hierarchical nesting of slow oscillations, spindles and ripples in the human hippocampus during sleep. *Nat Neurosci.* (2015) 18:1679–86. doi: 10.1038/nn.4119
42. Kudrimoti HS, Barnes CA, McNaughton BL. Reactivation of hippocampal cell assemblies: effects of behavioral state, experience, and EEG dynamics. *J Neurosci.* (1999) 19:4090–101. doi: 10.1523/JNEUROSCI.19-10-04090.1999
43. Buzsáki G. *Rhythms of the Brain*. Oxford University Press. Available online at: https://www.oxfordscholarship.com/view/10.1093/acprof:oso/9780195301069.001.0001/acprof-9780195301069 (accessed April 19, 2020).
44. Diba K, Buzsáki G. Forward and reverse hippocampal place-cell sequences during ripples. *Nat Neurosci.* (2007) 10:1241–2. doi: 10.1038/nn1961
45. von Ellenrieder N, Frauscher B, Dubeau F, Gotman J. Interaction with slow waves during sleep improves discrimination of physiologic and pathologic high-frequency oscillations (80-500 Hz). *Epilepsia.* (2016) 57:869–78. doi: 10.1111/epi.13380
46. Jacobs J, Staba R, Asano E, Otsubo H, Wu JY, Zijlmans M, et al. High-frequency oscillations (HFOs) in clinical epilepsy. *Prog Neurobiol.* (2012) 98:302–15. doi: 10.1016/j.pneurobio.2012.03.001
47. Cho JR, Koo DL, Joo EY, Seo DW, Hong S-C, Jiruska P, et al. Resection of individually identified high-rate high-frequency oscillations region is associated with favorable outcome in neocortical epilepsy. *Epilepsia.* (2014) 55:1872–83. doi: 10.1111/epi.12808
48. Kerber K, Dümpelmann M, Schelter B, Le Van P, Korinthenberg R, Schulze-Bonhage A, et al. Differentiation of specific ripple patterns helps to identify epileptogenic areas for surgical procedures. *Clin Neurophysiol.* (2014) 125:1339–45. doi: 10.1016/j.clinph.2013.11.030
49. Okanishi T, Akiyama T, Tanaka S-I, Mayo E, Mitsutake A, Boelman C, et al. Interictal high frequency oscillations correlating with seizure outcome in patients with widespread epileptic networks in tuberous sclerosis complex. *Epilepsia.* (2014) 55:1602–10. doi: 10.1111/epi.12761
50. van Klink NEC, Van't Klooster MA, Zelmann R, Leijten FSS, Ferrier CH, Braun KPJ, et al. High frequency oscillations in intra-operative electrocorticography before and after epilepsy surgery. *Clin Neurophysiol.* (2014) 125:2212–9. doi: 10.1016/j.clinph.2014.03.004
51. Wang S, Wang IZ, Bulacio JC, Mosher JC, Gonzalez-Martinez J, Alexopoulos AV, et al. Ripple classification helps to localize the seizure-onset zone in neocortical epilepsy. *Epilepsia.* (2013) 54:370–6. doi: 10.1111/j.1528-1167.2012.03721.x
52. Jacobs J, Banks S, Zelmann R, Zijlmans M, Jones-Gotman M, Gotman J. Spontaneous ripples in the hippocampus correlate with epileptogenicity and not memory function in patients with refractory epilepsy. *Epilepsy Behav.* (2016) 62:258–66. doi: 10.1016/j.yebeh.2016.05.025
53. Liu S, Gurses C, Sha Z, Quach MM, Sencer A, Bebek N, et al. Stereotyped high-frequency oscillations discriminate seizure onset zones and critical functional cortex in focal epilepsy. *Brain.* (2018) 141:713–30. doi: 10.1093/brain/awx374
54. Tamilia E, Park E-H, Percivati S, Bolton J, Taffoni F, Peters JM, et al. Surgical resection of ripple onset predicts outcome in pediatric epilepsy. *Ann Neurol.* (2018) 84:331–46. doi: 10.1002/ana.25295
55. Otárula KAG, von Ellenrieder N, Cuello-Oderiz C, Dubeau F, Gotman J. High-frequency oscillation networks and surgical outcome in adult focal epilepsy. *Ann Neurol.* (2019) 85:485–94. doi: 10.1002/ana.25442
56. Drake ME, Pakalnis A, Padamadan H, Weate SM, Cannon PA. Sleep Spindles in epilepsy. *Clin Electroencephalogr.* (1991) 22:144–9. doi: 10.1177/155005949102200305
57. Tezer FI, Rémi J, Erbil N, Noachtar S, Saygi S. A reduction of sleep spindles heralds seizures in focal epilepsy. *Clin Neurophysiol.* (2014) 125:2207–11. doi: 10.1016/j.clinph.2014.03.001
58. Selvitelli M, Krishnamurthy K, Herzog A, Schomer D, Chang B. Sleep spindle alterations in patients with malformations of cortical development. *Brain Dev.* (2008) 31:163–8. doi: 10.1016/j.braindev.2008.06.006
59. Kuhnke N, Klus C, Dümpelmann M, Schulze-Bonhage A, Jacobs J. Simultaneously recorded intracranial and scalp high frequency oscillations help identify patients with poor postsurgical seizure outcome. *Clin Neurophysiol.* (2019) 130:128–37. doi: 10.1016/j.clinph.2018.10.016
60. Zelmann R, Lina JM, Schulze-Bonhage A, Gotman J, Jacobs J. Scalp EEG is not a blur: it can see high frequency oscillations although their generators are small. *Brain Topogr.* (2014) 27:683–704. doi: 10.1007/s10548-013-0321-y
61. Kuhnke N, Schwind J, Dümpelmann M, Mader M, Schulze-Bonhage A, Jacobs J. High frequency oscillations in the ripple band (80-250 Hz) in scalp EEG: higher density of electrodes allows for better localization of the seizure onset zone. *Brain Topogr.* (2018) 31:1059–72. doi: 10.1007/s10548-018-0658-3
62. Papadelis C, Tamilia E, Stufflebeam S, Grant PE, Madsen JR, Pearl PL, et al. Interictal high frequency oscillations detected with simultaneous magnetoencephalography and electroencephalography as biomarker of pediatric epilepsy. *J Vis Exp JoVE.* (2016) 118:54883. doi: 10.3791/54883


**Conflict of Interest:** The authors declare that the research was conducted in the absence of any commercial or financial relationships that could be construed as a potential conflict of interest.

*Copyright © 2021 Bruder, Schmelzeisen, Lachner-Piza, Reinacher, Schulze-Bonhage and Jacobs. This is an open-access article distributed under the terms of the Creative Commons Attribution License (CC BY). The use, distribution or reproduction in other forums is permitted, provided the original author(s) and the copyright owner(s) are credited and that the original publication in this journal is cited, in accordance with accepted academic practice. No use, distribution or reproduction is permitted which does not comply with these terms.*

frontiers in Human Neuroscience

ORIGINAL RESEARCH
published: 24 February 2021
doi: 10.3389/fnhum.2021.613125

# Epileptic High-Frequency Oscillations in Intracranial EEG Are Not Confounded by Cognitive Tasks

*Ece Boran*[1], *Lennart Stieglitz*[1] *and Johannes Sarnthein*[1,2]*

[1]Klinik für Neurochirurgie, Universitäts Spital und Universität Zürich, Zurich, Switzerland, [2]Neuroscience Center Zurich, University of Zurich and ETH Zurich, Zurich, Switzerland

**Rationale**: High-frequency oscillations (HFOs) in intracranial EEG (iEEG) are used to delineate the epileptogenic zone during presurgical diagnostic assessment in patients with epilepsy. HFOs are historically divided into ripples (80–250 Hz), fast ripples (FR, >250 Hz), and their co-occurrence (FRandR). In a previous study, we had validated the rate of FRandRs during deep sleep to predict seizure outcome. Here, we ask whether epileptic FRandRs might be confounded by physiological FRandRs that are unrelated to epilepsy.

**Methods**: We recorded iEEG in the medial temporal lobe MTL (hippocampus, entorhinal cortex, and amygdala) in 17 patients while they performed cognitive tasks. The three cognitive tasks addressed verbal working memory, visual working memory, and emotional processing. In our previous studies, these tasks activated the MTL. We re-analyzed the data of these studies with the automated detector that focuses on the co-occurrence of ripples and FRs (FRandR).

**Results**: For each task, we identified those channels in which the HFO rate was modulated during the task condition compared to the control condition. However, the number of these channels did not exceed the chance level. Interestingly, even during wakefulness, the HFO rate was higher for channels within the seizure onset zone (SOZ) than for channels outside the SOZ.

**Conclusion**: Our prospective definition of an epileptic HFO, the FRandR, is not confounded by physiological HFOs that might be elicited by our cognitive tasks. This is reassuring for the clinical use of FRandR as a biomarker of the EZ.

**Keywords: epilepsy surgery, seizure onset zone, epileptogenic zone, medial temporal lobe, working memory, emotional processing, hippocampus, amygdala**

OPEN ACCESS

***Edited by:***
*Julia Jacobs, University of Freiburg Medical Center, Germany*

***Reviewed by:***
*Maxime Lévesque, McGill University, Canada*
*Rina Zelmann, Harvard Medical School, United States*
*William Stacey, University of Michigan, United States*

***Correspondence:**
*Johannes Sarnthein*
*johannes.sarnthein@usz.ch*

***Specialty section:***
*This article was submitted to Health, a section of the journal Frontiers in Human Neuroscience*

***Received:*** *01 October 2020*
***Accepted:*** *27 January 2021*
***Published:*** *24 February 2021*

***Citation:***
*Boran E, Stieglitz L and Sarnthein J (2021) Epileptic High-Frequency Oscillations in Intracranial EEG Are Not Confounded by Cognitive Tasks. Front. Hum. Neurosci. 15:613125. doi: 10.3389/fnhum.2021.613125*

## INTRODUCTION

When considering epilepsy surgery, the recording of intracranial EEG (iEEG) is a standard procedure to identify the seizure onset zone (SOZ; Jobst et al., 2020). There is accumulating evidence that high-frequency oscillations (HFOs > 80 Hz) in the iEEG are a reliable biomarker of epileptogenic tissue, bearing the potential to guide the surgical treatment of drug-resistant focal epilepsy (Jacobs et al., 2009; Fedele et al., 2016, 2017a, 2019; van 't Klooster et al., 2017; Jacobs and Zijlmans, 2020; Chen et al., 2021).

First reports in groups of patients showed that HFOs have higher rates in electrode contacts within the SOZ than outside the SOZ (non-SOZ; Jacobs et al., 2009). In individual patients, the aim is to delineate the epileptogenic zone (EZ). The EZ is defined as the area of the cortex whose resection leads to seizure freedom. HFOs have been shown to indicate the EZ both in intraoperative ECoG (Fedele et al., 2016, 2017b; van 't Klooster et al., 2017; Weiss et al., 2018; Boran et al., 2019c) and in presurgical iEEG recordings (Akiyama et al., 2011; Fedele et al., 2017a) while the results of a clinical trial are still pending (van 't Klooster et al., 2015). Furthermore, the HFO rate in surface EEG mirrors epilepsy severity (Boran et al., 2019d; Fan et al., 2020; Klotz et al., 2021).

HFOs are historically divided into ripples (80–250 Hz), fast ripples (FRs, >250 Hz), and their co-occurrence (FRandR). HFOs were first detected in the medial temporal lobe (MTL) of rodents, independent of epilepsy but associated with cognitive function (Buzsáki, 2006). Furthermore, HFOs occur in central and occipital brain regions without a relationship to epilepsy (Frauscher et al., 2018). These HFOs were therefore termed physiological HFOs. Unfortunately, different studies use the term "HFO" for different phenomena (Noorlag et al., 2019). The distinction between a physiological HFO and an epileptic HFO, which indicates the EZ, is a matter of ongoing research (Cimbalnik et al., 2018, 2020; Frauscher et al., 2018; Weiss et al., 2019, 2020; Arnulfo et al., 2020; Gliske et al., 2020; Pail et al., 2020). Can an epileptic HFO be confounded with a physiological HFO? The distinction has important implications: Confounding might entrain an erroneous delineation of the EZ and, in consequence, suboptimal surgical decisions.

To improve the clinical applicability of HFO, ideas on good practice have been summarized (Fedele et al., 2019; Chen et al., 2021). First, an epileptic HFO must aim to delineate the EZ and be validated against seizure outcome. Second, there must be a prospective definition of what should be marked as an epileptic HFO, as can be achieved by an automated detector (Fedele et al., 2016, 2017a; Weiss et al., 2018; Boran et al., 2019c,d; Nariai et al., 2019). Third, the data epochs should be carefully selected. In clinical research, presurgical iEEG data is usually selected from artifact-free epochs during deep sleep.

The detection of HFOs has been facilitated by automated or semi-automated detection algorithms (Remakanthakurup Sindhu et al., 2020. Of note, the vast literature on detection algorithms reflects the vast variety of definitions of what is considered to be an HFO. Here we apply a fully automated definition of HFOs, which we previously optimized on visual markings in a dataset of the Montreal Neurological Institute (Burnos et al., 2016b) and then validated on independently recorded data from Zurich (Fedele et al., 2017a). In that study, FRandRs turned out to predict seizure freedom after resective epilepsy surgery with the highest accuracy (Fedele et al., 2017a). In a further study on an independent dataset from Geneva, we again found high accuracy for outcome prediction (Dimakopoulos et al., 2020). From these studies, we deduce that FRandR are the best definition of an epileptic HFO in iEEG and therefore focus our analysis on FRandR.

Furthermore, we define as a physiological HFO an oscillation whose occurrence does not reflect the pathology and that may be induced by a cognitive task (Axmacher et al., 2008; Kucewicz et al., 2014; Arnulfo et al., 2020).

In the present study, we address the distinction between epileptic and physiological HFOs in the human MTL. For the selection of data, we build on earlier studies where we asked patients to perform cognitive tasks while we recorded iEEG. In these earlier studies, we recorded and associated the firing of single neurons with task performance, thereby confirming that the tasks were indeed activating regions of the MTL in the patients of this study (Boran et al., 2019a, 2020b). The datasets are published for re-analysis (Boran et al., 2019b, 2020a; Dimakopoulos et al., 2020; Fedele et al., 2020a, 2021).

We hypothesized that our prospective definition of an epileptic FRandR (Fedele et al., 2017a) is not confounded by physiological HFOs in the MTL. As our null hypothesis, the rate of FRandRs should be unaffected by the cognitive processing during task performance. We found a null result, i.e., cognitive processing did not modulate the FRandR rate greater than expected by chance.

# MATERIALS AND METHODS

## Subjects

The subjects were patients with epilepsy (17 subjects, age 18–56 years, 10 males, **Table 1**) that had iEEG electrodes implanted in their MTL during the presurgical diagnostic workup. All subjects had a normal or corrected-to-normal vision and were right-handed as confirmed by neurophysiological testing. Each subject performed at least one of the cognitive tasks.

## Data Acquisition and Selection

Depth electrodes (1.3 mm diameter, eight contacts of 1.6 mm length, and spacing between contact centers 3 mm or 5 mm; Ad-Tech[1], Racine, WI, UDA) were stereotactically implanted into the amygdala, hippocampus, and entorhinal cortex bilaterally (**Table 1**). iEEG was recorded against a common reference at a sampling frequency of 4,000 Hz with the ATLAS recording system (0.5–1,000 Hz pass-band, Neuralynx, www.neuralynx.com). For HFO analysis, iEEG signals were resampled at 2,000 Hz and transformed to a bipolar montage. We removed channels with high noise levels or many artifacts and invalid trials.

In parallel to the iEEG data presented here, we used microelectrodes and high-resolution equipment to record neuronal firing, which has been reported previously (Fedele et al., 2017a; Boran et al., 2019a, 2020b).

## Electrode Localization

Electrode localization and clinical data were taken from the published datasets (Boran et al., 2019b, 2020a; Fedele et al., 2020a, 2021). In brief, the patients were implanted with iEEG electrodes in MTL at Universitätsspital Zürich. Electrodes were localized using postimplantation CT scans and postimplantation

[1]www.adtechmedical.com

structural T1-weighted MRI scans. For each subject, the CT scan was registered to the postimplantation scan as implemented in FieldTrip (Oostenveld et al., 2011; Stolk et al., 2018). In the coregistered CT-MR images, the electrode contacts were visually marked. The contact positions were normalized to the MNI space and assigned to a brain region using the Brainnetome Atlas (Fan et al., 2016). Also, depth electrode positions were verified by the neurosurgeon (LS) after merging preoperative MRI with postimplantation CT images of each subject in the plane along the electrode (iPlan Stereotaxy 3.0, Brainlab, München, Germany). We grouped electrodes according to their anatomical region (Hipp: hippocampus, Ent: entorhinal cortex, Amg: amygdala) and whether they were recorded within the SOZ or outside the SOZ. **Figure 1** shows the localization of the electrode tips projected on a parasagittal plane (MNI space $x = -25.2$ mm).

## Clinical Data and SOZ

Patients underwent a presurgical diagnostic workup at Schweizerische Epilepsie-Klinik. The clinical information was taken from the hospital patient records. The SOZ was defined by experienced epileptologists independent of the studies.

## Tasks Activating the MTL Guided iEEG Data Selection

Our selection of iEEG data was guided by whether we had found neuronal firing in the same subjects that were associated with task performance (Boran et al., 2019a, 2020b; Fedele et al., 2020b). Our previous analysis of neuronal firing in the MTL served to characterize task demand and to predict subject behavior, thus demonstrating the involvement of MTL in cognitive task performance. Only then we could be assured that this structure of MTL in this subject was actually engaged in task processing.

### Verbal Working Memory Task

To activate verbal working memory, we used a modified Sternberg task where the subject had to memorize a string of letters (**Figure 2A**; Boran et al., 2019a). The number of letters in the string determined the working memory load (low workload: four letters; high workload: six or eight letters; 50 trials per session; 36 sessions in total). The mean duration of recording in each subject was 23.3 min. The behavioral results of the subjects were as expected from a working memory task: the rate of correct responses decreased with set size from 4 (98.5% correct responses) to set sizes of 6 (90.5%) and 8 (84.7%). The mean response time for the correct trials (1630 trials) increased with workload (48 ms per item). We analyzed a total of 773 MTL channels from nine subjects for this task (**Table 1**).

We have reported earlier (Boran et al., 2019a) that for the same task in the same subjects, we found neurons in the MTL that fired persistently during the maintenance period. Some of these neurons increased their firing rate for a high workload. We could also decode the workload of single trials from the neuronal population firing in the MTL. As a robust finding, hippocampal iEEG activity and hippocampal-cortical synchronization was high for trials with high workload and not for trials with

**TABLE 1** | Subject characteristics. Subjects were implanted in the medial temporal lobe (MTL) and performed at least one cognitive task.

| Subject number | Age | Sex | Pathology | Electrodes | SOZ | Verbal working memory | Visual working memory | Fearful faces |
|---|---|---|---|---|---|---|---|---|
| 1 | 31 | Male | Hippocampal sclerosis | AHL, AHR, AL, AR, ECL, ECR, PHL, PHR | AR, ECR | x | x | x |
| 2 | 18 | Female | Hippocampal sclerosis | AHL, AHR, AL, ECL, PHL | AHL, AL, ECL, PHL | x | x | x |
| 3 | 39 | Male | Gliosis | AHL, AHR, AL, AR, ECL, ECR, PHL, PHR | AHR, PHR | x | x | x |
| 4 | 28 | Male | Brain contusion | AHL, AHR, AL, AR, ECL, ECR, PHL, PHR | AHL, AHR, PHL, PHR | x | x | - |
| 5 | 47 | Male | Hippocampal sclerosis | AHL, AHR, AL, AR, ECL, ECR, PHL, PHR | AHR, PHR | x | - | x |
| 6 | 19 | Female | Hippocampal sclerosis | AHL, AHR, AL, AR, ECL, ECR, PHL, PHR | AR, ECR | x | - | - |
| 7 | 24 | Female | Xanthoastrozytoma WHO II | AHL, AL, ECL, LR, PHL, PHR | LR | x | - | - |
| 8 | 56 | Female | Hippocampal sclerosis | AHL, AHR, AL, AR, ECL, ECR, PHL, PHR | ECR | x | - | - |
| 9 | 20 | Female | Focal cortical dysplasia | AHL, AL, DRR, PHR | DRR | x | - | - |
| 10 | 31 | Female | Hippocampal sclerosis | AHR, ECR, PHR | AHR, PHR | - | x | - |
| 11 | 35 | Male | Unknown | AHL, AHR, AL, AR, ECL, ECR, PHL | AHL | - | x | - |
| 12 | 20 | Male | Focal cortical dysplasia | AHL, AHR, PHL, PHR | - | - | x | - |
| 13 | 19 | Male | Unknown | AHR, PHL, PHR | PHL | - | x | - |
| 14 | 51 | Female | Hippocampal sclerosis | AHL, AHR, AL, AR, ECL, ECR, PHL, PHR | AHL, PHL | - | x | - |
| 15 | 21 | Male | Hippocampal sclerosis | AL | | - | - | x |
| 16 | 22 | Male | Hippocampal sclerosis | AL, AR | AR | - | - | x |
| 17 | 21 | Male | Hippocampal sclerosis | AL, AR | | - | - | x |

*L, left; R, right; AH, hippocampal head; PH, hippocampal body; EC, entorhinal cortex; A, amygdala; DRR, LR: lesions, AIR, insular gyrus right; FR, frontal right; SOZ, seizure onset zone; (x) subject performed the task; (–) subject did not perform the task. The FR and R rates in SOZ channels and nonSOZ channels differed significantly in only 8/17 subjects (Wilcoxon rank-sum test $p < 0.05$).*

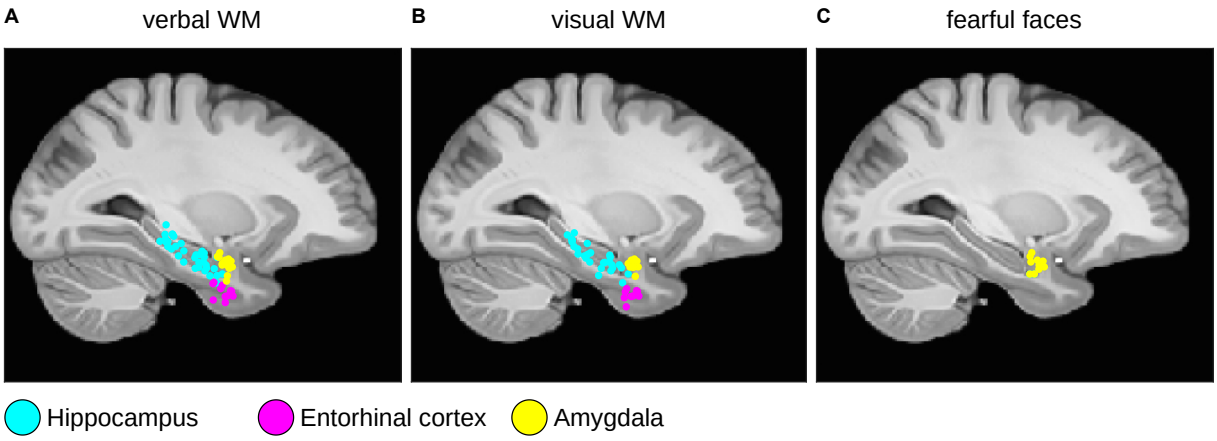


**FIGURE 1 |** Electrode localization. Anatomical locations of the tips of the depth electrodes in Montreal Neurological Institute's MNI152 space (Methods) for **(A)** verbal working memory task; **(B)** visual working memory task; **(C)** fearful faces task. Locations are projected on the parasagittal plane $x = -25.2$ mm and are color-coded (cyan, hippocampus; magenta, entorhinal cortex; and yellow, amygdala).

four letters. Therefore, trials with four letters were taken as the control condition.

### Visual Working Memory Task

To activate visual working memory, we used a change detection task where the subject had to memorize an array of colored squares (**Figure 2B**; Boran et al., 2020b). The number of squares determined the working memory load (low workload: one or two squares; high workload: four or six squares; 192 trials per session). For each subject, the duration of the session was 11.5 min. The rate of correct responses decreased with set size from a set size of 1 (98% correct responses) to 2 (99%), 4 (88%), and 6 (73%). The mean response time for the correct trials (2,678 trials) increased with set size (118 ms/item). We analyzed a total of 178 MTL channels from nine subjects for this task (**Table 1**).

We have reported earlier (Boran et al., 2020b) that for the same task in the same subjects, we found neurons in the MTL that fired persistently and increased their firing rate for trials with a high workload during the maintenance period. Neuronal population firing in the MTL during maintenance distinguished workload and we could decode workload of single trials. Therefore, trials with one or two squares were taken as the control condition.

### Fearful Faces Task

To activate the amygdala during emotional processing, we presented fearful faces as dynamic visual stimuli (**Figure 2C**; Fedele et al., 2020b). For trials of the aversive condition (eight trials), a 24 s block of short video clips (2–3 s) of fearful faces were shown. Video clips of fearful faces were extracted from thriller and horror movies and contained faces of actors showing fear. For trials of the control condition (nine trials, 24 s each), the video clips were from neutral landscapes. Each trial started with a repeated baseline of a 2 s video of a neutral landscape and there were seven sessions in total. For each subject, the duration of the task was 7 min.

We have reported earlier (Fedele et al., 2020b) that for the same task in the same subjects, for the aversive compared to the control condition, amygdalar high gamma power (>60 Hz) increased during the first 2 s and delta power (1–4 Hz) decreased for up to 18 s. Also, neuronal firing increased during the aversive condition. The high correlation of these measures with the BOLD response in the same subjects (Schacher et al., 2006) points to high gamma, delta, and neuronal firing being the electrophysiological counterparts to the observed increase in BOLD response during emotional processing in the amygdala. Since the task was designed to activate the amygdala (Schacher et al., 2006) and we found task-related neuronal firing only in the amygdala of these subjects (Fedele et al., 2020b), we here report only iEEG data from the 12 amygdalar channels of these subjects (**Table 1**).

## Automated HFO Detection

We used the prospective HFO detector previously validated to predict seizure outcome from iEEG recorded during intervals of NREM sleep (Fedele et al., 2017a). The detector captures the morphology of an HFO and was developed on data from the Montreal Neurological Institute (Burnos et al., 2016b). In brief, the detector has a baseline detection stage and an HFO detection stage that are performed separately for ripples and FRs (Burnos et al., 2016b). In the baseline detection stage, the segments of the signal corresponding to the baseline are determined using Stockwell entropy. The amplitude threshold is defined using these segments. In the HFO detection stage, events, where the filtered signal exceeded the amplitude threshold for at least 20 ms, were defined as ripples. Similarly, events, where the filtered signal exceeded the amplitude threshold for at least 10 ms, were defined as FR. Furthermore, we defined a FRandR as the co-occurrence of a ripple and an FR (Fedele et al., 2017a). **Figure 3** shows a representative example of a ripple, an FR, and the corresponding FRandR.

Similar to HFO detection during intervals of NREM sleep, HFOs were detected on the continuous data recorded while the

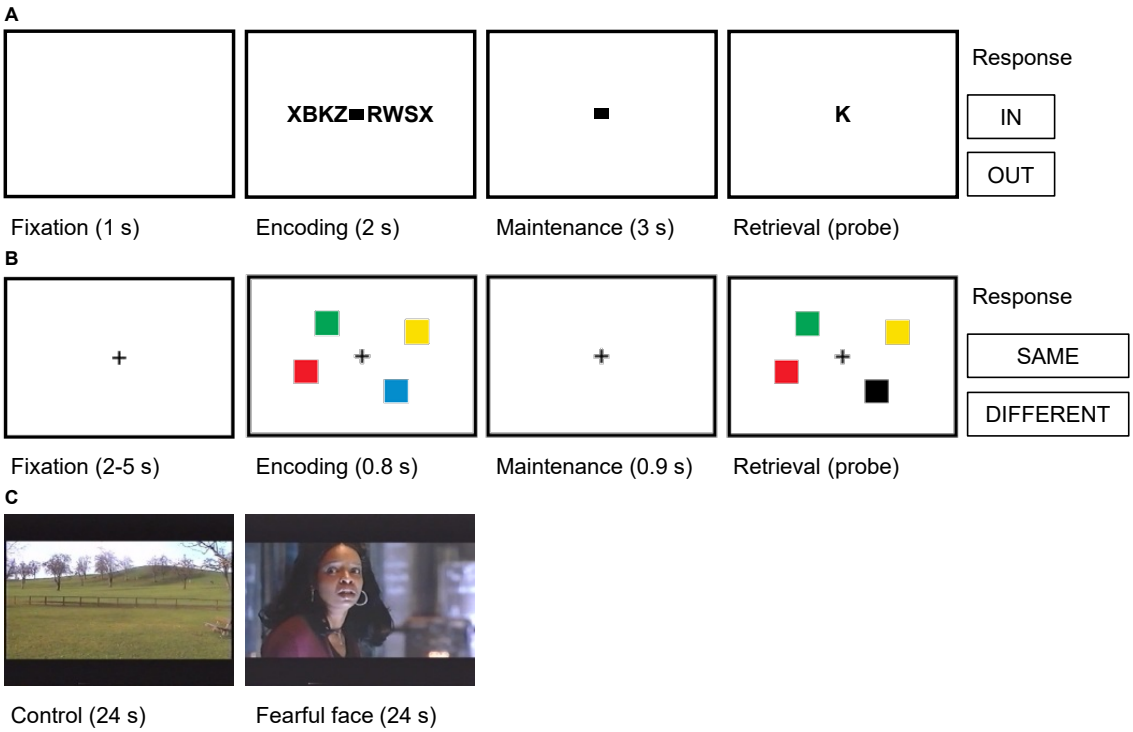


**FIGURE 2 |** Trial structures for the cognitive tasks. **(A)** Verbal working memory task. In this task, sets of consonants were presented and had to be memorized. Each trial (50 trials per session) started with a fixation period (1 s), followed by the presentation of a letter string (encoding, 2 s). The number of letters presented determined WM workload (task condition/high workload: six or eight letters; control condition/low workload: four letters). The encoding period was followed by a delay (maintenance, 3 s). After the delay, a probe letter was shown, and subjects indicated whether the probe was presented during the encoding period (In/Out). **(B)** Visual working memory task. In this task, visual working memory was examined using a change detection task. In each trial (192 trials per session), a fixation period (2–5 s) was followed by the presentation of the memory array of colored squares (encoding, 0.8 s). The number of squares determined WM workload (task condition/high workload: four or six squares; control condition/low workload: one or two squares). The encoding period was followed by a delay (maintenance 0.9 s). After the delay, a probe array was shown, and subjects indicated whether the probe array differed from the memory array (Same/Different). **(C)** Fearful faces. In this task, amygdalar response to fear was examined using fearful faces. Alternating blocks of fearful faces (task condition, eight trials) and neutral landscapes (control condition, nine trials) were shown. Each block lasted 24 s and consisted of short video clips of 2–3 s. Video clips of fearful faces were extracted from thriller and horror movies and contained faces of actors showing fear. In each trial, the block was preceded by a repeated baseline of 2 s of a neutral landscape.

subject performed the tasks. We used the timestamps of the HFOs to assign them to trials of task or control conditions. We computed the rate of ripples, FRs, and FRandRs during the cognitive tasks for each channel separately. We use the term HFO to comprise all three types of HFO (ripple, FR, and FRandR).

## HFO Rate Comparison Between Task and Control Conditions

We tested whether the HFO rates were modulated during the task condition as compared to the control condition. The choice of control condition was based on the design of the tasks and our previous reports of single neuron firing in the same patients (Boran et al., 2019a, 2020b; Fedele et al., 2020b). To assure that subjects were actually engaged in the task, we only used trials where the subject responded correctly.

For the verbal working memory task (Boran et al., 2019a), we compared the HFO rate during maintenance for low workload trials (set size 4) and high workload trials (set size 6 or 8) within each anatomical region.

For the visual working memory task (Boran et al., 2020b), we compared the HFO rate during maintenance for low workload trials (set size 1 or 2) and high workload trials (set size 4 or 6) within each anatomical region.

For the fearful faces task (Fedele et al., 2020b), we compared the HFO rate during the presentation of stimuli for trials with fearful faces (aversive condition) and trials with neutral landscapes (neutral condition).

## Statistics

To assess the significance of the difference of HFO rates across task conditions, we used the Wilcoxon rank-sum test. Next, we determined the number of channels where the HFO rate increased or decreased significantly (Wilcoxon rank-sum test). Furthermore, to assess the significance of the number of channels showing any effect, we used a permutation test with scrambled labels: we created a null distribution estimated from $n > 200$ permutations on data with scrambled labels. For the permutation test, the iEEG of each task condition was considered as 1 bin; we did not split the iEEG further. The minimum $p$-value is limited by the number of permutations as $p = 1/(\text{number of permutations} + 1)$. Reported $p$-values were based on the percentage of values in the empirically estimated null distribution

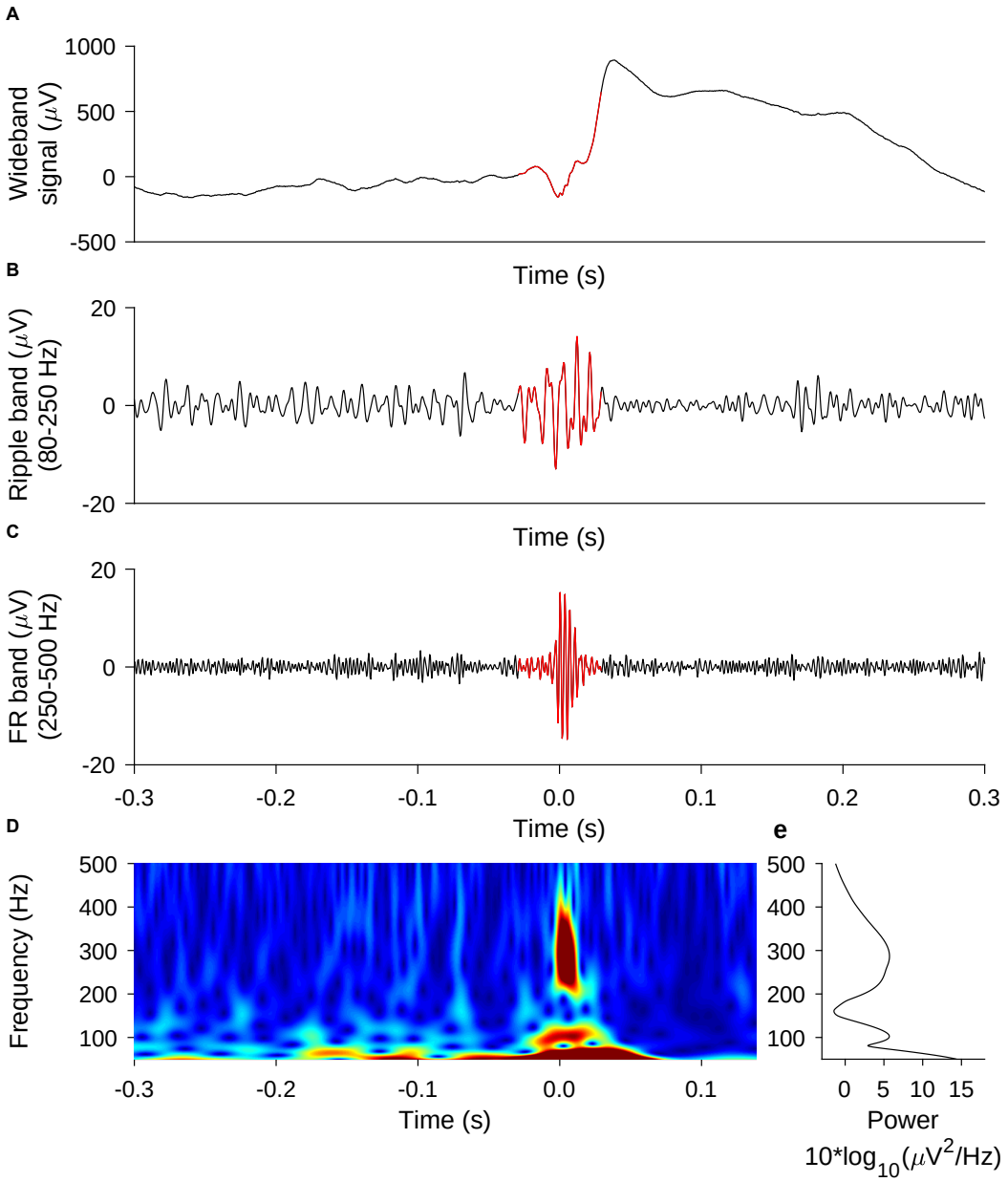


**FIGURE 3 |** Representative example of ripple, FR, FRandR. A ripple co-occurring with a fast ripple (FRandR) is shown **(A)** in the wideband signal, **(B)** the signal filtered in the ripple band (80–250 Hz), and **(C)** the signal filtered in the FR band (250–500 Hz). **(D)** The instantaneous frequency spectrum is smooth and does not allow a distinction between ripples and FR, in agreement with our earlier finding (Fedele et al., 2017a).

that was exceeded by the observed value. For all tasks and channels, we performed the analysis separately for all types of HFOs (ripples, FRs and FRandRs).

## RESULTS

### HFO Rate Does Not Differ Between Task and Control Condition

To test our primary hypothesis, we identified channels where the HFO rate was modulated by the task condition compared to the control condition. The median HFO rate over all the tasks was 4.14, 2.38, and 0.07 events/min for ripples, FRs, and FRandRs, respectively. The absolute and relative numbers of channels where task condition changed the HFO rate either up or down is given in (**Figure 4**).

For the verbal working memory task, ripple rates increased or decreased for the task condition (six or eight letters) compared to the control condition (low workload trials with four letters) during maintenance for a few channels. **Figure 4A** shows the number of channels for all subjects that show an increase (red

bars) or decrease (blue bars) in ripple rate with the workload for each anatomical region. For hippocampus, entorhinal cortex, and amygdala, 22, 1 and 3 channels had ripple rates that differed with workload ($p < 0.05$, Wilcoxon rank-sum test for individual channels). However, there is a large number of channels in each MTL region. We, therefore, tested the significance of the number of channels that show any effect by comparing against a random distribution. The number of channels with ripple rates that were modulated by the task for any MTL region was not significant ($p = 0.5150$, $p = 1.0000$, and $p = 0.9750$, permutation test against scrambled labels). Likewise, several channels show FR (**Figure 4B**) and FRandR (**Figure 4C**) rates that are modulated by the task. Similarly, these numbers did not exceed the chance level for any region ($p > 0.05$, permutation test against scrambled labels).

For the visual working memory task, we also found channels with modulation in HFO rate during the task (**Figure 4**; task condition, four or six squares; control condition, one or two squares). With the same statistical approach as above, the number of these channels did not exceed the chance level for any MTL region (for ripples, $p = 0.3450$, $p = 0.6650$, and $p = 0.1750$, permutation test against scrambled labels).

During the presentation of the fearful faces, there was one channel where ripple rate increased or decreased for the task condition, respectively. Similar to the working memory tasks, the number of channels that showed such effect was not significant ($p = 0.1000$, permutation test against scrambled labels).

There was no significant difference between channels recorded from the left or the right hemisphere of the brain. There was no significant association between channels in the five subjects that performed more than one task.

Overall, the number of channels in the MTL with HFO rates that were modulated by the task was not greater than expected by chance.

## HFO Rate During Task Performance Differs Between SOZ and Non-SOZ

In addition to our primary hypothesis, we tested whether HFO rates were higher within the SOZ than outside the SOZ.

For the verbal working memory task, the HFO rate in the SOZ (213 channels) exceeded the HFO rate outside the SOZ (560 channels) for ripples (**Figure 5**; $p = 1.486 \times 10^{-9}$, Wilcoxon rank-sum test), FRs ($p = 0.0128$, Wilcoxon rank-sum test) and for FRandRs ($p = 2.207 \times 10^{-6}$, Wilcoxon rank-sum test).

Similarly, for the visual working memory task, HFO rates were higher within the SOZ (56 channels) than outside the SOZ (122 channels) for ripples ($p = 0.0374$, Wilcoxon rank-sum test), FRs ($p = 0.0008$, Wilcoxon rank-sum test) and for FRandRs ($p = 0.0044$, Wilcoxon rank-sum test).

For the fearful faces task, HFO rates were higher within the SOZ (three channels) than outside the SOZ (nine channels). Due to the small number of channels, this difference did not reach significance for ripples ($p = 0.3727$, Wilcoxon rank-sum test), FRs ($p = 0.1000$, Wilcoxon rank-sum test) and for FRandRs ($p = 0.3455$, Wilcoxon rank-sum test).

For individual subjects, HFO rates average over tasks were higher within the SOZ than outside the SOZ for FRand R in only 8/17 subjects (FR 6/17; ripple 7/17). When averaging over all subjects and tasks, HFO rates were higher within the SOZ (77 channels) than outside the SOZ (197 channels) for ripples ($p = 0.0114$, Wilcoxon rank-sum test), FRs ($p = 0.0008$, Wilcoxon rank-sum test) and FRandRs ($p = 0.0001$, Wilcoxon rank-sum test).

# DISCUSSION

When comparing HFO rate between task and control condition, HFO rates did not change greater than expected by chance. This favors our main hypothesis: there was no indication that the HFOs as prospectively defined in (Fedele et al., 2017a) were confounded by physiological HFOs. As an additional finding on the group level, HFO detected during active wakefulness were found to be more abundant in the SOZ and therefore also reflected pathology.

## Methodological Considerations

Our primary methodological consideration is the definition of an HFO. We used our automated HFO detector which was designed to analyze long-term iEEG recordings during NREM sleep (Burnos et al., 2016b). The detection algorithm has been validated to predict seizure outcome after resective epilepsy surgery with good accuracy (Burnos et al., 2016b; Fedele et al., 2017a). Here we used this detector "off-label" on awake subjects performing cognitive tasks.

We based our prospective definition of a clinically relevant HFO on the co-occurrence of a ripple and a fast ripple (FRandR), where the majority of FRandR show an instantaneous frequency spectrum that does not distinguish between ripples and FR (**Figure 3**; Fedele et al., 2017a). We thus ignored the traditional distinction between ripples (80–250 Hz) and FR (250–500 Hz; Lévesque et al., 2018; Chen et al., 2021). As expected, the FRandR rate was much lower than the rates of ripples and FR separately.

In our HFO analysis, we used a bipolar montage, i.e., we subtracted the signal from two adjacent electrode contacts and considered the difference as a recording channel. The subtraction eliminates spatially extended background activity and artifacts, above all the line hum and its harmonics. Because of the small amplitude of HFOs (Fedele et al., 2017b), this subtraction was mandatory in all the datasets from several institutions that we analyzed (Burnos et al., 2016b; Fedele et al., 2016, 2017b; Dimakopoulos et al., 2020). Furthermore, the bipolar montage affects our certainty concerning the spatial origin of an HFO. On the mm scale, there is evidence that HFOs are generated by a tissue area in the millimeter range (Boran et al., 2019c; Zweiphenning et al., 2020). In principle, a FRandR might result from the superposition of a ripple at one contact and an FR at the other contact of a recording channel (spacing $\leq$5 mm) (Zaveri et al., 2006), if one would assume that FRandR were composed of distinct entities. On a larger scale, the bipolar montage ensures that the HFO is generated in the vicinity of the two contacts and not somewhere between one contact and the recording reference (spacing $\sim$5 cm). This agrees with the clinical standard where the SOZ is detected in a bipolar montage.

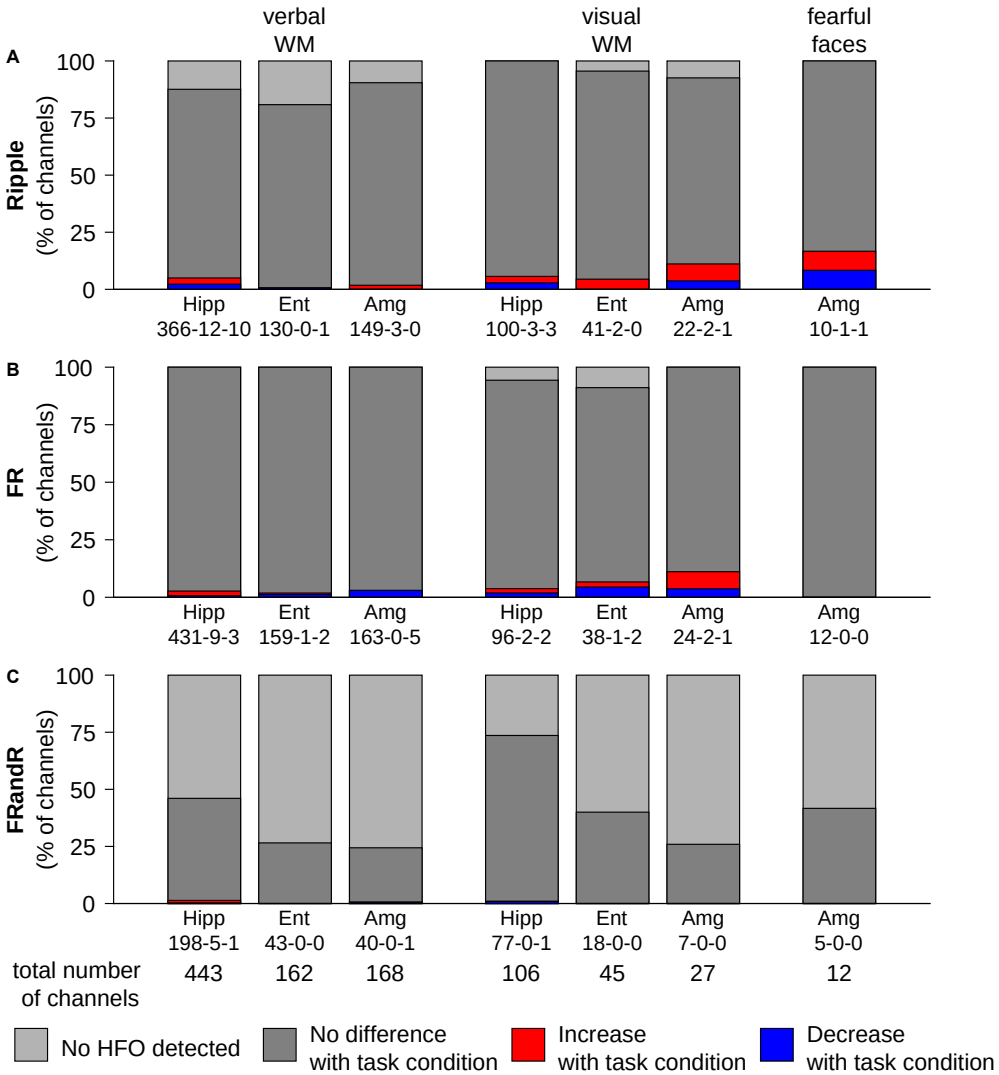


**FIGURE 4 |** HFO rate does not change with task condition. Percentage of channels with changes in **(A)** ripple, **(B)** FR, and **(C)** FRandR rates with task conditions during cognitive tasks. Left: verbal working memory task. Channels with modulation of HFO rates for the task condition (six or eight letters) vs. the control condition (four letters). From a total of 443 channels analyzed in the hippocampus, in 198 there were FRandRs detected. In five of these channels, the FRandR rate increased, and in one channel FR, and R rate decreased (198-5-1). Middle: visual working memory task. Channels with modulation of HFO rates for the task condition (four or six squares) vs. the control condition (one or two squares). Right: fearful faces task. Channels with modulation of HFO rates for fearful faces condition vs. control condition. The percentage of channels with increase or decrease with task conditions do not reach significance for any HFO type or task (permutation test with scrambled labels).

Finally, we addressed the problem of multiple comparisons. A large number of channels entered the analysis and a significant modulation of some channel's HFO rate would be expected simply by chance as a spurious effect. We, therefore, applied computational statistics to calculate the statistical significance of the percentage of channels where the cognitive tasks modulated HFO rate either up or down. We found that this number of channels was not greater than expected by chance.

## Physiological and Epileptic HFOs

Spontaneous physiological HFOs were first described in the hippocampus (Buzsáki, 2006). In neocortical areas, somatosensory stimulation elicited physiological HFOs (Burnos et al., 2016a; Fedele et al., 2017c). Spontaneous physiological HFO in the neocortex were mainly observed in central and occipital areas (Nagasawa et al., 2012; Frauscher et al., 2018). An attempt to distinguish individual physiological and epileptic HFOs by their morphology proved unsuccessful (Burnos et al., 2016b). For clinical applications of HFOs, distinguishing physiological and epileptic HFOs is a major concern. Including physiological HFOs in the analysis may lead to an erroneous estimation of the EZ, resulting in suboptimal surgical decisions and suboptimal clinical outcomes (Chen et al., 2021).

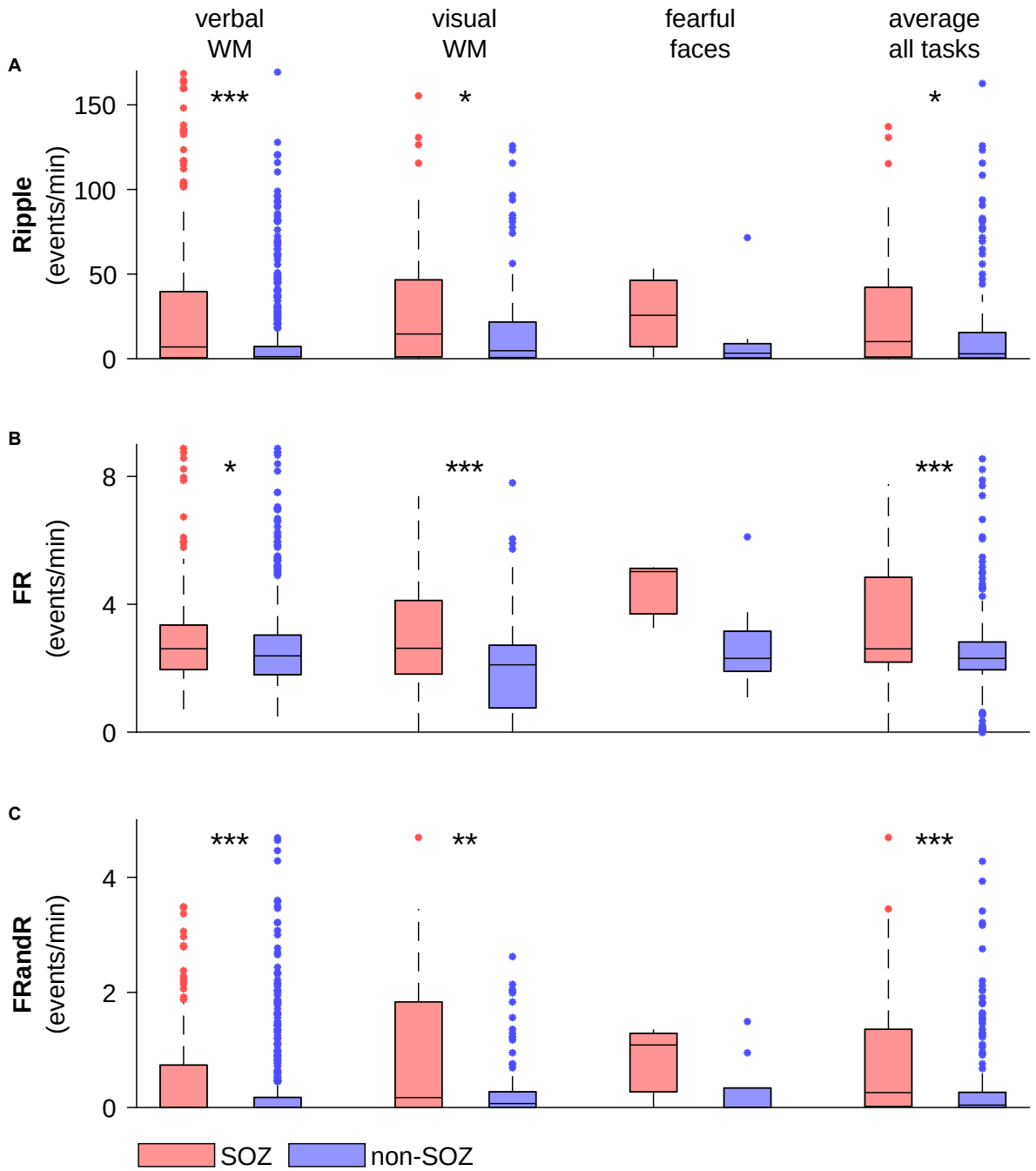


**FIGURE 5 |** HFO rate is higher within the SOZ than outside the SOZ during task performance. **(A)** Ripple, **(B)** FR, and **(C)** FRandR rates for channels within and outside the SOZ for each cognitive task (verbal WM: verbal working memory task, visual WM: visual working memory task, fearful faces: fearful faces task). The rightmost columns show average HFO rates over all the tasks and all sessions for each channel within and outside the SOZ. Over the patient group, HFO rates for channels within the SOZ are higher than for non-SOZ channels for all HFO types for the memory tasks and the average over all the tasks ($p$ <0.05, Wilcoxon rank-sum test). ***$p < 0.001$, **$p < 0.01$, *$p < 0.05$.

## FRandR Rate Was Not Modulated by Task Performance

As our main result, the FRandR rate during task performance did not change greater than the chance level, i.e., a null result (**Figure 4**). While we found the same null result for all three types of HFO (ripple, FR, and FRandR), we focus our discussion on FRandR because FRandR had the highest accuracy in predicting seizure outcome after resective epilepsy surgery

(Fedele et al., 2017a). From this null result, we conclude that FRandRs are not confounded by task-related HFOs. We discuss this conclusion because of the following questions.

Do these subjects perform these tasks without activating the brain regions where we record from? To prove that the recordings are indeed from activated brain areas, we have selected iEEG data from subjects where we had reported task-related neuronal firing in the MTL of the same subjects (Boran et al., 2019a, 2020b; Fedele et al., 2020b). This assured us that these subjects activated their MTL to perform the tasks.

Are FRandR valid biomarkers for epileptogenic tissue? In our search for an automated definition of an epileptic HFO, we aimed to predict the seizure outcome after resective epilepsy surgery (seizure-free vs. not seizure-free postoperatively; Fedele et al., 2019). Here, FRandR turned out to have the highest accuracy (Fedele et al., 2017a). Our approach is different from other approaches in the literature (Chen et al., 2021). For example, several studies in humans define the distinction of physiological and epileptic HFOs by assuming that an HFO that occurs in the SOZ is epileptic, while an HFO outside the SOZ or in the sensory or motor cortices is physiological (Cimbalnik et al., 2018; Frauscher et al., 2018; Weiss et al., 2019, 2020; Gliske et al., 2020; Remakanthakurup Sindhu et al., 2020). Similarly, we found increased FRandR activity in the SOZ (**Figure 5**). Thus, we deduce from the results presented in **Figure 5** and more comprehensive results presented earlier (Fedele et al., 2017a; Dimakopoulos et al., 2020), that FRandRs are indeed valid biomarkers of epileptogenic tissue.

How can this null-result be reconciled with the finding of physiological HFOs reported in other studies? Some studies use cognitive tasks and define as HFOs those oscillations in the HFO frequency band that are modulated by cognitive processing (Axmacher et al., 2008; Kucewicz et al., 2014; Jacobs et al., 2016; Cimbalnik et al., 2018, 2020; Arnulfo et al., 2020; Pail et al., 2020). These findings are in discrepancy with our null result, where we found no evidence for rate modulation of FRandRs by the cognitive tasks. The discrepancy might be reconciled by noting that the absence of evidence does not mean the evidence of absence. In the other studies, subjects performed other tasks. Our data are publicly available and can be tested for physiological HFOs (Boran et al., 2020b, 2019a; Fedele et al., 2020a, 2021). Still, it is conceivable that we recorded physiological FRandRs as well. However, these must have been masked by the consistently high rate of epileptic FRandRs whose overall rate was not modulated in a statistically significant way. This indicates that the number of physiological FRandRs, if at all present, must be small compared to the number of epileptic FRandRs.

## CONCLUSIONS

The most important conclusion from our study is that the rate of HFOs, especially the rate of FRandRs, was unaffected by the cognitive tasks. This indicates that the FRandR, our prospective definition of an epileptic HFO, is not confounded by physiological HFOs in the MTL. This is reassuring when using FRandR rate as a biomarker of the EZ.

## DATA AVAILABILITY STATEMENT

The iEEG recordings for two tasks are already publicly available (Boran et al., 2019b, 2020a,b; Fedele et al., 2020a, 2021). The remaining data will be made available after acceptance of the article.

## CODE AVAILABILITY STATEMENT

The code of the HFO detector is freely available at the GitHub repository (https://github.com/ZurichNCH/Automatic-High-Frequency-Oscillation-Detector). The verbal working memory task is available at https://www.neurobs.com/ex_files/expt_view?id=266. The fearful faces video is available in the original AVI format and read by a custom program at https://www.neurobs.com/ex_files/expt_view?id=283.

## ETHICS STATEMENT

The studies involving human participants were reviewed and approved by Kantonale Ethikkommission Zürich. The patients/participants provided their written informed consent to participate in this study.

## AUTHOR CONTRIBUTIONS

JS and EB designed the study. LS treated patients. EB analyzed data and prepared figures and tables. EB and JS wrote the article. All authors critically reviewed the manuscript. All authors contributed to the article and approved the submitted version.

## FUNDING

We acknowledge grants awarded by the Swiss National Science Foundation (SNSF 320030_176222 to JS), Mach-Gaensslen Stiftung (to JS), and Stiftung für wissenschaftliche Forschung an der Universität Zürich (to JS). The funders had no role in the design or analysis of the study.

## REFERENCES

Akiyama, T., McCoy, B., Go, C. Y., Ochi, A., Elliott, I. M., Akiyama, M., et al. (2011). Focal resection of fast ripples on extraoperative intracranial EEG improves seizure outcome in pediatric epilepsy. *Epilepsia* 52, 1802–1811. doi: 10.1111/j.1528-1167.2011.03199.x

Arnulfo, G., Wang, S. H., Myrov, V., Toselli, B., Hirvonen, J., Fato, M. M., et al. (2020). Long-range phase synchronization of high-frequency oscillations in human cortex. *Nat. Commun.* 11:5363. doi: 10.1038/s41467-020-18975-8

Axmacher, N., Elger, C. E., and Fell, J. (2008). Ripples in the medial temporal lobe are relevant for human memory consolidation. *Brain* 131, 1806–1817. doi: 10.1093/brain/awn103

Boran, E., Fedele, T., Klaver, P., Hilfiker, P., Stieglitz, L., Grunwald, T., et al. (2019a). Persistent hippocampal neural firing and hippocampal-cortical coupling predict verbal working memory load. *Sci. Adv.* 5:eaav3687. doi: 10.1126/sciadv.aav3687

Boran, E., Fedele, T., Steiner, A., Hilfiker, P., Stieglitz, L., Grunwald, T., et al. (2019b). Dataset of simultaneous scalp EEG and intracranial EEG recordings

and human medial temporal lobe units during a verbal working memory task. *G-Node*. doi: 10.12751/g-node.d76994. Available online at: https://gin.g-node.org/USZ_NCH/Human_MTL_units_scalp_EEG_and_iEEG.

Boran, E., Ramantani, G., Krayenbühl, N., Schreiber, M., König, K., Fedele, T., et al. (2019c). High-density ECoG improves the detection of high frequency oscillations that predict seizure outcome. *Clin. Neurophysiol.* 130, 1882–1888. doi: 10.1016/j.clinph.2019.07.008

Boran, E., Sarnthein, J., Krayenbuhl, N., Ramantani, G., and Fedele, T. (2019d). High-frequency oscillations in scalp EEG mirror seizure frequency in pediatric focal epilepsy. *Sci. Rep.* 9:16560. doi: 10.1038/s41598-019-52700-w

Boran, E., Fedele, T., Steiner, A., Hilfiker, P., Stieglitz, L., Grunwald, T., et al. (2020a). Dataset of human medial temporal lobe neurons, scalp and intracranial EEG during a verbal working memory task. *Sci. Data* 7:30. doi: 10.1038/s41597-020-0364-3

Boran, E., Hilfiker, P., Stieglitz, L., Grunwald, T., Sarnthein, J., and Klaver, P. (2020b). Neuronal firing in the medial temporal lobe reflects human working memory workload, performance and capacity. *bioRxiv* [Preprint]. doi: 10.1101/2020.06.15.152207

Burnos, S., Fedele, T., Schmid, O., Krayenbuhl, N., and Sarnthein, J. (2016a). Detectability of the somatosensory evoked high frequency oscillation (HFO) co-recorded by scalp EEG and ECoG under propofol. *Neuroimage Clin.* 10, 318–325. doi: 10.1016/j.nicl.2015.11.018

Burnos, S., Frauscher, B., Zelmann, R., Haegelen, C., Sarnthein, J., and Gotman, J. (2016b). The morphology of high frequency oscillations (HFO) does not improve delineating the epileptogenic zone. *Clin. Neurophysiol.* 127, 2140–2148. doi: 10.1016/j.clinph.2016.01.002

Buzsáki, G. (2006). *Rhythms of the Brain*. New York, NY: Oxford University Press.

Chen, Z., Maturana, M. I., Burkitt, A. N., Cook, M. J., and Grayden, D. B. (2021). High-frequency oscillations in epilepsy: what have we learned and what needs to be addressed. *Neurology* doi: 10.1212/WNL.0000000000011465. [Epub ahead of print].

Cimbalnik, J., Brinkmann, B., Kremen, V., Jurak, P., Berry, B., Gompel, J. V., et al. (2018). Physiological and pathological high frequency oscillations in focal epilepsy. *Ann. Clin. Transl. Neurol.* 5, 1062–1076. doi: 10.1002/acn3.618

Cimbalnik, J., Pail, M., Klimes, P., Travnicek, V., Roman, R., Vajcner, A., et al. (2020). Cognitive processing impacts high frequency intracranial EEG activity of human hippocampus in patients with pharmacoresistant focal epilepsy. *Front. Neurol.* 11:578571. doi: 10.3389/fneur.2020.578571

Dimakopoulos, V., Mégévand, P., Boran, E., Momjian, S., Seeck, M., Vulliémoz, S., et al. (2020). Prospectively defined high frequency oscillations to predict seizure outcome in the individual patient. *medRxiv* [Preprint]. doi: 10.1101/2020.12.24.20248799

Fan, Y., Dong, L., Liu, X., Wang, H., and Liu, Y. (2020). Recent advances in the noninvasive detection of high-frequency oscillations in the human brain. *J. Rev. Neurosci.* doi: 10.1515/revneuro-2020-0073. [Epub ahead of print].

Fan, L., Li, H., Zhuo, J., Zhang, Y., Wang, J., Chen, L., et al. (2016). The human brainnetome atlas: a new brain atlas based on connectional architecture. *Cereb. Cortex* 26, 3508–3526. doi: 10.1093/cercor/bhw157

Fedele, T., Boran, E., Chirkov, V., Hilfiker, P., Grunwald, T., Stieglitz, L., et al. (2020a). Dataset of neurons and intracranial EEG from human amygdala during aversive dynamic visual stimulation. *OpenNeuro* doi: 10.18112/openneuro.ds003374.v1.1.1. [Epub ahead of print].

Fedele, T., Tzovara, A., Steiger, B., Hilfiker, P., Grunwald, T., Stieglitz, L., et al. (2020b). The relation between neuronal firing, local field potentials and hemodynamic activity in the human amygdala in response to aversive dynamic visual stimuli. *NeuroImage* 213:116705. doi: 10.1016/j.neuroimage.2020.116705

Fedele, T., Boran, E., Chirkov, V., Hilfiker, P., Grunwald, T., Stieglitz, L., et al. (2021). Dataset of spiking and LFP activity invasively recorded in the human amygdala during aversive dynamic stimuli. *Sci. Data* 8:9. doi: 10.1038/s41597-020-00790-x

Fedele, T., Burnos, S., Boran, E., Krayenbuhl, N., Hilfiker, P., Grunwald, T., et al. (2017a). Resection of high frequency oscillations predicts seizure outcome in the individual patient. *Sci. Rep.* 7:13836. doi: 10.1038/s41598-017-13064-1

Fedele, T., Ramantani, G., Burnos, S., Hilfiker, P., Curio, G., Grunwald, T., et al. (2017b). Prediction of seizure outcome improved by fast ripples detected in low-noise intraoperative corticogram. *Clin. Neurophysiol.* 128, 1220–1226. doi: 10.1016/j.clinph.2017.03.038

Fedele, T., Schonenberger, C., Curio, G., Serra, C., Krayenbuhl, N., and Sarnthein, J. (2017c). Intraoperative subdural low-noise EEG recording of the high frequency oscillation in the somatosensory evoked potential. *Clin. Neurophysiol.* 128, 1851–1857. doi: 10.1016/j.clinph.2017.07.400

Fedele, T., Ramantani, G., and Sarnthein, J. (2019). High frequency oscillations as markers of epileptogenic tissue—end of the party? *Clin. Neurophysiol.* 130, 624–626. doi: 10.1016/j.clinph.2019.01.016

Fedele, T., van 't Klooster, M., Burnos, S., Zweiphenning, W., van Klink, N., Leijten, F., et al. (2016). Automatic detection of high frequency oscillations during epilepsy surgery predicts seizure outcome. *Clin. Neurophysiol.* 127, 3066–3074. doi: 10.1016/j.clinph.2016.06.009

Frauscher, B., von Ellenrieder, N., Zelmann, R., Rogers, C., Nguyen, D. K., Kahane, P., et al. (2018). High-frequency oscillations in the normal human brain. *Ann. Neurol.* 84, 374–385. doi: 10.1002/ana.25304

Gliske, S. V., Qin, Z. A., Lau, K., Alvarado-Rojas, C., Salami, P., Zelmann, R., et al. (2020). Distinguishing false and true positive detections of high frequency oscillations. *J. Neural Eng.* 17:056005. doi: 10.1088/1741-2552/abb89b

Jacobs, J., Banks, S., Zelmann, R., Zijlmans, M., Jones-Gotman, M., and Gotman, J. (2016). Spontaneous ripples in the hippocampus correlate with epileptogenicity and not memory function in patients with refractory epilepsy. *Epilepsy Behav.* 62, 258–266. doi: 10.1016/j.yebeh.2016.05.025

Jacobs, J., Levan, P., Châtillon, C.-E., Olivier, A., Dubeau, F., and Gotman, J. (2009). High frequency oscillations in intracranial EEGs mark epileptogenicity rather than lesion type. *Brain* 132, 1022–1037. doi: 10.1093/brain/awn351

Jacobs, J., and Zijlmans, M. (2020). HFO to measure seizure propensity and improve prognostication in patients with epilepsy. *Epilepsy Curr.* 20, 338–347. doi: 10.1177/1535759720957308

Jobst, B. C., Bartolomei, F., Diehl, B., Frauscher, B., Kahane, P., Minotti, L., et al. (2020). Intracranial EEG in the 21st century. *Epilepsy Curr.* 20, 180–188. doi: 10.1177/1535759720934852

Klotz, K. A., Sag, Y., Schönberger, J., and Jacobs, J. (2021). Scalp ripples can predict development of epilepsy after first unprovoked seizure in childhood. *Ann. Neurol.* 89, 134–142. doi: 10.1002/ana.25939

Kucewicz, M. T., Cimbalnik, J., Matsumoto, J. Y., Brinkmann, B. H., Bower, M. R., Vasoli, V., et al. (2014). High frequency oscillations are associated with cognitive processing in human recognition memory. *Brain* 137, 2231–2244. doi: 10.1093/brain/awu149

Lévesque, M., Wang, S., Gotman, J., and Avoli, M. (2018). High frequency oscillations in epileptic rodents: are we doing it right? *J. Neurosci. Methods* 299, 16–21. doi: 10.1016/j.jneumeth.2018.02.011

Nagasawa, T., Juhasz, C., Rothermel, R., Hoechstetter, K., Sood, S., and Asano, E. (2012). Spontaneous and visually driven high-frequency oscillations in the occipital cortex: intracranial recording in epileptic patients. *Hum. Brain Mapp.* 33, 569–583. doi: 10.1002/hbm.21233

Nariai, H., Hussain, S. A., Bernardo, D., Fallah, A., Murata, K. K., Nguyen, J. C., et al. (2019). Prospective observational study: fast ripple localization delineates the epileptogenic zone. *Clin. Neurophysiol.* 130, 2144–2152. doi: 10.1016/j.clinph.2019.08.026

Noorlag, L., van Klink, N., Huiskamp, G., and Zijlmans, M. (2019). What are you looking at? Unrippling terminology for high frequency activity. *Clin. Neurophysiol.* 130, 2132–2133. doi: 10.1016/j.clinph.2019.09.002

Oostenveld, R., Fries, P., Maris, E., and Schoffelen, J. M. (2011). FieldTrip: open source software for advanced analysis of MEG, EEG, and invasive electrophysiological data. *Comput. Intell. Neurosci.* 2011:156869. doi: 10.1155/2011/156869

Pail, M., Cimbálník, J., Roman, R., Daniel, P., Shaw, D. J., Chrastina, J., et al. (2020). High frequency oscillations in epileptic and non-epileptic human hippocampus during a cognitive task. *Sci. Rep.* 10:18147. doi: 10.1038/s41598-020-74306-3

Remakanthakurup Sindhu, K., Staba, R., and Lopour, B. A. (2020). Trends in the use of automated algorithms for the detection of high-frequency oscillations associated with human epilepsy. *Epilepsia* 61, 1553–1569. doi: 10.1111/epi.16622

Schacher, M., Haemmerle, B., Woermann, F. G., Okujava, M., Huber, D., Grunwald, T., et al. (2006). Amygdala fMRI lateralizes temporal lobe epilepsy. *Neurology* 66, 81–87. doi: 10.1212/01.wnl.0000191303.91188.00

Stolk, A., Griffin, S., van der Meij, R., Dewar, C., Saez, I., Lin, J. J., et al. (2018). Integrated analysis of anatomical and electrophysiological human intracranial data. *Nat. Protoc.* 13, 1699–1723. doi: 10.1038/s41596-018-0009-6

van 't Klooster, M. A., Leijten, F. S., Huiskamp, G., Ronner, H. E., Baayen, J. C., van Rijen, P. C., et al. (2015). High frequency oscillations in the intra-operative ECoG to guide epilepsy surgery ("The HFO Trial"): study protocol for a randomized controlled trial. *Trials* 16:422. doi: 10.1186/s13063-015-0932-6

van 't Klooster, M. A., van Klink, N. E. C., Zweiphenning, W., Leijten, F. S. S., Zelmann, R., Ferrier, C. H., et al. (2017). Tailoring epilepsy surgery with fast ripples in the intraoperative electrocorticogram. *Ann. Neurol.* 81, 664–676. doi: 10.1002/ana.24928

Weiss, S. A., Berry, B., Chervoneva, I., Waldman, Z., Guba, J., Bower, M., et al. (2018). Visually validated semi-automatic high-frequency oscillation detection aides the delineation of epileptogenic regions during intra-operative electrocorticography. *Clin. Neurophysiol.* 129, 2089–2098. doi: 10.1016/j.clinph.2018.06.030

Weiss, S. A., Song, I., Leng, M., Pastore, T., Slezak, D., Waldman, Z., et al. (2020). Ripples have distinct spectral properties and phase-amplitude coupling with slow waves, but indistinct unit firing, in human epileptogenic hippocampus. *Front. Neurol.* 11:174. doi: 10.3389/fneur.2020.00174

Weiss, S. A., Waldman, Z., Raimondo, F., Slezak, D., Donmez, M., Worrell, G., et al. (2019). Localizing epileptogenic regions using high-frequency oscillations and machine learning. *Biomark. Med.* 13, 409–418. doi: 10.2217/bmm-2018-0335

Zaveri, H. P., Duckrow, R. B., and Spencer, S. S. (2006). On the use of bipolar montages for time-series analysis of intracranial electroencephalograms. *Clin. Neurophysiol.* 117, 2102–2108. doi: 10.1016/j.clinph.2006.05.032

Zweiphenning, W. J. E. M., van Diessen, E., Aarnoutse, E. J., Leijten, F. S. S., van Rijen, P. C., Braun, K. P. J., et al. (2020). The resolution revolution: comparing spikes and high frequency oscillations in high-density and standard intra-operative electrocorticography of the same patient. *Clin. Neurophysiol.* 131, 1040–1043. doi: 10.1016/j.clinph.2020.02.006

**Conflict of Interest**: The authors declare that the research was conducted in the absence of any commercial or financial relationships that could be construed as a potential conflict of interest.

The handling Editor is currently organizing a Research Topic with one of the authors JS.

*Copyright © 2021 Boran, Stieglitz and Sarnthein. This is an open-access article distributed under the terms of the Creative Commons Attribution License (CC BY). The use, distribution or reproduction in other forums is permitted, provided the original author(s) and the copyright owner(s) are credited and that the original publication in this journal is cited, in accordance with accepted academic practice. No use, distribution or reproduction is permitted which does not comply with these terms.*

frontiers in Neurology

ORIGINAL RESEARCH
published: 05 March 2021
doi: 10.3389/fneur.2021.620670

# Effects of Spatial Memory Processing on Hippocampal Ripples

*Daniel Lachner-Piza[1]*, Lukas Kunz[1,2,3], Armin Brandt[1], Matthias Dümpelmann[1], Aljoscha Thomschewski[4] and Andreas Schulze-Bonhage[1]*

[1] Epilepsy Center, Medical Center–University of Freiburg, Faculty of Medicine, University of Freiburg, Freiburg im Breisgau, Germany, [2] Spemann Graduate School of Biology and Medicine (SGBM), University of Freiburg, Freiburg im Breisgau, Germany, [3] Faculty of Biology, University of Freiburg, Freiburg im Breisgau, Germany, [4] Department of Neurology, Paracelsus Medical University Salzburg, Salzburg, Austria

Human High-Frequency-Oscillations (HFO) in the ripple band are oscillatory brain activity in the frequency range between 80 and 250 Hz. HFOs may comprise different subgroups that either play a role in physiologic or pathologic brain functions. An exact differentiation between physiologic and pathologic HFOs would help elucidate their relevance for cognitive and epileptogenic brain mechanisms, but the criteria for differentiating between physiologic and pathologic HFOs remain controversial. In particular, the separation of pathologic HFOs from physiologic HFOs could improve the identification of epileptogenic brain regions during the pre-surgical evaluation of epilepsy patients. In this study, we performed intracranial electroencephalography recordings from the hippocampus of epilepsy patients before, during, and after the patients completed a spatial navigation task. We isolated hippocampal ripples from the recordings and categorized the ripples into the putative pathologic group *iesRipples*, when they coincided with interictal spikes, and the putative physiologic group *isolRipples*, when they did not coincide with interictal spikes. We found that the occurrence of *isolRipples* significantly decreased during the task as compared to periods before and after the task. The rate of *iesRipples* was not modulated by the task. In patients who completed the spatial navigation task on two consecutive days, we furthermore examined the occurrence of ripples in the intervening night. We found that the rate of ripples that coincided with sleep spindles and were therefore putatively physiologic correlated with the performance improvement on the spatial navigation task, whereas the rate of all ripples did not show this relationship. Together, our results suggest that the differentiation of HFOs into putative physiologic and pathologic subgroups may help identify their role for spatial memory and memory consolidation processes. Conversely, excluding putative physiologic HFOs from putative pathologic HFOs may improve the HFO-based identification of epileptogenic brain regions in future studies.

**Keywords: high-frequency oscillations, ripples, interictal epileptiform spikes, sleep spindles, hippocampus, cognition, memory consolidation, spatial memory**

OPEN ACCESS

***Edited by:***
*Maeike Zijlmans, University Medical Center Utrecht, Netherlands*

***Reviewed by:***
*Jan Cimbalnik, International Clinical Research Center (FNUSA-ICRC), Czechia*
*Eleonora Tamilia, Boston Children's Hospital and Harvard Medical School, United States*

****Correspondence:***
*Daniel Lachner-Piza*
*daniel.lachner@uniklinik-freiburg.de*

***Specialty section:***
*This article was submitted to Epilepsy, a section of the journal Frontiers in Neurology*

***Received:*** *26 October 2020*
***Accepted:*** *04 February 2021*
***Published:*** *05 March 2021*

***Citation:***
*Lachner-Piza D, Kunz L, Brandt A, Dümpelmann M, Thomschewski A and Schulze-Bonhage A (2021) Effects of Spatial Memory Processing on Hippocampal Ripples. Front. Neurol. 12:620670. doi: 10.3389/fneur.2021.620670*

## INTRODUCTION

High Frequency Oscillations (HFO) are an electrographic manifestation of hyper-synchronized neurons and are subdivided into Ripples and Fast-Ripples according to the frequency range of the oscillations (80–250 and 250–500 Hz, respectively) (1, 2). In the field of epilepsy, Ripples and Fast-Ripples were initially considered improved biomarkers of epileptogenic networks (3–8).

However, recent research has drawn a more complex picture (9–11) and has highlighted the importance of being able to differentiate between physiologic and pathologic HFOs.

Interictal Epileptic Spikes (IES) are another type of epileptic biomarker. IES are common in patients with epilepsy, have a waveform of a fast transient, are commonly generated in epileptic cortex and reflect a hyper-excitability of neural networks (12). IES are very sensitive but not specific to epileptogenic areas (13, 14). Ripples are known to coincide temporally and spatially with IES to some extent. These IES coincident Ripples appear to have different amplitude and waveform characteristics when compared to Ripples associated with physiologic events such as sleep spindles (15). IES coincident Ripples may be more sensitive to the seizure-onset-zone than Fast-Ripples and also more specific to it than Ripples occurring in isolation from IES (16). IES coincident Ripples may better predict post-surgical outcomes than Ripples not coinciding with IES (17) and Ripples coinciding with IES showed the highest correspondence with the resected volume in seizure-free patients as compared to other HFO subgroups (18). Moreover, a combined marker composed of IES and HFO occurrence rates appeared to be useful for estimating the epileptogenic zone (11). Together, the coincidence with IES may constitute a good criterion for separating pathologic Ripples from physiologic Ripples.

Sleep spindles are a third type of electrographic pattern which is observed in the human electroencephalogram (EEG) recorded with scalp or implanted electrodes (19). Sleep-spindle events have a distinct oscillatory waveform with durations between 0.5 and 3.0 s and frequencies between 11 and 16 Hz (20–22). Sleep spindles are generated and controlled by thalamic networks, with several hypotheses linking them to gating functions of sensory information flow. However, so far, the complete and definitive functional meaning of sleep spindles remains to be explored (23). Amongst others, sleep spindles may be relevant for memory consolidation during sleep, particularly when coupled to hippocampal Ripples (24–32). The occurrence rate of sleep spindle-coupled Ripples during sleep may thus reflect the intensity of memory consolidation.

Based on this prior knowledge, we hypothesized in the current study that hippocampal ripples could be differentiated into a putatively pathologic subgroup (*iesRipples*) and a putatively physiologic subgroup (*isolRipples*) based on their temporal and spatial coincidence with IES: *iesRipples* should coincide with an IES temporally (i.e., occurring within the duration of an IES) and spatially (i.e., when recorded on the same channel as an IES), whereas *isolRipples* should occur in isolation. Moreover, we hypothesized that ripples temporally co-occurring with ipsilateral hippocampal sleep spindles (*spindleRipples*) could serve as a marker for memory-consolidation processes. In our analyses, we therefore assessed whether the occurrence rates of *iesRipples* and of *isolRipples* were altered during the spatial navigation task. The spatial navigation task required the patients to form associative memories between objects and their corresponding locations and thus imposed an increased cognitive demand on the patients. Since physiological ripples are associated with cognitive functioning, we hypothesized that the rate of *isolRipples* should be altered during the task, whereas the activity of *iesRipples* should be unaffected. Additionally, in patients who performed the spatial navigation task on two consecutive days, we assessed the correlation between the occurrence rate of *spindleRipples* in the intervening night and the performance improvement of the patients between both days. Based on the proposed role of sleep spindle-coupled ripples in memory consolidation, we hypothesized that a higher rate of *spindleRipples* should be associated with a greater performance improvement.

# METHODS

## Patient Selection

Participating patients (**Table 1**) suffered from pharmaco-resistant focal epilepsy and underwent intracranial EEG (iEEG) recordings from the hippocampus to identify their seizure onset zone at the Freiburg Epilepsy Center, Germany. The clinical decision for the implantation of iEEG electrodes was made individually for each patient in cases when the epileptogenic zone remained unclear using non-invasive methods. All patients gave their informed consent to participate in a study aiming at the identification of electrophysiological correlates of cognitive processing, including a spatial navigation task. A total of 19 patients performing the spatial navigation task were included in the current study, 9 of which completed the spatial navigation task on two subsequent days. All patients gave their written informed consent and the study was approved by the Ethics Committee of the Freiburg University Medical Center.

## Spatial Navigation Paradigm

The spatial navigation paradigm was adapted from previous studies (33–35). In this paradigm, the patients performed an object-location memory task navigating freely in a circular virtual environment. The environment comprised a grassy plain bounded by a cylindrical cliff. Two mountains, a sun, and several clouds provided patients with distal orientation cues. Patients completed the task on a laptop using the arrow keys for moving forward and turning left and right and the spacebar to indicate their response. Patients were asked to complete up to 160 trials but were instructed to pause or quit the task whenever they wanted. At the very beginning, patients collected eight everyday objects (randomly drawn from a total number of 12 potential objects) from different locations in the arena. Objects appeared one after the other. Afterward, patients completed variable numbers of trials, depending on compliance. Each trial consisted of four different phases (**Figure 1**). First, one of the eight objects was presented for 2 s (cue presentation). Afterwards, patients were asked to navigate to the associated object location within the virtual environment (retrieval). After patients had indicated their response via a button press at the assumed object location, they received feedback depending on response accuracy. Response accuracy was measured as the distance between the remembered location and the correct location (drop error). Last, the object was presented in the correct location, and patients had to collect the object from there to further improve their associative memory between the object and its location. After each trial, a fixation crosshair was shown for a variable duration of 3–5 s. Triggers were detected using a phototransistor attached to the screen

**TABLE 1 |** Patient information.

| Patient ID | Age | Sex | Paradigm No. | No. trials | Duration pre-, intra- and post-paradigm phases (m) | No. hippocampal bipolar channels | Implantation side |
|---|---|---|---|---|---|---|---|
| 1 | 45 | F | 1 | 51 | 48 | 4 | Bilateral |
| 2 | 34 | M | 1 | 129 | 51 | 3 | Right |
| | | | 2 | 152 | 45 | | |
| 3 | 28 | F | 1 | 160 | 51 | 3 | Right |
| | | | 2 | 131 | 53 | | |
| 4 | 36 | F | 1 | 91 | 53 | 1 | Right |
| | | | 2 | 85 | 39 | | |
| 5 | 28 | M | 1 | 160 | 47 | 2 | Left |
| 6 | 29 | M | 1 | 160 | 54 | 4 | Bilateral |
| | | | 2 | 160 | 48 | | |
| 7 | 44 | F | 1 | 54 | 21 | 5 | Bilateral |
| | | | 2 | 60 | 43 | | |
| 8 | 23 | F | 1 | 98 | 41 | 4 | Bilateral |
| 9 | 25 | F | 1 | 151 | 72 | 2 | Left |
| | | | 2 | 81 | 39 | | |
| 10 | 27 | F | 1 | 76 | 36 | 2 | Left |
| 11 | 32 | M | 1 | 91 | 57 | 3 | Right |
| | | | 2 | 114 | 45 | | |
| 12 | 48 | M | 1 | 126 | 64 | 1 | Left |
| 13 | 49 | M | 1 | 160 | 81 | 4 | Bilateral |
| 14 | 25 | F | 1 | 82 | 46 | 3 | Right |
| 15 | 29 | M | 1 | 102 | 42 | 1 | Right |
| 16 | 49 | M | 1 | 54 | 39 | 4 | Bilateral |
| 17 | 43 | M | 1 | 102 | 57 | 1 | Left |
| 18 | 27 | F | 1 | 31 | 18 | 1 | Right |
| | | | 2 | 75 | 39 | | |
| 19 | 19 | M | 1 | 160 | 58 | 4 | Bilateral |
| | | | 2 | 160 | 50 | | |

marking onsets and offsets of the cue presentation phase. The intra-paradigm period of the iEEG was then delimited by the first and last phototransistor triggers. We calculated the patients' performance in each trial as the ratio between the drop error and the largest possible drop error (maximum random drop error):

$$Performance_{Single\ Trial} = 1 - \frac{Drop\ Error}{Maximum\ Random\ Drop\ Error}$$

The largest possible drop error in a given trial was determined by creating one million random locations within the virtual environment and then selecting the location with the largest Euclidean distance to the correct object location. The performance for the entire paradigm was calculated as the median performance across all trials.

## Identification of Hippocampal and White Matter Channels

Preimplantation and post-implantation MRI scans were available for all patients. Electrode localization was performed using FSL (https://fsl.fmrib.ox.ac.uk/fsl/fslwiki/FSL) and PyLocator (http://pylocator.thorstenkranz.de/). The post-implantation MR image was coregistered with the preimplantation MR image. Next, the preimplantation MR image was skull-stripped and normalized to MNI space, and the same normalization matrix was applied to the post-implantation MR image. Normalized post-implantation images were visually inspected using PyLocator, and channel locations were manually identified. For the analyses in this study, we only considered electrode channels located in the right or left hippocampus.

## Detection of Ripples, *isolRipples*, *iesRipples*, and IES

Intracranial EEG data were recorded using "Profusion EEG Software" (Compumedics Limited, Abbotsford Victoria, Australia). Original signals were low-pass filtered at 800 Hz and sampled at 2 kHz using Cz as a hardware reference. All signal analyses were performed using bipolar montages.

The detection of Ripples and IES on the hippocampal iEEG signals was accomplished by using automatic detectors (36), which were based on multivariate classifications of iEEG epochs using kernelized support-vector-machines. The spectral analysis

of these detections was performed using the Morlet wavelet transform, the maximum and minimum frequencies clustering the events' power corresponded to those frequency-bins with a power contribution within that one of the spectral peak (i.e., the frequency with the maximum power contribution) +/– the standard deviation of the power across all frequency bins.

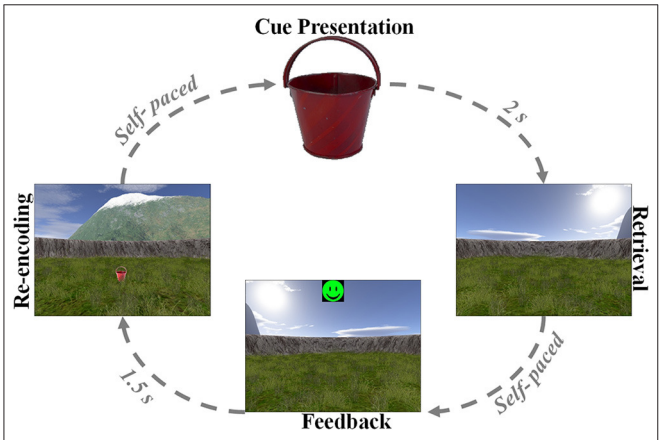


**FIGURE 1 |** Associative object-location memory task during virtual spatial navigation. At the beginning of the experiment, patients collected eight different objects from different locations within the virtual environment. Afterward, patients completed variable numbers of retrieval trials, during which they were first presented with one of the eight objects serving as cue (cue presentation). Patients then navigated to the remembered location of that object (retrieval) and made a response. Following this response, patients received feedback *via* an emoticon (feedback) and had to collect the object from its correct location (re-encoding).

The automatic detectors were run on time-selected segments of the hippocampal iEEG signals. These segments corresponded to the pre-, intra- and post-paradigm phases. The intra-paradigm phase was delimited by the first and last cue-presentation triggers. The duration of the pre- and post-paradigm phases was the same as for the intra-paradigm phase. The pre-paradigm phase ended 30 min before the start of the intra-paradigm phase and the post-paradigm phase started 30 min after the end of the intra-paradigm phase.

The automatic detectors provided discrete events of the classes Ripples and IES. Each event comprised a start time and an end time. We used custom scripts in MATLAB 2018b that determined the temporal and spatial coincidence of the Ripples and IES in order to identify ripples belonging to the class *iesRipples*. Ripples which were not coincident with IES formed the class *isolRipples*. For each class of ripples, we then calculated their occurrence rate per minute in each of the hippocampal channels. If a patient had more than one hippocampal electrode, we averaged the occurrence rates across the different hippocampal channels (**Figure 2**).

## Analysis of the Ripples, *isolRipples*, *iesRipples*, and IES Activity

We tested for the effect of the spatial navigation paradigm on the occurrence rate of Ripples, *isolRipples*, *iesRipples*, and IES

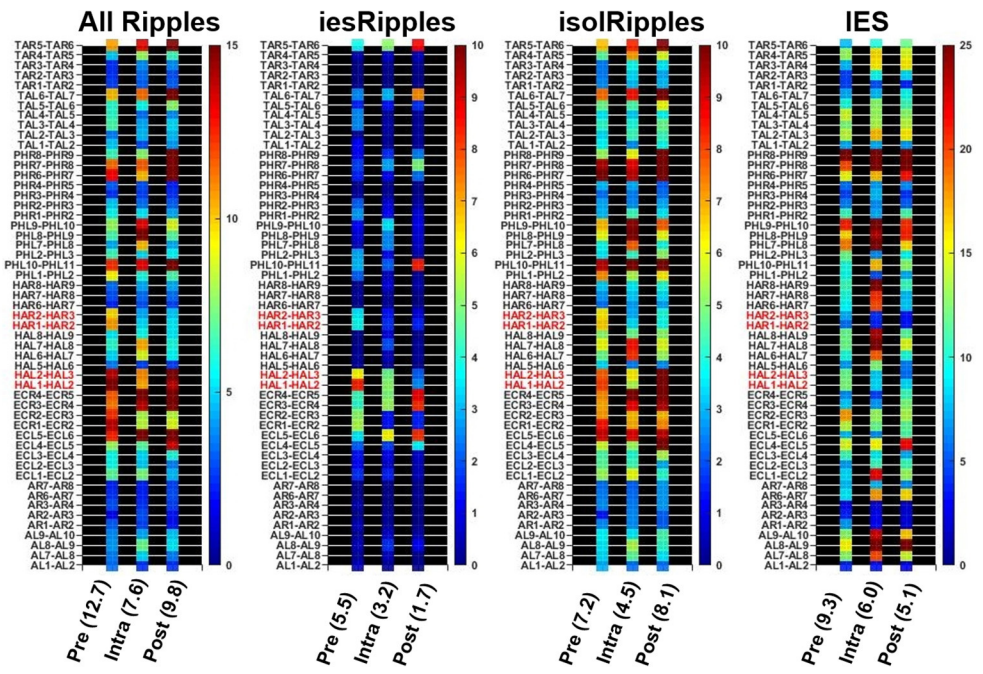


**FIGURE 2 |** Determining the hippocampal activity for Patient 16 and each event class. Firstly, the automatic detections of Ripples, *iesRipples*, *isolRipples*, and IES were used to characterize each channel (y-axes) with their occurrence rate per minute (heat-maps). The specific brain region Hippocampus (red channel labels) was then characterized by the average occurrence rate across all hippocampal channels. The average hippocampal activity for each event class and the pre-, intra- and post-paradigm segments is shown in parentheses on the x-axis.

using the data from all 19 patients. In patients who performed the task on two consecutive days, we only used the data from the first day for this analysis in order to avoid that these patients had a stronger effect on the statistical results. A mixed ANOVA was conducted to test for main effects and interactions between the factors "time period" (pre-, intra- and post-paradigm phase) and "ripple class" (*isolRipples* vs. *iesRipples*) on the occurrence rate of hippocampal ripples. In a *post-hoc* analysis, we firstly used a two-tailed, non-parametric Wilcoxon signed rank test to analyze whether the occurrence rates differed (i) between the pre-paradigm and the intra-paradigm phase, (ii) between the intra-paradigm phase and the post-paradigm phase, and (iii) between the control phases pre-paradigm and post-paradigm; at this stage no correction for multiple comparisons was applied since the families (i.e., pre vs. intra, intra vs. post, pre vs. post) had no repeated analyses (i.e., $\alpha = 0.05$) (37). Finally, as part of the same *post-hoc* analysis, we performed either a subsequent left-tailed or a right-tailed Wilcoxon signed rank test to analyze if the activity-difference between phases corresponded to an increase or a decrease; at this stage a Bonferroni correction was applied to the significance threshold (i.e., $\alpha = 0.025$) since two null hypotheses were considered (two-tailed and one-tailed Wilcoxon signed rank tests).

## Detection of *spindleRipples*

The *spindleRipple* events corresponded to those Ripples which were temporally and spatially coincident with hippocampal sleep spindles. The detection of hippocampal sleep spindles was achieved using an automatic detector (38) based on multivariate classifications of iEEG epochs using kernelized support-vector-machines. We used a custom MATLAB 2018b script to determine coinciding ripples and sleep spindles, which then composed the class *spindleRipples*. Only ripples that were completely within the start and end time of a sleep spindle were considered to be temporally coincident. The spatial coincidence of a ripple and a sleep spindle was present if they were both hippocampal and ipsilateral. All ripples complying with these rules of temporal and spatial coincidence comprised the *spindleRipples* class.

We estimated the occurrence rate of *spindleRipples* in patients who performed the spatial navigation task on two consecutive days. For all these patients, we used the data between 10:00 pm of the first day and 6:00 am of the second day to estimate the occurrence rate of *spindleRipples*. This time period was selected with the aim of maximizing the inclusion of non-rapid eye movement N2 sleep stages, since the occurrence and power of sleep spindles is highest during this sleep stage (21, 23, 39, 40). If a patient had more than one hippocampal electrode channel, we averaged the channel-specific *spindleRipple* rates across the different channels to obtain one overall occurrence rate, which quantified the number of *spindleRipples* per minute.

## Analysis of *spindleRipples* and Their Correlation With Spatial Navigation Performance

This analysis was only performed with the data from the patients who performed the spatial navigation task on two consecutive days. To test whether the occurrence rates of *spindleRipples* could be a marker of memory consolidation of the associative object-location memories that the patients formed during the spatial navigation task, we calculated the correlation between *spindleRipple* rates and the difference in performance obtained on days 1 and 2 (performance $\Delta$). A non-paired, non-parametric, left-tailed Mann–Whitney U test was applied to each patient using all their trials from days 1 and 2 to test if the performance $\Delta$ was significant. The correlation between the hippocampal *spindleRipple* rates and the performance $\Delta$ was measured using Spearman's rank correlation coefficient. As a control, we quantified this relationship while controlling for the potential effect of the number of trials on day 1 using a partial correlation.

# RESULTS

## Navigation Paradigm

A total of 19 patients completed the spatial navigation task (day 1). A subgroup of nine patients completed the spatial navigation task also on the subsequent day (day 2). The performance from each patient was measured as the median performance across all trials. For day 1, the maximum, minimum and mean performance corresponded to 86% (patient 9), 48% (patient 7) and 67 $\pm$ 11% (mean $\pm$ *SD*), respectively (**Figure 3A**).

In the subgroup of the 9 patients conducting the paradigm on two consecutive days, the maximum, minimum and mean performance on day 1 corresponded to 86% (patient 9), 48% (patient 7), and 72 $\pm$ 12%, respectively. On day 2, the maximum, minimum, and mean performance corresponded to 93% (patient 9), 53% (patient 7), and 79 $\pm$ 13%, respectively (**Figure 3B**). All patients showed a significant performance improvement, when comparing day 1 with day 2 (left-tailed Mann–Whitney *U*, all $p < 0.025$).

## Detection of *isolRipples* and *iesRipples*

The automatic detection on the hippocampal channels generated an average of 1,762 Ripple events and 1,042 IES events per patient across the pre-, intra- and post-paradigm phases. Of these Ripples, 74% occurred isolated from IES and were thus labeled *isolRipples*; the remaining 26% of the Ripples occurred spatially and temporally coinciding with an IES and were thus labeled *iesRipples*. A depiction of example waveforms and the corresponding spectrograms of *isolRipples* and *iesRipples* is provided in **Figure 4**.

A challenge when detecting HFOs is the correct handling of fast transients which, when filtered, can produce artifacts resembling authentic HFOs (41, 42). A depiction of the waveform and spectrogram of the IES detections is provided in **Figure 4** in order to show the handling of fast transients by the automatic detectors and to allow the comparison with the spectrogram from the detected Ripples. The *isolRipples* showed a distinct increase in power within a narrow band which resembled a blob in the spectrogram, the tuples (Hz) consisting of the spectral-peak, blob-lower-frequency and blob-higher-frequency for the single-event, averaged-events and patients-average were (117, 82, 144), (109, 82, 144), and (109, 88, 144), respectively. This

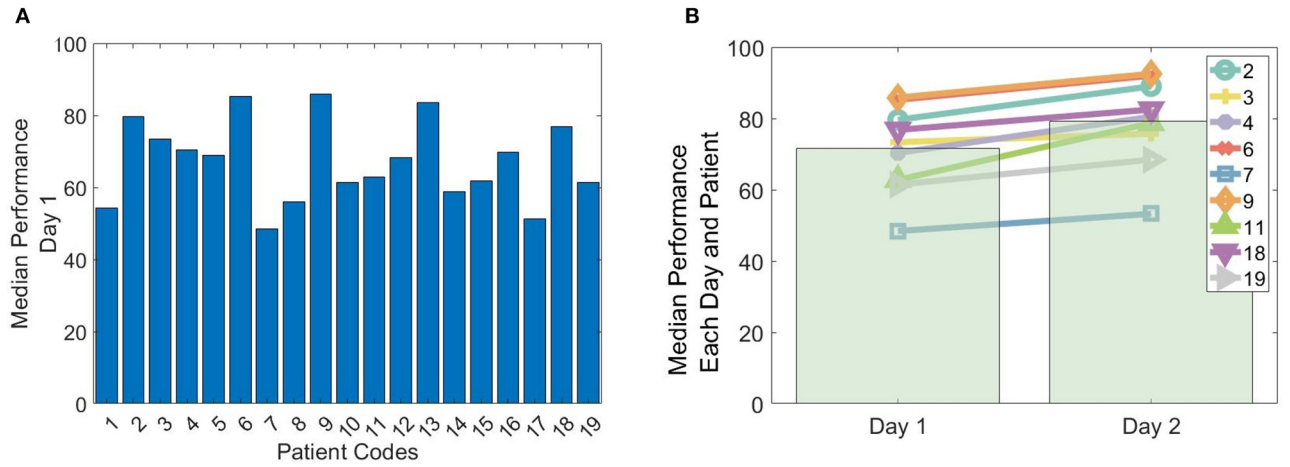


**FIGURE 3 |** Performance in the spatial navigation paradigm. **(A)** Median performance across trials obtained by the 19 patients on their first (or only) day of conducting the spatial-navigation task. **(B)** The line plots depict the median performance across trials for each of the nine patients that conducted the spatial navigation paradigm on 2 consecutive days (day 1 and 2). The bar plots depict the average across patients.

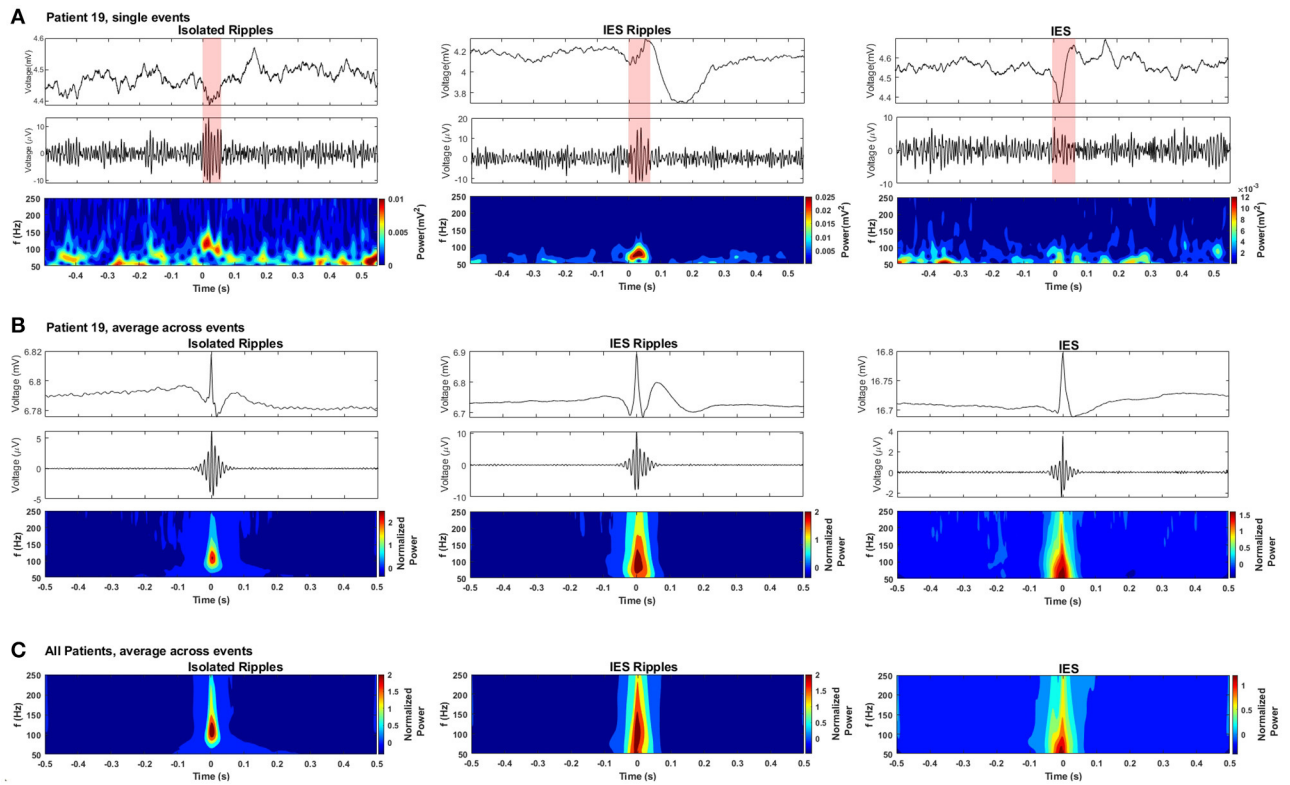


**FIGURE 4 |** Detected hippocampal ripples and spikes. **(A)** Selected events from each event type: the- first row shows the waveform from the raw EEG, the second row shows the waveform from the bandpassed EEG (80–250 Hz), the third row shows the spectrogram from each event-type obtained using a Morlet wavelet transform. **(B)** Average event-types from patient 19. **(C)** Grand average of the three event-types from all patients.

blob-like power increase was also shown by *iesRipples* when considering only patient 19. The same tuples for *iesRipples* were (82, 82, 102), (102, 82, 144), and (109, 82, 165), respectively.

The spectrogram of the IES depicted in the third column of **Figure 4** showed typical spectral characteristics of a fast-transient, which much like a single pulse are represented

in all frequency bins when analyzed by a time-frequency transformation. The key characteristic that differentiates a filtering artifact from a real HFO event is then this blob-like, narrow-band power increase which is shown by the spectrograms of both *isolRipples* and *iesRipples*.

The events forming the averages in **Figure 4** were centered using their maximum peak. Hence a peak was formed at the center of the raw averages while surrounding samples were canceled because of varying pre- and post-event waveforms across events.

## Modulation of Ripple Activity by Increased Cognitive Demands During the Spatial Navigation Task

The mixed ANOVA test showed a non-significant main effect of time period (pre-, intra-, post-paradigm) ($F = 0.679$, $p = 0.510$), a significant main effect of the ripple class (*isolRipples, iesRipples)* ($F = 8.948$, $p < 0.005$), and a significant interaction between both factors ($F = 4.069$, $p < 0.025$). To further understand this interaction, we performed *post-hoc* analyses (Wilcoxon signed rank tests).

We found no significant differences in the occurrence rates of *allRipples* for the pair-wise comparisons (pre-paradigm vs. intra-paradigm, $p < 0.717$; intra-paradigm vs. post-paradigm, $p < 0.243$; pre-paradigm vs. post-paradigm, $p < 0.314$). Hence, the increased cognitive load exerted by the spatial-navigation paradigm did not modulate the activity from the *allRipples* event class.

For *isolRipples*, the comparison pre-paradigm vs. intra-paradigm showed a significant difference ($p < 0.043$), the subsequent right-tailed test showed a significance of $p < 0.022$, hence the *isolRipples* presented an activity decrease when transitioning from the pre- to the intra-paradigm phase. Similarly, the comparison of *isolRipples* from the intra-paradigm vs. post-paradigm phase showed a significant difference ($p < 0.007$), the subsequent left-tailed test showed a significance of $p < 0.004$. Hence, the *isolRipples* presented an activity increase when transitioning from the intra- to the post-paradigm phase. When comparing the occurrence rates of *isolRipples* during the control phases pre-paradigm and post-paradigm, no significant difference was found ($p > 0.314$). In summary, the increased cognitive load exerted by the spatial navigation paradigm did modulate the activity from the *isolRipples* in a way that their activity was reduced during the paradigm (**Figure 5**), additionally, the *isolRipples* activity returned to the pre-paradigm control values after the phase of increased cognitive load.

We found no significant differences in the occurrence rates of *iesRipples* for the pair-wise comparisons (pre-paradigm vs. intra-paradigm, $p > 0.277$; intra-paradigm vs. post-paradigm, $p > 0.295$; pre-paradigm vs. post-paradigm, $p > 0.260$). Thus, the increased cognitive load exerted by the spatial navigation paradigm did not modulate the activity from the *iesRipples* event class.

For IES, we found no significant differences for the pair-wise comparisons pre-paradigm vs. intra-paradigm ($p > 0.778$) and intra-paradigm vs. post-paradigm phase ($p > 0.260$); however, the IES activity from the control phase pre-paradigm was significantly different from the post-paradigm activity ($p < 0.022$), the subsequent left-tailed test showed a significance of $p < 0.012$. These results suggest that the IES activity was not modulated by the increased cognitive load, however the IES activity from the post-paradigm control phase was higher than the IES activity during the pre-paradigm control phase.

The results described in this section are also shown in **Table 2** and summarized in **Figure 5**.

## Improvement in Performance and the Correlation With *spindleRipples*

An example of a detected sleep spindle is presented in **Figure 6**. The performances obtained by the patients when conducting the spatial navigation task on days 1 and 2 are presented in **Table 3**.

As previously mentioned, all the patients' performance for the navigation task improved on day 2 when comparing it with day 1 (left-tailed Mann–Whitney $U$ all $p < 0.025$). During the night between the two sessions of the spatial navigation task, hippocampal Ripples were detected and their occurrence rate (incidences per minute) was obtained. We found that the activity from the *allRipples* event class showed no correlation with the patients' performance improvement when repeating the spatial navigation task ($rho = 0.13$, $p = 0.74$; controlling for the number trials on day 1: $rho = 0.05$, $p = 0.90$). In contrast, the occurrence rate of the detected *spindleRipples* showed a significant positive correlation with performance improvement ($rho = 0.73$, $p = 0.03$; controlling for the number of trials on day 1, $rho = 0.77$, $p < 0.03$) (**Figure 7**).

As a control, we also computed correlations between the occurrence rate of ripples and the performance values on both days in order to present evidence that the association was presumably due to the learning process and not simply related to the patients' general performance level. These correlations were not significant (for performance on day 1 and *allRipples* rate, $rho = 0.17$, $p = 0.68$; performance on day 1 and *spindleRipples* rate, $rho = -0.14$, $p = 0.74$; performance on day 2 and *allRipples* rate, $rho = 0.32$, $p = 0.41$; performance on day 2 and *spindleRipples* rate, $rho = 0.05$, $p = 0.91$).

# DISCUSSION

In this study, we examined the activity of putatively physiologic and pathologic ripples in the human hippocampus during a spatial navigation task. We differentiated between the two groups of ripples by analyzing their coincidence with interictal spikes. We found that the rate of the putatively physiologic ripples, *isolRipples,* decreased during the task as compared to pre- and post-task phases, whereas the putatively pathologic ripples, *iesRipples*, did not show this effect. In addition, the ripples associated with hippocampal sleep spindles, *spindleRipples*, showed a positive correlation with the performance improvement of patients who completed the spatial navigation task on two consecutive days.

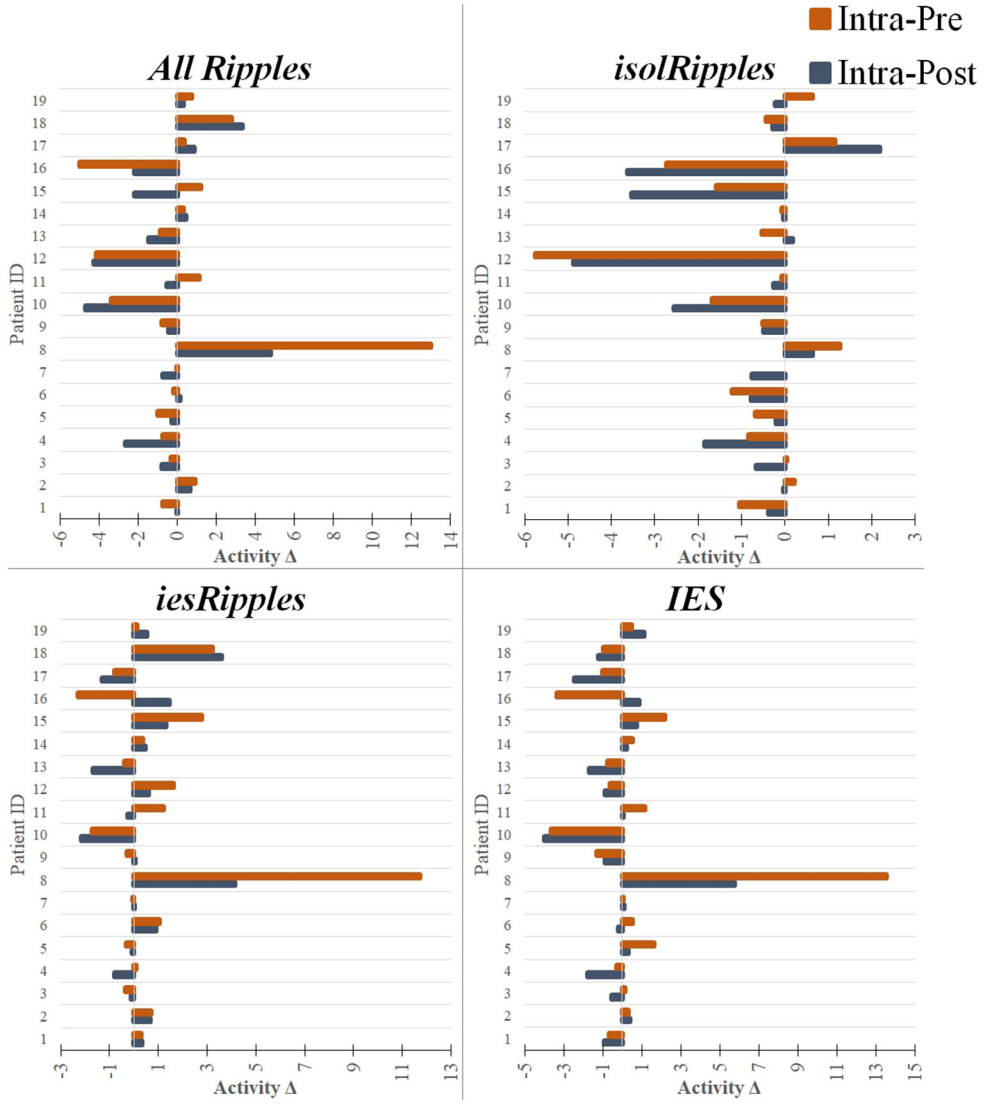


**FIGURE 5 |** Modulation of the event-classes by the increased cognitive load. The bar plots show pairs of activity differences between phases (Activity Δ), i.e., difference between the intra- and pre-paradigm phase (orange) and difference between the intra- and post-paradigm phase (blue), for each patient and using each of the event-classes. The bar plots with a negative value indicate a decrease in activity when entering or leaving the period of increased cognitive load (i.e., intra-paradigm phase). The bar plots with a positive value indicate an increase in activity during the paradigm when compared to the pre- or post-paradigm phases. The hippocampal *isolRipples* were the only event-class to show a significant modulation by the navigation task, presenting an activity decrease when comparing the intra-paradigm occurrence rates with those from both the preceding (pre-paradigm, $p < 0.043$) and succeeding (post-paradigm, $p < 0.007$) control phases.

In summary, the increased cognitive demands from the spatial navigation task exerted differential effects on *iesRipples* and *isolRipples*; these results [in addition to previously published evidence showing *iesRipples* as the most and *isolRipples* as the least accurate estimator of the epileptogenic-zone (18)] hence provide further evidence to support the putatively physiologic and pathologic nature initially attributed to *isolRipples* and *iesRipples*. Furthermore, our study suggests that ripples associated with sleep spindles may constitute a marker of memory-consolidation processes.

Our analysis was focused on the hippocampus, as it plays a major role for both spatial navigation (24–30) and declarative memory formation (43–50) and is a candidate region for generating epileptic activity (51, 52) and is therefore often assessed for the decision making and planning for surgical epilepsy therapy.

Our first goal was to analyze the activity of putative physiologic and putative pathologic Ripples during periods when the cognitive load was higher than normal and then compare this activity with controls coming from periods with a lower

**TABLE 2 |** Ripple and IES activity in the pre-, intra- and post-paradigm iEEG segments.

| Patient ID | iEEG segment duration (min) | Average hippocampal occurrence rate / min | | | | | | | | | | | |
|---|---|---|---|---|---|---|---|---|---|---|---|---|---|
| | | All Ripples | | | *isolRipples* | | | *iesRipples* | | | *IES* | | |
| | | Pre | Intra | Post | Pre | Intra | Post | Pre | Intra | Post | Pre | Intra | Post |
| 1 | 48 | 9.06 | 8.30 | 8.34 | 7.21 | 6.16 | 6.55 | 1.85 | 2.13 | 1.80 | 4.80 | 4.14 | 5.05 |
| 2 | 51 | 2.82 | 3.73 | 3.09 | 2.03 | 2.24 | 2.27 | 0.79 | 1.49 | 0.82 | 2.85 | 3.17 | 2.78 |
| 3 | 51 | 7.81 | 7.50 | 8.30 | 6.82 | 6.86 | 7.53 | 0.99 | 0.64 | 0.77 | 3.32 | 3.48 | 4.04 |
| 4 | 53 | 7.54 | 6.77 | 9.41 | 4.52 | 3.68 | 5.53 | 3.02 | 3.09 | 3.88 | 3.99 | 3.69 | 5.46 |
| 5 | 47 | 15.02 | 14.02 | 14.30 | 13.12 | 12.43 | 12.63 | 1.90 | 1.59 | 1.67 | 6.67 | 8.29 | 7.98 |
| 6 | 54 | 8.04 | 7.86 | 7.73 | 5.00 | 3.78 | 4.55 | 3.04 | 4.08 | 3.17 | 4.42 | 4.93 | 5.14 |
| 7 | 21 | 9.74 | 9.70 | 10.43 | 9.40 | 9.40 | 10.16 | 0.34 | 0.30 | 0.27 | 5.81 | 5.84 | 5.74 |
| 8 | 41 | 12.81 | 25.79 | 21.01 | 4.58 | 5.85 | 5.21 | 8.23 | 19.94 | 15.79 | 11.84 | 25.37 | 19.60 |
| 9 | 72 | 11.64 | 10.85 | 11.28 | 10.80 | 10.28 | 10.78 | 0.84 | 0.56 | 0.49 | 5.92 | 4.61 | 5.47 |
| 10 | 36 | 11.04 | 7.65 | 12.37 | 6.21 | 4.54 | 7.09 | 4.83 | 3.11 | 5.28 | 14.17 | 10.51 | 14.49 |
| 11 | 57 | 7.29 | 8.43 | 8.95 | 5.07 | 4.99 | 5.26 | 2.22 | 3.43 | 3.69 | 3.61 | 4.77 | 4.71 |
| 12 | 64 | 18.11 | 13.97 | 18.24 | 16.25 | 10.48 | 15.37 | 1.87 | 3.48 | 2.87 | 5.02 | 4.41 | 5.27 |
| 13 | 81 | 16.41 | 15.51 | 17.00 | 15.57 | 15.05 | 14.88 | 0.84 | 0.46 | 2.12 | 6.95 | 6.19 | 7.88 |
| 14 | 46 | 7.41 | 7.71 | 7.27 | 4.66 | 4.58 | 4.61 | 2.75 | 3.13 | 2.66 | 8.14 | 8.68 | 8.46 |
| 15 | 42 | 20.81 | 22.01 | 24.22 | 17.54 | 15.95 | 19.48 | 3.27 | 6.06 | 4.73 | 7.36 | 9.56 | 8.83 |
| 16 | 39 | 12.66 | 7.65 | 9.83 | 7.19 | 4.46 | 8.09 | 5.46 | 3.19 | 1.74 | 9.29 | 5.96 | 5.11 |
| 17 | 57 | 15.71 | 16.08 | 15.19 | 14.43 | 15.58 | 13.39 | 1.27 | 0.49 | 1.80 | 6.98 | 5.99 | 8.43 |
| 18 | 18 | 21.05 | 23.82 | 20.49 | 3.00 | 2.55 | 2.83 | 18.05 | 21.27 | 17.66 | 31.15 | 30.21 | 31.43 |
| 19 | 58 | 10.27 | 11.03 | 10.70 | 8.58 | 9.23 | 9.45 | 1.69 | 1.80 | 1.26 | 5.99 | 6.49 | 5.39 |
| Avg | 49.3 | 11.85 | 12.02 | 12.53 | 8.53 | 7.80 | 8.72 | 3.33 | 4.22 | 3.81 | 7.80 | 8.23 | 8.49 |
| Std.Dev. | 14.73 | 4.80 | 6.03 | 5.38 | 4.63 | 4.34 | 4.57 | 3.95 | 5.81 | 4.64 | 6.17 | 7.05 | 6.62 |

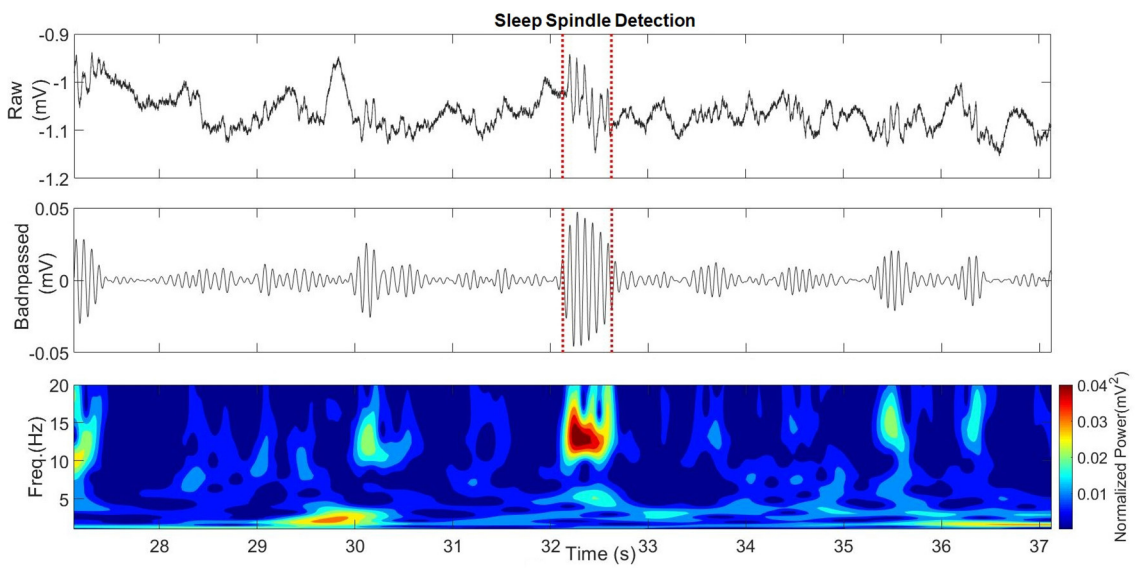


**FIGURE 6 |** Hippocampal sleep spindle from Patient 4.

**TABLE 3 |** Performance improvement and hippocampal Ripple and *spindleRipple* activity.

| Patient code | Perf. day 1 | Perf. day 2 | Performance Δ | Improvement (Mann-Whitney *U*, *p*-value) | All Ripples (Occ. Rate/min) | *spindleRipples* (Occ. Rate/min) | No. Trials day 1 | No. Trials day 2 |
|---|---|---|---|---|---|---|---|---|
| 2 | 79.6 | 89 | 9.4 | $4.9 \times 10^{-21}$ | 7.19 | 0.70 | 129 | 151 |
| 3 | 73.3 | 75.7 | 2.4 | $9.1 \times 10^{-3}$ | 8.3 | 0.36 | 160 | 130 |
| 4 | 70.4 | 80.5 | 10.1 | $4.9 \times 10^{-10}$ | 13.86 | 1.00 | 90 | 84 |
| 6 | 85.3 | 92 | 6.7 | $4.8 \times 10^{-20}$ | 14.75 | 0.75 | 160 | 160 |
| 7 | 48.4 | 53.3 | 4.9 | $1.3 \times 10^{-2}$ | 12.16 | 0.64 | 53 | 59 |
| 9 | 85.9 | 92.5 | 6.6 | $7.2 \times 10^{-15}$ | 14.67 | 1.83 | 150 | 80 |
| 11 | 62.8 | 78.7 | 15.9 | $8.0 \times 10^{-15}$ | 15.74 | 2.81 | 90 | 113 |
| 18 | 76.8 | 82.5 | 5.7 | $1.0 \times 10^{-2}$ | 23.3 | 0.06 | 30 | 74 |
| 19 | 61.5 | 68.5 | 7 | $3.7 \times 10^{-6}$ | 10.18 | 2.12 | 160 | 160 |

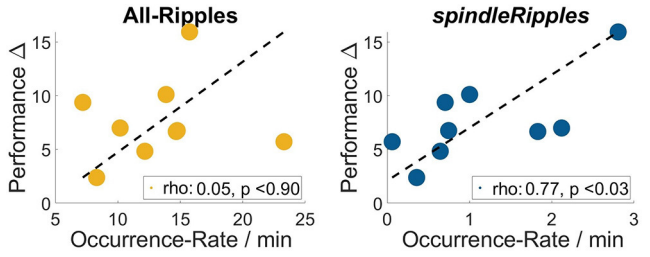


**FIGURE 7 |** Occurrence Rates of the event-class all hippocampal ripples and *spindleRipples* and their correlation with the patients' difference in performance when comparing day 1 and 2 (i.e., performance Δ).

demand on cognitive functioning. During these periods with a lower cognitive demand, all patients stayed in their hospital bed in the fairly quiet and stable environment of their room. It can thus be assumed that cognitive demands during these periods were indeed lower than during the spatial navigation task. Furthermore, all hippocampal activities reported corresponded to the average across the duration of the pre-, intra-, and post-paradigm phases; short increases of cognitive-load during the control phases would have been averaged out. In contrast, during the intra-paradigm phase it is conceivable that the reported average was derived from a period of a constant and increased cognitive-load.

The periods selected as controls before and after the paradigm showed no difference in the activity from either *allRipples*, *isolRipples*, or *iesRipples*, which in the case of the allRipples and iesRipples, as previously mentioned, evidences a lack of modulation exerted by the period of increased cognitive-load. In the case of *isolRipples* however, this equivalence between controls also shows that the isolRipples activity was modulated by the increased cognitive-load and then returned to the levels previous to the conducted navigation task.

## Differentiation of Pathologic and Physiologic Ripples

Numerous publications have reported, for both the human and non-human brain, on the occurrence of Ripples during wakefulness and while conducting cognitive tasks (43–50); despite this, to our knowledge, only the studies from (47) and those from the Brázdil1 group (48–50), have analyzed the effects of cognitive processes on the activity of putatively physiologic and putatively pathologic Ripples during the awake state and in humans. The study from (50) presents the largest patient cohort with 36 patients and will thus be considered for further discussion. This study explored if the effect of cognitive load in the form of different tasks (visual oddball, Go/NoGo, Ultimatum Game, Mismatch Negativity) on putative-pathologic ripples (i.e., ripples from epileptic hippocampi, hereinafter referenced as *pathoBrazRipples*) differed from the effect on putative-physiologic ripples (i.e., from non-epileptic hippocampi, hereinafter referred to as *physioBrazRipples*). Both *pathoBrazRipples* and *physioBrazRipples* were reported to show a significant activity reduction when transitioning from the pre- to the intra-paradigm phase, however this reduction was more significant for the *physioBrazRipples* than for the *pathoBrazRipples* when averaging the activity across the analyzed hippocampal channels.

Our results agree with (50) in that both *isolRipples* and *physioBrazRipples* showed a decrease in their activity during the intra-paradigm phase when compared to either the resting states pre-paradigm or post-paradigm. Our results disagree with (50) in that in contrast to the decrease in activity of *pathoBrazRipples* during the task, our *iesRipples* did not show any modulation exerted by the increased cognitive load. The differences between our results and those from (50) are likely due to the fact that neither approach is exhaustive, i.e., both approaches are likely to increase the proportion of physiologic to pathologic Ripples but it is still possible that this formed sub-groups of Ripples are not exclusively physiologic or pathologic.

Another recent study, (47), examined ripple-occurrence rates across two cognitive tasks and a resting state during wakefulness.

This study detected ripples firstly in the time domain by thresholding the power in the ripple band, and secondly by only accepting those detections with spectral power bursts narrowed down to the ripple range. This procedure used for the removal of potential artifactual ripples will produce detected events with spectral characteristics resembling those from our *isolRipples* class (**Figure 4**). Interestingly, in agreement with our findings for *isolRipples*, the results from (47) showed their ripple occurrence-rate to be higher during the resting state than during the cognitive tasks.

## Modulation of IES Activity

Interactions between epileptic activity and cognition have been discussed for many years (53). We compare our results with those obtained by other studies analyzing IES activity changes during cognitive tasks. The studies from (54–56) give evidence that cognitive tasks and movements can change the properties of epileptogenic networks and thus the occurrence of IES, these studies however provide disagreeing conclusions on the activity patterns followed by the reported IES. The work from (54) reported a reduction of the spike rate during successful encoding while conducting a visual recognition memory task in amygdala, hippocampus, and temporal cortex. In agreement with the latter study, (55) showed a decrease of IES activity during movement in two patients with a focal cortical dysplasia in the pre- and/or post-central gyrus. The more recent study by (56) presented an increase of temporal lobe interictal spikes in the hippocampus during a spatial memory task and both in hippocampus and lateral temporal lobe during an episodic memory task.

In contrast with the mentioned conflicting studies, our results did not show any significant modulation, whether increasing or decreasing, of the IES activity during the period of increased cognitive load. We did find, however, a difference between the control phases pre-paradigm and post-paradigm. The difference in activity from our control periods then calls for a further exploration of the importance of selecting a control period, which can then allow the comparison of results between studies.

## Correlation of *spindleRipples* and Memory Consolidation

The fact that all patients improved their performance when repeating the spatial-navigation paradigm provides evidence that the used paradigm did in fact exert a cognitive load which lead to the learning of newly acquired information. Interestingly, we found a strong correlation between *spindleRipple* activity and performance improvement.

To our knowledge only one other study has analyzed Ripple-rates and their correlation with cognitive-performance. This study from (24) analyzed the rates of ripples in the hippocampus and rhinal cortex during a short nap of 1 h, a set of images was presented pre- and post-nap and then again at the control stage, where patients had to distinguish known from novel images. Their results showed firstly, that the ripple events were circumscribed to the frequency range between 80 and 120 Hz. Secondly, that the ripple rate in the hippocampus was on average 1.90/min. Thirdly, that only rhinal, but not hippocampal ripples were correlated with the number of correctly recognized items. Our results differ from (24) in that our average rate of hippocampal ripples is higher (**Table 3**, *allRipples*: 13.35/min, *spindleRipples*: 1.14/min), which can be explained by the different detection methods used (amplitude thresholding vs. multivariate analysis). Our results slightly differ with (24) in that the frequency range of the detected ripples was circumscribed to a broader frequency range spanning between 88 and 144 Hz for the *isolRipples*, and 82 to 165 Hz for the *iesRipples*. An important agreement between our results and those from (24) is that hippocampal ripples, when undifferentiated (i.e., *allRipples*), do not present a correlation with performance improvement (measured by the difference in performances obtained pre-sleep and post-sleep).

The strong correlation shown by the *spindleRipples* with the performance improvement provides further evidence for their involvement in memory consolidation processes, moreover, these findings may contribute to the separation of physiological and non-physiological high frequency oscillations in the human hippocampus.

## Limitations

This study presents a grand average of the Ripple activity during cognitive load and does not look into more local phenomena which could arise at specific time points, e.g., the *isolRipples*' activity dynamics at specific time intervals after cue-presentation.

The selection of *spindleRipples* was based on mere co-occurrence, however previous research has shown that Ripples strongly cluster around the troughs of the sleep spindles (15, 25, 26). A selection of *spindleRipples* while considering their clustering around the spindle trough could provide a more depurated sub-set of Ripples promoting the memory-consolidation mechanism.

# CONCLUSIONS

In conclusion, the proposed method for the differentiation of physiological and pathological Ripples could help to understand the neural processes that allow the brain to execute cognitive functions such as spatial navigation and may also help to identify specific forms of ripples as biomarkers of epileptogenicity and ictogenicity. We also presented evidence supporting the role of sleep spindle-coincident ripples in memory consolidation processes, which may contribute to better understand the neural interactions allowing the storage of newly acquired information in the brain.

# DATA AVAILABILITY STATEMENT

The original contributions presented in the study are included in the article/supplementary material, further inquiries can be directed to the corresponding author/s.

# ETHICS STATEMENT

The studies involving human participants were reviewed and approved by Ethics Committee of the Freiburg

University Medical Center. The patients/participants provided their written informed consent to participate in this study.

## AUTHOR CONTRIBUTIONS

DL-P and LK conducted the navigation tasks with the patients, analyzed the data, and co-wrote the manuscript. AB conducted parts of the navigation tasks with the patients and provided assistance with the EEG measurements. MD provided assistance with the EEG measurements and co-wrote the manuscript. AT helped with the data analysis. AS-B co-wrote the manuscript. All authors contributed to the article and approved the submitted version.

## FUNDING

This work was supported by the Medical Infomatics Platform for Stereoencephalography (SEEGMIP), grant agreement No.: 650003 Human Brain Project and the BrainLinks-BrainTools Cluster of Excellence funded by the German Research Foundation (DFG; EXC 1086). LK was supported by the Federal Ministry of Education and Research (BMBF; grant number 01GQ1705A), National Science Foundation (NSF) grant BCS-1724243, NIH/NINDS grant U01 NS1113198-01, and by a travel grant from the Boehringer Ingelheim Fonds (Mainz, Germany). AT was partially financed by the Austrian Science Fund (FWF), project KLI657-B31. The article processing charge was funded by the Baden-Württemberg Ministry of Science, Research and Art and the University of Freiburg in the funding programme Open Access Publishing.

## REFERENCES

1. Buzsáki G, Silva FL da. High frequency oscillations in the intact brain. *Progr Neurobiol.* (2012) 98:241–9. doi: 10.1016/j.pneurobio.2012.02.004
2. Bragin A, Engel J, Wilson C L, Fried I, Buzsáki G. High-frequency oscillations in human brain. *Hippocampus.* (1999) 9:137–42. doi: 10.1002/(SICI)1098-1063(1999)9:2<137::AID-HIPO5>3.0.CO;2-0
3. Jacobs J, LeVan P, Châtillon C-É, Olivier A, Dubeau F, Gotman J. High frequency oscillations in intracranial EEGs mark epileptogenicity rather than lesion type. *Brain.* (2009) 132:1022–37. doi: 10.1093/brain/awn351
4. Jacobs J, Zijlmans M, Zelmann R, Chatillon C-E, Hall J, Olivier A, et al. High-frequency electroencephalographic oscillations correlate with outcome of epilepsy surgery. *Ann Neurol.* (2010) 67:209–20. doi: 10.1002/ana.21847
5. Crépon B, Navarro V, Hasboun D, Clemenceau S, Martinerie J, Baulac M, et al. Mapping interictal oscillations >200 Hz recorded with intracranial macroelectrodes in human epilepsy. *Brain.* (2010) 133:33–45. doi: 10.1093/brain/awp277
6. Malinowska U, Boatman-Reich D. Cross-frequency coupling during auditory perception in human cortex. (*2016*). In: *38th Annual International Conference of the IEEE Engineering in Medicine and Biology Society (EMBC)*. Orlando, FL (2016). p. 5521–4. doi: 10.1109/EMBC.2016.7591977
7. Worrell G A, Parish L, Cranstoun SD, Jonas R, Baltuch G, Litt B. High-frequency oscillations and seizure generation in neocortical epilepsy. *Brain.* (2004) 127:1496–506. doi: 10.1093/brain/awh149
8. Zijlmans M, Jacobs J, Kahn YU, Zelmann R, Dubeau F, Gotman J. Ictal and interictal high frequency oscillations in patients with focal epilepsy. *Clin Neurophysiol.* (2011) 122:664–71. doi: 10.1016/j.clinph.2010.09.021
9. Jacobs J, Wu JY, Perucca P, Zelmann R, Mader M, Dubeau F, et al. Removing high-frequency oscillations: a prospective multicenter study on seizure outcome. *Neurology.* (2018) 91:e1040–52. doi: 10.1212/WNL.0000000000006158
10. Gliske SV, Irwin ZT, Chestek C, Hegeman GL, Brinkmann B, Sagher O, et al. Variability in the location of high frequency oscillations during prolonged intracranial EEG recordings. *Nat Commun.* (2018) 9:2155. doi: 10.1038/s41467-018-04549-2
11. Roehri N, Pizzo F, Lagarde S, Lambert I, Nica A, McGonigal A, et al. High-frequency oscillations are not better biomarkers of epileptogenic tissues than spikes. *Ann Neurol.* (2018) 83:84–97. doi: 10.1002/ana.25124
12. Staley KJ, Dudek FE. Interictal spikes and epileptogenesis. *Epilepsy Curr.* (2006) 6:199–202. doi: 10.1111/j.1535-7511.2006.00145.x
13. Ward AA. The epileptic spike. *Epilepsia.* (1959) 1:600–6. doi: 10.1111/j.1528-1157.1959.tb04293.x
14. Hufnagel A, Dümpelmann M, Zentner J, Schijns O, Elger CE. Clinical relevance of quantified intracranial interictal spike activity in presurgical evaluation of epilepsy. *Epilepsia.* (2000) 41:467–78. doi: 10.1111/j.1528-1157.2000.tb00191.x
15. Bruder JC, Dümpelmann M, Lachner Piza D, Mader M, Schulze-Bonhage A, Julia J-L. Physiological ripples associated with sleep spindles differ in waveform morphology from epileptic ripples. *Int J Neural Syst.* (2016) 27:1750011. doi: 10.1142/S0129065717500113
16. Wang S, Wang IZ, Bulacio JC, Mosher JC, Gonzalez-Martinez J, Alexopoulos AV, et al. Ripple classification helps to localize the seizure-onset zone in neocortical epilepsy. *Epilepsia.* (2013) 54:370–6. doi: 10.1111/j.1528-1167.2012.03721.x
17. Wang S, So NK, Jin B, Wang IZ, Bulacio JC, Enatsu R, et al. Interictal ripples nested in epileptiform discharge help to identify the epileptogenic zone in neocortical epilepsy. *Clin Neurophysiol.* (2017) 128:945–51. doi: 10.1016/j.clinph.2017.03.033
18. Lachner-Piza D, Jacobs J, Schulze-Bonhage A, Stieglitz T, Dümpelmann M. Estimation of the epileptogenic-zone with HFO sub-groups exhibiting various levels of epileptogenicity*. In: *41st Annual International Conference of the IEEE Engineering in Medicine and Biology Society (EMBC)*. Berlin (2019). p. 2543–6. doi: 10.1109/EMBC.2019.8856733
19. Andrillon T, Nir Y, Staba RJ, Ferrarelli F, Cirelli C, Tononi G, et al. Sleep spindles in humans: insights from intracranial EEG, unit recordings. *J Neurosci.* (2011) 31:17821–34. doi: 10.1523/JNEUROSCI.2604-11.2011
20. Iber C, Ancoli-Israel S, Chesson AL Jr, Quan SF. *The AASM Manual for the Scoring of Sleep and Associated Events: Rules, Terminology, and Technical Specifications, 1st edn*. Westchester, IL: American Academy of Sleep Medicine. (2007).
21. Rechtschaffen A, Kales A, University of California LABIS. NINDB Neurological Information Network (U.S.). In: Allan Rechtschaffen and Anthony Kales, editors. *A Manual of Standardized Terminology, Techniques and Scoring System for Sleep Stages of Human Subjects*. Bethesda, MD: U. S. National Institute of Neurological Diseases and Blindness, Neurological Information Network. (1968). p. 6.
22. Silber MH, Ancoli-Israel S, Bonnet MH, Chokroverty S, Grigg-Damberger MM, Hirshkowitz M, et al. The visual scoring of sleep in adults *J Clin Sleep Med.* (2007) 3:121–31. doi: 10.5664/jcsm.26814
23. De Gennaro L, Ferrara M. Sleep spindles: an overview. *Sleep Med Rev.* (2003) 7:423–40. doi: 10.1053/smrv.2002.0252
24. Axmacher N, Elger CE, Fell J. Ripples in the medial temporal lobe are relevant for human memory consolidation. *Brain.* (2008) 131:1806–17. doi: 10.1093/brain/awn103
25. Clemens Z, Mölle M, Eross L, Jakus R, Rásonyi G, Halász P, et al. Fine-tuned coupling between human parahippocampal ripples and sleep spindles: ripple-spindle events in human sleep. *Eur J Neurosci.* (2011) 33:511–20. doi: 10.1111/j.1460-9568.2010.07505.x
26. Staresina BP, Bergmann TO, Bonnefond M, Meij R van der, Jensen O, Deuker L, et al. Hierarchical nesting of slow oscillations, spindles and ripples in the human hippocampus during sleep. *Nat Neurosci.* (2015) 18:1679–86. doi: 10.1038/nn.4119

27. Rasch B, Born J. About sleep's role in memory. *Physiol Rev.* (2013) 93:681–766. doi: 10.1152/physrev.00032.2012
28. Diekelmann S, Born J. The memory function of sleep. *Nat Rev Neurosci.* (2010) 11:114–26. doi: 10.1038/nrn2762
29. Mölle M, Bergmann T O, Marshall L, Born J. Fast and slow spindles during the sleep slow oscillation: disparate coalescence and engagement in memory processing. *Sleep.* (2011) 34:1411–21. doi: 10.5665/SLEEP.1290
30. Buzsáki G. Hippocampal sharp wave-ripple: a cognitive biomarker for episodic memory and planning. *Hippocampus.* (2015) 25:1073–188. doi: 10.1002/hipo.22488
31. Siapas AG, Wilson MA. Coordinated interactions between hippocampal ripples and cortical spindles during slow-wave sleep. *Neuron.* (1998) 21:1123–8. doi: 10.1016/S0896-6273(00)80629-7
32. Buzsáki G. The hippocampo-neocortical dialogue. *Cerebral Cortex.* (1996) 6:81–92. doi: 10.1093/cercor/6.2.81
33. Kunz L, Schröder TN, Lee H, Montag C, Lachmann B, Sariyska R, et al. Reduced grid-cell–like representations in adults at genetic risk for Alzheimer's disease. *Science.* (2015) 350:430–3. doi: 10.1126/science.aac8128
34. Chen D, Kunz L, Wang W, Zhang H, Wang W-X, Schulze-Bonhage A, et al. Hexadirectional modulation of theta power in human entorhinal cortex during spatial navigation. *Curr Biol.* (2018) 28:3310–5.e4. doi: 10.1016/j.cub.2018.08.029
35. Kunz L, Wang L, Lachner-Piza D, Zhang H, Brandt A, Dümpelmann M, et al. Hippocampal theta phases organize the reactivation of large-scale electrophysiological representations during goal-directed navigation. *Sci Adv.* (2019) 5:eaav8192. doi: 10.1126/sciadv.aav8192
36. Lachner-Piza D, Jacobs J, Bruder JC, Schulze-Bonhage A, Stieglitz T, Duempelmann M. Automatic detection of high-frequency-oscillations and their sub-groups co-occurring with interictal-epileptic-spikes. *J Neural Eng.* (2019) 17:016030. doi: 10.1088/1741-2552/ab4560
37. Läuter J. HochbergY, Ajit C. Tamhane: multiple comparison procedures. John Wiley & Sons, New York – Chichester – Brisbane – Toronto – Singapore 1987, XXII, 450 S., £ 38.95. *Biometr J.* (1989) 31:122. doi: 10.1002/bimj.4710310115
38. Lachner-Piza D, Epitashvili N, Schulze-Bonhage A, Stieglitz T, Jacobs J, Dümpelmann M. A single channel sleep-spindle detector based on multivariate classification of EEG epochs: MUSSDET. *J Neurosci Methods.* (2018) 297:31–43. doi: 10.1016/j.jneumeth.2017.12.023
39. Himanen S-L, Virkkala J, Huhtala H, Hasan J. Spindle frequencies in sleep EEG show U-shape within first four NREM sleep episodes *J Sleep Res.* (2002) 11:35–42. doi: 10.1046/j.1365-2869.2002.00273.x
40. Dijk D-J, Hayes B, Czeisler CA. Dynamics of electroencephalographic sleep spindles and slow wave activity in men: effect of sleep deprivation. *Brain Res.* (1993) 626:190–9. doi: 10.1016/0006-8993(93)90579-C
41. Bénar C G, Chauvire L, Bartolomei F, Wendling F. Pitfalls of high-pass filtering for detecting epileptic oscillations: a technical note on false? Ripples. *Clin Neurophysiol.* (2010) 121:301–10. doi: 10.1016/j.clinph.2009.10.019
42. Gibbs J W. Fourier's series. *Nature.* (1898) 59:200. doi: 10.1038/059200b0
43. Joo HR, Frank LM. The hippocampal sharp wave–ripple in memory retrieval for immediate use and consolidation. *Nat Rev Neurosci.* (2018) 19:744–57. doi: 10.1038/s41583-018-0077-1
44. Nokia MS, Mikkonen JE, Penttonen M, Wikgren J. Disrupting neural activity related to awake-state sharp wave-ripple complexes prevents hippocampal learning. *Front Behav Neurosci.* (2012) 6:84. doi: 10.3389/fnbeh.2012.00084
45. Papale AE, Zielinski MC, Frank LM, Jadhav SP, Redish AD. Interplay between hippocampal sharp-wave-ripple events and vicarious trial and error behaviors in decision making. *Neuron.* (2016) 92:975–82. doi: 10.1016/j.neuron.2016.10.028
46. Kucewicz MT, Cimbalnik J, Matsumoto JY, Brinkmann BH, Bower MR, Vasoli V, et al. High frequency oscillations are associated with cognitive processing in human recognition memory. *Brain.* (2014) 137:2231–44. doi: 10.1093/brain/awu149
47. Chen YY, Yoshor D, Sheth SA, Foster BL. Stability of ripple events during task engagement in human hippocampus. *bioRxiv.* (2020) 2020.10.17.342881. doi: 10.1101/2020.10.17.342881
48. Brázdil M, Cimbálník J, Roman R, Shaw DJ, Stead MM, Daniel P, et al. Impact of cognitive stimulation on ripples within human epileptic and non-epileptic hippocampus. *BMC Neurosci.* (2015) 16:47. doi: 10.1186/s12868-015-0184-0
49. Pail M, Cimbálník J, Roman R, Daniel P, Shaw DJ, Chrastina J, et al. High frequency oscillations in epileptic and non-epileptic human hippocampus during a cognitive task. *Sci Rep.* (2020) 10:18147. doi: 10.1038/s41598-020-74306-3
50. Cimbalnik J, Pail M, Klimes P, Travnicek V, Roman R, Vajcner A, et al. Cognitive processing impacts high frequency intracranial EEG activity of human hippocampus in patients with pharmacoresistant focal epilepsy. *Front Neurol.* (2020) 11:578571. doi: 10.3389/fneur.2020.578571
51. Engel J. Mesial temporal lobe epilepsy: what have we learned? *Neuroscientist.* (2001) 7:340–52. doi: 10.1177/107385840100700410
52. Elger CE, Helmstaedter C, Kurthen M. Chronic epilepsy and cognition. *Lancet Neurol.* (2004) 3:663–72. doi: 10.1016/S1474-4422(04)00906-8
53. Aarts JH, Binnie CD, Smit AM, Wilkins AJ. Selective cognitive impairment during focal and generalized epileptiform EEG activity. *Brain.* (1984) 107:293–308. doi: 10.1093/brain/107.1.293
54. Matsumoto JY, Stead M, Kucewicz MT, Matsumoto AJ, Peters PA, Brinkmann BH, et al. Network oscillations modulate interictal epileptiform spike rate during human memory. *Brain.* (2013) 136:2444–56. doi: 10.1093/brain/awt159
55. Yanagisawa T, Hirata M, Kishima H, Goto T, Saitoh Y, Oshino S, et al. Movement induces suppression of interictal spikes in sensorimotor neocortical epilepsy. *Epilepsy Res.* (2009) 87:12–7. doi: 10.1016/j.eplepsyres.2009.07.002
56. Vivekananda U, Bush D, Bisby JA, Diehl B, Jha A, Nachev P, et al. Spatial and episodic memory tasks promote temporal lobe interictal spikes. *Ann Neurol.* (2019) 86:304–9. doi: 10.1002/ana.25519


**Conflict of Interest:** The authors declare that the research was conducted in the absence of any commercial or financial relationships that could be construed as a potential conflict of interest.

*Copyright © 2021 Lachner-Piza, Kunz, Brandt, Dümpelmann, Thomschewski and Schulze-Bonhage. This is an open-access article distributed under the terms of the Creative Commons Attribution License (CC BY). The use, distribution or reproduction in other forums is permitted, provided the original author(s) and the copyright owner(s) are credited and that the original publication in this journal is cited, in accordance with accepted academic practice. No use, distribution or reproduction is permitted which does not comply with these terms.*

frontiers in Neurology

ORIGINAL RESEARCH
published: 24 March 2021
doi: 10.3389/fneur.2021.645925

# Are HFOs in the Intra-operative ECoG Related to Hippocampal Sclerosis, Volume and IQ?

*Paula Agudelo Valencia[1†], Nicole E. C. van Klink[1*†], Maryse A. van 't Klooster[1], Willemiek J. E. M. Zweiphenning[1], Banu Swampillai[1], Pieter van Eijsden[1], Tineke Gebbink[1], Martine J. E. van Zandvoort[1], Maeike Zijlmans[1,2] and the RESPect Database Study Group*

[1] Department of Neurology and Neurosurgery, University Medical Center Utrecht Brain Center, University Utrecht, Utrecht, Netherlands, [2] Stiching Epilepsie Instellingen Nederland (SEIN), Heemstede, Netherlands

Temporal lobe epilepsy (TLE) is the most common form of refractory focal epilepsy and is often associated with hippocampal sclerosis (HS) and cognitive disturbances. Over the last decade, high frequency oscillations (HFOs) in the intraoperative electrocorticography (ioECoG) have been proposed to be biomarkers for the delineation of epileptic tissue but hippocampal ripples have also been associated with memory consolidation. Healthy hippocampi can show prolonged ripple activity in stereo- EEG. We aimed to identify how the HFO rates [ripples (80–250 Hz, fast ripples (250–500 Hz); prolonged ripples (80–250 Hz, 200–500 ms)] in the pre-resection ioECoG over subtemporal area (hippocampus) and lateral temporal neocortex relate to presence of hippocampal sclerosis, the hippocampal volume quantified on MRI and the severity of cognitive impairment in TLE patients. Volumetric measurement of hippocampal subregions was performed in 47 patients with TLE, who underwent ioECoG. Ripples, prolonged ripples, and fast ripples were visually marked and rates of HFOs were calculated. The intellectual quotient (IQ) before resection was determined. There was a trend toward higher rates of ripples and fast ripples in subtemporal electrodes vs. the lateral neocortex (ripples: 2.1 vs. 1.3/min; fast ripples: 0.9 vs. 0.2/min). Patients with HS showed higher rates of subtemporal fast ripples than other patients ($Z = -2.51$, $p = 0.012$). Prolonged ripples were only found in the lateral temporal neocortex. The normalized ratio (smallest/largest) of hippocampal volume was correlated to pre-resection IQ ($r = 0.45$, $p = 0.015$). There was no correlation between HFO rates and hippocampal volumes or HFO rates and IQ. To conclude, intra-operative fast ripples were a marker for HS, but ripples and fast ripples were not linearly correlated with either the amount of hippocampal atrophy, nor for pre-surgical IQ.

**Keywords: high frequency oscillations, epilepsy surgery, mesial temporal lobe epilepsy, hippocampal volumetry, cognition**

OPEN ACCESS

***Edited by:***
*Kette D. Valente,*
*Universidade de São Paulo, Brazil*

***Reviewed by:***
*Shennan Aibel Weiss,*
*SUNY Downstate Medical Center, United States*
*Richard Staba,*
*University of California, Los Angeles, United States*

***Correspondence:**
*Nicole E. C. van Klink*
*n.vanklink-2@umcutrecht.nl*

*† These authors have contributed equally to this work and share first authorship*

***Specialty section:***
*This article was submitted to Epilepsy, a section of the journal Frontiers in Neurology*

***Received:*** *04 January 2021*
***Accepted:*** *02 March 2021*
***Published:*** *24 March 2021*

***Citation:***
*Agudelo Valencia P, van Klink NEC, van 't Klooster MA, Zweiphenning WJEM, Swampillai B, van Eijsden P, Gebbink T, van Zandvoort MJE, Zijlmans M and the RESPect Database Study Group (2021) Are HFOs in the Intra-Operative ECoG Related to Hippocampal Sclerosis, Volume and IQ? Front. Neurol. 12:645925. doi: 10.3389/fneur.2021.645925*

## INTRODUCTION

Temporal lobe epilepsy (TLE) is the most common epileptic syndrome of focal refractory epilepsy and is subcategorized in neocortical and mesial temporal epilepsy (MTLE). MTLE is often associated with hippocampal sclerosis (HS) (1). Neurosurgery is a therapeutic option for patients with focal refractory MTLE, with a high chance of seizure freedom (2, 3).

Intraoperative electrocorticography (ioECoG) can be used to demarcate the epileptogenic tissue and guide the neurosurgeon in verification whether the hippocampus is affected and the extent of the temporal resection that is required (4).

High frequency oscillations (HFOs) (ripples: 80–250 Hz, fast ripples: 250–500 Hz) are a new electrophysiological biomarker in the ioECoG (5). Ripples and fast ripples have been identified at the seizure onset zone, occurring both interictally and ictally, suggesting a relationship with the mechanisms of seizure onset (6). However, relatively long periods of high amplitude ripple activity occurring in healthy hippocampi were not associated with epilepsy and may relate to physiological brain functioning (7, 8). For this reason, recently a new type of HFO has been proposed: prolonged ripples, described as a ripple event lasting more than 200 ms (9, 10). Nonetheless, the differentiation between physiological and pathological HFOs in the hippocampus remains challenging and the overall significance of this biomarker is unclear.

MTLE, and HS in particular, is strongly associated with memory and cognitive impairment (11). The degree of hippocampal atrophy in HS is negatively associated with memory loss and IQ (12, 13). We compare fast ripples, ripples and prolonged ripples in subtemporal strip electrodes and lateral neocortical electrodes to hippocampal volume, HS and IQ. We hypothesize that increased fast ripples and decreased prolonged ripples are associated with a reduced hippocampal volume on MRI and are related to the severity of IQ impairment in MTLE.More specifically, we expect an increased rate of pathological HFOs, i.e., fast ripples and short ripples and a decreased rate of prolonged ripples to be associated with reduced hippocampal volume and IQ score. This study will provide insight on the relationship between electrophysiology, pathology and cognitive function in TLE, in an attempt to enable prediction of the effects of removing the hippocampus on seizure outcome and cognitive functioning.

# MATERIALS AND METHODS

## Study Population

People who underwent surgical resection of the hippocampus in the UMC Utrecht between 2008 and 2017 were selected from the RESPect database (**R**egistry for **E**pilepsy **S**urgery **P**atients in the UMC Utrecht). Patients were included when they had a diagnosis of MTLE, underwent ioECoG with a sampling frequency of 2,048 Hz, and had surgical resection of the hippocampus. Only patients with subtemporal strip electrodes recording the entorhinal cortex of the parahippocampal gyrus (aimed at recording the hippocampal activity) available for HFO analysis (**Figure 1**) and a pre-operative 3DT1 and FLAIR or T2 MRI available for hippocampus volumetry were selected. We excluded patients with dual pathology and continuous burst suppression on the ioECoG. We determined if the side of surgery was in the dominant hemisphere, using clinical information on handedness and results from fTCD, fMRI and Wada tests. In our center, no language lateralization test is performed if the planned resection does not include possible Wernicke's areas.

The Medal Ethical Committee of the UMC Utrecht waived the need for informed consent for all retrospectively collected data before 2018 and approved the use of coded data in the RESPect database for retrospective research.

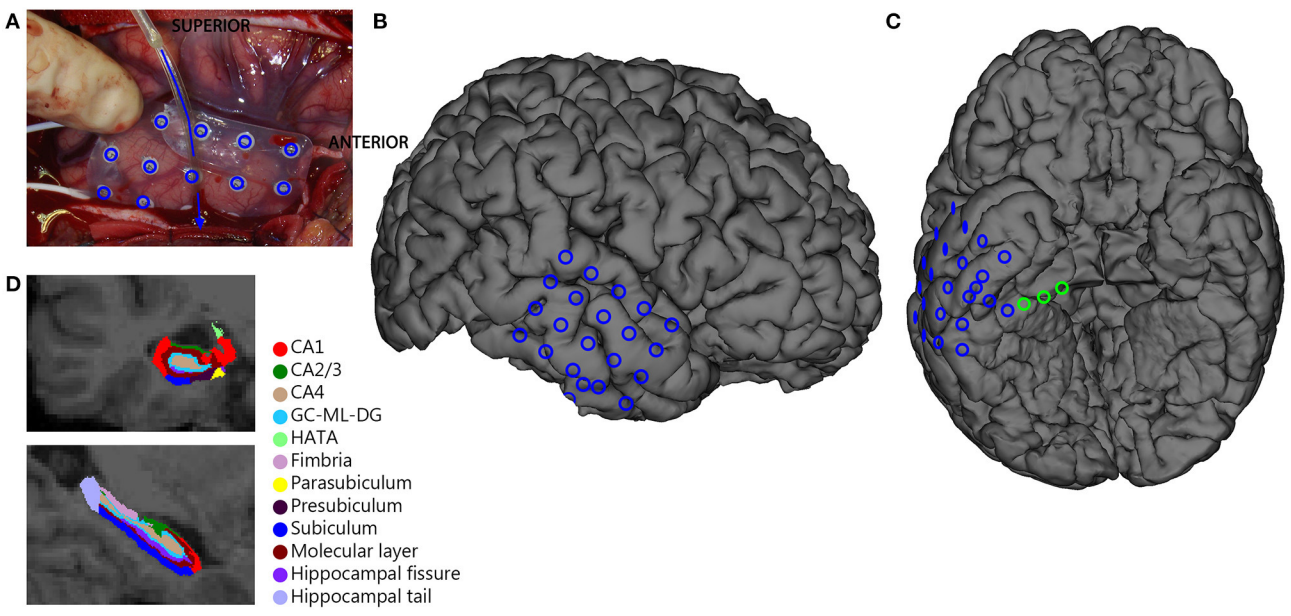


**FIGURE 1 |** Overview of ioECoG grid placement in anterior temporal lobe surgery. A 4x5 grid is placed on the lateral convexity of the right anterior temporal lobe (blue in **A–C**), and a 1x8 strip is placed under the base of the temporal pole (arrow in **A**)The three deepest contacts of the subtemporal strip sample the hippocampus and the entorhinal cortex and are analyzed separately (green in **C**). **(D)** Example of Freesurfer segmentation of hippocampal subregions.

## Pathology

Pathology findings were classified into five categories: HS, central nervous system (CNS) tumors (incl. DNETs), malformations of cortical development [incl. focal cortical dysplasia (FCD)], other (incl. cavernoma, vascular abnormalities, gliosis) and no abnormalities. Subsequently, patients were dichotomized in two groups based on pathology: HS group (ILAE type 1, 2, or 3) and non-HS group (pathological results from hippocampus showing normal tissue or neurons with reactive gliosis only).

## MRI Acquisition

The clinical pre-surgical MRI scans were performed in the UMC Utrecht with Philips MRI-scanners with a protocol designed for epilepsy patients. The parameters of the sequences, the field strengths and the planes changed over time and could be different amongst patients. This study includes 1T, 1.5T, 3T, and 7T scans. All patients had a 3D T1 scan, with a maximum isotropic resolution of 1 mm. T2 scans could be 3D T2, 3D FLAIR, or FLAIR scans and T2 scans in axial or sagittal plane. The images were saved as DICOM files and converted to Nifti for further analysis.

## Hippocampal Volumetry

Image processing and volumetric measurement of hippocampal subregions was done using FreeSurfer image analysis (version 6.0). An automated segmentation of the hippocampal subregions was performed based on a 3D T1-weighted scan and a 3D FLAIR sequence. In case there was no 3D FLAIR available, a FLAIR sequence was used and in absence of a FLAIR any available presurgical T2-weighted scan with the highest resolution was used. Volumes of the following subregions were calculated: CA1, CA3, CA4, subiculum, presubiculum, parasubiculum, granule cells in the molecular layer of the dentate gyrus (GC-ML-DG), hippocampal tail, fimbria, hippocampal amygdaloid transition area (HATA), hippocampal fissure and the total hippocampus. The hippocampal segmentations in different planes were reviewed for correctness in the Freesurfer imaging software (**Figure 1D**, Freeview; https://surfer.nmr.mgh.harvard.edu/). All volumes were corrected by division over the total intracranial volume to be able to compare across patients, therefore all volumes are reported as percentage of total intracranial volume (% ICV). As a quick check of the validity of the automated volumetry, we compared volumes of the CA1, CA3, and CA4 subregions between patients with HS ILAE type 1 and ILAE type 2 (14), expecting more pronounced atrophy of the CA1 region in ILAE type 2. For further analysis, the ratio of the total hippocampal volume was calculated by dividing the total hippocampal volume of the surgical side by the non-surgical side. This ratio appeared larger than 1 for some people, indicating a larger hippocampus on the surgical side. To be able to perform correlation analysis, we also computed the normalized ratio of the total hippocampal volume, by dividing the smallest hippocampus by the largest hippocampus, irrespective of the surgical side.

## Intra-Operative ECoG Recordings

IoECoG was recorded using 2 × 4, 4 × 5, or 4 × 8 electrode-grids placed directly on the anterior laterotemporal cortex and one 1 × 8 electrode-strip placed subtemporally over the entorhinal cortex of the parahippocampal gyrus toward the hippocampus (**Figure 1**). The grids and strips (Ad-Tech, Racine, WI, USA) consist of platinum electrodes, embedded in silicone, with a contact surface of 4.2 $mm^2$ and an inter-electrode distance of 1 cm. Recordings were made with a 64 channel EEG system (MicroMed, Veneto, Italy) at 2,048 Hz sampling rate with an anti-aliasing filter at 538 Hz. The signal was recorded referenced to an external electrode placed on the mastoid. Propofol was used as an anesthetic during surgery and was interrupted during recording until a continuous ioECoG background pattern was achieved. The ioECoG was repeated after the resection. Only the pre-resection ioECoG recording, sampling the anterior temporal pool plus hippocampus, was used for analysis.

## HFO Analysis

The last minute of ioECoG recording was selected for analysis to diminish propofol effect and artifacts. HFOs were visually marked by one reviewer (PA) and checked by a second reviewer (MZ). Marking was performed in Stellate Harmonie Reviewer in a bipolar montage. The display was split vertically with an 80 Hz high-pass filter and an amplitude of 5 μV/mm on the left side and a 250 Hz high-pass filter and 1 μV/mm on the right side. Ripples and fast ripples were marked if they clearly stood out from the baseline and contained at least four consecutive oscillations (15). An event was considered a prolonged ripple if there existed a clear oscillatory event lasting between 200 and 500 ms on the ripple screen (10). Rates of ripples, fast ripples and prolonged ripples were divided between subtemporal, if located on the first three channels of the strip, and neocortical, if located on other channels. Rates were calculated as the total number of events per channel divided by the total number of analyzed subtemporal, respectively, neocortical channels for each patient. The rates (events/minute) of HFOs were used for further analysis.

## Cognitive Assessments

Routine neuropsychological evaluation was performed in the year before surgery to assess the pre-surgical cognitive functioning of the patients. Standardized intelligence and cognitive tests, according to the age of the patient were applied. The Dutch versions of the Wechsler Intelligence Scale of Children III (WISC-III) (for children between 6 and 15 years) and the Wechsler Adult Intelligence Scale III (WAIS-III) (for patients age 16 or older) were administered by a clinical neuropsychologist to assess the total intellectual quotients (IQ), verbal IQ and performal IQ.

## Statistical Analyses

A non-parametric Wilcoxon signed rank test was used to compare the volume of each hippocampal subregion between surgical and non-surgical side and to compare HFO rates between subtemporal and neocortical channels. Mann-Whitney U tests were used to test for differences in hippocampal ratios and HFO rates between HS and non-HS patients. We compared localization of epilepsy in dominant or non-dominant hemispheres to IQ scores and HFO rates (Mann-Whitney U). We used a Spearman's Rho test for correlations between

**TABLE 1** | Patient demographics.

| | HS | Non-HS | | | |
|---|---|---|---|---|---|
| | | CNS tumor | MCD | Other | No abnormalities |
| No. | 10 | 16 | 4 | 11 | 6 |
| Gender (No. female) | 6 | 9 | 2 | 6 | 3 |
| Age at surgery [Mn (range)] | 26 (12–59) | 15 (4–53) | 49 (19–62) | 40 (12–61) | 32 (8–47) |
| Age at onset [Mn (range)] | 6 (0–12) | 9 (0–39) | 20 (1–48) | 20 (1–56) | 18 (4–39) |
| Surgical side (L:R) | 6:4 | 5:11 | 2:2 | 3:8 | 3:3 |

*HS, hippocampal sclerosis; CNS, central nervous system; MCD, malformation of cortical development; L, left; R, right; Mn, mean.*

HFO rates and hippocampal volumes and HFO rates and IQ scores. Hippocampal volumes and IQ scores showed a normal distribution, so differences between ILAE type 1 and type 2 volumes were assessed with an independent sample *t*-test, and correlation between the hippocampal volumes and IQ was assessed with a Pearson correlation test. *P*-values $<0.05$ were considered to indicate statistical significance. We did not correct for multiple comparisons because this study is exploratory in nature and most comparisons are complementary, and sensibly planned based on hypotheses arising from existing evidence. Statistical analysis was performed in IBM SPSS Statistics 25 (IBM Corp., Armonk, NY).

# RESULTS

## Population

Sixty-two patients diagnosed with MTLE had surgical resection of the hippocampus with ioECoG with grid and strip electrodes recorded at 2,048 Hz between 2008 and 2017. Thirteen patients had to be excluded from analyses because they presented dual pathology [FCD and HS ($n = 5$), cavernoma and HS ($n = 3$), glioma and HS ($n = 3$), Sturge-weber syndrome and HS ($n = 1$), glioneuronal tumor, ganglioglioma and FCD ($n = 1$)]. Two patients were excluded because of the presence of burst suppression in the epochs. Analyses were performed in 47 patients with an average age of 28 (range 2–62 years), of whom were 26 female. Nineteen patients underwent left temporal lobectomy (40%). Pathology results showed 10 patients with HS, 16 with a CNS tumor, four with a malformation of cortical development, 11 with other abnormalities and six without abnormalities (**Table 1**). *Forty-four* patients were right-handed, 28 had one or more language lateralization investigations (Wada $n = 18$, fTCD $n = 14$, fMRI $n = 14$), including all three left-handed patients. One left-handed patient had a right dominant hemisphere, one left-handed patient and two right-handed patients had bilateral language localization (based on fTCD + fMRI). The other 24 patients who underwent language lateralization were left dominant. Twenty patients had a dominant hemisphere surgery, assuming all right-handed patients without Wada, fTCD or fMRI were left dominant.

## Hippocampal Volumetry

Six patients had a tumor located in or close to the hippocampus, which made reliable segmentation of hippocampal subregions impossible. These six patients were excluded in volumetry statistics. For the remaining 41 patients the total hippocampus on the surgical side was significantly smaller than the hippocampus on the nonsurgical side (median 0.22 vs. 0.23%, $Z = -2.57$, $p = 0.01$). When splitting into subregions, the CA1, CA3, CA4, hippocampal tail, subiculum, GC-ML-DG, fimbria, and HATA were smaller on the surgical side.

In HS-patients, the total hippocampus on the surgical side was significantly smaller compared to the nonsurgical side. All subregions except for the presubiculum and fimbria were significantly smaller on the surgical side (**Figure 2A**). In patients without HS, there was no significant difference in total hippocampal volume between the surgical and nonsurgical side. Only the hippocampal tail was significantly smaller on the surgical side than on the nonsurgical side (median 0.03 vs. 0.04%, $Z = -2.19$, $p = 0.028$, **Figure 2B**).

Eight out of the 10 hippocampal sclerosis patients were ILAE type 1, the other two were ILAE type 2 (CA1 predominant). The mean volumes of the CA1, CA3 and CA4 areas were all non-significantly smaller in type 2 than in type 1 HS, but the difference was most prominent in CA1 [0.036% of ICV vs. 0.027% of ICV, t (8) = 1.50, $p = 0.17$] and CA3 [0.011% of ICV vs. 0.0086% of ICV, t (8) = 2.02, $p = 0.08$]. The difference in mean volume of the CA4 area was less pronounced (type 2 HS volume was 91% of type 1 HS volume).

The ratio of the total hippocampus of the resected hemisphere divided by the non-resected hemisphere was on average 0.9. This ratio was lower for HS compared to non-HS patients (median 0.78 vs. 0.99, $Z = -4.19$, $p < 0.001$) (**Figure 3**). Twenty-one of 41 patients had a resected hippocampus that was more than 10% smaller than the non-resected hippocampus. Seven patients had a resected hippocampus that was more than 10% larger than the non-resected hippocampus. Three of them showed tumor mass, one had an MCD, two had other pathology and in one pathology showed no abnormalities.

## HFO Analysis

A total of 835 bipolar channels (657 grid and 178 strip) was analyzed (mean 18 (range: 10–35) per patient). A total of 1598 ripples ($n = 37$, mean 6.0 channels with events per patient), 259 fast ripples ($n = 22$, mean 3.2 channels with events per patient) and 285 prolonged ripples ($n = 23$, mean 2.8 channels with events per patient) were identified. Nine patients showed no HFOs at all, an additional 15 patients showed no

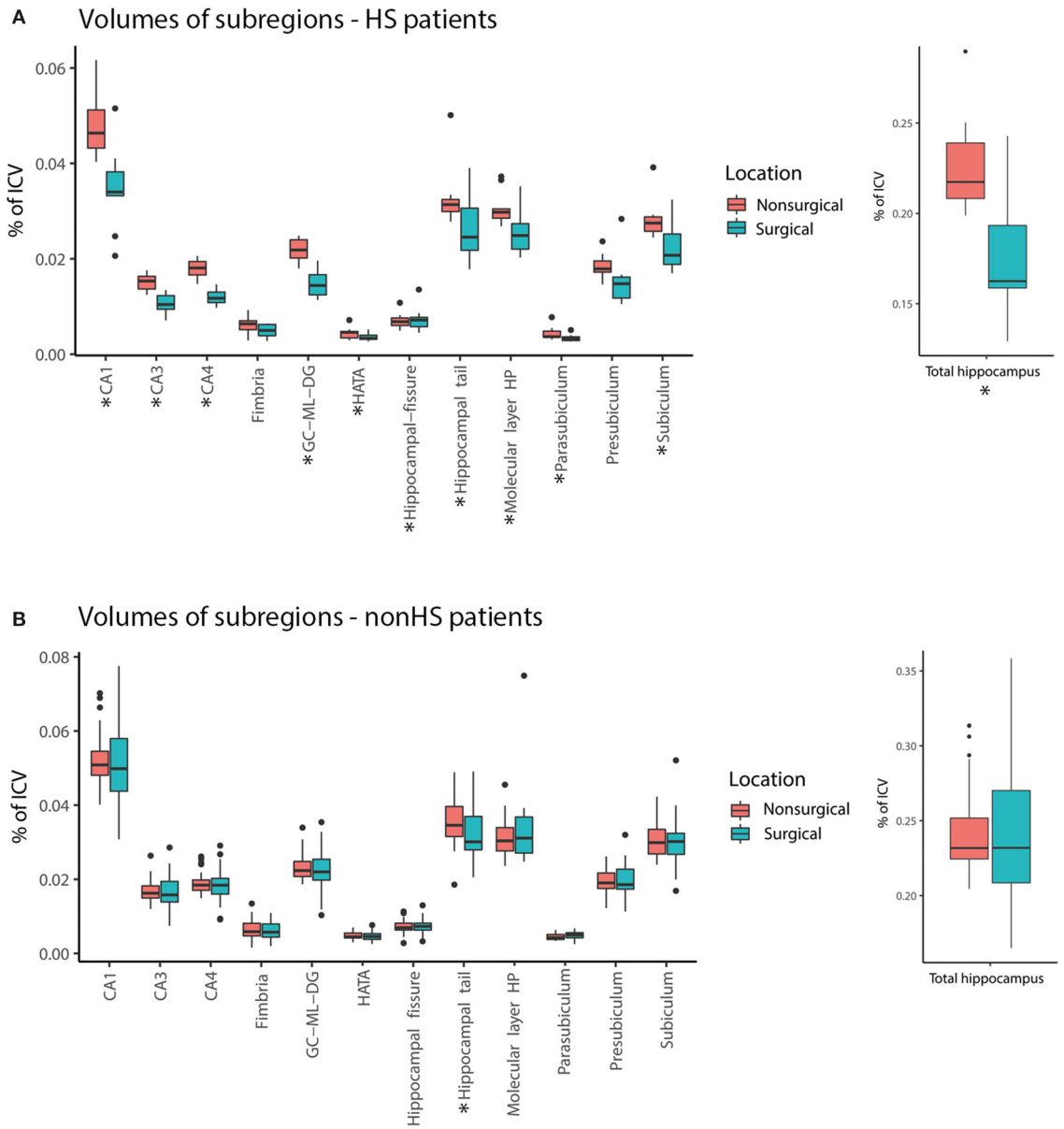


**FIGURE 2 |** Comparison of volume [in % of total intracranial volume (ICA)] of hippocampal subregions surgical (blue) and nonsurgical (pink) hemispheres for hippocampal sclerosis patients (HS) **(A)** and non-hippocampal sclerosis (non-HS) patients **(B)**. The total hippocampus and many subregions were smaller in the surgical hemisphere compared to the nonsurgical hemisphere in the HS group, but not in patients without HS (* = statistically significant, $p < 0.05$).

fast ripples. One patient showed only prolonged ripples. Fast ripples were located only subtemporal, only lateral neocortical or both subtemporal and lateral neocortical in eight, eight and six patients respectively. Ripples were located only subtemporal in seven, only lateral neocortical in 10 and both subtemporal and lateral neocortical in 20 patients. Six of the 10 patients with HS showed subtemporal fast ripples and seven showed subtemporal ripples.

There seemed to be a trend toward higher HFOs rates in the subtemporal compared to neocortical channels (ripples: 2.1 vs. 1.3/min, $Z = -1.28$, $p = 0.20$; fast ripples: 0.9 vs. 0.2/min, $Z = -1.74$, $p = 0.08$; **Figure 4**). Prolonged ripples were only found in the lateral neocortical channels.

HFOs and HS Both HS patients and non-HS patients showed fast ripples in the subtemporal channels, but the rate in non-HS patients was so low that the median rate was 0.0/min. The fast ripple rates in the subtemporal channels in HS patients were significantly higher than in non-HS patients (median 0.3 vs. 0.0/min, $Z = -2.51$, $p = 0.012$).

HFOs and hippocampal volume There was no significant correlation between lateral neocortical or subtemporal ripple, fast ripple, or prolonged ripple rates and the total volume or any of

the subregions of the removed hippocampus or the (normalized) ratio of total hippocampal volumes (**Figure 5**). When specifically looking into patients with HS ($n = 10$), there was no significant correlation between total hippocampal volume and fast ripple rate in subtemporal channels (Spearman's $r = 0.44$, $p = 0.21$), nor between any of the subregions and subtemporal ripple or fast ripple rates. There was also no difference between the presence of lateral neocortical or subtemporal ripples or fast ripples (yes vs. no) and the total volume of the resected hippocampus or the (normalized) ratio of total hippocampal volumes.

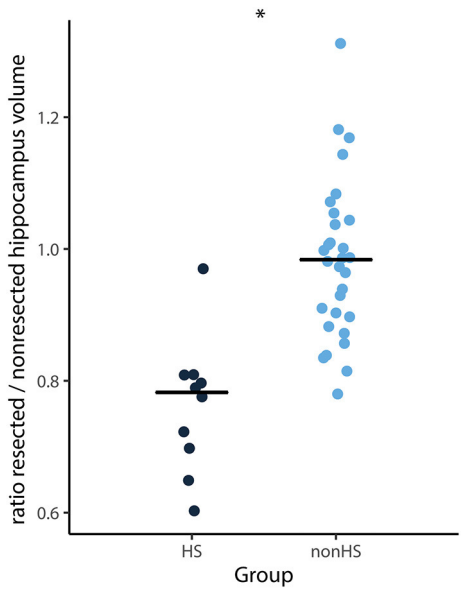


**FIGURE 3 |** Ratio of total hippocampal volume (surgical side divided by non-surgical side) of each patient and median (horizontal lines) of HS (black) and non-HS (blue) patients. The ratio was significantly smaller for patients with HS compared to non-HS patients (*$p < 0.001$).

## Intellectual Coefficient

Total IQ was available in 33 patients who underwent routine pre-surgical neuropsychological assessment. Twenty-two of them also had the verbal and performal IQ reported. Total, verbal and performal IQ did not differ between dominant hemisphere epilepsies and non-dominant hemisphere epilepsies (total IQ $p = 0.16$; verbal IQ $p = 0.74$ and performal $P = 0.41$). Hemispheric dominance did not yield different subtemporal or lateral temporal neocortical ripple, fast ripple or long ripple rates.

The total IQ showed a significant correlation to the normalized ratio of total hippocampal volume ($r = 0.45$, $p = 0.015$, **Figure 6**), indicating a lower IQ in patients with a lower normalized ratio, and therefore a larger left-right difference of hippocampal volume. The pre-surgical verbal IQ showed the same significant correlation ($r = 0.51$, $p = 0.024$), while the pre-surgical performal IQ showed no significant correlation ($r = 0.29$, $p = 0.23$). Total, verbal and performal IQ did not differ between dominant hemisphere epilepsies and non-dominant hemisphere epilepsies (total IQ $p = 0.16$; verbal IQ $p = 0.74$ and performal IQ $p = 0.41$). There was also no difference in pre-surgical total IQ between patients with a right or a left sided temporal resection.

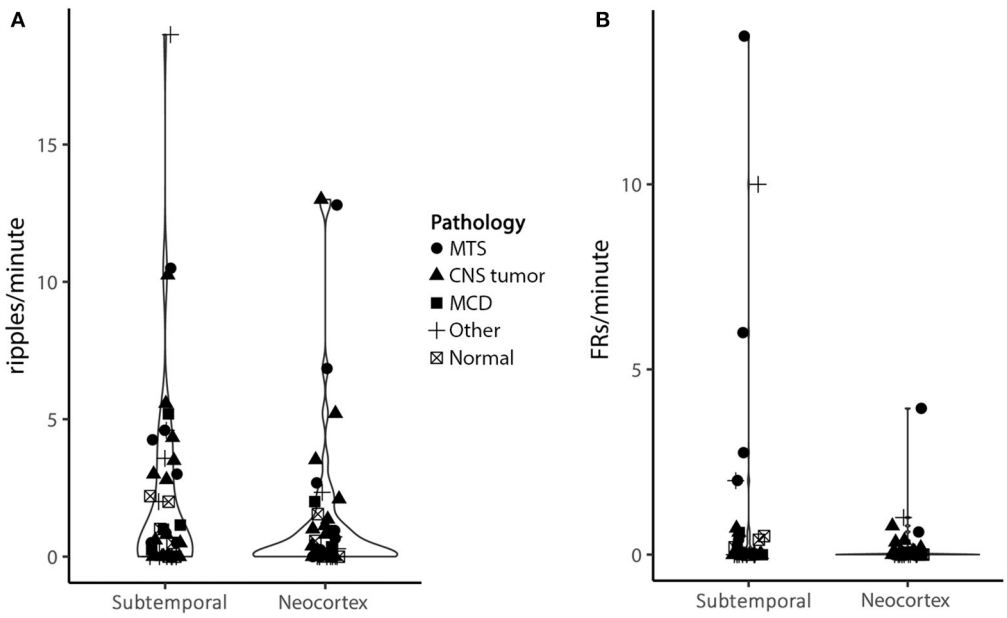


**FIGURE 4 |** Violin plot of ripple **(A)** and fast ripple **(B)** rates in subtemporal and neocortical channels. Each character represents a patient, different characters represent different pathologies. The width of the violin represents the number of dots at a certain y value. Although not significant, there is a trend toward higher HFO rates in the subtemporal compared to the neocortex (ripples: 2.1/min vs. 1.3/min, $Z = -1.28$, $p = 0.20$; fast ripples: 0.9/min vs. 0.2/min, $Z = -1.74$, $p = 0.08$) (MTS, mesiotemporal sclerosis; CNS, central nervous system; MCD, malformation of cortical development).

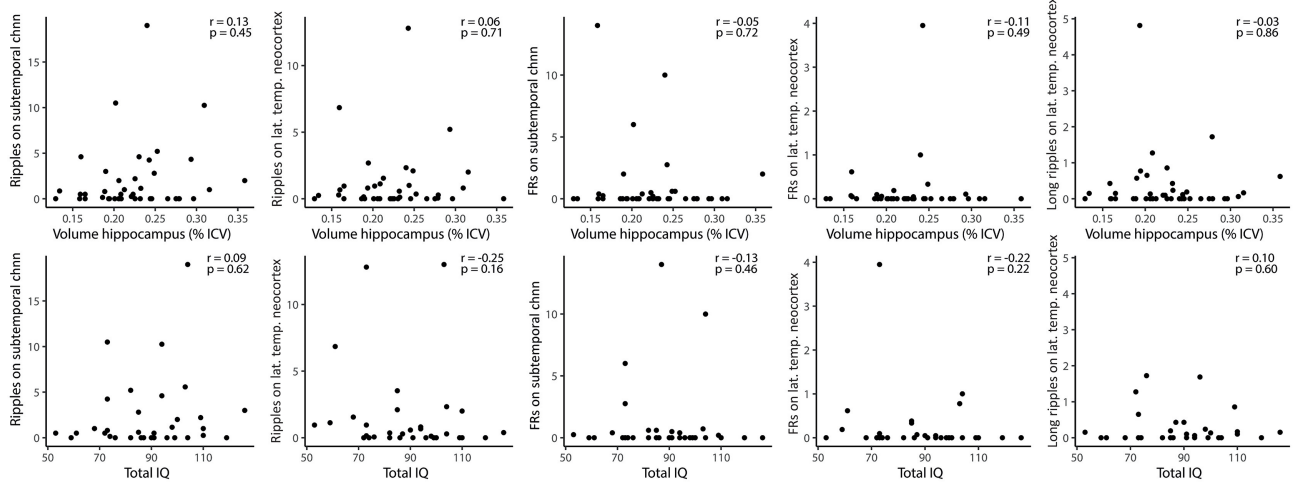


**FIGURE 5 |** Correlations between HFO rates and volume of resected hippocampus (upper row), and HFO rates (subtemporal and lateral temporal neocortical channels) and total pre-resection IQ (lower row). None of the Spearman correlations was significant. FRs, fast ripples; Chnn, channel; lat., lateral; temp., temporal.

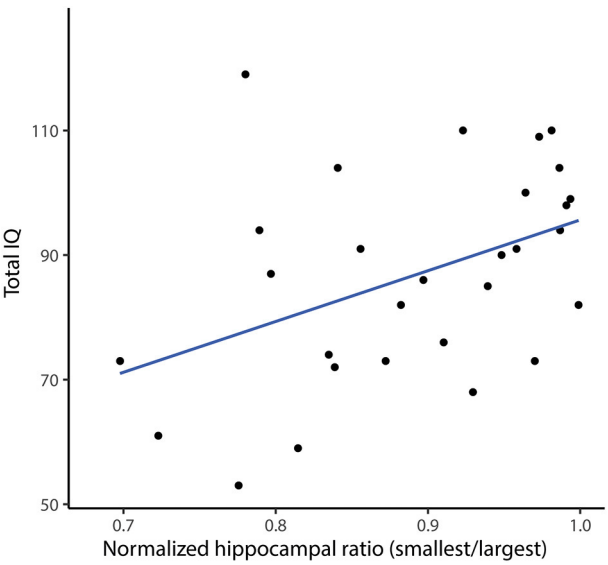


**FIGURE 6 |** Correlation between pre-resection total IQ and normalized hippocampal ratio (smallest/largest). Each dot represents a patient, the blue line is the fitted linear regression line. There is a positive correlation between pre-resection total IQ and normalized hippocampal ratio, indicating a lower IQ when the left-right hippocampal volume difference is lager (Spearmans $r = 0.45$, $p = 0.015$).

The total IQ showed a non-significant trend toward a positive correlation with the volume of the removed hippocampus ($r = 0.32$, $p = 0.095$). There was no significant correlation between neocortical or subtemporal ripple, fast ripple, or long ripple rates and total IQ (**Figure 5**). Hemispheric dominance did not yield different subtemporal or neocortical ripple, fast ripple or long ripple rates.

## DISCUSSION

Patients with HS showed higher rates of subtemporal fast ripples than other patients. We found no relation between HFO rates and hippocampal volumes or IQ. We found a trend toward higher rates of HFOs in the subtemporal channels compared to the neocortex, and significantly higher fast ripple rates in the subtemporal channels in patients with HS. Prolonged ripples were only found in the neocortex. Patients with a large left-right difference in hippocampal volumes had a lower pre-surgical IQ.

As expected, our data showed volume reduction of the ipsilateral total hippocampus in HS patients, supporting the results from other studies (12, 16–18). This volume reduction was present in almost all subregions (CA1, CA3, CA4, hippocampal tail, subiculum, GC-ML-DG, fimbria and HATA), in agreement with previous studies (12, 18, 19). The distribution of atrophy is in line with the typical volume loss pattern described by histopathological studies (1, 18). We found only atrophy of the hippocampal tail in a subselection of non-HS patients. Interestingly, in 17% of the patients (all non-HS; three with tumors, one MCD, two other and one without pathological abnormalities) the resected hippocampus was >10% bigger than the non-resected hippocampus. An explanation for a bigger hippocampus on surgical side could be ipsilateral swelling, for example due an subtle underlying pathology (e.g., FCD or tumor), or contra-lateral atrophy, as has been described for the amygdala in MTLE without HS (20, 21). We did not analyze amygdala volumes in this study. We found a lower pre-resection IQ was associated with a lower total volume of the resected hippocampus, which was expected as both worsen with longer duration of epilepsy (22).

Fast ripples arose at a higher rate in the HS- vs. non-HS patients. This is in line with previous studies that found higher rates of fast ripples in patients with hippocampal sclerosis (15, 23, 24). Even though the mechanisms underlying the generation

of HFOs are still unclear (6), it is suggested that this is due to excitotoxicity occurring in HS (25). *Ex vivo* studies have found high levels of extracellular potassium ($K^+$) in the sclerotic hippocampal tissue generating fast ripples, but no fast ripples were found in a non-HS group with the same levels of $K^+$ (26). Neuronal loss would interrupt the recapture pathway of $K^+$, leading to an accumulation of $K^+$ in extracellular spaces that influence neuronal excitability and high frequency neuronal activity in the sclerotic hippocampus (26).

HFO rates did not correlate with hippocampal volumes. This is in contrast with other studies that found an association between fast ripples rate and atrophy (25) or fast ripples to ripples rate ratio and atrophy (27) with the degree of hippocampal atrophy. Our data shows that the fast ripple rate in the subtemporal channels is higher in case of hippocampal sclerosis, but the rate was not linearly related to the amount of atrophy. We know that HFOs are related to the seizure frequency at that time point (28). Seizure frequency is not necessarily related to the amount of atrophy at that time point, but mainly to the duration of epilepsy (22). We do not have information about current seizure frequency of this cohort but this could explain our findings. The reason for the discrepancy with previous literature might also be the difference in the recording methods. We used subtemporal strip macro electrodes to sample the entorhinal cortex which covers the hippocampus, while both studies that found a correlation used micro-electrodes stereotactically inserted in the hippocampus. Worrell et al. (23) compared HFO rates recorded with micro- and macroelectrodes and hypothesized that these differences in ripples and fast ripples rate are due to the spatial undersampling of focal HFO activity with macro-electrodes. Our study included only 10 patients with hippocampal sclerosis, which might be too small to show a relation between hippocampal volume and HFO rates.

Recent research performed on sEEG recordings, has suggested that continuous rippling (with a longer duration $>$ 200 ms) found in mesiotemporal and occipital areas is independent of epileptogenicity as they do not correlate with the seizure onset zone, lesions or surgical resection area. Thus continuous rippling might reflect a particular type of physiological discharge (7–10). The hippocampus above all other structures typically generates physiological ripples, which are involved in memory consolidation, and their occurrence is strongly linked to neocortical slow waves during natural sleep (29, 30). Although propofol anesthesia is a sleep-like state that also shows slow waves, these waves are, in comparison to natural sleep, more spatially blurred and without spindling in comparison to natural sleep (31).

We marked prolonged ripples in an attempt to differentiate between physiological and pathological ripples. We found prolonged ripples only in lateral temporal, neocortical, channels. This is in contrast with other sEEG studies, that found physiological ripples in presumed normal hippocampi (29). Earlier studies have shown that differentiation between individual physiological and pathological ripples based on duration alone is not adequate (30, 32, 33), but our hypothesis was that the majority of the prolonged ripples would be physiological. The fact that we did not record prolonged ripples from the hippocampus means either that physiological ripples were not prolonged, or the hippocampus did not produce physiological ripples due to the surgical circumstances including administration of propofol before the recording. It is remarkable in this context that we do not remember seeing the typical pattern of continuous ripples in the hippocampal areas that can be seen in sEEG recordings (7). We did not see this in our intra-operative data, neither in this study, neither in previous studies nor in the onsite intra-operative review of HFOs for the HFO trial (34). We are used to seeing prolonged ripples in neocortical grid electrodes covering Broca's area, the central area and occipital area. This difference from sEEG recordings may result from the surgical conditions and would be interesting to study in more detail in the future.

We chose IQ as measure for cognitive function, even though hippocampal pathology affects memory most specifically. We did this because of the wide age range and diversity in testing, which always included an IQ score but not always a numerical memory score. IQ gives the measurement of the patient's general cognitive functioning and can be corrected for age. It has been demonstrated that patients with MTLE not only encounter memory deficits, but also impairment in all their cognitive functions (11). We recently showed that children in whom the area showing fast ripples on ioECoG was removed, had better chance at IQ improvement after surgery, irrespective of seizure recurrence (35). To date studies have only found the relationship between high HFO rates with memory impairment in MTLE (36, 37) while the role of HFOs in overall cognitive functioning have not been documented yet. In this study we could not confirm the relation between HFO rates and cognitive functioning. Since we do not have a cohort with MRIs of control subjects without epilepsy, we could not quantify the amount of atrophy compared to a normal hippocampus. When patients have bilateral atrophy, this will also affect the ratio of the hippocampal volume, which will be closer to one the more equally both hippocampi are affected. We tried to minimize this effect by focusing most on between-subject analyses on the volume of the resected hippocampus, corrected by total intracranial volume.

The use of intra-operative ECoG recordings has several limitations for data analysis and interpretation. First, in contrast to extra-operative recordings, intra-operative recordings are usually 3–4 min, of which the first minutes are often contaminated by burst suppression (38–40). Availability of epochs longer than 1 min might have resulted in different HFO rates with especially more chance to capture fast ripples. Second, intra-operative ECoG recordings are limited to recording the presumed affected hippocampus, making it impossible to compare HFO rates between hippocampi. Third, we used the HFO rates on the first three channels of the subtemporal strip recording the entorhinal cortex of the parahippocampal gyrus as a proxy for the hippocampus. We considered the hippocampus to be the source of events observed on the first three channels of the subtemporal strip, because on these channels typical hippocampal spikes, similar to those in sEEG, can be seen. At least part of the signal however arises from

the overlapping entorhinal cortex, which can also show HFOs and atrophy, but is often secondarily to hippocampal atrophy (41). This could explain why we did not find a correlation between hippocampal volume and subtemporal strip HFOs. We did not analyze the volume of the entorhinal cortex as it was often affected by the epileptogenic lesion. SEEG records directly from within hippocampi and the electrode positions are verified by MRI. It would be of interest to investigate how these intra-operative HFO rates relate to extra-operative HFO rates in the same patient. To conclude, we found increased fast ripple rates on the subtemporal channels in ioECOG in patients with HS, but ripple, fast ripple or prolonged ripple rates did not correlate with the hippocampal volume nor with IQ. We found prolonged ripples only in neocortical but not in subtemporal channels, and they were not related to IQ or volume reduction. Further research is needed to understand prolonged ripples and their role played in epilepsy and cognition.

## DATA AVAILABILITY STATEMENT

The raw data supporting the conclusions of this article will be made available by the authors, without undue reservation.

## ETHICS STATEMENT

The studies involving human participants were reviewed and approved by METC Utrecht. Written informed consent from the participants' legal guardian/next of kin was not required to participate in this study in accordance with the national legislation and the institutional requirements.

## AUTHOR CONTRIBUTIONS

PA, NK, MK, BS, WZ, TG, MZa, PE and MZi in collaboration with the RESPect database study group were involved in data collection. PA, NK, WZ, and MZi were responsible for the design of the study, and the HFO analysis. PA and NK performed the statistical analysis. PA, NK, MK, and MZi drafted the manuscript. MK, PA, and NK prepared the figures. All authors were involved in review, editing, and approval of the final version of the manuscript.

## FUNDING

WZ was financially supported by the UMC Utrecht Alexandre Suerman Stipendium 2015, MK and MZi were supported by the ERC starting grant 803880. The project was co-funded by the PPP Allowance made available by Health Holland, Top Sector Life Sciences and Health, to stimulate public-private partnerships.

## ACKNOWLEDGMENTS

We thank the following colleagues at the University Medical Center Utrecht: F. S. S. Leijten, C. Ferrier, P. H. Gosselaar, and P. van Rijen for their collaboration and clinical work related to the surgeries and ioECoG recordings.

## RESPECT DATABASE STUDY GROUP

Dorien van Blooijs, Kees Braun, Matteo Demuru, Cyrille Ferrier, Peter Gosselaar, Geertjan Huiskamp, Frans Leijten, Janine Ophorst, Peter van Rijen, Sandra van der Salm, Anouk Velders.

## REFERENCES

1. Malmgren K, Thom M. Hippocampal sclerosis-origins and imaging. *Epilepsia*. (2012) 53:19–33. doi: 10.1111/j.1528-1167.2012.03610.x
2. Jobst BC, Cascino GD. Resective epilepsy surgery for drug-resistant focal epilepsy: a review. *J Am Med Assoc*. (2015) 313:285–93. doi: 10.1001/jama.2014.17426
3. Lamberink HJ, Otte WM, Blümcke I, Braun KPJ, Aichholzer M, Amorim I, et al. Seizure outcome and use of antiepileptic drugs after epilepsy surgery according to histopathological diagnosis: a retrospective multicentre cohort study. *Lancet Neurol*. (2020) 19:748–57. doi: 10.1016/S1474-4422(20)30220-9
4. Stefan H, Quesney L, Abou-Khalil B, Olivier A. Electrocorticography in temporal lobe epilepsy surgery. *Acta Neurol Scand*. (1991) 83:65–72. doi: 10.1111/j.1600-0404.1991.tb04651.x
5. Urrestarazu E, Chander R, Dubeau F, Gotman J. Interictal high-frequency oscillations. (100-500 Hz) in the intracerebral EEG of epileptic patients. *Brain*. (2007) 130:2354–66. doi: 10.1093/brain/awm149
6. Jiruska P, Alvarado-Rojas C, Schevon CA, Staba R, Wendling F, Avoli M. Update on the mechanisms and roles of high-frequency oscillations in seizures and epileptic disorders. *Physiol Behav*. (2019) 176:139–48. doi: 10.1111/epi.13830
7. Mari F, Zelmann R, Andrade-Valenca L, Dubeau F, Gotman J. Continuous high-frequency activity in mesial temporal lobe structures. *Epilepsia*. (2012) 53:797–806. doi: 10.1111/j.1528-1167.2012.03428.x
8. Kerber K, Dümpelmann M, Schelter B, Le Van P, Korinthenberg R, Schulze-Bonhage A, et al. Differentiation of specific ripple patterns helps to identify epileptogenic areas for surgical procedures. *Clin Neurophysiol*. (2014) 125:1339–45. doi: 10.1016/j.clinph.2013.11.030
9. Melani F, Zelmann R, Mari F, Gotman J. Continuous high frequency activity: a peculiar SEEG pattern related to specific brain regions. *Clin Neurophysiol*. (2013) 124:1507–16. doi: 10.1016/j.clinph.2012.11.016
10. Noorlag L, van Klink N, Huiskamp G, Zijlmans M. What are you looking at? Unrippling terminology for high frequency activity. *Clin Neurophysiol*. (2019) 130:2132–3. doi: 10.1016/j.clinph.2019.09.002
11. Bell B, Lin JJ, Seidenberg M, Hermann B. The neurobiology of cognitive disorders in temporal lobe epilepsy. *Nat Rev Neurol*. (2011) 7:154–64. doi: 10.1038/nrneurol.2011.3
12. Ji C, Zhu L, Chen C, Wang S, Zheng L, Li H. Volumetric changes in hippocampal subregions and memory performance in mesial temporal lobe epilepsy with hippocampal sclerosis. *Neurosci Bull*. (2018) 34:389–96. doi: 10.1007/s12264-017-0186-2
13. Bennett IJ, Stark SM, Stark CEL. Recognition memory dysfunction relates to hippocampal subfield volume: a study of cognitively normal and mildly impaired older adults. *J Gerontol Ser B Psychol Sci Soc Sci*. (2019) 74:1132–41. doi: 10.1093/geronb/gbx181
14. Blümcke I, Thom M, Aronica E, Armstrong DD, Bartolomei F, Bernasconi A, et al. International consensus classification of hippocampal sclerosis in temporal lobe epilepsy: a Task Force report from the ILAE Commission on Diagnostic Methods. *Epilepsia*. (2013) 54:1315–29. doi: 10.1111/epi.12220
15. Jacobs J, LeVan P, Chander R, Hall J, Dubeau F, Gotman J. Interictal high-frequency oscillations (80-500 Hz) are an indicator of seizure onset areas

independent of spikes in the human epileptic brain. *Epilepsia*. (2008) 49:1893–907. doi: 10.1111/j.1528-1167.2008.01656.x
16. Thom M, Liagkouras I, Elliot KJ, Martinian L, Harkness W, McEvoy A, et al. Reliability of patterns of hippocampal sclerosis as predictors of postsurgical outcome. *Epilepsia*. (2010) 51:1801–8. doi: 10.1111/j.1528-1167.2010.02681.x
17. Witt JA, Coras R, Schramm J, Becker AJ, Elger CE, Blümcke I, et al. The overall pathological status of the left hippocampus determines preoperative verbal memory performance in left mesial temporal lobe epilepsy. *Hippocampus*. (2014) 24:446–54. doi: 10.1002/hipo.22238
18. Kim JB, Suh SI, Kim JH. (2015). Volumetric and shape analysis of hippocampal subfields in unilateral mesial temporal lobe epilepsy with hippocampal atrophy. *Epilepsy Res* 117:74–81. doi: 10.1016/j.eplepsyres.2015.09.004
19. Caciagli L, Bernasconi A, Wiebe S, Koepp MJ, Bernasconi N, Bernhardt BC. A meta-Analysis on progressive atrophy in intractable temporal lobe epilepsy: time is brain? *Neurology*. (2017) 89:506–16. doi: 10.1212/WNL.0000000000004176
20. Coan AC, Morita ME, Campos BM, Bergo FPG, Kubota BY, Cendes F. Amygdala enlargement occurs in patients with mesial temporal lobe epilepsy and hippocampal sclerosis with early epilepsy onset. *Epilepsy Behav*. (2013) 29:390–4. doi: 10.1016/j.yebeh.2013.08.022
21. Beheshti I, Sone D, Farokhian F, Maikusa N, Matsuda H. Gray matter and white matter abnormalities in temporal lobe epilepsy patients with and without hippocampal sclerosis. *Front Neurol*. (2018) 9:107. doi: 10.3389/fneur.2018.00107
22. Duarte JTC, Jardim AP, Comper SM, De Marchi LR, Gaça LB, Garcia MTFC, et al. The impact of epilepsy duration in a series of patients with mesial temporal lobe epilepsy due to unilateral hippocampal sclerosis. *Epilepsy Res*. (2018) 147:51–7. doi: 10.1016/j.eplepsyres.2018.08.009
23. Worrell GA, Gardner AB, Stead SM, Hu S, Goerss S, Cascino GJ, et al. High-frequency oscillations in human temporal lobe: simultaneous microwire and clinical macroelectrode recordings. *Brain*. (2008) 131:928–37. doi: 10.1093/brain/awn006
24. Rehulka P, Cimbálník J, Pail M, Chrastina J, Hermanová M, Brázdil M. Hippocampal high frequency oscillations in unilateral and bilateral mesial temporal lobe epilepsy. *Clin Neurophysiol*. (2019) 130:1151–9. doi: 10.1016/j.clinph.2019.03.026
25. Ogren JA, Wilson CL, Bragin A, Lin JJ, Salamon N, Dutton RA, et al. Three-dimensional surface maps link local atrophy and fast ripples in human epileptic hippocampus. *Ann Neurol*. (2009) 66:783–91. doi: 10.1002/ana.21703
26. Kitaura H, Shirozu H, Masuda H, Fukuda M, Fujii Y, Kakita A. Pathophysiological characteristics associated with epileptogenesis in human hippocampal sclerosis. *EBioMedicine*. (2018) 29:38–46. doi: 10.1016/j.ebiom.2018.02.013
27. Staba RJ, Frighetto L, Behnke EJ, Mathern GW, Fields T, Bragin A, et al. Increased fast ripple to ripple ratios correlate with reduced hippocampal volumes and neuron loss in temporal lobe epilepsy patients. *Epilepsia*. (2007) 48:2130–8. doi: 10.1111/j.1528-1167.2007.01225.x
28. Zijlmans M, Jacobs J, Zelmann R, Dubeau F, Gotman J. High frequency oscillations and seizure frequency in patients with focal epilepsy. *Epilepsy Res*. (2009) 85:287–92. doi: 10.1016/j.eplepsyres.2009.03.026
29. Frauscher B, von Ellenrieder N, Zelmann R, Rogers C, Nguyen DK, Kahane P, et al. High-frequency oscillations in the normal human brain. *Ann Neurol*. (2018) 84:374–85. doi: 10.1002/ana.25304
30. Weiss SA, Song I, Leng M, Pastore T, Slezak D, Waldman Z, et al. Ripples have distinct spectral properties and phase-amplitude coupling with slow waves, but indistinct unit firing, in human epileptogenic hippocampus. *Front Neurol*. (2020) 11:1–8. doi: 10.3389/fneur.2020.00174
31. Murphy M, Bruno MA, Riedner BA, Boveroux P, Noirhomme Q, Landsness EC, et al. Propofol anesthesia and sleep: a high-density EEG study. *Sleep*. (2011) 34:283–91. doi: 10.1093/sleep/34.3.283
32. Matsumoto A, Brinkmann BH, Stead SM, Matsumoto J, Kucewicz MT, Marsh WR, et al. Pathological and physiological high-frequency oscillations in focal human epilepsy. *J Neurophysiol*. (2013) 110:1958–64. doi: 10.1152/jn.00341.2013
33. Alkawadri R, Gaspard N, Goncharova II, Spencer DD, Gerrard JL, Zaveri H, et al. The spatial and signal characteristics of physiologic high frequency oscillations. *Epilepsia*. (2014) 55:1986–95. doi: 10.1111/epi.12851
34. van 't Klooster MA, Leijten FSS, Huiskamp G, Ronner HE, Baayen JC, van Rijen PC, et al. High frequency oscillations in the intra-operative ECoG to guide epilepsy surgery ("The HFO Trial"): Study protocol for a randomized controlled trial. *Trials*. (2015) 16:1. doi: 10.1186/s13063-015-0932-6
35. Sun D, van 't Klooster MA, van Schooneveld MMJ, Zweiphenning WJEM, van Klink NEC, Ferrier CH, et al. High frequency oscillations relate to cognitive improvement after epilepsy surgery in children. *Clin Neurophysiol*. (2020) 131:1134–41. doi: 10.1016/j.clinph.2020.01.019
36. Jacobs J, Banks S, Zelmann R, Zijlmans M, Jones-Gotman M, Gotman J. Spontaneous ripples in the hippocampus correlate with epileptogenicity and not memory function in patients with refractory epilepsy. *Epilepsy Behav*. (2016) 62:258–66. doi: 10.1016/j.yebeh.2016.05.025
37. Waldman ZJ, Camarillo-Rodriguez L, Chervenova I, Berry B, Shimamoto S, Elahian B, et al. Ripple oscillations in the left temporal neocortex are associated with impaired verbal episodic memory encoding. *Epilepsy Behav*. (2018) 88:33–40. doi: 10.1016/j.yebeh.2018.08.018
38. Van Klink NEC, Van't Klooster MA, Zelmann R, Leijten FSS, Ferrier CH, Braun KPJ, et al. High frequency oscillations in intra-operative electrocorticography before and after epilepsy surgery. *Clin Neurophysiol*. (2014) 125:2212–9. doi: 10.1016/j.clinph.2014.03.004
39. van't Klooster MA, van Klink NE, Leijten FS, Zelmann R, Gebbink TA, Gosselaar PH, et al. Residual fast ripples in the intraoperative corticogram predict epilepsy surgery outcome. *Neurology*. (2015) 85:120–8. doi: 10.1212/WNL.0000000000001727
40. van 't Klooster MA, van Klink NEC, Zweiphenning WJEM, Leijten FSS, Zelmann R, Ferrier CH, et al. Tailoring epilepsy surgery with fast ripples in the intraoperative electrocorticogram. *Ann Neurol*. (2017) 81:664–76. doi: 10.1002/ana.24928
41. Salmenperä T, Kälviäinen R, Partanen K, Pitkänen A. Quantitative MRI volumetry of the entorhinal cortex in temporal lobe epilepsy. *Seizure*. (2000) 9:208–15. doi: 10.1053/seiz.1999.0373

**Conflict of Interest:** The authors declare that the research was conducted in the absence of any commercial or financial relationships that could be construed as a potential conflict of interest.

*Copyright © 2021 Agudelo Valencia, van Klink, van 't Klooster, Zweiphenning, Swampillai, van Eijsden, Gebbink, van Zandvoort, Zijlmans and the RESPect Database Study Group. This is an open-access article distributed under the terms of the Creative Commons Attribution License (CC BY). The use, distribution or reproduction in other forums is permitted, provided the original author(s) and the copyright owner(s) are credited and that the original publication in this journal is cited, in accordance with accepted academic practice. No use, distribution or reproduction is permitted which does not comply with these terms.*

# Advantages of publishing in Frontiers

**OPEN ACCESS**
Articles are free to read for greatest visibility and readership

**FAST PUBLICATION**
Around 90 days from submission to decision

**HIGH QUALITY PEER-REVIEW**
Rigorous, collaborative, and constructive peer-review

**TRANSPARENT PEER-REVIEW**
Editors and reviewers acknowledged by name on published articles

**Frontiers**
Avenue du Tribunal-Fédéral 34
1005 Lausanne | Switzerland

**Visit us:** www.frontiersin.org
**Contact us:** frontiersin.org/about/contact

**REPRODUCIBILITY OF RESEARCH**
Support open data and methods to enhance research reproducibility

**DIGITAL PUBLISHING**
Articles designed for optimal readership across devices

**FOLLOW US**
@frontiersin

**IMPACT METRICS**
Advanced article metrics track visibility across digital media

**EXTENSIVE PROMOTION**
Marketing and promotion of impactful research

**LOOP RESEARCH NETWORK**
Our network increases your article's readership